



University  
of Glasgow

<https://theses.gla.ac.uk/>

Theses Digitisation:

<https://www.gla.ac.uk/myglasgow/research/enlighten/theses/digitisation/>

This is a digitised version of the original print thesis.

Copyright and moral rights for this work are retained by the author

A copy can be downloaded for personal non-commercial research or study,  
without prior permission or charge

This work cannot be reproduced or quoted extensively from without first  
obtaining permission in writing from the author

The content must not be changed in any way or sold commercially in any  
format or medium without the formal permission of the author

When referring to this work, full bibliographic details including the author,  
title, awarding institution and date of the thesis must be given

Enlighten: Theses

<https://theses.gla.ac.uk/>  
[research-enlighten@glasgow.ac.uk](mailto:research-enlighten@glasgow.ac.uk)

# COMPUTER-AIDED DESIGN OF SWITCHED-CAPACITOR FILTERS

*A Thesis submitted to the  
Faculty of Engineering  
of the University of Glasgow  
for the degree of  
Doctor of Philosophy*

*by*

ROBERT KERR HENDERSON

December 1989

ProQuest Number: 11003341

All rights reserved

INFORMATION TO ALL USERS

The quality of this reproduction is dependent upon the quality of the copy submitted.

In the unlikely event that the author did not send a complete manuscript and there are missing pages, these will be noted. Also, if material had to be removed, a note will indicate the deletion.



ProQuest 11003341

Published by ProQuest LLC (2018). Copyright of the Dissertation is held by the Author.

All rights reserved.

This work is protected against unauthorized copying under Title 17, United States Code  
Microform Edition © ProQuest LLC.

ProQuest LLC.  
789 East Eisenhower Parkway  
P.O. Box 1346  
Ann Arbor, MI 48106 – 1346



此圖為一九四九年所作，當時作者在  
 上海，正值抗戰勝利後，社會氣氛  
 熱烈，故畫此圖以表慶祝之意。

此圖為一九四九年所作，當時作者在  
 上海，正值抗戰勝利後，社會氣氛  
 熱烈，故畫此圖以表慶祝之意。

## SUMMARY

This thesis describes a series of computer methods for the design of switched-capacitor filters. Current software is greatly restricted in the types of transfer function that can be designed and in the range of filter structures by which they can be implemented. To solve the former problem, several new filter approximation algorithms are derived from Newton's method, yielding the Remez algorithm as a special case (confirming its convergency properties). Amplitude responses with arbitrary passband shaping and stopband notch positions are computed. Points of a specified degree of tangency to attenuation boundaries (touch points) can be placed in the response, whereby a family of transfer functions between Butterworth and elliptic can be derived, offering a continuous trade-off in group delay and passive sensitivity properties. The approximation algorithms have also been applied to arbitrary group delay correction by all-pass functions.

Touch points form a direct link to an iterative passive ladder design method, which bypasses the need for Hurwitz factorisation. The combination of iterative and classical synthesis methods is suggested as the best compromise between accuracy and speed. It is shown that passive ladder prototypes of a minimum-node form can be efficiently simulated by SC networks without additional op-amps. A special technique is introduced for canonic realisation of SC ladder networks from transfer functions with finite transmission at high frequency, solving instability and synthesis difficulties. SC ladder structures are further simplified by synthesising the zeros at  $\pm 2f_s$  which are introduced into the transfer function by bilinear transformation. They cause cancellation of feedthrough branches and yield simplified LDI-type SC filter structures, although based solely on the bilinear transform.

Matrix methods are used to design the SC filter simulations. They are shown to be a very convenient and flexible vehicle for computer processing of the linear equations involved in analogue filter design. A wide variety of filter structures can be expressed in a unified form. Scaling and analysis can readily be performed on the system matrices with great efficiency.

Finally, the techniques are assembled in a filter compiler for SC filters called PANDDA. The application of the above techniques to practical design problems is then examined. Exact correction of  $\text{sinc}(x)$ , LDI termination error, pre-filter and local loop telephone line weightings are illustrated. An optimisation algorithm is described, which uses the arbitrary passband weighting to pre-distort the transfer function for response distortions. Compensation of finite amplifier gain-bandwidth and switch resistance effects in SC filters is demonstrated. Two commercial filter

specifications which pose major difficulties for traditional design methods are chosen as examples to illustrate PANDDA's full capabilities. Significant reductions in order and total area are achieved. Finally, test results of several SC filters designed using PANDDA for a dual-channel speech-processing ASIC are presented. The speed with which high-quality, standard SC filters can be produced is thus proven.

## ACKNOWLEDGEMENTS

I would like to thank Professor J. Lamb for the facilities provided by the Department of Electronics and Electrical Engineering. I am grateful to Professor J. I. Sewell for his encouragement and considerate supervision of this work. Thanks are also due to my industrial supervisors, Mr K. Jones and Mr S. Laurenson of GEC Hirst Research Centre for providing the motivation for this project. Financial support for this research was provided by the Science and Engineering Research Council in a CASE award with GEC Hirst Research Centre, Wembley, London.

My special thanks go to my good friend and colleague Li Ping. His enthusiastic co-operation has made this research a pleasure to undertake. I am greatly indebted to him for many inspired suggestions, explanations and ideas. Many thanks also to my friends and fellow research students Douglas Leith, Rebecca Cheung, Majeed Ali Ahmed Foad, Gail Hughes and Michael Manness whose humour, kindness and companionship have been a great source of support to me over these years.

The advice and assistance of Neil Amos and Dave Gee of the AMSYS group at GEC Hirst Research Centre is most gratefully acknowledged. Their detailed understanding of the practical problems of SC filter design has been invaluable in directing the aims of this research.

The help of Ann Mackinnon, Janet Sutherland, Elaine McArthur, Dugald Campbell and Stephen Gallacher has been indispensable in sorting out the myriad of small but troublesome problems of working with computers. The painstaking efforts of secretaries, Janice Whitelaw and Vi Winnie, in the preparation of unintelligible papers are also greatly appreciated.

I am grateful also to my friend and flatmate David Alexander for tolerating my anti-social work habits of the last three years and for providing such a welcome distracting influence.

Finally, this thesis is the product of a long, arduous and impeccable education for which I am indebted to my parents; it is to them that I dedicate this work.

## TABLE OF CONTENTS

SUMMARY	i
ACKNOWLEDGEMENTS	iii
TABLE OF CONTENTS	iv

### CHAPTER 1: INTRODUCTION

1.1 INTRODUCTION AND GENERAL AIM	2
1.2 SWITCHED- CAPACITOR FILTER SYSTEMS	4
1.2.1 A switched- capacitor filter system	4
1.2.2 Non- ideal effects in SC filters	6
1.2.3 Design methods	8
1.2.4 Present and future applications of SC filters	10
1.3 FILTER DESIGN SOFTWARE	13
1.3.1 Aims of computer- aided design	13
1.3.2 Design of integrated filters by computer	14
1.3.3 Survey of design software	17
1.4 PURPOSE OF THE RESEARCH	21
1.5 STATEMENT OF ORIGINALITY	23
REFERENCES	24

### CHAPTER 2 : FILTER AMPLITUDE APPROXIMATION

2.1 INTRODUCTION	30
2.2 CLASSICAL FILTER AMPLITUDE APPROXIMATION	31
2.2.1 Definitions	31
2.2.2 Classical approximation methods	33
2.2.3 Limitations of classical approximations	37
2.3 GENERAL AMPLITUDE APPROXIMATION	37
2.3.1 Curve fitting problem	38
2.3.2 Interpolation	38
2.3.3 Bilateral method	41
2.3.4 Newton's method	42
2.3.5 Generalised Remez methods	46
2.3.6 Unilateral method	47
2.4. COMPUTER IMPLEMENTATION	49



2.4.1 Computer algorithm	49
2.4.2 Software considerations	50
2.5 RATIONAL APPROXIMATION	52
2.5.1 Approximation of minimum— phase rational functions	52
2.5.2 Multi— band cases	56
2.5.3 Computed examples	59
2.6 SUMMARY	67
REFERENCES	67

## CHAPTER 3 : FILTER GROUP DELAY APPROXIMATION

3.1 INTRODUCTION	72
3.2 GROUP DELAY APPROXIMATION BY ALL— PASS FUNCTIONS	73
3.2.1 Definitions	73
3.2.2 The delay approximation problem	73
3.3 ALL— PASS FILTER DESIGN METHOD	74
3.3.1 Amplitude and group delay relations	74
3.3.2 New Remez— type algorithm	75
3.3.3 Computer implementation	77
3.3.4 Computed examples	78
3.4 SUMMARY	84
REFERENCES	84

## CHAPTER 4 : FILTER PROTOTYPE DESIGN

4.1 INTRODUCTION	87
4.2 PASSIVE LADDER PROTOTYPE DESIGN	88
4.2.1 Passive ladder synthesis	88
4.2.2 Computational issues in synthesis	94
4.2.3 Iterative design of passive ladder networks	95
4.2.4 Computational issues	95
4.3 COUPLED ITERATIVE DESIGN METHOD	96
4.3.1 Computer method	96
4.3.2 Computational issues	96
4.3.3 High order ladder design	97
4.4 DESIGN OF LADDER PROTOTYPES FOR SC SIMULATION	97
4.4.1 Special topologies	97
4.4.2 Negative element values	98

4.4.3 Zeros at $\pm 2f_s$ by bilinear transformation	98
4.4.4 Realisation of zeros at $\pm 2f_s$	100
4.4.5 Synthesis for exact—LDI type SC ladder filters	102
4.4.6 Special transfer functions	104
4.5 CONCLUSIONS	108
REFERENCES	109

## CHAPTER 5 : FILTER REALISATION

5.1 INTRODUCTION	111
5.2 SWITCHED—CAPACITOR FILTER DESIGN METHODS	111
5.2.1 Cascade biquad design	111
5.2.2 Passive ladder simulation	117
5.2.3 Overview	127
5.3 SYSTEMATIC DESIGN METHODS	127
5.3.1 A general matrix form	127
5.3.2 Matrix description for SC filters	129
5.3.3 Bilinear ladder design	129
5.3.4 Ladders with finite transmission at high frequency	137
5.3.5 Bilinear/LDI ladder design	143
5.3.6 Biquad design	145
5.3.7 Analysis and scaling	147
5.3.8 Network realisation from matrix form	149
5.3.9 Computational issues	151
5.4 CAPACITANCE SPREAD REDUCTION TECHNIQUES	152
5.4.1 Dynamic range tradeoff	152
5.4.2 Pole removal permutations for ladders	154
5.4.3 Pole—zero pairing for biquads	154
5.5 SUMMARY	157
REFERENCES	157

## CHAPTER 6 : A COMPUTER—AIDED FILTER DESIGN SYSTEM

6.1 INTRODUCTION	161
6.2 AN INTEGRATED FILTER COMPILER : PANDDA	162
6.2.1 Design philosophy	162
6.2.2 Internal structure	163
6.2.3 Specifications	163

6.2.4 Filter approximation	163
6.2.5 Prototype design	183
6.2.6 Circuit design and scaling	183
6.2.7 Optimisation	185
6.3 DESIGN OF A FM RADIO FILTER	186
6.4 DESIGN OF A TELECOMMUNICATIONS FILTER	193
6.5 A SWITCHED- CAPACITOR FILTER ASIC	200
6.6 SUMMARY	212
REFERENCES	212

## CHAPTER 7 : CONCLUSIONS

7.1 DISCUSSION OF RESULTS	216
7.2 PROPOSALS FOR FUTURE WORK	220
REFERENCES	222

## APPENDIX A : DESCRIPTION OF PANDDA FILTER DESIGN SOFTWARE

A.1 FUNCTIONAL SPECIFICATIONS	223
A.1.1 Filter specification (USER)	223
A.1.2 Amplitude approximation (APPROX)	236
A.1.3 Group delay approximation (DLA)	236
A.1.4 Prototype design (LAD)	236
A.1.5 All- pass ladder design (ALPLAD)	236
A.1.6 Transfer function plotting (TFPLOT)	237
A.1.7 Circuit design (DSN)	237
A.1.8 Internal filter analysis (ANALYSIS)	237
A.1.9 Network linker (LINKER)	237
A.1.10 Netlist output (SCOUT)	237
A.1.11 Optimisation (OPTM)	239
A.1.12 Schematic generation	239
A.1.13 Automatic layout	239

## APPENDIX B : ANALYSIS OF DISTRIBUTED- RC NETWORKS

B.1 Distributed- RC networks	248
B.2 Program for analysis of distributed- RC networks	248
B.3 Analysis examples	250
REFERENCES	250

## **CHAPTER 1**

### **INTRODUCTION**

#### **1.1 INTRODUCTION AND GENERAL AIM**

#### **1.2 SWITCHED—CAPACITOR FILTER SYSTEMS**

- 1.2.1 A switched—capacitor filter system
- 1.2.2 Non—ideal effects in SC filters
- 1.2.3 Design methods
- 1.2.4 Present and future applications of SC filters

#### **1.3 FILTER DESIGN SOFTWARE**

- 1.3.1 Aims of computer—aided design
- 1.3.2 Design of integrated filters by computer
- 1.3.3 Survey of design software

#### **1.4 PURPOSE OF THE RESEARCH**

#### **1.5 STATEMENT OF ORIGINALITY**

#### **REFERENCES**

## 1.1 INTRODUCTION AND GENERAL AIM

Switched-capacitor filters (SCFs) are analogue integrated circuits found as building-blocks in a variety of communications and signal processing systems [1–3]. Their low cost, precision and compactness make them an ideal choice for telephone networks where they are used in modems, signalling systems and voice coders-decoders in digital transmission systems. Success in telephony led to further application in audio equipment, speech analysers, test instruments and electronic musical instruments. Continued interest is being shown in extending the operating frequency range of SCFs to permit application to video and radar/sonar systems.

The introduction of the SCF in the 1970s solved many of the problems associated with other analogue filter technologies [4–8]. Traditional passive RLC networks were made up of bulky, lossy discrete components which could not be integrated on a silicon chip. Active resistor-capacitor (RC) filters – composed of op-amps, resistors and capacitors – may only be partially integrated. External resistors are required which make the filter large and expensive. Fully integrated active-RC filters are not successful because neither capacitors nor resistors can be fabricated precisely enough on silicon and the resistors particularly take up too much room. The switched-capacitor, a component consisting of a capacitor continuously switched between voltages, provides an accurate, integrateable replacement for the continuous-time resistor. An SCF is composed of op-amps, capacitors and switching transistors integrated on a silicon chip in a combination of continuous-time elements (op-amps) and sampled-data elements (switches and capacitors). The precision of the filter characteristics is determined by capacitor ratios which may be set to an accuracy of better than 0.1 per cent in MOS technology. These ratios are also very stable, negating fabrication process errors, temperature and signal level variations and ageing. Several filters may be integrated on a single chip as the circuits themselves are very small.

A modern alternative to the SCF is the digital filter which samples analogue signals and processes them in digital form [9–10]. These filters have greater flexibility and lower noise but suffer from large power consumption, design complexity and high cost. In digital filters there is always a trade-off between the accuracy, in terms of the number of bits, and the processing rate. They require analogue-to-digital (A/D) conversion at input and output, and the speed and accuracy of the A/D and D/A converters is often the limiting factor to the performance of the digital system. Internally, signals must be manipulated by

arithmetic operations which are time-consuming, especially multiplication. In this respect, SCFs will always have a speed advantage due to their direct processing of analogue signals.

Sampled-data filters also possess certain inherent drawbacks such as clock-feedthrough, aliasing and signal distortion due to  $\text{sinc}(x)$  effects. Thus, the pursuit of fully integrated continuous-time filters has continued, with much research devoted to solving the problems of active-RC technology. Accurate RC time constants can be obtained by controlling the nonlinear drain-source resistance of the MOSFET by an adaptive feedback system. These so-called integrated C-T filters have relatively good performance for lower frequency signals [11]. Various problems due to parasitic effects, power supply noise and intermodulation still undermine the quality of integrated C-T filters. For low-power, precision and compactness SCFs are still the best choice against these rival technologies.

The design of integrated SCFs is often considered a fairly mature area, with a great number of design techniques for synthesizing high-performance precision SCFs. There are a series of distinct stages common to the synthesis process;

1. Calculation of a transfer function to meet specifications of amplitude and delay of signal frequencies.
2. Choice of a suitable filter network structure and calculation of capacitor values to realise the transfer function.
3. Layout of network on a silicon or GaAs chip.

The quality of the resulting filter is strongly dependent on how well these steps have been completed. Factors such as size, sensitivity to capacitor value errors, noise and tolerance of switch and amplifier non-idealities are important. For example, a well-designed transfer function can provide a circuit with minimum size and passband sensitivity. The choice of a suitable filter structure influences the capacitor area and sensitivity to capacitor value deviation and careful layout can reduce noise and ensure good capacitor ratio accuracy. Since these stages involve much laborious numerical calculation and many design decisions they are time-consuming and tedious to perform manually. It is natural, then, to apply computer-aided design (CAD) techniques to SCFs since, unlike other analogue circuits, their design process is well-defined and relatively regular. Automated filter design can greatly reduce chip turn-around time and expense. The quick delivery of good quality, error-free filters has already been proven feasible for a range of standard applications [12–15].

The aim of this thesis is to study the development of advanced CAD tools for SCFs. Current software demonstrates the lack of a unified approach to the design process which has led to a variety of restrictions being placed on the designer, impairing his/her ability to tackle the more difficult kinds of filtering problems. Some examples are low clock-to-signal frequency ratio distortions, asymmetric response specifications, amplitude and group delay equalisation and a limited choice of filter structure. These difficulties will be detailed in the remainder of this Chapter. The techniques presented in the succeeding Chapters will offer solutions, and will form the basis of a software package for integrated filter design called PANDDA.

## 1.2 SWITCHED-CAPACITOR FILTER SYSTEMS

### 1.2.1 A switched-capacitor filter system

The architecture of a switched-capacitor filter system is shown in Fig. 1.1. It is composed of a number of different stages in cascade [4-8,16]. At the input, it employs a continuous-time anti-aliasing filter to avoid any ambiguity of the signal frequencies detected by periodical sampling. Similarly, at the output an anti-imaging filter smooths the sampled waveform, removing higher frequency spectral images. Both these filters require MOS resistors which occupy a large silicon area, and so they are normally kept as simple as possible, implying very low order and selectivity.

The demands on the continuous-time filtering can be further reduced by including some decimator/interpolator filter stages in the system [17]. In effect, these are switched-capacitor anti-aliasing/imaging filters which operate at a higher clock frequency than the main SC filtering. Decimator stages are used to reduce the sampling rate towards that of the central SC filter stage and interpolator stages increase it again. This has an additional benefit, since a switched-capacitor filter operating at lower clock-to-signal frequency ratio will be accompanied by smaller capacitors and less silicon area. The central SC filter may be subdivided into an amplitude selective filter and an all-pass group delay equaliser.

Although designed separately, the blocks of a SCF system are not completely independent and some interactions are apparent. The most obvious is the effect of the group delay of an all-pass equaliser on that of the amplitude filter.

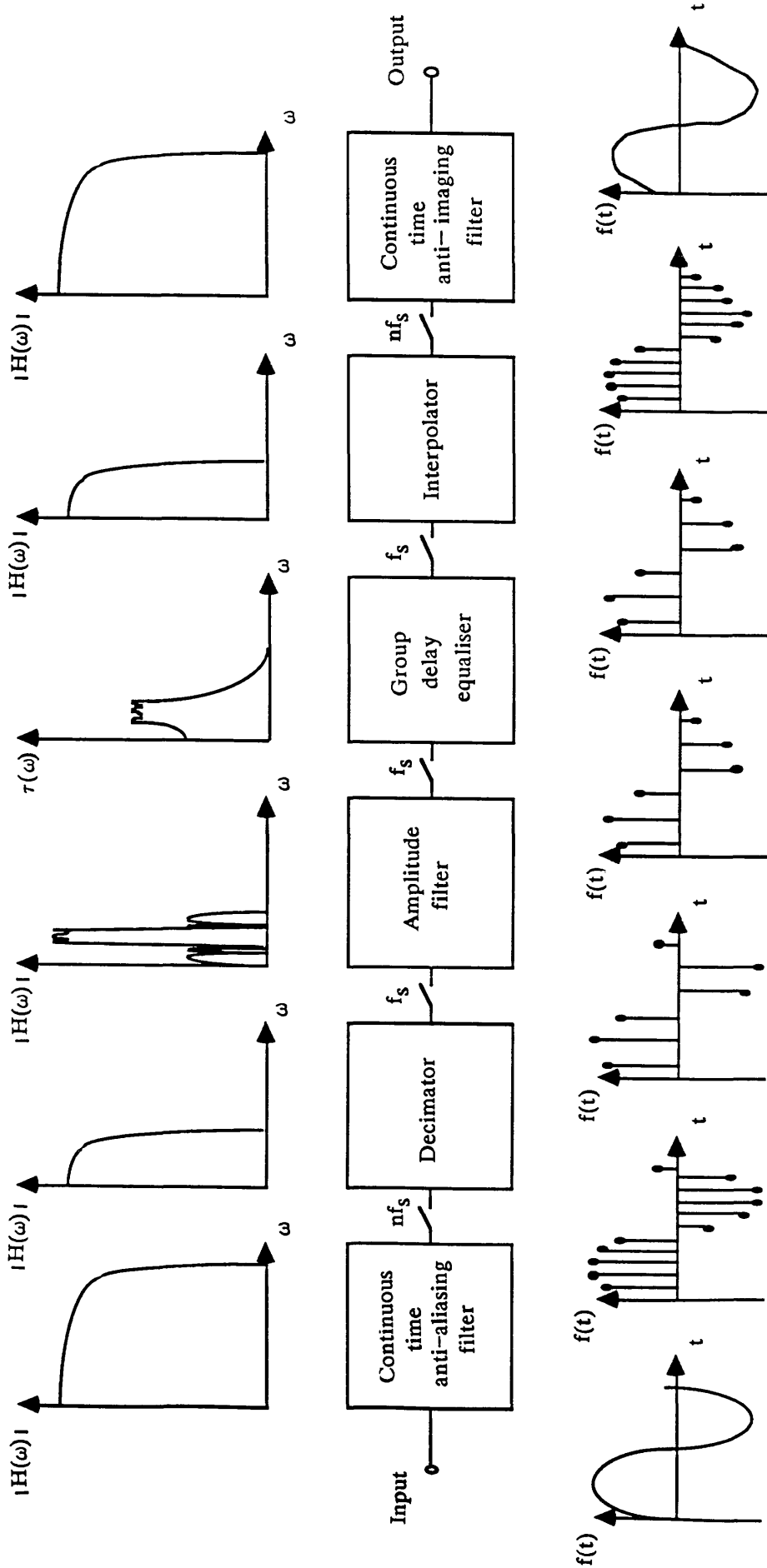


Fig. 1.1 A switched-capacitor filter system



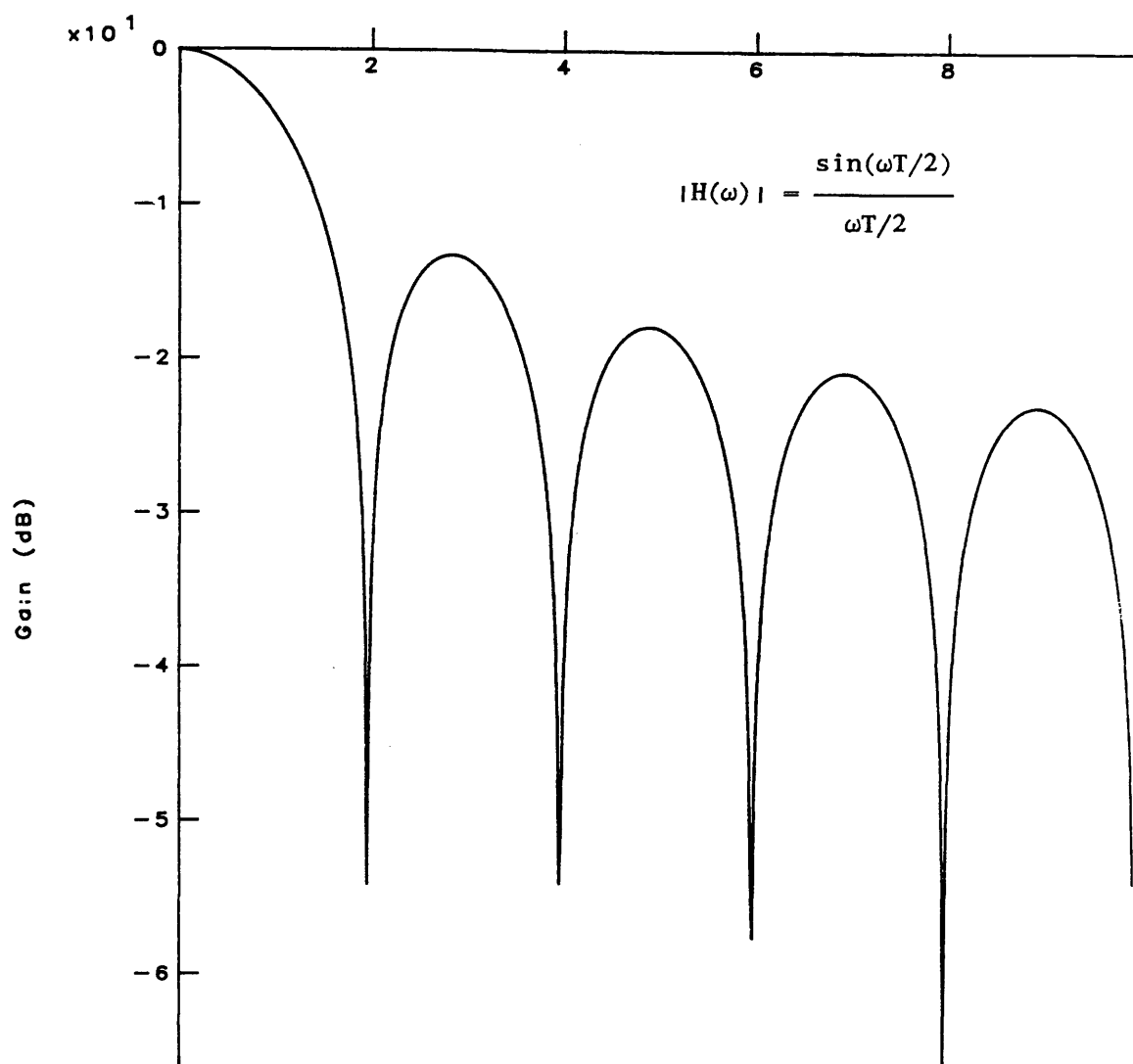
Although this is accounted for in the design process, some distortions are not e.g. the additional amplitude and group delay contributed by decimator/interpolator and continuous-time filters. Furthermore, each stage operating with a different sampling frequency adds an associated  $\text{sinc}(x)$  weighting effect. It is difficult at present to trade-off the characteristics of each block to improve the overall response of the system. This is one of the objectives of the work in this thesis.

### 1.2.2 Non-ideal effects in SC filters

Switched-capacitor filters are prone to various errors in the designed frequency response [18–20]. One unavoidable distortion is due to the sampled-and-held nature of the internal time-domain signals and takes the form of a  $\text{sinc}(x)$  weighting of the amplitude response (Fig. 1.2). The influence of this function becomes greater as the clock-to-signal frequency ratio decreases. Normally the clock frequency is chosen to be much higher than the centre frequency of the filter response. This ensures that the anti-aliasing/imaging continuous time filters are kept as simple as possible (typically second order). However, a large clock-to-centre frequency ratio (e.g. 100:1) will normally also entail a large capacitance spread which is costly in silicon area. It is therefore desirable to reduce this ratio towards the feasible limit set by the Nyquist criterion of 2:1. Practically, ratios in the range 8:1 upwards are used because of the selectivity limitations of the anti-aliasing/imaging filters. At these lower ratios the  $\text{sinc}(x)$  effect and errors due to approximate design methods become quite significant [21]. Thus there are two conflicting pressures on the choice of clock-to-centre frequency; one to increase the ratio to reduce distortion, the other to reduce it to ease the capacitance spread.

Other distortions are caused by random errors in manufacture or the non-ideal behaviour of MOS components in the filter [19]. Parasitic capacitances exist at each and every node in an integrated filter. Unless the circuits are carefully designed, the charge injection from these parasitic capacitances will significantly disturb the signals being processed by the filter. Capacitance ratios are also affected by stray-capacitance as well as layout inaccuracies. Large ratios are particularly prone to error, whereas more common small ratios (close to unity) can be realised to better than 0.1–0.5% tolerance.

Switches are realised by MOS transistors and they have a certain finite resistance in the 'on' state which, depending on the size of the switch, can range between 1–30K (in the 'off' state the resistance is very large ( $\approx 10^{12}\Omega$ ) [19]).



Multiples of the Nyquist frequency ( $f_s/2$ )

Fig. 1.2 Sinc(x) weighting effect in sampled-data systems

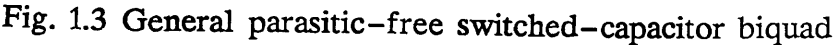
Switches with small resistances will occupy a larger area and consume more power and therefore it is desirable to use poorer, small switches. However, switch resistance causes delay in the charging of capacitors which limits the maximum operation speed of the circuit. If the clock frequency is too high, the capacitors will not charge completely in each cycle, leading to signal errors and a distorted frequency response.

Operational amplifiers are afflicted by gain and bandwidth limitations [20]. This is a particular problem in high-frequency GaAs circuits where the gain can be lower than 1000 despite a very wide bandwidth. All such 'non-idealities' distort the desired filter response in the frequency domain by disturbing the ideal pole and zero positions. Other problems are caused by amplifier offset voltages and phase errors.

### 1.2.3 Design methods

In the design of an SC filter the tolerance of the non-ideal effects mentioned in Section 1.2.2. is very important. A filter which is sensitive to such influences will often fail to meet the specified performance criteria, resulting in low yields in manufacture. It is essential therefore, to choose filters with good sensitivity properties. This leads immediately to the rejection of filter structures that are sensitive to stray-capacitance, e.g. voltage-inverter switch (VIS) approaches, component simulation and wave filters [22–24]. In addition those with notoriously high sensitivity to capacitance ratio errors must also be rejected, e.g. follow-the-leader, FIR [25–26]. Remaining, are two popular architectures; biquad cascade and operational ladder simulation filters. Further discussion will be restricted to these categories.

A biquad is a second order filter section (Fig. 1.3), realised using a loop of an inverting and non-inverting integrator [27]. A higher order filter is realised as a cascade of these circuits. The design of a biquad filter is accomplished by taking the filter transfer function to be realised, factorising it into second order terms in the  $z$ -domain and comparing each term in turn with the coefficients of a symbolic formula for the transfer function of an SC biquad section. The capacitor values are calculated by solving the set of resulting overdetermined equations. The simplicity of this process has made this design approach a popular one.



Doubly-terminated passive ladder networks (Fig.1.4a), designed for maximum power transfer over the filter passband, are known to have very low sensitivity to variations in their component values [4–8]. SC filter structures which simulate the internal workings of the ladder inherit this property (Fig. 1.4b). Their design procedure is much more complicated than biquads; a passive ladder filter must first be synthesised, and then a SC filter composed of a connection of first order blocks must be determined to implement the internal current–voltage ( $I-V$ ) relationships of the  $L$  and  $C$  elements in the prototype. An approximate method using the lossless discrete integrator (LDI) transform, results in SC ladders which do not properly simulate the resistive terminations of the prototype [28–31]. An upward sloping distortion of the amplitude response, becoming worse with decreasing clock–to–signal frequency ratio, is observed. Nevertheless, LDI ladders are efficient realisations of certain prototypes and remain popular.

Synthesis methods which result in an SC filter whose transfer function is identical to the desired one are termed *exact*, and they make use of the bilinear transformation. The design procedures are not as straightforward as for LDI filters, as the correspondence between prototype and SC implementation is no longer by simple  $I-V$  relationships. There are a number of different ladder simulation methods, the most popular of these provide the so-called leapfrog (Fig. 1.4b) and coupled–biquad filter structures [32–35].

In summary, ladder filters excel by their inherent low sensitivity properties. However, their multi–feedback nature and the need to synthesise a prototype complicate their design procedure. The class of transfer function that may be realised must normally be of the minimum–phase type and is often restricted in order and form. Biquad filters, on the other hand, are very simple to design and can *exactly* realise a general class of transfer function. Unfortunately, their sensitivity is normally poorer than that of a comparable ladder, although there is a great deal of flexibility in their design procedure, offering many possible trade–offs to the designer. The implementation cost of both structures, in terms of numbers of components, is almost identical, but the range of component values may differ widely.

#### 1.2.4 Present and future applications of switched–capacitor filters

In this section, the present applications of SCFs are reviewed. Difficulties in the design process of present filter systems are highlighted. Potential application areas of SCFs are then indicated, together with the limitations which are

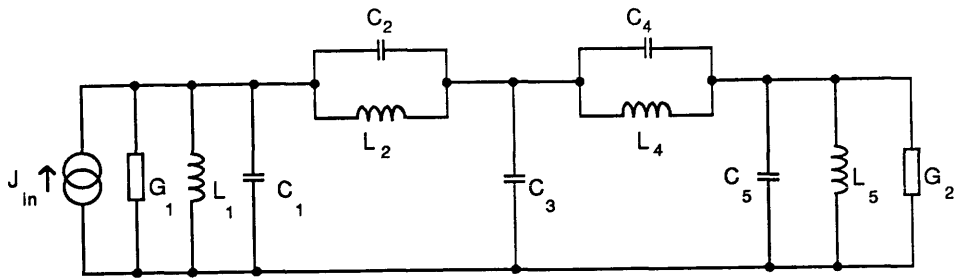


Fig. 1.4a Doubly-terminated passive ladder

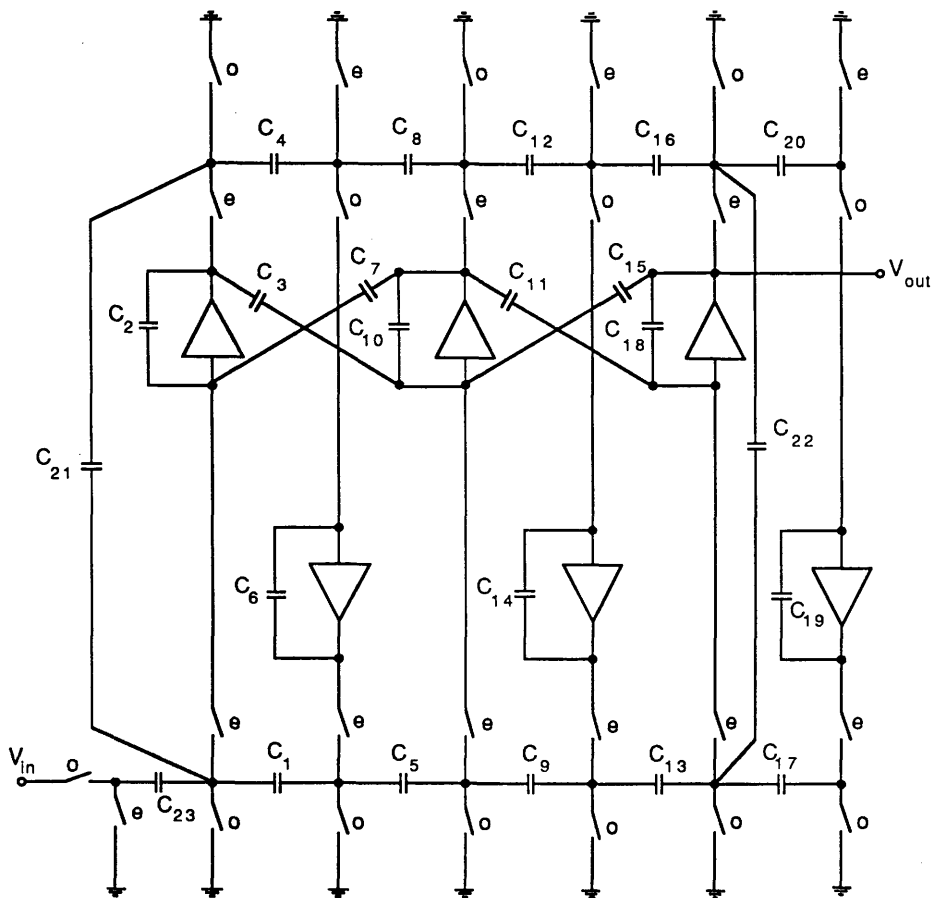


Fig. 1.4b Simulation of passive ladder by leapfrog SC filter

preventing their exploitation. The rôle of CAD in tackling these problems is then discussed.

Currently, SC filters are most commonly found as a component in voice-band communications systems, typically in modems and echo-cancellers. As they normally form part of a larger system, the correction of distortions introduced by other signal processing stages is necessary. For example, a local loop telephone line can introduce a signal loss of as much as  $-16\text{dB}$  at  $1\text{kHz}$  [37]. Another example is the  $\text{sinc}(x)$  attenuation introduced by external sampling processes. Some degree of amplitude equalisation is therefore called for, realised either by special circuits or more conveniently combined with the filtering process itself. The latter approach requires some developments in the field of filter approximation to obtain non-flat passband filter characteristics. Non-uniform stopband characteristics are also important since, for example, modem channel filters often have extremely asymmetric stopband requirements. It is concluded that some general approach to the approximation of both passband and stopband characteristics is necessary. Further applications exist in FM radio filters, transducer compensation filters and class-E transmitter filters [38].

Another problem exists in the realisation of notch filters for hum rejection. These notches occur at low frequency (e.g.  $50\text{Hz}$ ,  $60\text{Hz}$ ,  $180\text{Hz}$ ) and they imply large time constants which demand enormous capacitor ratios ( $>1000$ ) [39]. CAD can assist by optimising the  $Q$ -factors in transfer function which influence the capacitance spread and also by designing area-efficient circuit configurations [39].

A very promising future application for SCFs is within FM radio receivers where very narrow bandwidth, high-selectivity filters are required [40]. They cannot be made at present with the quality necessary for high-fidelity reception. Narrowband filters are difficult to realise with low order, small capacitor ratios and low sensitivity. Further applications exist in bioelectronic applications, such as pacemakers, hearing aids and other implantable measurement devices [40]. The low power, low voltage and low noise operation of the SCF makes it ideal for these purposes. Hearing aids require some general hearing-loss compensation implying a reconsideration of the traditional rôle of the SCF [41]. It must now perform as a general spectrum shaping device rather than simply pass or stop signals. General non-minimum phase filter design techniques are needed.

Research is progressing into implementation of SCFs on GaAs for high frequency applications such as video filters [40]. Technological constraints make

high-gain amplifiers and low-resistance switches difficult to realise. The response distortion introduced by the low gain ( $<1000$ ) and high switch resistance can be removed by appropriate computer optimisation techniques [42].

### 1.3 FILTER DESIGN SOFTWARE

#### 1.3.1 Aims of computer-aided design

Computer-aided design (CAD) software is able to assist the designer to produce an integrated filter circuit in the following ways;

1. Reduced design time and cost. Designs which would take weeks to complete by hand calculation can be done in minutes. In this way many possible alternatives may be assessed.
2. Fast estimation of silicon area and implementation cost. This is important to assess the feasibility of filter specifications and for chip floorplanning.
3. Detail and numerical calculation are conveniently handled, so that no specialised knowledge is needed to derive a filter.
4. An optimal design of filter can be obtained. Improvements may be made to filter attributes such as capacitor area, dynamic range and sensitivity to component deviation. Computer assistance is essential in this computationally expensive task.
5. Error-free network construction and layout. Mistakes in the filter network which go undetected to manufacture cost a great deal of money and time. Layout is particularly prone to human error. The computer can provide a filter layout which is correct by construction.
6. Advanced design techniques are made accessible. New filter structures are continually being developed. However, they are often slow to gain acceptance because of the complicated design process. Computer software can ensure that all designs are produced with equal ease and that the use of a given filter structure is not prejudiced by the effort demanded to construct it.

In concept, a designer should be able to specify a filter frequency response in an arbitrary manner with respect to both magnitude and group delay. A set of



switched-capacitor filter structures which efficiently meet these specifications should then quickly be presented. After a preliminary assessment of the offered designs, the selected one should be optimised for various physical parameters. Finally, the circuit should be translated to a layout for a silicon chip. Results should be able to be viewed rapidly in graphical form at all stages. The designer should be freed as much as possible from constraints on order, bandwidth, response symmetry, applicable types of structure, prototype.

The following section will indicate the techniques involved in translating this ideal scheme into computer software. A survey of the currently available software will then show the extent to which the imagined objective has been achieved.

### 1.3.2 Design of integrated filters by computer

Filters are particularly amenable to computer-aided design because, unlike other analogue circuits, the design process can be broken down into a series of well-defined steps [43]. Many of the steps involve either evaluation of explicit mathematical design formulae or numerical algorithms. They are laborious and time-consuming to execute manually and are ideally suited to implementation on a computer. The main steps and actions performed therein are now detailed (Fig. 1.5).

#### i. Specification

The principal requirement of an electronic filter is that it should process an input spectrum to pass certain bands of frequencies and to suppress all others. Amplitude response constraints are therefore of greatest importance, specified by frequencies of band edges and passband and stopband attenuation tolerances. Filter responses fit into five main categories according to which frequency bands are to be passed; low-pass, band-pass, high-pass, band-stop and all-pass.

In digital telecommunications, the group delay must also be considered to avoid inter-symbol interference. For minimum signal distortion, the group delay should be constant over the filter passband although, in practice, some deviation must be allowed.

Circuit performance may also be specified by placing acceptable limits on such measures as noise, sensitivity, power supply rejection ratio (PSRR) and harmonic distortion.

Specification and approximation	
Prototype design	$H(s) = \frac{\prod_{i=1}^N (s^2 + \omega_i^2)}{\prod_{i=1}^N (s^2 + a_i s + b_i)}$ $Z(s) = \frac{1}{s + \alpha_0} \frac{1}{s + \alpha_1} \frac{1}{s + \alpha_2} \dots$
Filter realisation	<p style="text-align: center;">biquad                      ladder</p>
Optimisation	<ol style="list-style-type: none"> <li>1. Total capacitance and capacitance spread</li> <li>2. Sensitivity</li> <li>3. Dynamic range and noise</li> <li>4. Finite op-amp gain-bandwidth and switch resistance effects</li> <li>5. Pre-distortion for frequency response weightings e.g. sinc(x), LDI error</li> </ol>
Layout	

Fig. 1.5 Conceptual stages of integrated filter design

## ii. Approximation

Design of a transfer function to meet frequency response specifications is called *approximation*. The transfer function of an analogue filter network is a rational polynomial function of frequency. Its coefficients must be determined such that its amplitude and group delay response lie within a given tolerance scheme. The order of the function must be minimised to lower the complexity of the resulting filter network.

The simplest approximations are classical functions with flat or equi-ripple amplitude behaviour in the passband or stopband e.g. Butterworth, Chebyshev, Inverse Chebyshev, Elliptic. They have closed-form or simple algorithmic solutions and can be consulted in tabular form [4]. However, these functions do not offer optimal solutions for asymmetric or irregular specifications of either amplitude or delay and so some more general approximation methods are required [44].

Amplitude specifications are commonly satisfied by designing a minimum phase transfer function which takes no account of the group delay. An all-pass function can then be designed to equalise the resultant group delay without disturbance of the amplitude response [45].

## iii. Prototype Design

In prototype design the transfer function is expanded into a form which represents a realisable network. This is commonly done in one of two ways;

a. factorisation into second-order rational terms. This represents a series of simple second-order networks (biquads) connected in cascade.

b. continued-fraction expansion of an impedance function. This process is known as classical synthesis and results in a passive RLC ladder network. It is very ill-conditioned and often incurs severe accuracy loss within finite precision computer arithmetic, even in the design of relatively low-order filters of high selectivity. Accuracy preservation entails advanced numerical methods which greatly complicate the software [46].

Many different prototype functions can be derived from a given transfer function. Each instance of a prototype function results in a different network. The choice of prototype function will later influence the capacitor spread and dynamic range of switched-capacitor implementations.

#### iv. Filter Design

At this stage the prototype function is realised as a filter network. The network structure must be established and the component values must be calculated. Two topologies dominate active circuit realisations due to their insensitivity to parasitic capacitance; biquad cascades and ladder simulations. Both possess a family of alternative equivalent realisations. For instance, a biquadratic prototype can be simulated by biquads due to Laker or Sanchez-Sinencio [4,7]. Likewise, ladder prototypes can be simulated by leapfrog, LUD or coupled-biquad ladders [32,33,36]. Each structure will have different properties of dynamic range, capacitor spread and sensitivity to component value errors. In general, filters based on ladder prototypes have lower sensitivity than those based on biquads. It is difficult, however, to generalise on which network should be chosen for a given problem. The design procedures for different prototype simulations are usually quite different and this prevents easy comparison.

Various scaling operations and optimisations may be performed to improve the dynamic range, capacitance spread and tolerance of non-ideal effects.

#### v. Realisation and Layout

Techniques to improve circuit performance are employed at this stage e.g. special amplifier designs, switching schemes and noise cancelling techniques [16]. The layout of the network on silicon is a straightforward but laborious task. Careful layout can reduce noise and ensure good capacitor ratio accuracy.

### **1.3.3 Survey of design software**

A number of filter design programs have been presented in the literature, all originating from university sources. The earliest programs for passive RLC filter design, FILSYN [47] and FILTOR2 [48], have been included, since they are used for RLC prototype design within S/FILSYN [49] and AUTO-SC (SICOMP) [50,12] respectively. Their capabilities will now be examined under the headings of Section 1.3.2. Table 1.1 offers a brief comparison of their main features.

Name	Ref	Date	Special Features
FILSYN	47	1977	Best known passive ladder synthesis program. Filters up to 40th order. Classical approximations. Pole placer program.
FILTOR2	48	1979	Good classical passive ladder synthesis program. Classical approximations. Pole placer approximation.
S/FILSYN	49	1988	Updated version of FILSYN. Switched-capacitor filter design by approximate LDI leapfrog and biquad methods.
AUTO-SC	50	1988	SC ladder filter design with FILTOR2. Exact and approximate LDI and resistor equivalence ladder designs. DR+CS scaling
SICOMP	12	1987	FILTOR2 + AUTO-SC. Automatic layout and user interface. Biquad design.
FILCAD	58	1987	Classical approximation. Ladder design. Bilinear leapfrog SC simulation. Automatic layout.
VITOLD	14	1987	Classical approximation. Pole placer. Group delay equaliser z-domain approximation and ladder synthesis. Leapfrog and biquad design. Sensitivity and harmonic distortion optimisation. DR+CS scaling. Automatic layout. Commercial package.
IMAN	15	1988	Classical approximation. Exact LDI ladder synthesis and leapfrog simulation. DR+CS scaling. Automatic layout.
MASFIL	54	1988	Simulated annealing optimisation algorithm for amplitude approximation. Biquad design. Decimator/interpolator design Anti-aliasing filter design. DR+CS optimisation.
AROMA	13	1985	Classical approximation. Bilinear biquad design. Capacitance area, sensitivity and dynamic range trade-offs. Exhaustive pole-zero pairing.
SCSYN	53	1987	Exact LDI ladder synthesis by LADNET. Structure transforms to ensure regular SC circuits for mask-programmable chip. Biquad design. Auto routing and layout. Capacitance spread and noise optimisation. No approximation.
?	55	1986	Classical approximation. Biquad design. Automatic layout.
PANDDA	52	1988	Classical approximations. Arbitrary passband and stopband approximation. High order touch points. Group delay equalisation. Classical synthesis and iterative ladder design. Leapfrog, LUD, coupled-biquad, TWINTOR simulations. Exact bilinear/LDI simulation. Biquad design. Pole-zero pairing. DR+CS optimisation. All-pass ladder and biquads. Internal analysis. Optimisation for non-ideal switch and amplifier parameters.

N.B. DR+CS = Dynamic Range and Capacitance Spread

**Table 1.1 Comparison of filter design software**

### i. Specification

Only amplitude specifications are accepted by most programs. If these are to be solved by classical approximations certain standard parameters will be requested (order, passband ripple, stopband attenuation or passband edges). A template defining the bounds on the stopband attenuation is required by FILTER2 and FILSYN. This is entered by a series of frequency/attenuation breakpoints. Graphical specification entry is being investigated for SICOMP.

PANDDA [51–52] accepts templates defining amplitude and group delay bounds. Amplitude boundaries may be weighted in both passband and stopband.

### ii. Approximation

The ability to derive classical functions (Butterworth, Chebyshev, Inverse Chebyshev and Elliptic) is common to all programs.

Both FILSYN and FILTER2, permit more general approximation. These programs will determine the zero positions and minimum order of a transfer function with arbitrary stopband shape. The poles positions for a flat, equiripple passband are then determined. SCSYN is handicapped by being without approximation capability [53].

VITOLD [14] includes a quasi–Newton minimisation method for group delay as well as general stopband attenuation. MASFIL [54] uses a simulated annealing method to adjust the poles and zeros of the transfer function to meet simultaneous amplitude and delay specifications. The method seems successful but demands long computation time.

PANDDA supports a full range of classical functions as well as a general rational approximation capability. Both passband and stopband characteristics can be tailored to arbitrary templates. Points of a specified degree of flatness (high order touch points) can be used to create hybrid equiripple/maximally–flat responses to trade–off amplitude and group delay. The specifications can be weighted automatically to compensate for distortion due to sinc(x) weighting, LDI termination error or telephone line attenuation. Group delay can be equalised by all–pass functions.

### iii. Prototype Design

FILSYN is the pre-eminent program in passive ladder synthesis. It was the first to solve the inherent ill-conditioning in the filter synthesis problem in finite computer arithmetic. The order of the ladder networks which could be accurately derived was raised to around 40. It has been expanded to encompass switched-capacitor design methods in S/FILSYN. A rival program called FILTOR2 has also been developed, and incorporated similarly into SICOMP.

However, these programs are predominantly concerned with the constraints on passive filter technology, e.g. positive element values and minimum-phase transfer functions. These properties can be relaxed when the passive ladder is simulated by active circuits. For this reason, LADNET, IMAN and VITOLD [53,15,14] perform synthesis in the  $z$ -domain so that the ladder is directly implementable as a switched-capacitor network without further transformation. LADNET is a special  $z$ -domain synthesis program for LDI filters which synthesises and transforms the ladder prototype for regular gate-array type layout.

PANDDA employs an iterative method for ladder design combined with classical synthesis in order to avoid the accuracy problem, allowing passive prototypes to be designed well beyond typical orders of around 20 (up to 100 in certain special cases). Special ladder structures with negative element values can be synthesised to reduce the complexity of SC simulations. The ladders can all be *exactly* realised by regular bilinear SC filter structures.

Factorisation of a polynomial for biquad implementation is a straightforward numerical task compared to ladder synthesis and is performed by all programs.

### iv. Filter Design

Two types of switched-capacitor filter have achieved popularity for practical design due to their insensitivity to parasitic capacitance; the biquadratic cascade and leapfrog ladder. AROMA [13] specialises in biquad design and permits many tradeoffs between various performance parameters such as spread and dynamic range. S/FILSYN employs approximate LDI simulation of a passive ladder designed by FILSYN. AUTO-SC, VITOLD, IMAN and SCSYN choose exact LDI leapfrog structures to avoid distortion from approximate design methods. Scaling of circuits

for maximum dynamic range and minimum capacitance spread is a commonly available. S/FILSYN, SICOMP, SCSYN and VITOLD can also realise biquad filters. SCSYN includes a feature to tradeoff total capacitance and dynamic range. A total capacitance area can be specified and the filter capacitors will be expanded or reduced to make best use of the available area.

VITOLD is the only program to provide a design centreing capability. The component values are assigned an allowable percentage deviation and optimised for maximum yield.

PANDDA can design both ladder and biquad filters. A wide variety of implementations is offered including leapfrog, LUD and coupled-biquad ladders with either LDI or bilinear topology. Special techniques are available to realise highpass and bandstop ladders [56–57]. Laker's type-E or F biquadratic sections are also available [4]. All-pass group delay equalisers can be designed by new low-sensitivity ladder topologies or by special all-pass biquads.

#### v. Layout

Switched-capacitor filters, being very regular structures are quite convenient for automatic computer layout. SCSYN constructs layouts from second-order integrator loops and synthesises the ladder networks to be a simple connection of these blocks. SICOMP constructs the filter from general first-order blocks. Routing and capacitor layout are done to minimise charge injection and stray-capacitance.

PANDDA has no internal layout software, since this step is highly dependent on fabrication process and style of a design house.

### 1.4 PURPOSE OF THE RESEARCH

The purpose of the research presented in this thesis is to study computer techniques for the design of switched-capacitor filter systems. Chapters 2 to 5 present a series of efficient computer methods for each of the main stages of the design process. Chapter 6 illustrates their application within a software package to tackle several difficult practical filter problems.

Since  $\text{sinc}(x)$  and LDI termination error are frequency response distortions inherent to SC filters there is a need for some degree of amplitude equalisation



in the design of the filter frequency response. In addition, since an SC filter must exist in an environment of anti-aliasing stages, there must be some capability to trade-off the influences on the frequency responses of each stage. These call for more general transfer approximation capabilities in both amplitude and delay. These topics will be approached in Chapters 2 and 3 respectively.

Chapter 4 covers the design of prototype ladder filters for simulation by SC circuits. Methods of designing ladders with weighted frequency response are considered. The accuracy of the synthesised ladder is maintained without excessively complicating the software by a combination of iterative and synthesis approaches. Certain restrictions in the design of passive ladders can be removed, when they are to be simulated by SC circuits. Negative element values are acceptable and are even shown to be useful in the design of LDI-type filter structures. It is of importance that the prototype ladder can be simulated by canonical SC networks. Certain rules are presented to ensure that this will always be the case.

In Chapter 5 the design of SC circuit structures to simulate a prototype transfer function is considered. At present, the design techniques for SC filters vary greatly and are as a result not easy to implement in computer form. Current filter CAD packages reflect this lack of uniformity by adopting only a single architecture. Matrix methods, which have been successfully applied to circuit analysis, are now shown to be an excellent means for processing filter designs in computer form. The regularity achieved permits a wide variety of filter structures to be quickly compared. Scaling and realisation steps become greatly simplified.

A software package, PANDDA (Program for Advanced Network Design : Digital and Analogue), has been constructed employing the design methods described in this thesis. Chapter 6 explores a range of design problems and illustrates the improved solutions available by the application of the filter design tools. Several practical design examples are considered which cannot be satisfactorily solved by traditional methods. The use of PANDDA to design a commercial speech processing chip is demonstrated and test results of the integrated circuit are given.

Chapter 7 summarises the achievements of the research in this thesis and proposes some extensions of the work.

## 1.5 STATEMENT OF ORIGINALITY

The following results of the research in this thesis are, as far as is known, original and have been published or submitted for publication:

In Chapter 2, the derivation of efficient approximation methods for arbitrary amplitude boundary functions and the use of high-order touch points. The relationship of Newton's method to Remez approximation methods is demonstrated. A new approximation technique is proposed called the unilateral algorithm.

[Li Ping, R.K.Henderson and J.I.Sewell, "A New Filter Approximation and Design Algorithm", Proc. IEEE ISCAS '89, pp., Portland, Oregon, U.S.A., May 1989.]

[R.K.Henderson, Li Ping and J.I.Sewell, "Extended Remez algorithms for filter amplitude and group delay approximation", in preparation.]

In Chapter 3, the use of the Remez amplitude approximation methods for group delay approximation by all-pass functions.

[R.K.Henderson and J.I.Sewell, "A new design algorithm for all-pass delay equalisers", Proc. IEE Saraga Colloquium on Electronic Filters, London, June, 1989.]

[R.K.Henderson, Li Ping and J.I.Sewell, "Extended Remez algorithms for filter amplitude and delay approximation", in preparation.]

In Chapter 4, the unified use of touch points by approximation and iterative ladder design algorithm affords a direct connection which can avoid the ill-conditioned Hurwitz factorisation step. The development of special prototypes for simulation by bilinear/LDI filter structures. Zeros at  $\pm 2fs$  introduced by applying the bilinear transform to  $z$ -domain designed transfer functions. An exact scheme to correct distortion due to improperly realised resistive terminations by LDI-type SC filters. A method to design canonical simulations of passive ladder networks with finite transmission at high frequency.

[Li Ping, R.K.Henderson and J.I.Sewell, "A New Filter Approximation and Design Algorithm", Proc. IEEE ISCAS '89, pp. 1063–1066, Portland, Oregon, U.S.A., May 1989.]

[Li Ping, R.K.Henderson and J.I.Sewell, "Matrix methods for switched-capacitor filter design", IEEE ISCAS '88, pp. 1044–1048, Espoo, Helsinki, Finland, 1988.]

In Chapter 5. the use of matrix methods for the description and processing of SC filters on a computer. Scaling for maximum dynamic range and minimum capacitance spread by matrix operations. Zero removal permutations as a means of reducing total capacitance of ladder simulations.

[Li Ping, R.K.Henderson and J.I.Sewell, "Matrix methods for switched- capacitor filter design", IEEE ISCAS '88, pp. 1044-1048, Helsinki, Finland, June 1988.]

[Li Ping, R.K.Henderson and J.I.Sewell, "Switched- capacitor filter design by matrix methods", submitted for publication.]

[R.K.Henderson, Li Ping and J.I.Sewell, "A unified approach to the design of canonical integrated ladder filters", submitted for publication.]

In Chapter 6 the software package PANDDA is presented. A series of novel design examples, demonstrating the use of high order touch point responses to ease group delay equalisation requirements, exact correction of  $\text{sinc}(x)$  distortion and filter optimisation by pre-distortion of the specifications.

[R.K.Henderson, Li Ping and J.I.Sewell, "A design program for digital and analogue filters : PANDDA", Proc. ECCTD '89, pp. 289-293, Brighton, U.K., Sept. 1989.]

[R.K.Henderson, Li Ping and J.I.Sewell, "PANDDA : A program for advanced network design : digital and analogue", Digest of Saraga Colloquium on Electronic Filters, pp. 4/1-4/8, London, 1988.]

## REFERENCES

- [1] C. W. Solomon, "Switched- capacitor filters : precise, compact, inexpensive", IEEE Spectrum, pp.28-32, June 1988.
- [2] K. Nakayama and Y. Kuraishi, "Present and future applications of switched- capacitor circuits", IEEE Circuits and Devices magazine, pp. 10-20, Sept. 1987.
- [3] R. W. Broderson, P. R. Gray and D. A. Hodges, "MOS switched- capacitor filters", Proc. IEEE, Vol. 67, No.1, pp. 61-74, Jan. 1979.
- [4] M. S. Ghausi and K. R. Laker, "Modern filter design : active RC and switched- capacitor", Prentice- Hall, Englewood Cliffs, New Jersey, 1981.
- [5] A. S. Sedra and P. O. Brackett, "Filter Theory and Design: Active and Passive", Pitman, London, 1979.
- [6] R. Gregorian and G. C. Temes, "Analog MOS Integrated Circuits for

Signal Processing", Wiley, 1986.

[7] E. Sanchez-Sinencio, "Switched-capacitor circuits", Van-Nostrand Reinhold, 1985.

[8] G. S. Moschytz, ed., "MOS switched-capacitor filters : analysis and design", IEEE Press, New York, 1984.

[9] A. Antoniou, "Digital filters : analysis and design", McGraw-Hill, 1979.

[10] L. R. Rabiner, B. Gold, "Theory and application of digital signal processing", Prentice-Hall, Englewood Cliffs, NJ, 1975.

[11] R. Schaumann, "Design of continuous-time fully integrated filters : a review", Proc. IEE, Part G, Vol. 136, No. 4, pp. 184-190, Aug. 1989.

[12] G. V. Eaton, D. G. Nairn, W. M. Snelgrove and A. S. Sedra, "SICOMP : A silicon compiler for switched-capacitor filters", Proc. ISCAS, pp.321-324, Philadelphia 1987.

[13] E. Sanchez-Sinencio and J. Ramirez-Angulo, "AROMA : An area optimised CAD program for cascade SC filter design", IEEE Trans. CAD, Vol. CAD-4, No. 3, pp.296-303, July 1985.

[14] Y. Therasse, L. Reynders, R. Lannoo and B. Dupont, "A switched-capacitor filter compiler", VLSI Systems Design, pp. 85-88, Sept. 1987.

[15] J. Assael, P. Senn and M. S. Tawfik, "A switched-capacitor filter compiler", IEEE Journal of Solid-State Circuits, Vol. SC-23, pp. 166-174, Feb. 1988.

[16] R. Gregorian, K. W. Martin and G. C. Temes, "Switched-capacitor circuit design", Proc. IEEE, Vol. 71, No. 8, pp. 941-966, Aug. 1983.

[17] J. DeFranca, "Switched Capacitor Systems for Narrow Bandpass Filtering", PhD Thesis, University of London, 1985.

[18] P. R. Gray and R. Castello, "Performance limitations in switched-capacitor filters", Proc. IEEE ISCAS, pp. 247-250, Kyoto, Japan, 1985.

[19] D. J. Allstot and W. C. Black, "Technological design considerations for monolithic MOS switched-capacitor filtering systems", Proc. IEEE, Vol. 71, pp.967-986, Aug. 1983.

[20] K. Martin and A. S. Sedra, "Effects of op-amp finite gain and bandwidth on the performance of switched-capacitor filters", IEEE Trans. Circuits and Systems, Vol. CAS-28, pp.822-829, Aug. 1981.

[21] T. Choi and R. W. Broderson, "Considerations for high-frequency switched-capacitor ladder filters", IEEE Trans. Circ. and Syst., Vol. CAS-27, pp. 545-552., June 1980.

[22] A. Fettweis, "Basic principles of switched capacitor filters using voltage inverter switches", Arch. Elektronik Ubertragung, vol. 33, no.1, pp. 13-19, 1979.

- [23] A. M. Davis and H. P. Nuygen, "Exact SC synthesis of bilinearly transformed all-pole analog filters using cascaded GCT sections", Proc. IEEE ISCAS, pp. 746-749, 1987.
- [24] B. J. Hosticka, G. S. Moschytz, "Switched-capacitor simulation of grounded inductors and gyrators", Electron. Lett., Vol. 14, pp. 788-790, 1978.
- [25] A. Limperis, I. Haritantis, "Wave SC filters based on two-port equivalents", Proc. IEEE ISCAS, pp. 1017-1020, Helsinki, Finland, 1988.
- [26] G. Fischer, "A switched-capacitor building block for analog FIR filters", Proc. ISCAS, Proc. IEEE ISCAS, pp. 1445-1448, Portland, Oregon, 1989.
- [27] R. Gregorian, "Switched capacitor filter design using cascaded sections", IEEE Trans. Circs and Syst., vol. CAS-27, pp. 515-521, June 1980.
- [28] A. Kaelin and G. S. Moschytz, "Exact design of arbitrary parasitic-insensitive elliptic SC-ladder filters in the  $z$ -domain", Proc. IEEE ISCAS, pp. 2485-2488, Helsinki, Finland, 1988.
- [29] S. O. Scanlan, "Analysis and synthesis of switched-capacitor state variable ladder filters", IEEE Trans. Circ. and Syst., vol. CAS-28, pp. 85-93, Feb. 1981.
- [30] J. Taylor, "Exact design of elliptic switched-capacitor filters by synthesis", Electronics Letters, Vol. 18, No. 19, pp. 807-809, Sept. 1982.
- [31] H. M. Yassine, "Exact discrete time synthesis", Proc. IEE, Vol. 133, Pt. G, No. 4, pp. 209-215, Aug. 1986.
- [32] M. S. Lee and C. Chang, "Switched-capacitor filters using the LDI and bilinear transformations", IEEE Trans. Circuits and Systems, Vol. CAS-30, No. 12, pp. 873-887.
- [33] Li Ping and J. I. Sewell, "The LUD approach to switched-capacitor filter design", IEEE Trans. Circuits Syst., vol. CAS-34, Dec. 1987.
- [34] E. Hokenek and G. S. Moschytz, "Design of parasitic-insensitive bilinear-transformed admittance-scaled (BITAS) switched capacitor ladder filters", IEEE Trans. on Circuits and Systems, Vol. CAS-28, pp811-821, Aug. 1981
- [35] M. S. Lee, G. Temes, C. Chang and M. Ghaderi, "Bilinear switched capacitor ladder filters", IEEE Trans. on Circuits and Systems, Vol. CAS-28, pp811-821, Aug. 1981
- [36] K. Martin and A. S. Sedra, "Exact design of switched-capacitor bandpass filters using coupled biquad structures", IEEE Trans. Circuits and Systems, vol. CAS-27, pp.469-474, June 1980.
- [37] Y. Tsividis and P. Antognetti, eds, "Design of MOS VLSI circuits for telecommunications", Prentice-Hall, Englewood Cliffs, NJ, 1985.
- [38] N. O. Sokal, "Unsolved theoretical problem in design of optimal

low-pass filter for harmonic suppression in radio-transmitter output", IEEE Trans. on Circuits and Systems, Vol. CAS-27, No. 3, p235, March 1980.

[39] K. Nagaraj, "A parasitic-insensitive area-efficient approach to realizing very large time constants in switched-capacitor circuits", IEEE Trans. Circuits and Systems, Vol. CAS-36, No. 9, pp. 1210-1216, Sept. 1989.

[40] G. C. Temes, L. E. Larson and K. W. Martin, "State-of-the-art and future prospects for analogue signal processing - a tutorial", Proc. ISCAS, pp. 1655-1660, Helsinki, Finland, 1988.

[41] F. Callais, F. H. Salchli and D. Girard, "A set of four IC's in CMOS technology for a programmable hearing aid", IEEE J. Solid-State Circs, Vol. SC-24, No. 2, pp.301-312, April 1989.

[42] D. G. Haigh, C. Toumazou, S. J. Harrold, J. I. Sewell and K. Steptoe, "Design and optimisation of a GaAs switched-capacitor filter", Proc. IEEE ISCAS, pp. 1449-1454, Portland, Oregon, 1989.

[43] G. Szentirmai, "Computer-aided filter design", IEEE Press, New York, 1973.

[44] R. W. Daniels, "Approximation methods for electronic filter design", McGraw-Hill, New York, 1974.

[45] R. Gregorian and G. C. Temes, "Design techniques for digital and analog all-pass circuits", IEEE Trans. Circuits and Systems, Vol. CAS-25, No. 12, pp. 981-988, Dec. 1978.

[46] J. A. C. Bingham, "A new method of solving the accuracy problem in filter design", IEEE Trans. on Circuit Theory, Vol. CT-11, pp. 327-341, Sept. 1964.

[47] G. Szentirmai, "FILSYN - A general purpose filter synthesis program", Proc. IEEE, Vol. 65, No. 10, pp.1443-1458, Oct. 1977.

[48] W. M. Snelgrove and A. S. Sedra, "FILTOR2 : A computer filter design Package", Matrix Publishers, Ill. 19.

[49] G. Szentirmai, S/FILSYN user manual, DGS Associates, Santa Clara, CA.

[50] D. G. Nairn and A. S. Sedra, "Auto-SC, automated switched-capacitor ladder filter design program", IEEE Circuits and Devices Magazine, pp. 5-9, March 1988.

[51] R.K.Henderson, Li Ping and J.I.Sewell, "A design program for digital and analogue filters : PANDDA", Proc. ECCTD '89, pp. 289-293, Brighton, U.K., Sept. 1989.

[52] R.K.Henderson, Li Ping and J.I.Sewell, "PANDDA : A program for advanced network design : digital and analogue", Digest of Saraga Colloquium on Electronic Filters, pp. 4/1-4/8, London, 1988.

[53] R. P. Sigg, A. Kaelin, A. Murault, W. C. Black Jr and G. S. Moschytz, "A switched-capacitor filter compiler : fully automated filter synthesizer and mask generator for a CMOS gate-array-type filter chip", Proc. IEEE ICCAD, Nov. 1987.

[54] K. Theqvist, H. Alarolu, P. Ylisirnio and H. Kaskela, "Adaptive simulated annealing used in the synthesis of switched-capacitor Filters", Proc. IEEE ISCAS, pp. 1729-1733, Helsinki, 1988.

[55] W. J. Helms and K. C. Russell, "A switched capacitor filter compiler", IEEE 1986 Custom Integrated Circuits Conference, pp. 125-128.

[56] F. Montecchi, "Bilinear design of high-pass switched-capacitor ladder filters", IEEE ISCAS, pp. 547-550, Kyoto, Japan 1985.

[57] Li Ping and J. I. Sewell, "The TWINTOR in bandstop switched-capacitor ladder filter realisation", IEEE Trans. Circuits and Systems, Vol. CAS-36, No.7, pp.1041-1044, July 1989.

[58] E. Preiss, "FILCAD : Werkzeug fur den Entwurf Kundenspezifischer Filter", Elektronik Industrie, pp. 76-87, Oct. 1987.

## CHAPTER 2

### FILTER AMPLITUDE APPROXIMATION

#### 2.1 INTRODUCTION

#### 2.2 CLASSICAL FILTER AMPLITUDE APPROXIMATION

##### 2.2.1 Definitions

##### 2.2.2 Classical approximation methods

##### 2.2.3 Limitations of classical approximations

#### 2.3 GENERAL AMPLITUDE APPROXIMATION

##### 2.3.1 Curve fitting problem

##### 2.3.2 Interpolation

##### 2.3.3 Bilateral method

##### 2.3.4 Newton's method

##### 2.3.5 Generalised Remez methods

##### 2.3.6 Unilateral method

#### 2.4. COMPUTER IMPLEMENTATION

##### 2.4.1 Computer algorithm

##### 2.4.2 Software considerations

#### 2.5 RATIONAL APPROXIMATION

##### 2.5.1 Approximation of minimum-phase rational functions

##### 2.5.2 Multi-band cases

##### 2.5.3 Computed examples

#### 2.6 SUMMARY

#### REFERENCES



## 2.1 INTRODUCTION

In Chapter 2, computational methods for the design of filter amplitude functions will be examined. Classical functions which approximate ideal filter specifications are reviewed. These functions have special properties of symmetry and constant equiripple attenuation in passband or stopband. Their coefficients can be calculated conveniently by explicit formulae or simple iterations [1–7]. However, classical approximations are not suitable for highly asymmetric specifications or amplitude equalisation tasks commonly encountered in modern communications systems [8]. Approximation methods for such specifications are not well developed. They are usually highly specific to a given filtering task and are not flexible enough for a general, easy-to-use software package [9–17]. Although, general multiple-criterion optimisation techniques can certainly be applied, they tend to involve a large amount of computation and do not always guarantee convergence [18–21]. Frequently, this is because they do not make enough use of the special properties of filter functions, which are special cases of rational polynomials with well-confined root locations. Moreover, the approximation problem is often not expressed conveniently for a filter designer without detailed knowledge of optimisation theory [22].

In the remainder of the Chapter, methods for the approximation of polynomial filter functions within arbitrarily weighted amplitude specifications are considered. Several new algorithms are proposed bearing some interesting relationships to the Remez minimax approximation technique [23–25]. The concept of maximal flatness is generalised to allow compromises between equiripple and flat band properties. The computational aspects of the algorithms are discussed. Accuracy is particularly critical in the approximation of filter functions in finite wordlength computer arithmetic. Methods to preserve accuracy without recourse to the complications of transformed variables are given [1–2,26].

The design of minimum-phase rational functions with arbitrary passband and stopband tolerance schemes is investigated. These functions are of particular importance because they can be efficiently realised as the transfer functions of linear analogue networks, including SCFs. Numerator and denominator polynomials have special properties which are best designed by a combination of two different methods. The four main classes of filter can be handled and computed examples meeting arbitrary passband and stopband specifications are given.

## 2.2. CLASSICAL FILTER APPROXIMATION

### 2.2.1 Definitions

The magnitude response of an ideal filter is defined by the "brick wall" template in Fig. 2.1. It is not feasible to obtain a transmission function which exactly matches these characteristics and so certain tolerances must be introduced (Fig. 2.2). The function is allowed some small deviation from full transmission in the passband and from zero transmission in the stopband, and a transition region is provided to allow the function to move between levels. This introduces a series of design parameters which control how closely the filter function approximates the ideal specifications.

$f_{plo}, f_{phi}$  : lower and upper passband edge frequencies (Hz)

$f_{slo}, f_{shi}$  : lower and upper stopband edge frequencies (Hz)

$A_s$  : Minimum stopband attenuation (dB)

$A_p$  : Maximum passband attenuation (dB)

In general, as these parameters are made more severe, e.g. very small transition region, or very large stopband attenuation, an increasingly high order (N) of approximating function will be required.

A transmission function is designed by working with a magnitude squared function. It has the following property;

$$T(s)T(-s) \Big|_{s=j\omega} = T(x) \Big|_{x=-\omega^2} \quad (2.1)$$

The phase information has been removed and the function has been linearised in terms of a single real variable, avoiding the use of complex arithmetic. Besides the transfer function  $T(x)$  another function called the *characteristic function*  $K(x)$  is useful in classical approximation.

$$K(s)K(-s) = 1/(T(s)T(-s)) - 1 \quad (2.2)$$

Since the transmission function must vary between 0 and 1, the characteristic function will vary between 0 and  $\infty$ . It is normally a simpler computational task to design such a function [1].

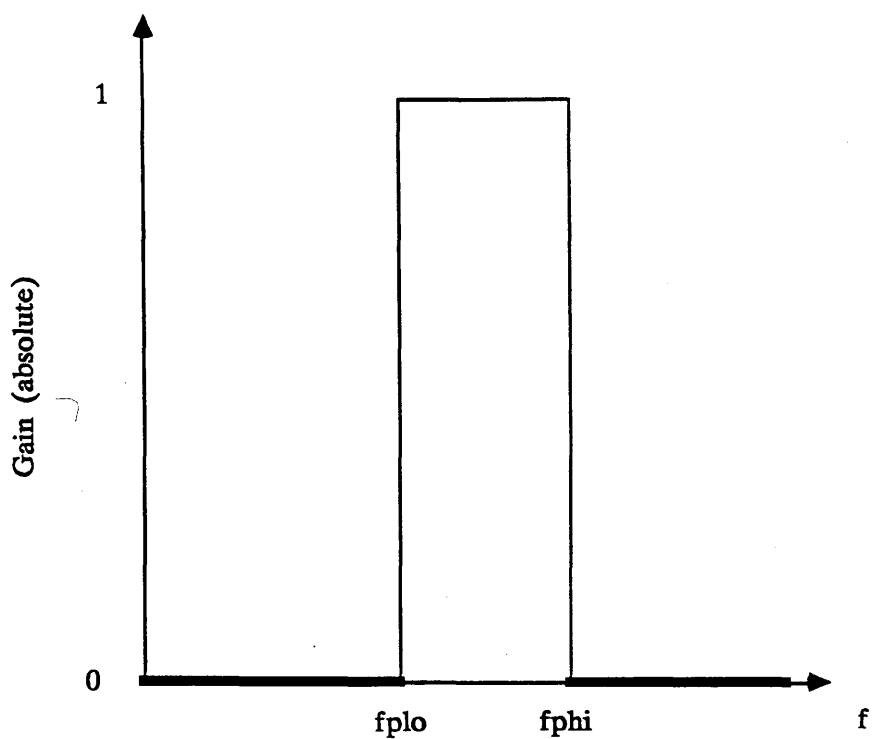


Fig. 2.1 Ideal filter amplitude specifications

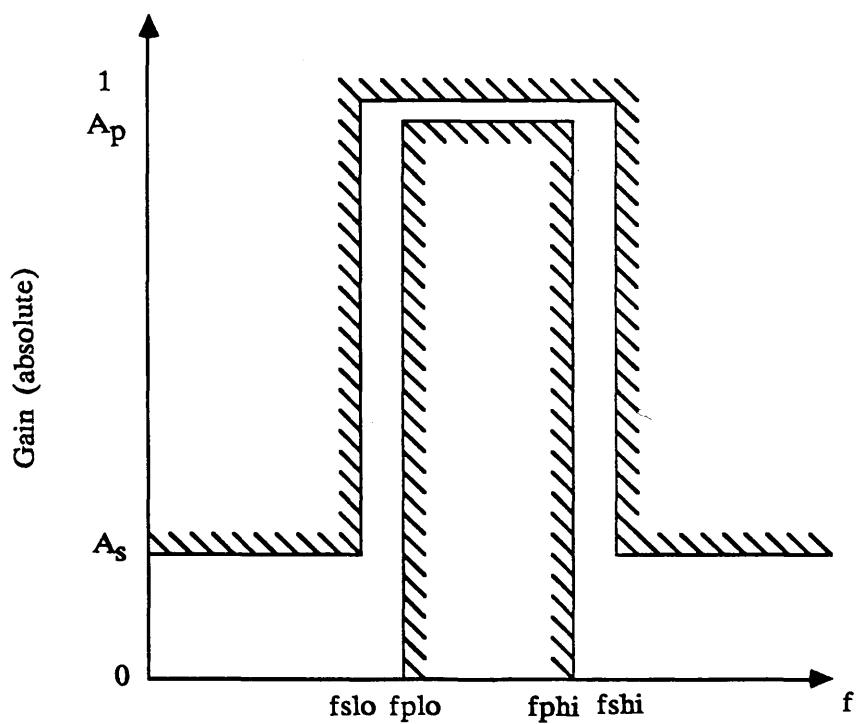


Fig. 2.2 Filter amplitude template with tolerances

### 2.2.2 Classical Approximation Methods

Classical functions are approximations to ideal filter specifications. They have the following general form

$$T(s)T(-s) = \frac{1}{1 + K(s)K(-s)} \quad (2.3)$$

The zero and pole frequencies of  $K(s)$  correspond exactly to the positions of the maxima in the passband and minima in the stopband of the transmission function. The positioning of the poles and zeros frequencies of  $K(s)$  is done to control the maximum deviation of the transmission function in passband and stopband. In each band the transmission function will usually have one of two forms; maximally flat and equiripple. The permutation of these properties in passband and stopband yields the four best-known classical functions; elliptic, Chebyshev, inverse Chebyshev, Butterworth (Fig. 2.4).

Table 2.1 gives a set of formulae for the pole and zero frequencies of these approximations. Conventionally, a lowpass prototype function is designed with normalised passband edge  $1\text{rads}^{-1}$  and stopband edge  $\omega_{\text{slo}} = 2\pi f_{\text{phi}}/f_{\text{plo}}$ . In general, it is not possible to satisfy all the above parameters simultaneously and only a subset can be defined. For example, in a Chebyshev function if  $N$ ,  $f_{\text{plo}}$ ,  $f_{\text{phi}}$  and  $A_p$  are specified then  $f_{\text{slo}}$ ,  $f_{\text{shi}}$  and  $A_s$  are determined uniquely. Table 2.1 adopts the convention that the order, passband ripple and stopband edges will be met where possible. Note that the poles and zeros of  $K(s)$  lying on the imaginary axis are calculated here, the complex natural modes of  $T(s)$  can be obtained by equally direct formulae or root extraction applied to (2.3).

It can be seen from Table 2.1 that only simple formulae or iterations are required to compute the classical functions. Thus the computational expense is minimal and the software relatively straightforward.

The four main classes of filter; lowpass, bandpass, bandstop or highpass (Fig. 2.3); can all be obtained by the application of frequency transformations to the lowpass prototype (Table 2.2). Filters obtained by lowpass-bandpass and lowpass-bandstop transformations exhibit geometrical symmetry about  $1\text{rads}^{-1}$ . Multi-band filters can also be obtained by frequency transformations [2].

$\text{Characteristic function } K(s)K(-s) = \frac{\prod_{i=0}^{N/2-1} (s^2 + \omega_{zi}^2)}{\prod_{j=0}^{N/2-1} (s^2 + \omega_{pj}^2)}$ $C = \frac{\prod_{j=0}^{N/2-1} (1 + \omega_{pj}^2)}{\prod_{i=0}^{N/2-1} (1 + \omega_{zi}^2)}$ $\text{Calculate } \epsilon = \sqrt{(10^{(A_p/10)} - 1)} \quad \gamma = \sqrt{(10^{(A_s/10)} - 1)} \quad g = \epsilon/\gamma \quad \omega_s = \omega_{slo}$			
Approximation type	Numerator zeros	Denominator poles	Necessary order N
BUTTERWORTH	$\omega_{zi} = 0$	$\omega_{pj} = \infty$	$N = \frac{\log_{10}(g)}{\log_{10}(\omega_s)}$
CHEBYSHEV	$\omega_{zi} = \cos\left(\frac{(2i+1)\pi}{2N}\right)$	$\omega_{pj} = \infty$	$N = \frac{\log_{10}(g + \sqrt{(g^2 - 1)})}{\log_{10}(\omega_s + \sqrt{(\omega_s^2 - 1)})}$
INVERSE CHEBYSHEV	$\omega_{zi} = 0$	$\omega_{pj} = \omega_s / \cos\left(\frac{(2j+1)\pi}{2N}\right)$	$N = \frac{\log_{10}(g + \sqrt{(g^2 - 1)})}{\log_{10}(\omega_s + \sqrt{(\omega_s^2 - 1)})}$
ELLIPTIC	$\omega_{zi} = \omega_{ci}$	$\omega_{s0} = \omega_s$ $k = 0$ repeat $k = k + 1$ $\omega_{sk} = \omega_{sk-1}^2 / (\omega_{sk-1}^4 - 1)$ until $\omega_{sk} > 99$ $\omega_{s0} = 1$ $\omega_{cj} = \omega_{sj} / \cos\left(\frac{(2j+1)\pi}{2N}\right)$ for $i = k$ downto 0 $\omega_{ci} = (\omega_{ci+1} / \omega_{ci}) / 2\omega_{si}$ $\omega_{pj} = \omega_s / \omega_{cj}$	$J = \log_{10}(g)$ repeat $\omega_s = \omega_s^2 + \sqrt{(\omega_s^4 - 1)}$ $J = \log_{10}(2) + 2J$ until $\omega_s > 99$ $N = \frac{\log_{10}(2) + J}{\log_{10}(2\omega_s)}$

Table 2.1 Formulae for pole and zero frequencies of classical filter approximations

Type	Lowpass prototype stopband edge	Transformation	Notes
LOWPASS	$\omega_s = f_{slo}/f_{phi}$	$s = p/\omega_{phi}$	$\omega_{plo} = 2\pi f_{plo}$ $\omega_{phi} = 2\pi f_{phi}$ $\omega_{slo} = 2\pi f_{slo}$ $\omega_{shi} = 2\pi f_{shi}$ $\omega_0^2 = \omega_{plo}\omega_{phi}$ $\omega_0^2 = \omega_{slo}\omega_{shi}$ $B = \omega_{phi} - \omega_{plo}$
HIGHPASS	$\omega_s = f_{plo}/f_{shi}$	$s = \omega_{plo}/p$	
BANDPASS	$\omega_s = \frac{f_{shi} - f_{slo}}{f_{phi} - f_{plo}}$	$s = \frac{p^2 + \omega_0^2}{pB}$	
BANDSTOP	$\omega_s = \frac{f_{phi} - f_{plo}}{f_{shi} - f_{slo}}$	$s = \frac{pB}{p^2 + \omega_0^2}$	

Note: in the above table, s is used for the lowpass prototype domain, while p is used for the actual filter domain (denormalised).

Table 2.2 Symmetrical frequency transformations

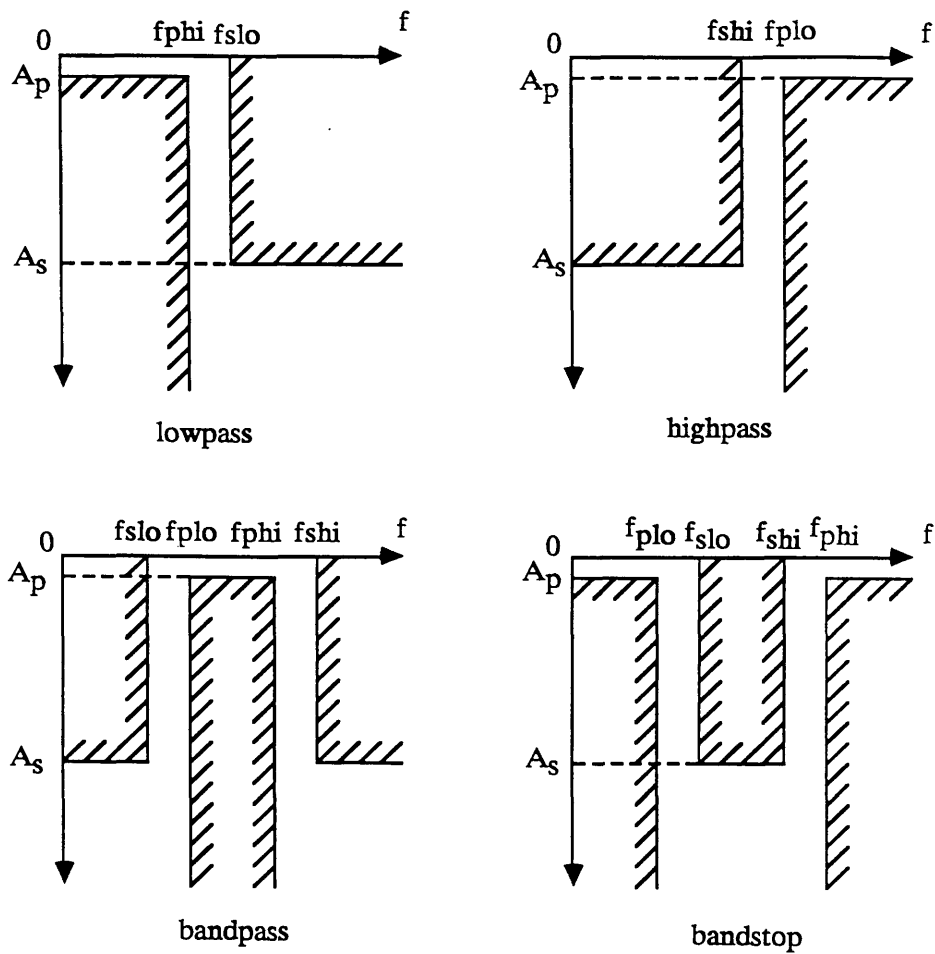
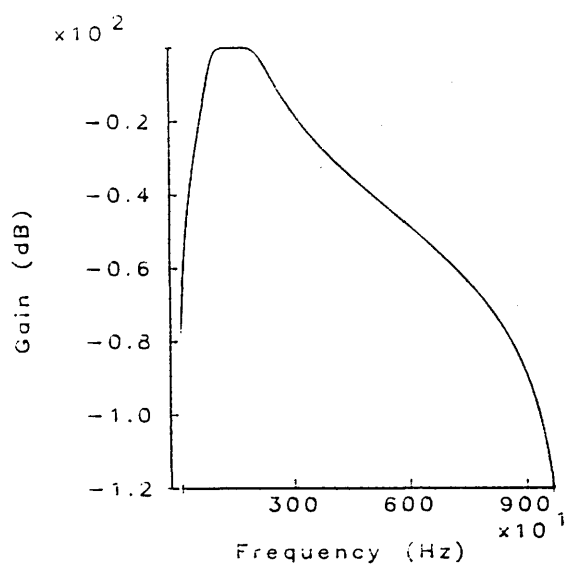
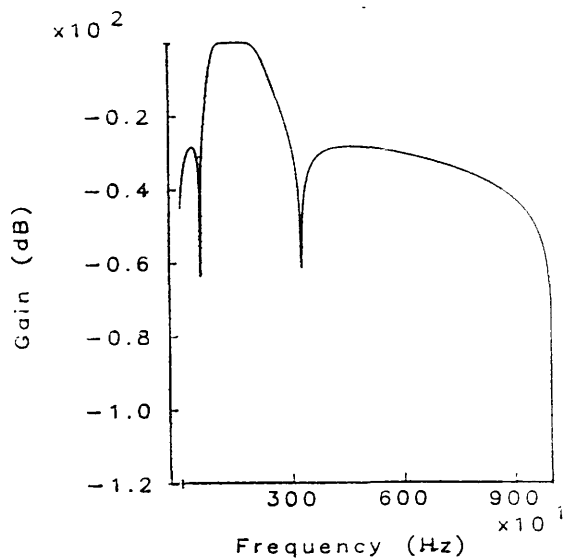


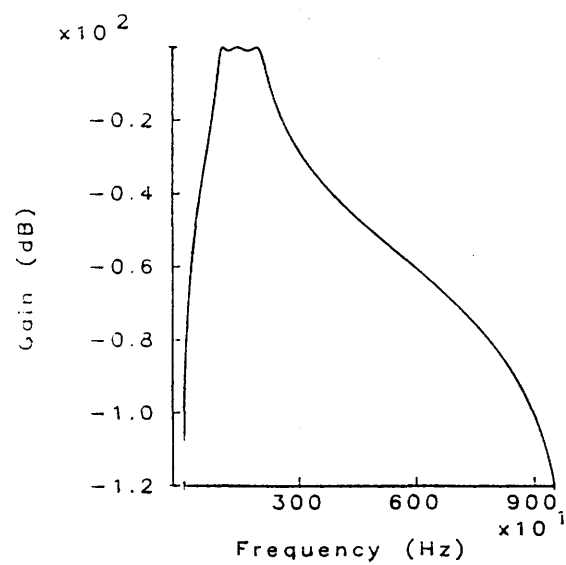
Fig. 2.3 Templates for various filter classes



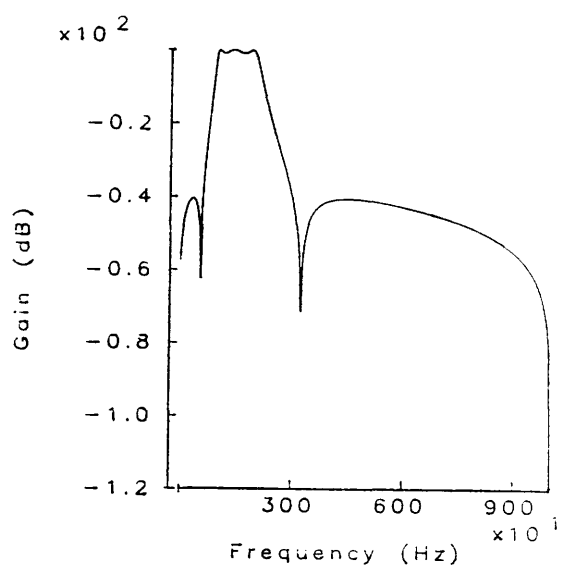
**Butterworth**



**Inverse Chebyshev**



**Chebyshev**



**Elliptic**

**Fig. 2.4 Classical filter approximations**

### 2.2.3 Limitations of classical functions

Classical approximation functions are optimal with respect to various properties such as roll-off, stopband attenuation or degree of flatness. However each devotes all its approximation power to making only one property optimal, neglecting the others. In this way, for example an elliptic function will have optimal roll-off into the stopband but will have very poor group delay characteristics. A Butterworth filter has optimal passband flatness but poor roll-off and stopband attenuation. There is a lack of freedom to trade-off between these characteristics, to say have sub-optimal degree of flatness in the passband in order to improve the roll-off into the stopband.

The symmetrical frequency transforms introduce additional inconvenience and lack of design freedom. An inherently asymmetric specification, such as a bandpass filter with unequal attenuation in lower and upper stopband, can be met by a symmetrically transformed filter. However the filter will have equal numbers of zeros in either band and equal attenuation, rather than concentrating the zeros where they are most necessary, in the high attenuation band. Similar inefficiencies result from the geometrical symmetry of the stopband edges. A sharp roll-off required in the lower band must be accompanied by an equally sharp roll-off in the upper band, regardless of the relative transition bandwidths.

Classical functions have flat or equiripple characteristics over the passband and stopband. Although this is satisfactory for ideal filter systems, often some external influences create a need for amplitude equalisation and non-flat attenuation. Examples are prevalent in digital and switched-capacitor filter systems which, by their sampled-data nature, introduce various systematic frequency response distortions such as LDI termination error and  $\text{sinc}(x)$  effects. In general, some degree of amplitude equalisation must be combined with filtering operations without increasing the order of the system. The classical approximations are therefore quite unsuitable and some generalised approximations are required.

## 2.3 GENERAL FILTER AMPLITUDE APPROXIMATION

Approximation methods for functions with more arbitrary behaviour including amplitude weightings and degree of flatness are now presented. The theoretical development is given initially for single polynomials. It will later be shown how the methods can be extended to rational functions.



### 2.3.1 Curve Fitting Problem

Consider the problem of fitting a polynomial  $p(x) = a_n x^n + \dots + a_0$  in a *minimax* sense to some prescribed function  $m(x)$  on the interval  $[a, b]$  such that the maximum error  $\max |p(x) - m(x)|$  is minimised. A variant of this problem is of interest for filter designers, Fig. 2.5. Two curves,  $u(x) = m(x) + \delta$  and  $l(x) = m(x) - \delta$ , can be seen as boundary functions and  $p(x)$  is sought to fit between them. At a series of points, the so-called *touch points*,  $p(x)$  will touch  $u(x)$  and  $l(x)$  alternately, which implies that  $p(x)$  will have the same zero and first order derivative values of  $u(x)$  or  $l(x)$ . In a general sense  $u(x)$  and  $l(x)$  can be any functions satisfying  $u(x) > l(x)$  on  $[a, b]$  and the order of tangency at the touch points can be greater than one. At  $M$  points (the touch points) on the upper and the lower function,  $\{x_{ti} | a < x_{ti} < x_{ti+1} < b\}$

$$p^{(r)}(x_{ti}) = u^{(r)}(x_{ti}) \text{ or } l^{(r)}(x_{ti}) \quad r=0, 1, 2, \dots, \mu_i \quad (2.4)$$

where  $i=1, 2, 3, \dots, M$ . The exact locations of  $\{x_{ti}\}$  are unknown but the sequence  $\{\mu_i\}$  is specified (Fig. 2.6). For convenience we fix the two end points by

$$\begin{aligned} p(a) &= A & p(b) &= B & l(a) &\leq A \leq u(a) & (2.5) \\ & & & & l(b) &\leq B \leq u(b) \end{aligned}$$

then altogether there are  $N_C$  specifications on the values and the derivatives of  $p(x)$ , where

$$N_C = 2 + \sum_{i=1}^M (\mu_i + 1) \quad (2.6)$$

The aim of the curve fitting problem is to find the lowest order approximating polynomial which fits the specification (2.4) and (2.5).

### 2.3.2. Interpolation

The unknown positions of  $\{x_{ti}\}$  provide  $M$  degrees of freedom, which can be used to reduce the order of the polynomial from the nominal problem order  $N_C$ . Thus  $N_C - M$  of the specifications can be chosen as constraints to form a polynomial of order  $N$ , where

$$N + 1 = N_C - M \quad (2.7)$$

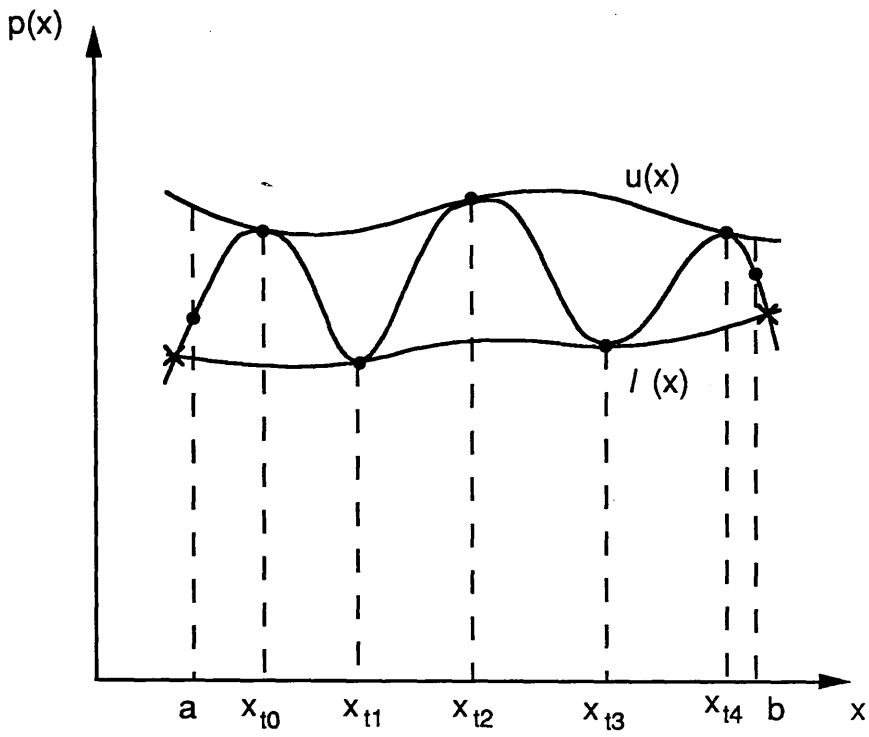


Fig. 2.5 Solution of minimum curve fitting problem by polynomial  $p(x)$

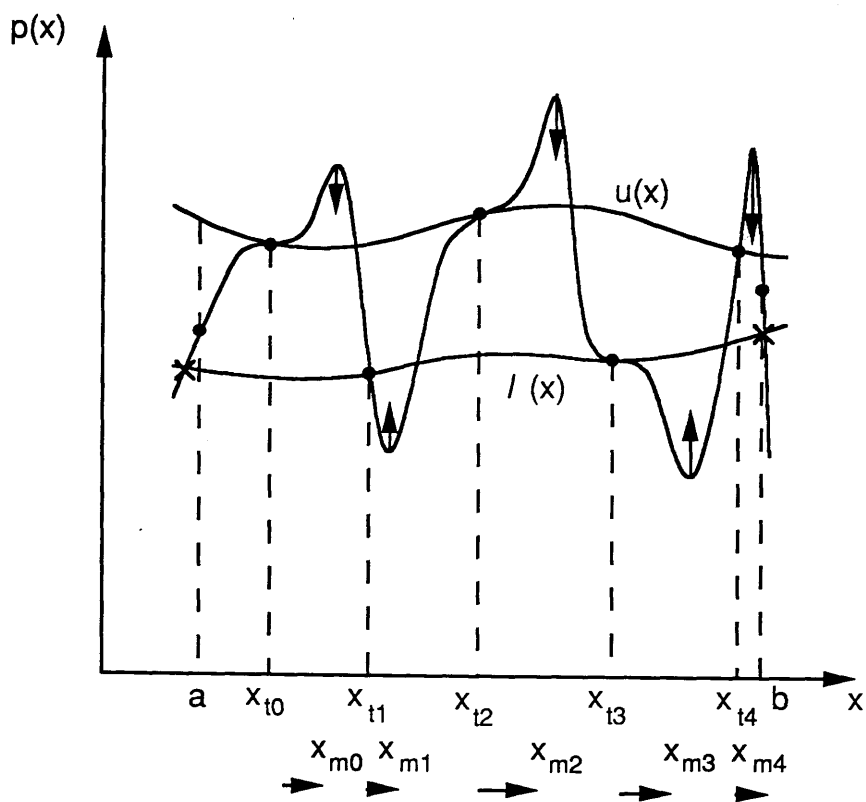


Fig. 2.6 Bilateral approximation

The remaining  $M$  specifications must be met by adjusting the  $M$  positions of the touch points.

The relation between the behaviour and the order of a polynomial is a complicated issue. To decide the minimum order is a difficult problem and some theoretical discussion can be found in [27], however in most cases the order determined by (2.7) is satisfactory. A  $N^{\text{th}}$  order polynomial can always be interpolated by  $N+1$  constraints. *Osculatory Newton interpolation* [28] can be used to interpolate a number of derivatives with certain computational advantages over other interpolation methods [29].

### 2.3.3 Bilateral Method

Assume that for the specifications,

i) all  $\mu_i$  are odd,

ii) the touch points are assigned alternately to  $u(x)$  and  $l(x)$ , i.e.  $\{x_{ti} | i=1,3,\dots,M_u\}$  and  $\{x_{ti} | i=2,4,\dots,M_l\}$  are the set of touch points on  $u(x)$  and  $l(x)$  respectively (where  $M_u=M$  and  $M_l=M-1$  if  $M$  is odd and  $M_u=M-1$  and  $M_l=M$  if  $M$  is even).

These assumptions are true for a Chebyshev function where all  $\mu_i=1$  (osculatory points) and are valid for most filter functions. The Weierstrass polynomial approximation theorem guarantees that if the filter order is high enough then a solution lying between the two boundary functions will exist [27].

Interpolate  $p(x)$  such that,

$$\begin{aligned} p^{(r)}(x_{ti}) &= u^{(r)}(x_{ti}) & r &= 0, 1, \dots, \mu_i - 1 \\ & & i &= 1, 3, 5, \dots, M_u \end{aligned} \quad (2.8a)$$

$$\begin{aligned} p^{(r)}(x_{ti}) &= l^{(r)}(x_{ti}) & r &= 0, 1, \dots, \mu_i - 1 \\ & & i &= 2, 4, 6, \dots, M_l \end{aligned} \quad (2.8b)$$

$$\text{and} \quad p(a) = A \quad p(b) = B \quad (2.8c)$$

Thus exactly  $N_c - M$  specifications are met by interpolation. It now remains to adjust  $\{x_{ti}\}$  to make  $\{p^{(\mu_i)}(x_{ti})\}$  satisfy the other  $M$  specifications.

*Definitions:*

$$\begin{aligned}
 \text{upper error function} & \quad e_u(x) = p(x) - u(x) \\
 \text{lower error function} & \quad e_l(x) = l(x) - p(x) \\
 \text{mid function} & \quad m(x) = (l(x) + u(x))/2 \\
 \text{search function} & \quad s(x) = \max [ e_u(x), e_l(x) ]
 \end{aligned}$$

$$\text{combined error function} \quad e(x) = \begin{cases} -e_u(x) & \text{if } p(x) > m(x) \\ e_l(x) & \text{if } p(x) \leq m(x) \end{cases}$$

From assumption i)  $\{\mu_i - 1\}$  are restricted to be even, so in general the touch points are now points of inflection (Fig.2.3) and  $s(x)$  will change sign in the neighbourhood of each touch point  $\{x_{ti}\}$ . If the polynomial is manipulated such that  $p(x)$  does not cross  $u(x)$  or  $l(x)$  at these points, then  $p(x)$  must possess an extra order of tangency to  $u(x)$  or  $l(x)$ , having then up to the  $\mu_i$ th order tangency at  $\{x_{ti}\}$  required for  $p(x)$  to be a solution. At this stage,  $\max[s(x)] = 0$  in the neighbourhood of  $\{x_{ti}\}$ . Notice that from assumption ii) there must be at least one minima of  $e(x)$ , denoted as  $x_{mi}$ , on  $[x_{ti-1}, x_{ti+1}]$ . Therefore if

$$x_{mi} = x_{ti} \quad i=1, 2, 3, \dots, M \quad (2.9)$$

is achieved then  $p(x)$  is a solution. Some approximation scheme can be adopted to generate an adjustment  $\{\Delta x_{ti}\}$

$$\{x_{ti}\} \leftarrow \{x_{ti} + \Delta x_{ti}\} \quad i=1, 2, 3, \dots, M \quad (2.10)$$

to reduce  $\{e(x_{mi})\}$ .

#### 2.3.4. Newton's Method

Obviously  $\{\Delta x_{ti}\}$  can be generated by a technique based on Newton's method which is found by solving a Jacobian system [28]

$$\begin{bmatrix} g_1(x_{m1}) & g_2(x_{m1}) & \dots & g_M(x_{m1}) \\ g_1(x_{m2}) & & \dots & \vdots \\ \vdots & & & \vdots \\ g_1(x_{mM}) & g_2(x_{mM}) & \dots & g_M(x_{mM}) \end{bmatrix} \begin{bmatrix} \Delta x_{t1} \\ \Delta x_{t2} \\ \vdots \\ \Delta x_{tM} \end{bmatrix} = \begin{bmatrix} e(x_{m1}) \\ e(x_{m2}) \\ \vdots \\ e(x_{mM}) \end{bmatrix} \quad (2.11)$$

where

$$g_i(x) = \frac{\partial p(x)}{\partial x_{ti}} \quad (2.12)$$

The computational cost of setting up the Jacobian matrix  $J$  and solving the Newton system is usually large ( $O(n^3)$ ). Efficient methods to obtain the derivatives  $g_i(x_{mj})$  and to solve for the touch point increments  $\{\Delta x_{ti}\}$  are now presented.

### Theorem 1

Define a  $N^{th}$  order polynomial  $q(x)$  subject to the following  $N+1$  interpolation conditions

$$q(x_{mi}) = e(x_{mi}) \quad i = 1, 2, \dots, M \quad (2.13a)$$

$$\begin{aligned} q^{(r)}(x_{ti}) &= 0 & r &= 0, 1, \dots, \mu_i - 2 \\ & & i &= 1, 2, \dots, M \end{aligned} \quad (2.13b)$$

and

$$\delta_i(x) = \frac{(x - x_{ti})q(x)}{\mu_i e(x)} \quad i = 1, 2, \dots, M \quad (2.13c)$$

then the Newton system (2.11) can be solved for the touch point increments  $\{\Delta x_{ti}\}$  by

$$\Delta x_{ti} = \lim_{x \rightarrow x_{ti}} \delta_i(x) \quad (2.14)$$

### Proof of Theorem 1

Consider the solution of the Newton system for touch point movements  $\Delta x_{ti}$  by interpolation of  $q(x)$ . Two remarks are necessary for the proof.

#### Remark 1:

Suppose  $u(x)$  or  $l(x)$  (and so  $e(x)$ ) are differentiable up to  $\mu_i^{th}$  order at all the touch points. Then the function  $g_i(x)$  formed by differentiating the interpolated polynomial  $p(x)$  with respect to a touch point  $x_{ti}$  is itself an  $N^{th}$

order polynomial of  $x$ . It can be calculated by interpolation subject to the following constraints

$$\begin{aligned} g_i^{(r)}(x_{tj}) &= 0 & r &= 0, 1, \dots, \mu_j - 1 \\ & & j &= 1, 2, \dots, M \\ & & j &\neq i \end{aligned} \quad (2.15a)$$

$$g_i^{(\mu_i - 1)}(x_{ti}) = e^{(\mu_i)}(x_{ti}) \quad r = 0, 1, \dots, \mu_i - 1 \quad (2.15b)$$

Proof:

Equation (2.15a) is evident since the  $\mu_j$  interpolated derivatives of  $p(x_{tj})$  are fixed with respect to another touch point  $x_{ti}$ ,  $i \neq j$ . The proof of (2.15b) follows. Suppose that one of the touch points on  $u(x)$ ,  $x_{ti}$ , changes to  $x_{ti}' = x_{ti} + h$  and the abscissa from  $u(x_{ti})$  to  $u(x_{ti} + h)$ . Define the new polynomial interpolated from  $\{x_{t1}, x_{t2}, \dots, x_{ti}', \dots, x_{tM}\}$  by  $p_h(x)$ . As the polynomial is interpolated up to  $\mu_i - 1$ th tangency to  $u(x)$  at this touch point,

$$p_h^{(r)}(x_{ti} + h) = u^{(r)}(x_{ti} + h) \quad r = 0, 1, 2, \dots, \mu_i - 1 \quad (2.16)$$

Expand  $p_h(x)$  at  $x_{ti}'$  by a Taylor series and evaluate  $p_h^{(r)}(x)$  at  $x = x_{ti}$  and notice (2.16)

$$\begin{aligned} p_h^{(r)}(x_{ti}) &= \left\{ \sum_{k=0}^{\infty} \frac{p_h^{(k)}(x_{ti} + h)}{k!} (-h)^k \right\}^{(r)} \\ &= u^{(r)}(x_{ti} + h) - p_h^{(r+1)}(x_{ti} + h)h + O(h^2) \end{aligned} \quad (2.17)$$

for  $r = 0, 1, 2, \dots, \mu_i - 1$ .

$$g_i^{(r)}(x_{ti}) = \frac{\partial p^{(r)}(x)}{\partial x_{ti}} \bigg|_{x=x_{ti}} = \lim_{h \rightarrow 0} \frac{p_h^{(r)}(x_{ti}) - p^{(r)}(x_{ti})}{h} \quad (2.18)$$

$$\begin{aligned} &= \lim_{h \rightarrow 0} \frac{[u^{(r)}(x_{ti} + h) - p_h^{(r+1)}(x_{ti} + h)h] - u^{(r)}(x_{ti}) + O(h^2)}{h} \\ & \quad (2.19) \end{aligned}$$

$$= u^{(r+1)}(x_{ti}) - p_h^{(r+1)}(x_{ti}) \quad (2.20)$$

Eq. (2.15b) follows by noting that  $\lim_{h \rightarrow 0} p_h^{(r+1)}(x_{ti} + h) = p^{(r+1)}(x_{ti})$  as  $h \rightarrow 0$  and the definition of  $e(x)$  for  $r=0,1,2,\dots,\mu_i-1$ . In general, the above proof can be applied to all  $\{x_{ti}\}$ , which may be touch points on either  $u(x)$  or  $l(x)$ .

Remark 2:

*The Newton system can be solved for the touch point increments  $\{\Delta x_{ti}\}$  by*

$$\Delta x_{ti} = \frac{q^{(\mu_i-1)}(x_{ti})}{g_i^{(\mu_i-1)}(x_{ti})} = \frac{q^{(\mu_i-1)}(x_{ti})}{e_i^{(\mu_i)}(x_{ti})} \quad i = 1, 2, \dots, M \quad (2.21)$$

Proof:

A single row of the Jacobian system (2.11) is

$$\sum_{i=1}^M g_i(x_{mj}) \Delta x_{ti} = e(x_{mj}) \quad j = 1, 2, \dots, M \quad (2.22)$$

and define

$$q(x) = \sum_{i=1}^M g_i(x) \Delta x_{ti} \quad (2.23)$$

From Theorem 1  $q(x)$  is also a polynomial and meets the constraints (2.13). Substitute  $x = x_{tj}$  into (2.23) and

$$q_j^{(\mu_j-1)}(x_{tj}) = \sum_{i=1}^M g_i^{(\mu_j-1)}(x_{tj}) \Delta x_{ti} = g_j^{(\mu_j)}(x_{tj}) \Delta x_{tj} \quad (2.24)$$

Eq.(2.21) follows.

From (2.13b) and (2.8a)  $x_{ti}$  is a  $\mu_i-2^{\text{th}}$  order zero of  $q(x)$  and  $\mu_i-1^{\text{th}}$  order zero of  $e(x)$ . They can be expanded by a Taylor expansion at  $x_{ti}$  as,



$$q(x) = A_q (x-x_{ti})^{\mu_i-1} + O[(x-x_{ti})^{\mu_i}] \quad (2.25)$$

$$e(x) = A_e (x-x_{ti})^{\mu_i} + O[(x-x_{ti})^{\mu_i+1}] \quad (2.26)$$

From (2.21), (2.25) and (2.26)

$$\Delta x_{ti} = \frac{q^{(\mu_i-1)}(x_{ti})}{e^{(\mu_i)}(x_{ti})} \cong \frac{(\mu_i-1)! A_q}{\mu_i! A_e} = \frac{A_q}{\mu_i A_e} \quad (2.27)$$

From (2.25), (2.26) and (2.27) it is easily seen that (2.14) is true.

As both numerator and denominator of (2.13c) tend to zero at  $x_{ti}$ , each touch point increment  $\Delta x_{ti}$  can only be calculated from the limiting values of the increment polynomial  $q(x)$  and error function  $e(x)$  in the proximity of the touch point,  $x_{ti}+h$ . The distance  $h$  must be chosen suitably according to wordlength and order of touch point. A suggested rule is  $\mu_i \times 10^{-6}/N$  for double precision arithmetic.

Involving only repeated interpolation, the computational cost of the whole procedure is very small. The  $O(n^3)$  step of solving the Newton system has been reduced to an  $O(n^2)$  interpolation. Each evaluation of the interpolated polynomial costs  $O(n)$  multiplications.

### 2.3.5 Generalised Remez Methods

As has been shown,  $\Delta x_{ti}$  can be approximately evaluated by  $\delta_f(x)$  at a point close to  $x_{ti}$ . If this point is selected as  $x=x_{mi}$ , then a very simple adjustment to the touch point positions is revealed, {notice (2.13a)}

$$\Delta x_{ti} = \delta_i(x_{mi}) = \frac{(x_{mi}-x_{ti}) q(x_{mi})}{\mu_i e(x_{mi})} = \frac{x_{mi}-x_{ti}}{\mu_i} \quad (2.28)$$

In the special case of the curve fitting problem with all  $\mu_i=1$ , then (2.28) results in the well-known Remez method which updates the variable vector by

$$\{x_{ti}\} \leftarrow \{x_{mi}\} \quad i=1, 2, \dots, M \quad (2.29)$$

This indicates that the interpolation ordinates are simply exchanged with the locations of the extrema and re-interpolated (Fig. 2.6). It may be expected that ordinates separated by an excessively large ripple will be brought together and those separated by an insufficiently large ripple will be moved apart. When the  $\{x_{ti}\}$  are close to the solution, the  $\{x_{mi}\}$  are also close to  $\{x_{ti}\}$ , and the adjustment given by (2.28) becomes similar to that given by a Newton method. This confirms that the Remez method achieves the good convergency of Newton iteration on approach to the solution. Convergency of this algorithm is guaranteed [30] for sufficiently large  $N$  and it has been widely adopted in FIR and IIR digital filter design [31–37]. For the case of  $\mu_i > 1$ , the simple exchange process of (2.29) is unsuitable. Instead the adjustment given by (2.28) is applicable,

$$\{x_{ti}\} \leftarrow \{x_{ti} + (x_{mi} - x_{ti})/\mu_i\} \quad i=1,2,\dots,M \quad (2.30)$$

This can be seen as a generalisation of the Remez method of (2.29) in which instead of moving the ordinate all the way to the extremum it is moved by a fraction of the distance dependant on the order of the touch point.

### 2.3.6 Unilateral Method

In most filter applications, emphasis is given to one of the bounding functions. For example, in the passband region of a filter,  $u(x)$  is most important as it determines the points of maximum transmission. All the high order touch points (with  $\mu_i > 1$ ) could be assigned to  $u(x)$  for greatest effect. In a unilateral method the  $N_c - M$  specifications can be met by directly interpolating  $p(x)$  to  $\mu_i$ th order tangency at all the touch points on  $u(x)$ . The lower curve  $l(x)$  is used only as a bound for the ripple, so that all touch points on  $l(x)$  should be adjusted to  $\mu_i = 1$ , Fig. 2.7. The difference between  $p(x)$  and  $l(x)$  is used as the objective function. Only half of the touch points are kept as variables compared with the bilateral method.

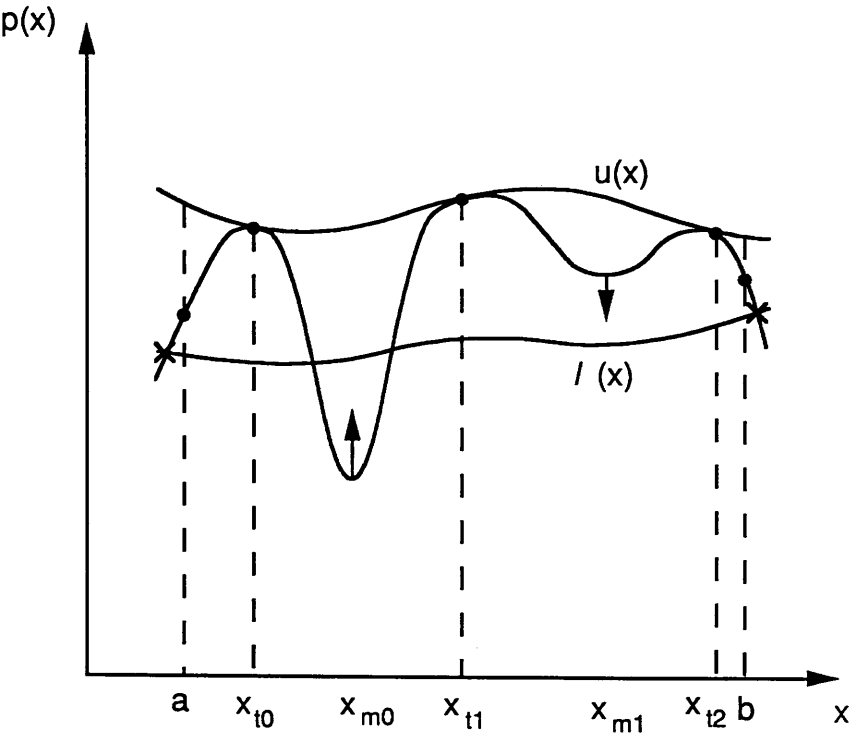


Fig. 2.7 The unilateral method

## 2.4 COMPUTER IMPLEMENTATION

### 2.4.1 Computer algorithm

The approximation methods proposed in the previous section can be implemented on a computer by the following algorithm.

*Step 1 : read the boundary functions  $u(x)$  and  $l(x)$  as piece-wise linear functions on range  $[a,b]$ . Read number of touch points and specified orders  $\mu_i$ .*

*Step 2 : distribute  $\{x_{ti}\}$  uniformly spaced over  $[a,b]$  assigning  $x_{t0}=a$  and  $x_{tn}=b$ .*

*Step 3 : interpolate  $\{x_{ti}\}$  alternately to boundaries  $u(x)$  and  $l(x)$ .*

*Step 4 : set  $x_{m0}=a$*

$$\begin{aligned} i=0,2,4,\dots,n ; \text{ choose } x_{mi} \text{ to maximise} \\ \{p(x)-u(x), x_{mi-1} < x < x_{ti+1}\} \\ i=1,3,5,\dots,n-1 ; \text{ choose } x_{mi} \text{ to maximise} \\ \{l(x) - p(x), x_{mi-1} < x < x_{ti+1}\} \end{aligned}$$

*Step 5 : compute improved touch point estimates by one of the methods in Section 2.3. The extended Remez method indicates that,*

$$x_{ti} = x_{ti} + ((x_{mi} - x_{ti})/\mu_i)$$

*Step 6 : compute convergence estimate for  $k^{\text{th}}$  iteration as*

$$\epsilon_k = \frac{\sum_{i=1}^n e(x_{mi})}{\sum_{i=1}^n |u(x_{mi}) - l(x_{mi})|}$$

*Terminate if  $\epsilon_k < \text{tolerance}$  or  $\epsilon_k > \epsilon_{k+1}$  (divergent)*

## 2.4.2 Software considerations

### a. Interpolation

The interpolation of the polynomial at Step 2 can be done by *osculatory* Newton interpolation. This is an extended form of the well-known Newton interpolation whereby a number of derivatives can be matched to the specified function.

It is particularly important in a filter problem that care is taken with the accuracy of construction and representation of the polynomials within finite wordlength arithmetic. Cancellation errors can be seen to be particularly severe as the touch points of a filter function become closely spaced near a band edge. A typical calculation would be,

$$f[x_{t0}, x_{t1}] = \frac{f(x_{t0}) - f(x_{t1})}{x_{t0} - x_{t1}} \quad (2.31)$$

where cancellation errors occur in numerator and denominator as  $x_{t0}$  approaches  $x_{t1}$ .

The effects of these cancellation errors can be minimised by calculating interpolated values by the *zig-zag path* method [29]. The principle is that a path is taken through the Newton table such that the coefficients with the largest errors are multiplied by ordinates with the smallest differences. By using this accurate interpolation and representation of polynomials high order functions can be obtained (up to length 110 FIR designs). This avoids the complications of transformed variable methods [26].

### b. Searching

At Step 4 a search must be made for the touch point extrema. For reliability, the best method is found to be a single linear search over a uniform grid of points. Normally only 10–20 points are required per touch point for a terminating accuracy better than 1%. The linear search requires a fairly large number of function evaluations for higher order approximation. Faster searching is available by applying cubic, quadratic or golden section search methods requiring only 5 or 6 steps per touch point for very high accuracy ( $10^{-8}\%$ ). However

when the attenuation boundaries are specified in piece-wise linear form and not by a smooth function with continuous derivatives these search methods can be misled and may determine the extrema erroneously. Some combination of the reliability of the linear search with the speed of gradient search methods is discussed by Antoniou [38–40].

#### c. Cluster method

In most cases the boundary functions are only given by values and the derivatives are not available. Although the derivatives can be calculated by numerical differentiation, it is notoriously inaccurate for high orders. The polynomial obtained by a Newton interpolation may become totally unreliable in the neighbourhood of a high order touch points. A better conditioned method is to interpolate the polynomial at a *cluster* of points with first order tangency to the boundary function. A  $\mu_i^{\text{th}}$  order touch point with  $\mu_i$  odd, requires  $(\mu_i+1)/2$  first order touch points distributed in the neighbourhood of  $x_{ti}$ . In practice it is found spacing of  $10^{-6}$  (with normalised passband width of 1) can be chosen. The error caused by this approximate method can be controlled and made much smaller than the allowed ripple (the separation of  $u(x)$  and  $l(x)$ ).

#### d. Damping

*Damping* is the term used for the process whereby the step sizes determined by Newton's method may be reduced to avoid divergence. A form of damping is found useful where Newton's method is used to predict adjustments  $\Delta x_{ti}$  and the touch points would cross one another or move entirely outside the approximating region  $[a,b]$ . In these cases (usually far from solution), it is found useful to limit the movement of the touch points to half the distance in the direction of its closest neighbour. In this way, no touch point may cross or escape the region  $[a,b]$  and yet the direction required to reduce the extrema is observed.

#### e. Convergency, accuracy and storage

Computation costs are  $O(n^2)$  for passband approximation. Stopband approximation requires solution of a matrix system with  $O(n^3)$  efficiency. Convergence is quadratic near solution, a property of algorithms based on Newton's method. Divergence occurs only in those cases where the boundary functions are too severe for the selected order of the function. The accuracy of the algorithm is limited solely by the fineness of the search grid used to

determine the positions of the extrema. Storage is dominated by the matrix system and Newton interpolation tables and is of  $O(n^2)$  size.

## 2.5 RATIONAL APPROXIMATION

### 2.5.1 Approximation method for minimum phase rational functions

Filter approximations based on a single polynomial e.g. FIR or all–pole functions have generally lower selectivity than comparable functions based on a ratio of two polynomials (rational functions). A study of a typical elliptic approximation reveals that zeros from the numerator of the transfer function enable much steeper roll–off into the stopband than for a similar order all–pole Chebyshev approximation. Thus rational functions are much more efficient to satisfy filter problems requiring high amplitude selectivity without severe constraints on group delay. They are also highly suitable for realisation by active integrated circuits since feedback of signals is straightforward, yielding recursive filter structures.

In this section, a design technique for rational filter transfer functions will be considered. The filter amplitude specifications need not be ideal, and can have arbitrary weightings in both passband and stopband. The approximating function can be designed in a minimax fashion with high order touch points assigned to certain positions in each band. Classical functions result as special cases from a general algorithm.

For simplicity, a lowpass filter specification will be considered first. The filter specification is defined as a piece–wise template of attenuation in dB against frequency in Hz. The following parameters must be specified by a designer.

- fplo, fphi : passband edge frequencies (Hz)
- fslo, fshi : stopband edge frequencies (Hz)
- NN, ND : numerator and denominator orders

The transfer function to be designed is

$$T(x) = \frac{N(x)}{D(x)} \qquad x=-\omega^2 \qquad (2.32)$$

The zeros of  $T(x)$  are contained in the numerator polynomial. In a filter transfer function they are most effectively assigned to the imaginary axis of the  $s$ -plane (real  $x$ -plane locations) and placed in the stopband region for maximum attenuation. By making this restriction the rational polynomial becomes a minimum phase function. The denominator polynomial contains the complex pole locations which must be positioned in order to control the passband transmission characteristics.

The following procedure is used to design a rational filter approximation

*Step 1 : read ND, NN,  $f_{plo}$ ,  $f_{phi}$ ,  $f_{slo}$ ,  $f_{shi}$ , touch point orders  $\{\mu_{tsi}\}$ ,  $\{\mu_{tpi}\}$  and piece-wise linear descriptions of  $L(\omega)$  and  $U(\omega)$ .*

*Step 2 : initialise  $\{x_{tpi}\}$  in the passband region  $[x_{plo}, x_{phi}]$  and  $\{x_{tsi}\}$  in the stopband region  $[x_{slo}, x_{shi}]$ , equidistantly spaced. Set  $N(x)=1$ .*

*Step 3 : solve passband approximation problem on  $[x_{plo}, x_{phi}]$  using  $D(x)$  such that*

$$u(x) = N(x)/L(x)$$

$$l(x) = N(x)/U(x)$$

*and compute initial convergence estimate  $\epsilon_p$ .*

*Step 4 : solve stopband approximation problem on  $[x_{slo}, x_{shi}]$  using  $N(x)$  such that*

$$u(x) = \beta U(x)/D(x)$$

$$l(x) = \beta L(x)/D(x)$$

*and compute initial convergence estimate  $\epsilon_s$ .*

*Step 5 : terminate if  $\epsilon_p$  and  $\epsilon_s < \text{tolerance}$  or  $k > \text{maxiter}$*

Due to the special properties of the numerator and denominator polynomials two different approaches are appropriate to solve Steps 3 and 4. Note that a multiplying factor  $\beta$  is introduced in Step 4 so that the stopband attenuation will only be met to a constant dB error. In general it is not possible to meet the stopband and passband specifications exactly and some error margin must be allowed in either passband or stopband or both. In this approach, the passband specifications will be met as closely as possible, and the stopband attenuation



characteristics will have some error above or below the specified attenuation. This expression of the filtering problem is practically useful since good control of the passband characteristics is usually of greater importance than the stopband. Note that if the factor  $\beta$  is greater than 1 then the specifications have been exceeded and it may be possible to reduce the order of the function or the number of zeros. Conversely if  $\beta < 1$  then the order must be increased or more zeros should be introduced.

### Passband Design

Any of the methods of Sections 2.3–4 are suitable for the design of the passband function  $N(x)$ . It is found that the bilateral method has very good global convergence. The unilateral method is then useful to ensure that the function does not exceed maximum transmission ( $T(x) > 1$ ) for passive filter realisation. The touch points are all fixed to the upper boundary.

### Stopband Design

The numerator polynomial is of the following particular form

$$N(x) = Kx^{n_0} \prod_{i=1}^{n_f} (x - x_{tsi})^{\mu_{tsi}} \tag{2.33}$$

This corresponds to a special case of the unilateral method where all touch points are tangent to the lower boundary which is 0. It remains to compute the attenuation margin  $\beta$  (Fig. 2.8). Two methods can be applied; the heuristic method of [36] permits the approximation methods of Sections 2.3–4 to be used. However a variant of the method of Temes and Smith [26] has been found more stable and more easily extended to multi-band approximations. A Jacobian matrix of the peak positions with respect to the touch points must be set up and solved.

$$\left[ \begin{array}{ccc|c} \frac{\partial T(x_{ms0})}{\partial x_{ts0}} & \dots & \frac{\partial T(x_{ms0})}{\partial x_{tsn}} & -U(x_{ms0}) \\ \vdots & & \vdots & \vdots \\ \frac{\partial T(x_{msn})}{\partial x_{ts0}} & \dots & \frac{\partial T(x_{msn})}{\partial x_{tsn}} & -U(x_{msn}) \end{array} \right] \left[ \begin{array}{c} \Delta x_{ts0} \\ \vdots \\ \Delta x_{tsn} \\ \beta \end{array} \right] = \left[ \begin{array}{c} -T(x_{ms0}) \\ \vdots \\ -T(x_{msn}) \end{array} \right] \tag{2.34}$$

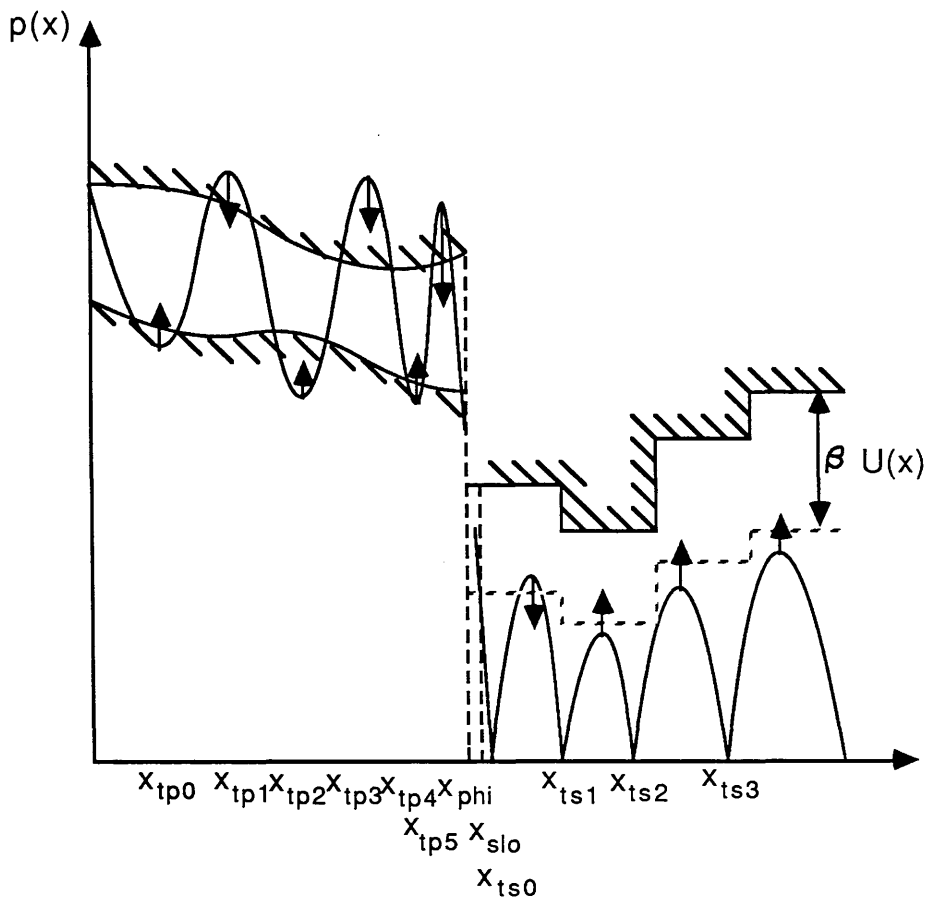


Fig. 2.8 Scheme for approximation of arbitrary lowpass filter by rational function

and since

$$\frac{\partial T(x)}{\partial x_{tsi}} = \frac{-\mu_i}{(x - x_{tsi})} T(x) \quad (2.35)$$

Eq. (2.34) can be rearranged and evaluated as

$$\left[ \begin{array}{ccc|c} \frac{\mu_0}{(x_{ms0}-x_{ts0})} & \dots & \frac{\mu_n}{(x_{ms0}-x_{tsn})} & \frac{U(x_{ms0})}{T(x_{ms0})} \\ \vdots & & \vdots & \vdots \\ \frac{\mu_0}{(x_{msn}-x_{ts0})} & \dots & \frac{\mu_n}{(x_{msn}-x_{tsn})} & \frac{U(x_{msn})}{T(x_{msn})} \end{array} \right] \left[ \begin{array}{c} \Delta x_{ts0} \\ \vdots \\ \Delta x_{tsn} \\ \beta \end{array} \right] = \left[ \begin{array}{c} 1 \\ \vdots \\ 1 \end{array} \right] \quad (2.36)$$

The touch points are updated as

$$x_{tsi} = x_{tsi} + \Delta x_{tsi} \quad (2.37)$$

and some damping may be necessary.

Note that the constant  $K$  must also be determined. A good method of assigning a value to  $K$  is to fix the passband edge position between passband and stopband iterations.

$$K = L(x_{phi})/T(x_{phi}) \quad (2.38)$$

### 2.5.2 Multi-band cases

Since frequency transformations are only appropriate to the design of symmetric filters, the design of general multi-band rational filter approximations is no longer a trivial extension of the lowpass case. Special design techniques for the four most popular classes of filter are considered; lowpass, bandpass, bandstop and highpass and generalisations drawn from these.

Highpass approximations are obtained in the same manner as lowpass, with passband and stopband regions transposed.

Bandpass filters have three bands, one passband and two stopbands. The numerator polynomial must now be divided into two parts, one containing zeros assigned to the lower stopband the other containing zeros assigned to the upper stopband (Fig. 2.9). The number of constraints in the problem requires that two unknown parameters be introduced. These take the form of lower and upper stopband error margins  $\beta_1$  and  $\beta_2$ . The new Newton system is

$$\left[ \begin{array}{ccc|cc} \frac{\mu_0}{(x_{ms0}-x_{ts0})} & \dots & \frac{\mu_n}{(x_{ms0}-x_{tsn})} & \frac{U(x_{ms0})}{T(x_{ms0})} & 0 \\ \vdots & & \vdots & \vdots & \vdots \\ \frac{\mu_0}{(x_{msr}-x_{ts0})} & \dots & \frac{\mu_n}{(x_{msr}-x_{tsn})} & \frac{U(x_{msr})}{T(x_{msr})} & 0 \\ \vdots & & \vdots & \vdots & \vdots \\ \frac{\mu_0}{(x_{msr+1}-x_{ts0})} & \dots & \frac{\mu_n}{(x_{msr+1}-x_{tsn})} & 0 & \frac{U(x_{msr+1})}{T(x_{msr+1})} \\ \vdots & & \vdots & \vdots & \vdots \\ \frac{\mu_0}{(x_{msn}-x_{tsn})} & \dots & \frac{\mu_n}{(x_{msn}-x_{tsn})} & 0 & \frac{U(x_{msn})}{T(x_{msn})} \end{array} \right] \begin{bmatrix} \Delta x_{ts0} \\ \vdots \\ \Delta x_{tsr} \\ \vdots \\ \Delta x_{tsr+1} \\ \vdots \\ \Delta x_{tsn} \\ - \\ \beta_1 \\ \beta_2 \end{bmatrix} = \begin{bmatrix} 1 \\ \vdots \\ 1 \\ \vdots \\ 1 \\ \vdots \\ 1 \\ \vdots \\ 1 \end{bmatrix} \quad (2.39)$$

The constant  $k$  can be determined in a similar manner to the lowpass case. The allocation of the zeros of  $N(x)$  between lower and upper stopband must initially be guessed. If the approximation exceeds the specification in one stopband and falls below in the other, some re-distribution will be necessary.

Bandstop filters also have three bands, one stopband and two passbands. As before, the number of constraints demands two additional degrees of freedom. In this case only one of these may be met by introducing a stopband error margin  $\beta$ . The other degree of freedom can be chosen to be either the stopband or a passband edge frequency or a passband error margin. The latter choice requires the solution of a system of equations as in the McLellan-Parks algorithm [31-34]. Relaxation of the passband edge can be done by omitting the fixed interpolation point at the edge of the upper passband. The algorithm then proceeds as for the lowpass case.

Each increase in the number of bands of the filter demands a single extra degree of freedom. These can be satisfied by relaxing the band edge of each additional passband. An alternative method is to allow all passbands and stopbands to have ripple errors [39]. Multi-band filters can generally be created by parallel

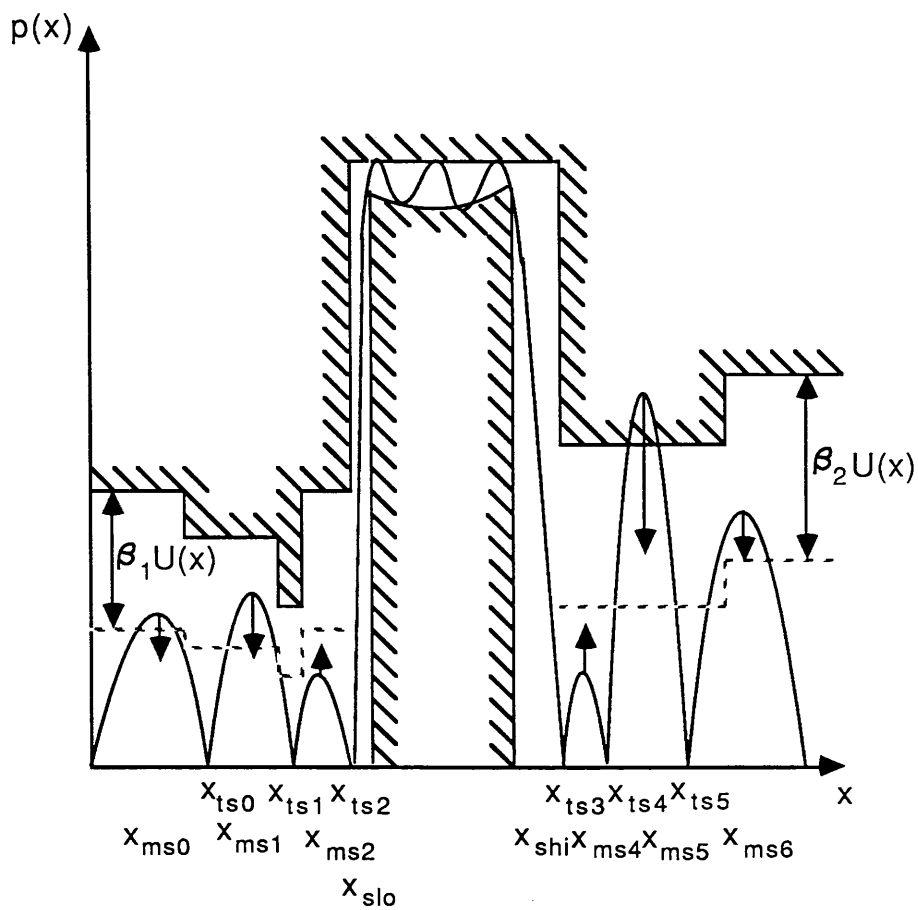


Fig. 2.9 Approximation scheme for stopband of asymmetric bandpass filter

connection of the four popular filter classes. This avoids very high—order single filters which have severe noise and accuracy problems in practical intergrated circuit realisations.

### 2.5.3 Computed examples

A series of computed approximation examples is now given to illustrate the power and flexibility of the above methods. Fig. 2.10 shows a polynomial (FIR) approximation to arbitrarily shaped boundaries. A touch point of fifth order tangency is seen at the centre of the function. High order approximations to filter bounding functions are computed in Figs. 2.11 and 2.12. FIR approximations up to length 110 ( $N=55$ ) have been obtained using double precision arithmetic.

A series of rational polynomial (IIR) filter approximations is displayed next. Fig. 2.13 shows a lowpass filter with arbitrary passband and stopband specifications. An 11th order function is fitted touching the passband boundaries and meeting the stopband boundary to within some constant dB error. Fig. 2.14 illustrates the application of high order touch points in passband and stopband. This 18th order lowpass filter has a sequence of two 3rd order followed by a 5th order touch point incident to upward sloping passband boundaries. By placing a 9th order touch point at the lower stopband edge a very deep notch is created. Figs. 2.15 and 2.16 show arbitrary bandpass approximations with asymmetric stopbands. Fig. 2.17 shows an arbitrary bandstop approximation of 18th order.

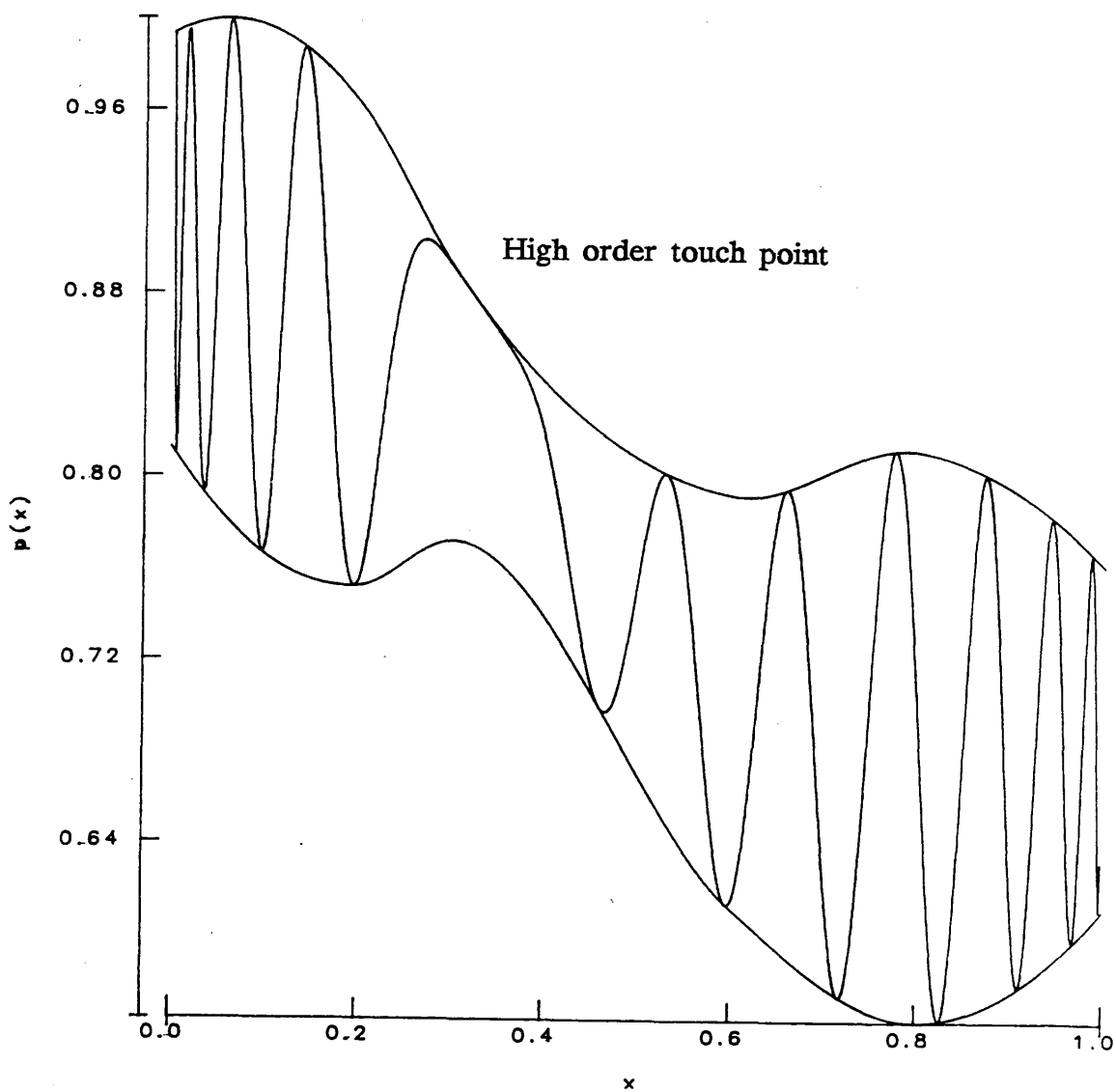


Fig. 2.10 Length 51 FIR approximation to arbitrary boundaries

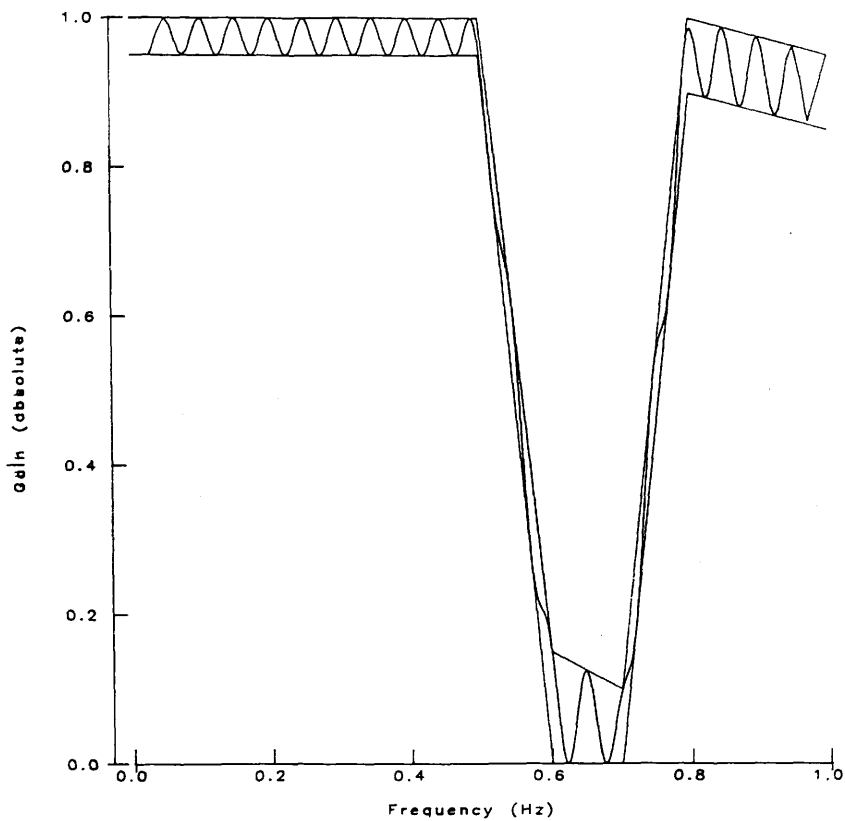


Fig. 2.11 Length 81 bandstop FIR filter approximation

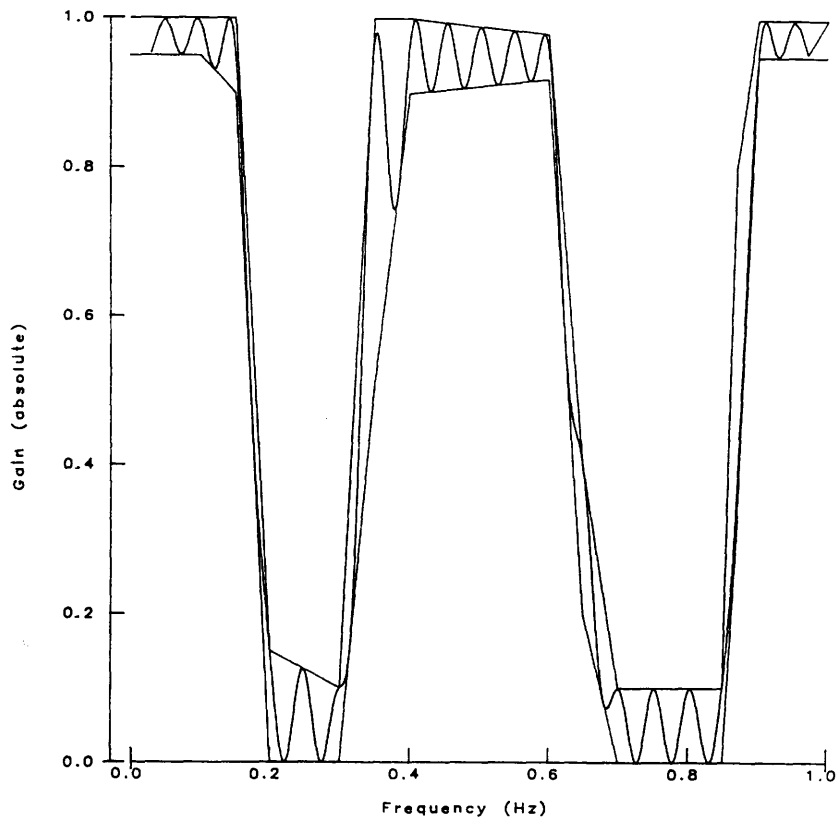


Fig. 2.12 Length 81 multi-band FIR filter approximation



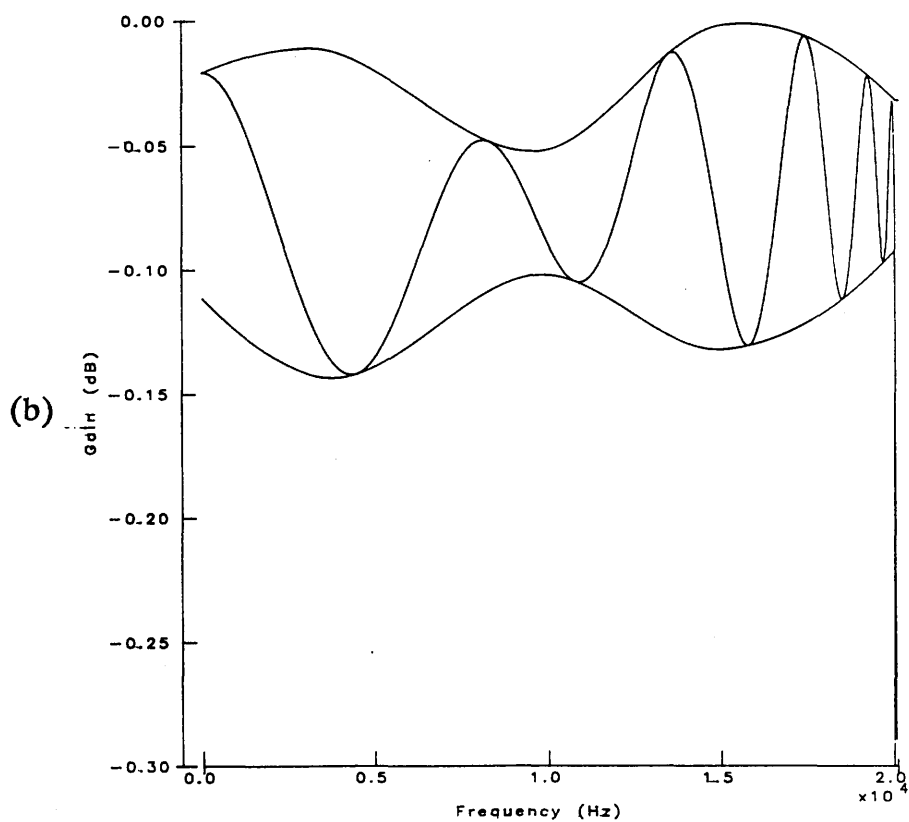
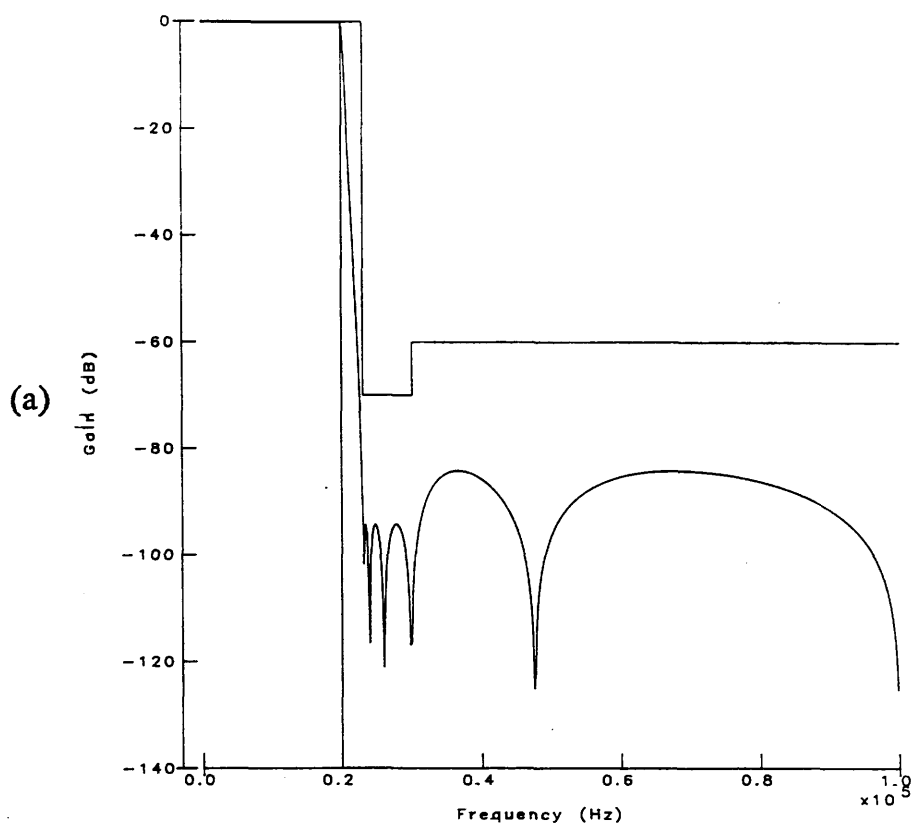


Fig. 2.13 (a) 11th order lowpass filter with arbitrary passband and stopband specifications  
(b) Passband detail

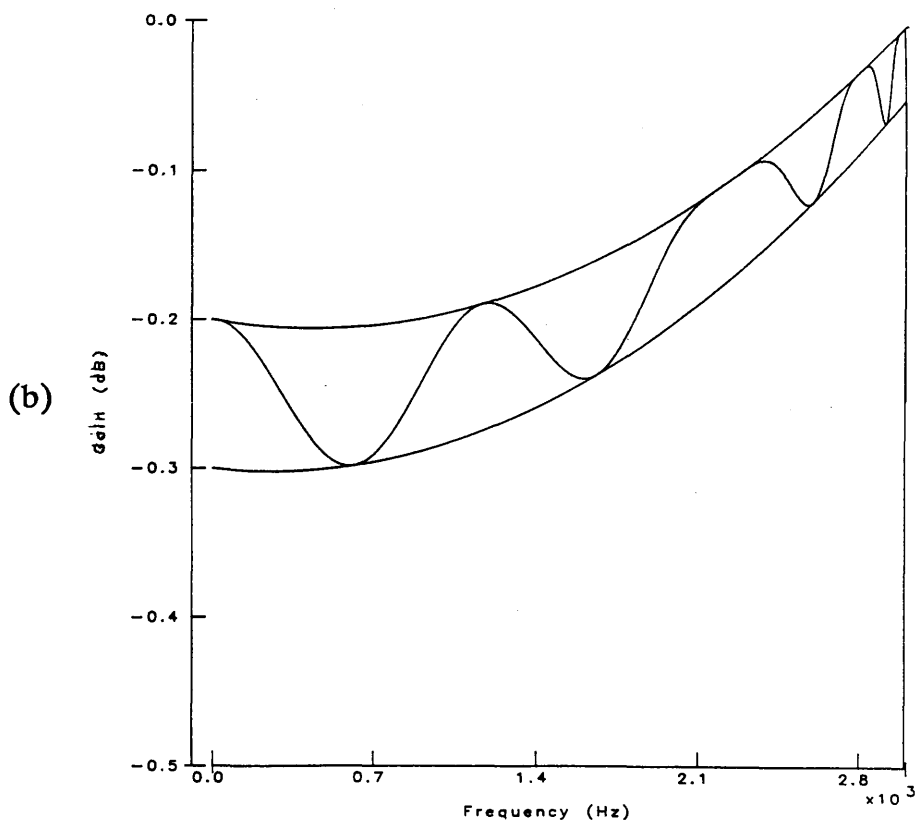
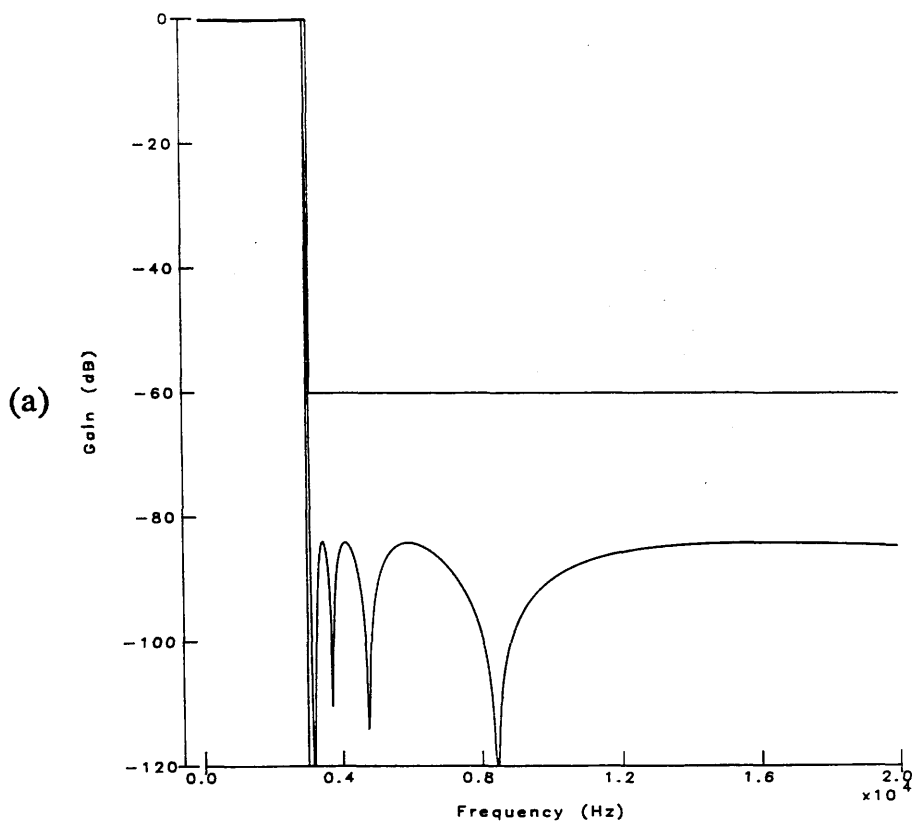


Fig. 2.14 (a) 17th order lowpass filter with high order touch points in both passband and stopband  
(b) Passband detail

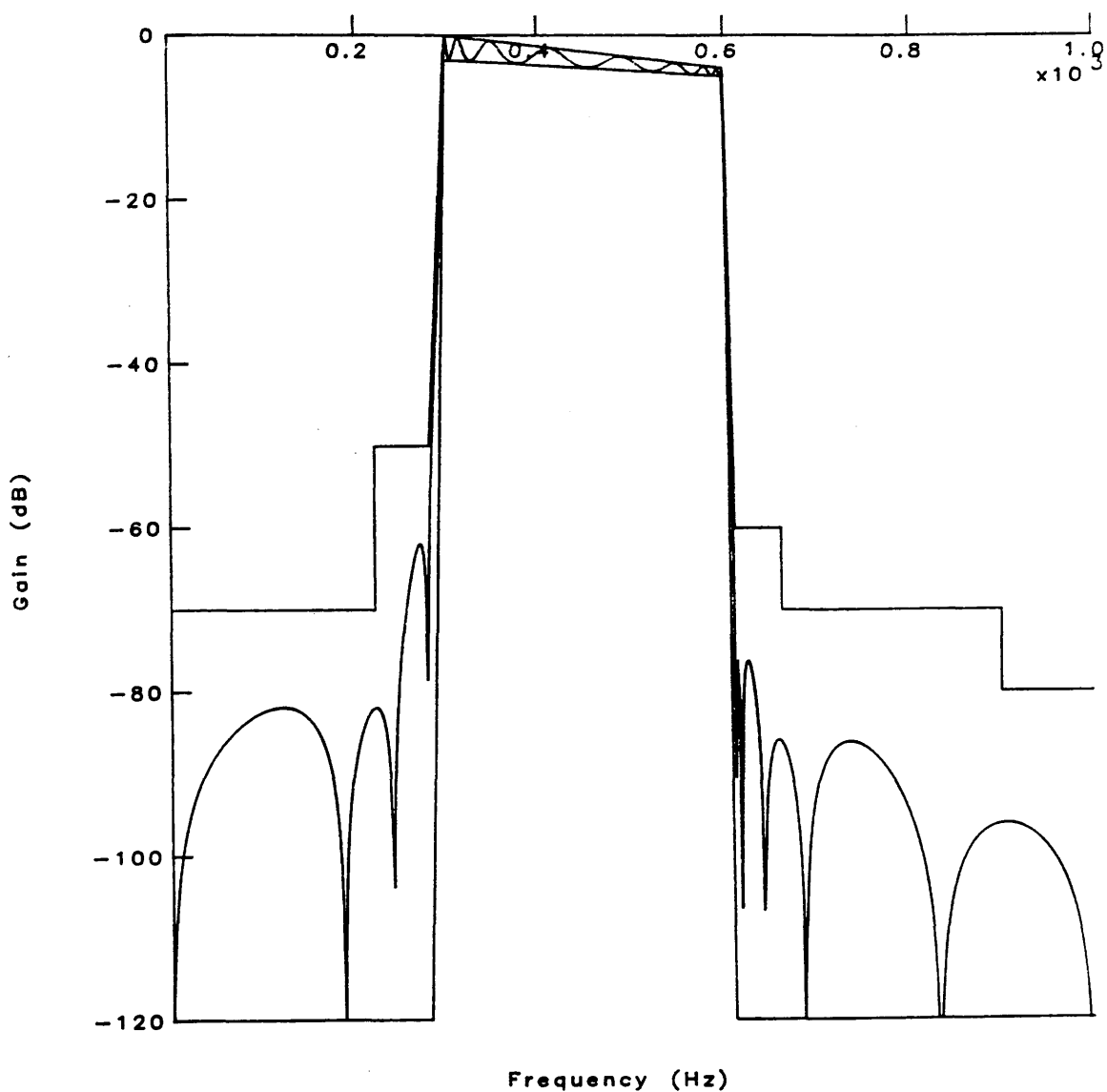


Fig. 2.15 18th order bandpass filter approximation with arbitrary passband and stopband specifications

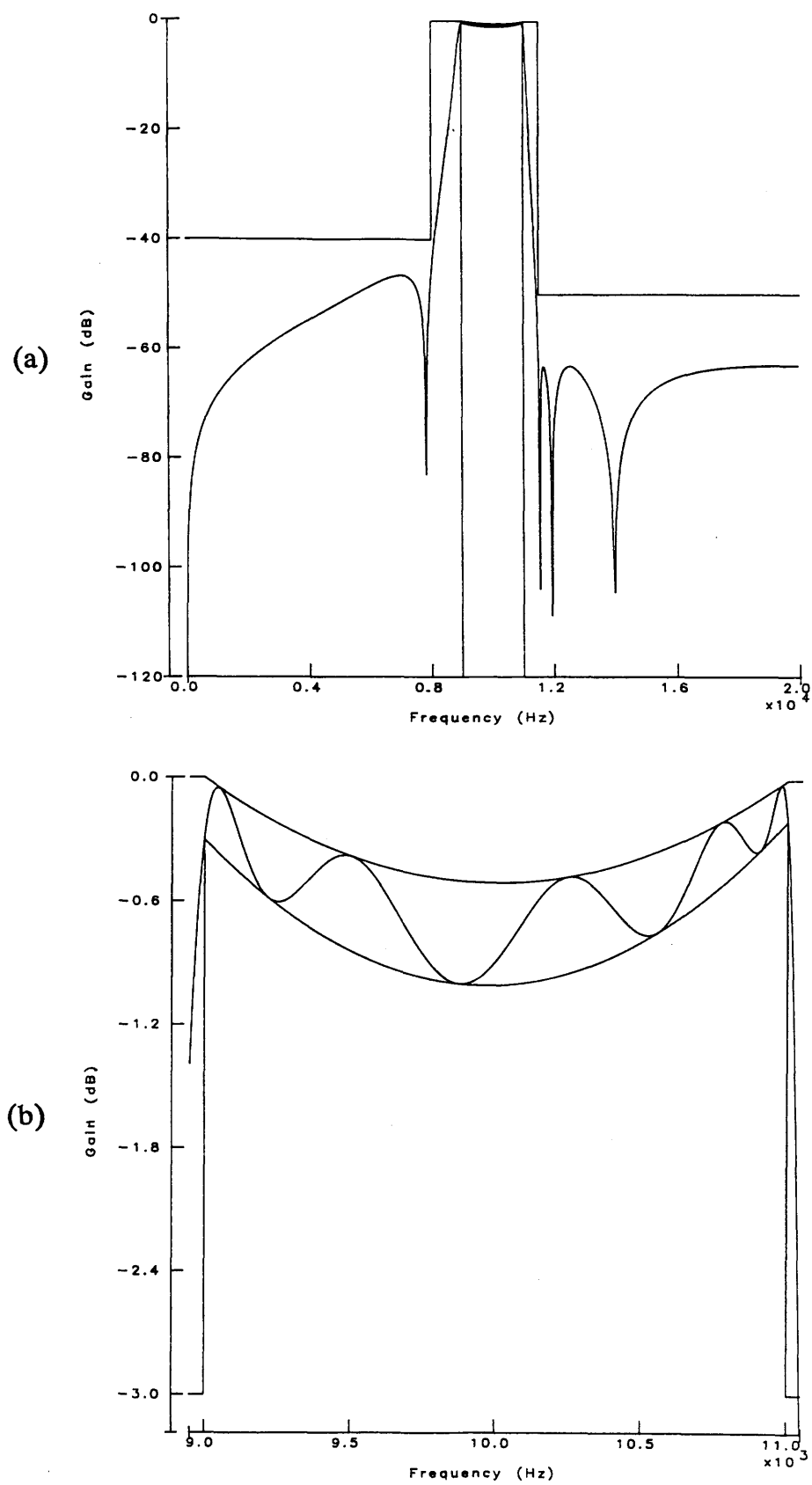


Fig. 2.16 (a) 10th order asymmetric bandpass filter with sagging passband  
(b) Passband detail

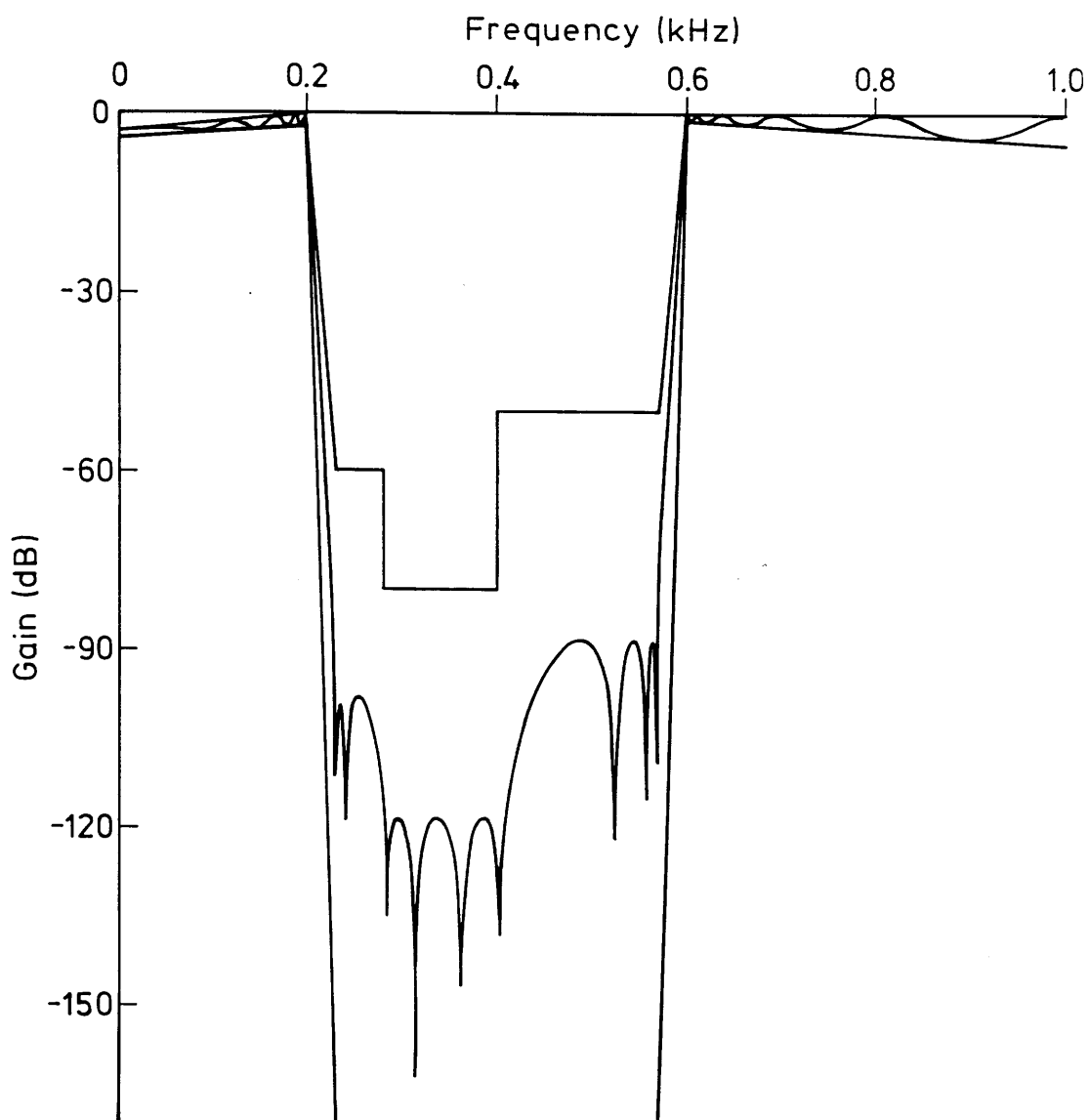


Fig. 2.17 18th order asymmetric bandstop filter approximation

## 2.6 SUMMARY

The chapter began by reviewing the design methods and properties of classical filter approximations. It was seen that, despite the convenience with which the functions can be derived, they will provide inefficient or inappropriate solutions to irregular filter specifications. To overcome this inadequacy, a set of approximation methods to fit single polynomials within arbitrarily bounded amplitude specifications was proposed. Based originally on Newton's method, the Remez algorithm appears as a special case, confirming its quadratic convergency property near solution. The formulation of the methods includes a generalisation of the maximal flatness concept, known from classical approximations. In this way compromises between equiripple and flat band properties can be obtained. The computational costs of the methods are assessed. Accuracy loss due to calculation within finite wordlength is particularly severe in filter problems. It was combatted by careful interpolation and polynomial storage schemes. Finally, since minimum-phase rational polynomials can be used to form the transfer functions of analogue networks their approximation is specially investigated. Since numerator and denominator polynomials have different properties a combination of techniques is used to design these in turn. Filters of the four main filter classes, low-pass, band-pass, band-stop and highpass can then be constructed with arbitrary passband and stopband properties.

## REFERENCES

- [1] A. S. Sedra and P. O. Brackett, "Filter Theory and Design: Active and Passive", Pitman, London, 1979.
- [2] R. W. Daniels, "Approximation methods for electronic filter design", McGraw-Hill, New York, 1974.
- [3] S. Darlington, "Simple algorithms for elliptic filters and generalisations thereof", IEEE Trans. Circuits and Systems, Vol. CAS-25, No. 12, pp. 975-980, Dec. 1978.
- [4] L. F. Lind, "Simple computation of elliptic function filters", Digest of IEE Saraga Colloquium on Electronic Filters, London, 1984.
- [5] L. F. Lind, "On finding the degree of an elliptic function filter", Digest of IEE Saraga Colloquium on Electronic Filters", pp. 11/1-11/4, London, 1988.
- [6] D. Baez-Lopez and L. P. Huelsman, "Computational aspects of elliptic filter approximation and synthesis", 28th Midwest Symposium on Circs and Syst., pp. 290-293, 1985.

[7] A. H. Gray and J. D. Markel, "Computer program for designing digital elliptic filters", IEEE Trans. on Acoustics, Speech and Signal Processing, Vol. ASSP-24, No. 6, pp.529-538, Dec. 1976.

[8] Y. Tsividis and P. Antognetti, eds, "Design of MOS VLSI circuits for telecommunications", Prentice-Hall, Englewood Cliffs, NJ, 1985.

[9] M. S. Nakhla, "Approximation of lowpass filters with frequency dependent input gain characteristic", IEEE Trans., vol. CAS-26, pp. 198-202, 1979.

[10] G. W. Medlin, "A new design technique for maximally linear differentiators", Proc. ICASSP, pp. 825-828, Glasgow, Scotland, 1989.

[11] S. N. Filho, R. Seara and J. C. M. Bermudez, "A new method for the compensation of the  $\sin(x)/x$  distortion in discrete time to continuous time signal conversions", Proc. ISCAS, pp. 1668-1671, Portland, Oregon, 1989.

[12] A. C. M. de Queiroz and L. P. Caloba, "Physically symmetrical and antisymmetrical ladder filters with finite transmission zeros", Proc. 30th Midwest Symposium on Circuits and Systems, pp. 639-643, 1987.

[13] Che-Ho Wei and Shyue-Win Wei, "Lowpass filters with single ripple in both passband and stopband", Proc. ISCAS, pp. 1632-1635, Portland, U.S.A., 1989.

[14] P. P. Vaidyanathan, "Optimal design of linear-phase FIR digital filters with very flat passbands and equiripple stopbands", IEEE Trans. on Circuits and Systems, Vol. CAS-32, No. 9, pp. 904-917, Sept. 1985.

[15] F. Brophy and A. C. Salazar, "Synthesis of spectrum shaping digital filters of recursive design", IEEE Trans. on Circuits and Systems, Vol. CAS-22, No. 3, pp. 197-204, March 1975.

[16] S. Natarajan, "A simple pre-distortion technique for active filters", IEEE Trans. on Circuits and Systems, Vol. CAS-31, No. 4, pp. 398-400, April 1984.

[17] M. Markiewicz-Wrzeciono and N. O. Sokal, "Filters with unequal ripples in the passband for class-E power amplifiers", Proc. ISCAS, pp. 1628-1631, Portland, U.S.A., 1989.

[18] G. Cortelazzo and M. R. Lightner, "Simultaneous design in both magnitude and group delay of IIR and FIR filters based on multiple criterion optimisation", IEEE Trans. Acoustics, Speech and Signal Processing, Vol. ASSP-32, No.5, pp.949-967, Oct. 1984.

[19] C. Charalambous and H. Khreishi, "Minimax design of one-dimensional recursive digital filters of a given approximation type: a closed form approach", Proc. IEE, Pt.G, No.1, pp.38-44, Feb. 1987.

[20] K. Steiglitz, "Computer-aided design of recursive digital filters", IEEE

Trans. on Audio and Electroacoustics, Vol. AU-18, No. 2, pp.123-129, June 1970.

[21] G. C. Temes and D. A. Calahan, "Computer-aided network optimisation : the state-of-the-art", Proc. IEEE, Vol. 53, pp. 1832-1863, Nov. 1967.

[22] G. Szentirmai, "Computer-aided Filter Design", IEEE Press, New York, 1973.

[23] E. Y. Remes, "Sur un procede convergent d'approximations successives pour determiner les polynomes d'approximation", Comptes Rendues, Vol. 198, pp. 2063-2065, 1934.

[24] E. Ya. Remez, "General computation methods of Tchebysheff approximation", Kiev USSR, Atomic Energy Translation 4491, pp. 1-85, 1957.

[25] Li Ping, R. K. Henderson and J. I. Sewell, "A new filter approximation and design algorithm", Proc. ISCAS, pp. 1063-1066, Portland, Oregon, 1989.

[26] B. R. Smith and G. C. Temes, "An iterative approximation procedure for automatic filter synthesis", IEEE Trans. Circ. Theory, Vol. CT-12, No.1, pp.107-112, March 1967.

[27] E. Isaacson and H. B. Keller, "Analysis of numerical methods", J. Wiley and Sons, New York, 1966.

[28] S. D. Conte and C. de Boor, "Elementary numerical analysis", McGraw-Hill, pp. 120-125, 1980.

[29] F. B. Hildebrand, "Introduction to Numerical Analysis", Second Edition, McGraw-Hill, New York, 1974.

[30] M. T. McCallig and B. J. Leon, "Constrained ripple design of FIR digital filters", Trans. on Circuits and Systems, Vol. CAS-25, No. 11, pp. 893-901, Nov. 1978.

[31] L. R. Rabiner, J. H. McClellan and T. W. Parks, "FIR digital filter design techniques using weighted Chebyshev approximation", Proc. IEEE, Vol. 63, No. 4, pp. 595-609, April 1975.

[32] T. W. Parks and J. H. McClellan, "Chebyshev approximation for nonrecursive digital filters with linear phase", IEEE Trans. on Circuit Theory, Vol. CT-19, No. 2, pp. 189-194, March 1972.

[33] J. H. McClellan and T. W. Parks, "A unified approach for the design of optimum FIR linear-phase digital filters", IEEE Trans. on Circuit Theory, Vol. CT-20, pp. 697-701, Nov. 1973.

[34] J. H. McClellan and T. W. Parks, "A computer program for designing optimum FIR linear-phase digital filters", IEEE Trans. on Audio and Electroacoustics, Vol. AU-21, No. 6, Dec. 1973.



[35] J-K. Liang and R. J. P. De Figueiredo, "An efficient iterative algorithm for designing optimal recursive digital filters", IEEE Transactions on Acoustics, Speech and Signal Processing, Vol. ASSP-31, No. 5, pp. 1110-1120, Oct. 1983.

[36] H. G. Martinez and T. W. Parks, "Design of recursive digital filters with optimum magnitude and attenuation poles on the unit circle", IEEE Transactions on Acoustics, Speech and Signal Processing, Vol. ASSP-26, No. 2, pp. 150-156, April 1978.

[37] K. Shenoi and B. P. Agrawal, "A design algorithm for constrained equiripple digital filters", IEEE Transactions on Acoustics, Speech and Signal Processing, Vol. ASSP-30, No. 2, pp. 206-211, April 1983.

[38] A. Antoniou, "New improved method for the design of weighted-chebyshev, nonrecursive digital filters", IEEE Trans. on Circuits and Systems, Vol. CAS-30, No. 10, pp. 740-748, Oct. 1983.

[39] D. J. Shpak and A. Antoniou, "Two robust Remez methods for the design of FIR digital filters meeting prescribed specifications", IEEE ISCAS, pp. 47-51, Helsinki, 1988.

[40] W. Stehle, "Closed form minimum search in equal ripple filter design", Proc. ISCAS, pp. 378-381,

## CHAPTER 3

### FILTER GROUP DELAY APPROXIMATION

#### 3.1 INTRODUCTION

#### 3.2 GROUP DELAY APPROXIMATION BY ALL-PASS FUNCTIONS

##### 3.2.1 Definitions

##### 3.2.2 The delay approximation problem

#### 3.3 ALL-PASS FILTER DESIGN METHOD

##### 3.3.1 Amplitude and group delay relations

##### 3.3.2 New Remez-type algorithm

##### 3.3.3 Computer implementation

##### 3.3.4 Computed examples

#### 3.4 SUMMARY

#### REFERENCES

### 3.1 INTRODUCTION

In the previous section, various methods were proposed to approximate filter amplitude specifications ignoring the group delay. However, modern digital communications and signal processing systems often require filters which satisfy simultaneous specifications on amplitude *and* group delay. A common practical design approach is to separate the two approximation problems by employing an all-pass function to equalise the group delay of a minimum phase amplitude function. The latter function should first be optimised to reduce the peaking of the delay towards the passband edges, either by smoothing the passband amplitude function (e.g. Butterworth) or reducing the roll-off into the stopband. The general amplitude approximation methods of the previous chapter offer various ways to trade-off between the amplitude and group delay characteristics. High order touch points can be introduced into the passband and notches can be placed to tailor the stopband roll-off. Although, the demands on the group delay correction can be reduced in these ways, it is still costly to use all-pass functions. They are known to offer a non-canonic solution to the combined amplitude and group delay approximation problem. Greater efficiency can be achieved by employing a general non-minimum phase function [1–8]. However, these functions cannot be simulated by low-sensitivity SCFs at present. The argument for all-pass equalisation is strengthened by the recent development of low-sensitivity all-pass SC ladder structures [9–10].

This chapter is concerned with efficient computer methods for the approximation of all-pass transfer functions to meet arbitrary group delay specifications. In particular, a method is sought whereby the techniques developed to approximate the amplitude of a transfer function can also be applied to the group delay of an all-pass function. Unfortunately, when this group delay function is interpolated, a system of ill-conditioned non-linear equations arise which becomes very difficult to solve with increasing order [11]. Since Newton and Remez-type approximation methods depend on an efficient interpolation step they are difficult to apply with efficiency or reliability [12]. Alternative methods based on optimisation techniques have therefore been studied [13–14].

A new algorithm is proposed which permits direct application of Remez-type approximation methods to the problem [15]. By observing the similarity between the group delay function and a filter amplitude function, the techniques and theorems for amplitude approximation are still valid. A stable, accurate algorithm is then developed for arbitrary group delay correction.

## 3.2 GROUP DELAY APPROXIMATION BY ALL-PASS FUNCTIONS

### 3.3.1 Definitions

The all-pass function in the continuous time  $s$ -domain is

$$T(s) = \frac{X(-s)}{X(s)} \quad (3.1)$$

where

$$X(s) = \sum_{i=0}^n d_i s^i \quad (3.2)$$

and the phase is given by

$$\beta(\omega) = -2 \tan^{-1} \left[ \frac{-\sum_{\text{odd } i} d_i \omega^i}{\sum_{\text{even } i} d_i \omega^i} \right] \quad (3.3)$$

The group delay is defined as

$$\tau(\omega) \triangleq - \frac{d\beta(\omega)}{d\omega} \quad (3.4)$$

### 3.3.2 Delay approximation problem

The filter *amplitude* approximation problem has been most successfully solved by stable, accurate Remez-type algorithms [12,16–17]. Two main steps are necessary in a Remez algorithm; interpolation and determination of the extrema. Unfortunately the group delay function is not amenable to direct interpolation by the simple Newton or Lagrange schemes. In fact, a set of nonlinear equations must be set up and solved. If the roots of  $X(s)$  are  $s_i = a_i + jb_i$  and the specified group delay is  $\tau_s(\omega)$  then the following nonlinear system is implied,

$$\frac{1}{2} \sum_{i=1}^{n/2} \left\{ \frac{a_i}{a_i^2 + (\omega_j + b_i)^2} + \frac{a_i}{a_i^2 + (\omega_j - b_i)^2} \right\} - \tau_s(\omega_j) = 0$$

$$\text{for } j= 1, \dots, n+1 \quad (3.5)$$

Solution of this system is a necessarily iterative procedure and becomes difficult for moderate values of  $n$  [11]. Alternatively, it is possible to interpolate the phase function directly through solution of the following Vandermonde-type matrix system, set up by solving (3.3) at a series of frequency points.

$$\begin{bmatrix} \omega_0 & \tan(\beta_S(\omega_0))\omega_0^2 & \omega_0^3 & \dots & \tan(\beta_S(\omega_0))\omega_0^n \\ \omega_1 & \tan(\beta_S(\omega_1))\omega_1^2 & \omega_1^3 & \dots & \tan(\beta_S(\omega_1))\omega_1^n \\ \vdots & \vdots & \vdots & \ddots & \vdots \\ \omega_n & \tan(\beta_S(\omega_n))\omega_n^2 & \omega_n^3 & \dots & \tan(\beta_S(\omega_n))\omega_n^n \end{bmatrix} \begin{bmatrix} d_1 \\ d_2 \\ \vdots \\ d_n \end{bmatrix} = \begin{bmatrix} -\tan(\beta_S(\omega_0)) \\ -\tan(\beta_S(\omega_1)) \\ \vdots \\ -\tan(\beta_S(\omega_n)) \end{bmatrix} \quad (3.6)$$

with  $d_0=1$  and  $\beta_S(\omega)$  is the specified phase function.

Gregorian and Temes [11] found that this system is very ill-conditioned and proposed an improved interpolation method for both phase *and* group delay. Despite being better conditioned, this method does have certain drawbacks. The necessity to specify the phase at certain frequencies as well as the group delay means that the form of the group delay function cannot be completely controlled. The extrema cannot then be manipulated by a Remez scheme. Additionally, polynomials are interpolated in coefficient form which is known to be an inaccurate representation in finite computer arithmetic, leading to problems for high order or narrow-band filters. So, although the scheme can provide good initial parameter values for a Remez iteration, it does not remove the need to solve nonlinear equations.

Other schemes involving least pth optimisation or linear programming have thus been considered to avoid the problems of the Remez algorithm [13–14]. These methods involve extensive computation and do not necessarily guarantee the stability of the solution.

### 3.3 ALL-PASS FILTER DESIGN METHOD

#### 3.3.2 Amplitude and group delay relations

The group delay function can be expressed as

$$\tau(\omega) = \frac{2\operatorname{Re} \left\{ X(s) \frac{dX(-s)}{ds} \right\}}{X(s)X(-s)} \bigg|_{s=j\omega} = \frac{N(\omega)}{D(\omega)} \quad (3.7)$$

Since the denominator of (3.7) is a magnitude squared function it can be designed by standard Remez-type methods. The numerator function is an even function of  $s$  which can be formed by Hurwitz factorisation of the denominator polynomial.

### 3.3.2 New Remez-type algorithm

Consider now the problem of fitting the delay function to lower and upper boundaries  $L(\omega)$  and  $U(\omega)$  in a minimax sense over a frequency interval  $\omega_{l0}$  to  $\omega_{hi}$  (Fig. 3.1). It is required that

$$L(\omega) + C \leq \frac{N(\omega)}{X(j\omega)X(-j\omega)} \leq U(\omega) + C \quad (3.8)$$

Where the unknown constant delay offset  $C$  is necessary to ensure that

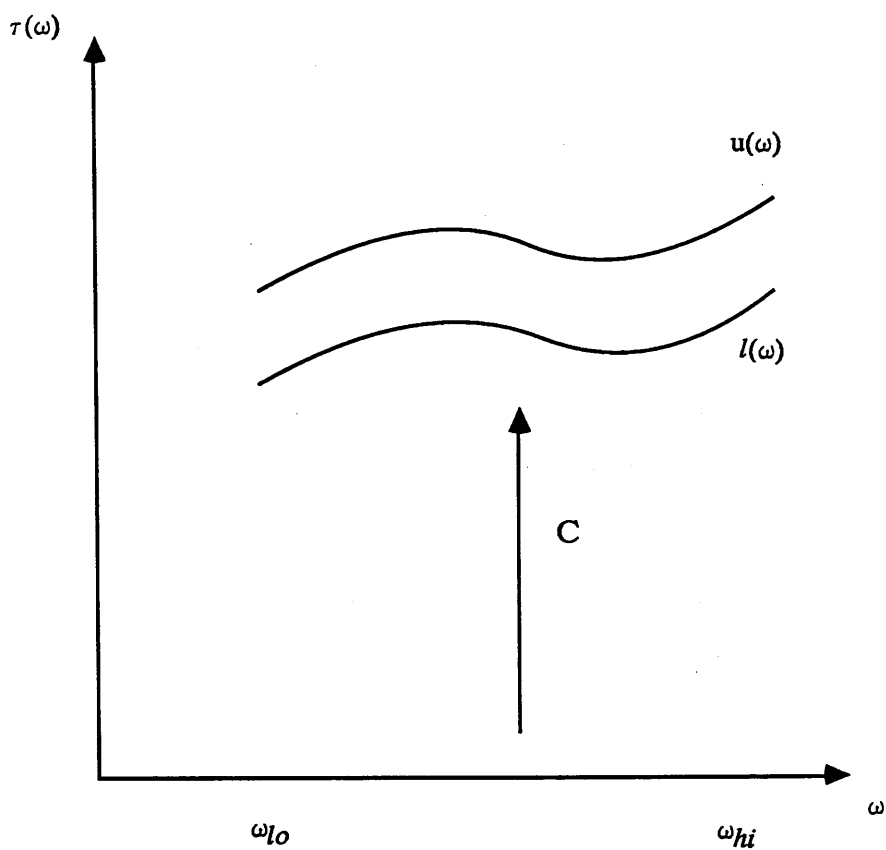
$$\int_0^\infty \tau(\omega) d\omega = n\pi \quad (3.9)$$

The constant  $C$  can be added in as necessary without affecting the relative delay variation over the approximating region.

The all-pass approximation method may be summarised by the following steps

*Step 1 : read lower and upper delay boundaries as piece-wise boundaries  $L(\omega)$  and  $U(\omega)$  and equaliser order  $n$ .*

*Step 2 : Set numerator function  $N(\omega)=1$  and guess constant  $C=n\pi/(\omega_{hi}-\omega_{l0})$*



**Fig. 3.1** Approximation scheme for allpass group delay

*Step 3 : Apply Remez approximation techniques to solve*

$$\begin{aligned} u(\omega) &= N(\omega)/(L(\omega)+C) \\ l(\omega) &= N(\omega)/(U(\omega)+C) \end{aligned} \quad (3.10)$$

*over the range  $\omega_{lo}$  to  $\omega_{hi}$  using  $D(x)$ .*

*Step 4 : Recalculate C as average delay constant between specified and approximated  $\tau(\omega)$  over  $\omega_{lo}$  to  $\omega_{hi}$ .*

*Step 5 : Form numerator function by Hurwitz factorisation of  $D(\omega)$ . Let the roots be  $s_i = -a_i + jb_i$ , then the delay function is*

$$\tau(\omega) = 2 \sum_{i=1}^{n/2} \left\{ \frac{a_i}{a_i^2 + (\omega + b_i)^2} + \frac{a_i}{a_i^2 + (\omega - b_i)^2} \right\} \quad (3.11)$$

*The numerator function can be calculated from (3.11) and (3.12).*

$$N(\omega) = D(\omega) \times \tau(\omega) \quad (3.12)$$

*Step 6 : Repeat from Step 2 until converged.*

### 3.3.3 Computer implementation

The factorisation at Step 4 can be made very efficient by utilising root positions from the previous factorisation as good initial guesses of roots for the present factorisation. Using Muller's quadratic interpolation method this typically only requires 2 to 3 iterations per root [18].

Accuracy is preserved in the algorithm by avoiding representation of polynomials in coefficient form. Instead Newton interpolated form is used at step 3 and factored form at Step 4. Both forms are well-conditioned on the approximation region allowing high order functions and narrow band all-pass functions to be designed.

No theoretical proof has been obtained of convergence. However experience has shown that convergence is good and that 5 or 6 cycles will generally suffice. The mechanism of the algorithm is dependent on the similarity between the group



delay function  $\tau(\omega)$  and the denominator magnitude function  $D(\omega)$  in (3.2). The numerator is observed to be a smooth function over the approximating region which warps the delay function of the denominator. Further theoretical investigation is being undertaken.

Digital all-pass functions can be obtained by bilinear transformation. The delay specifications must be pre-warped by a factor of  $\cos(\omega T/2)^2$ .

Group delay equalisation can be performed by combining  $L(\omega)$  and  $U(\omega)$  with the additive inverse of the group delay function of the amplitude filter. In this case, the total group delay of the all-pass and amplitude filter stages will meet the desired specifications.

### 3.3.4 Computed examples

A series of unusual group delay approximations is presented. Fig. 3.2 shows the group delay of a 16th order all-pass function fitted within peaked boundaries  $U(\omega)$  and  $L(\omega)$ . Figs 3.3 and 3.4 show sloping and stepped forms of group delay respectively. High order touch points can be introduced into the delay function by the approximation methods of Chapter 2. Fig. 3.5 shows a 12th order maximally flat group delay response (11th order touch point). Fig. 3.6 shows a 28th order stepped group delay response with a 5th order touch point at the lower band edge.

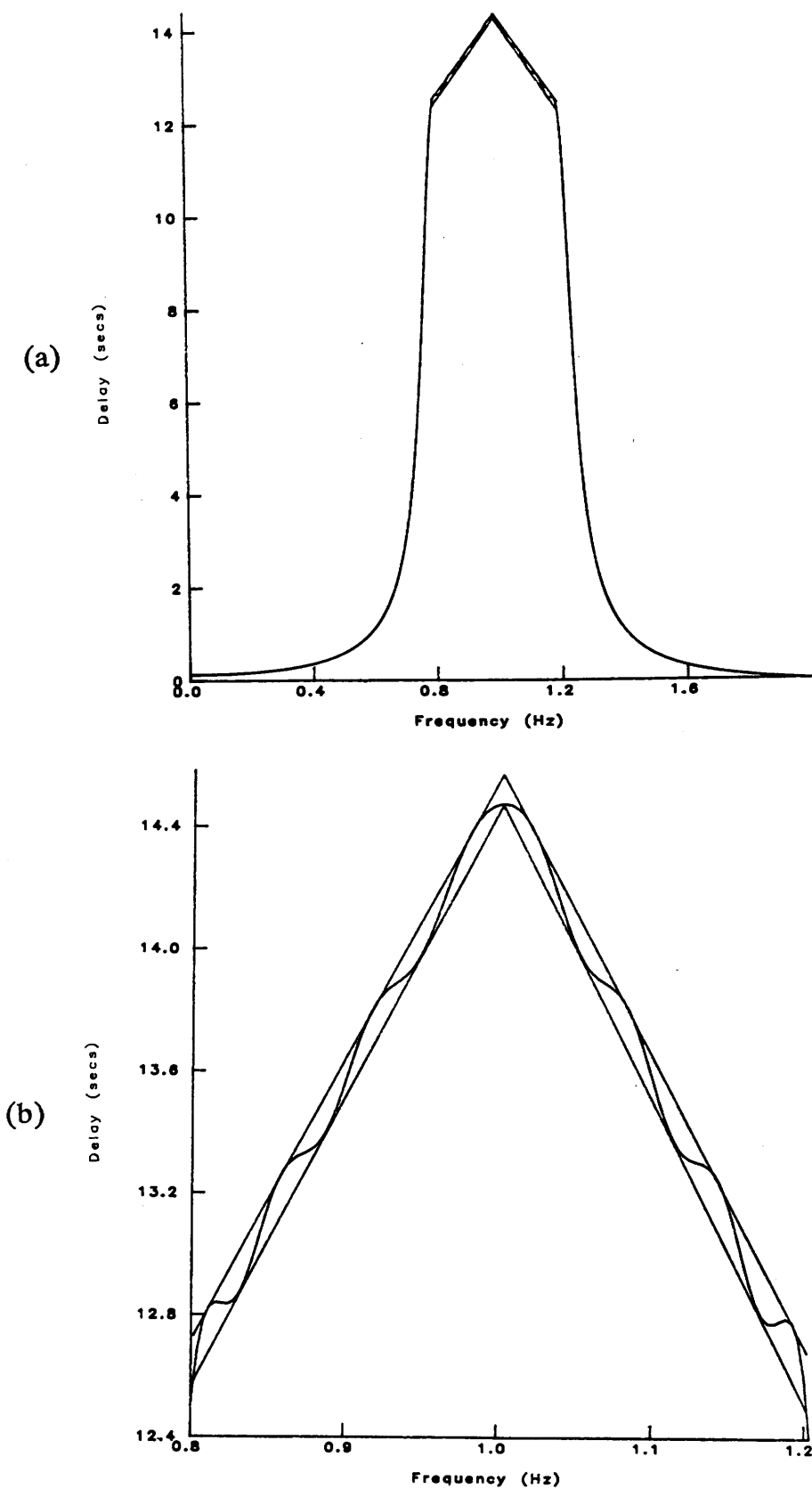


Fig. 3.2 (a) 16th order allpass group delay approximation with peaked boundaries

(b) Detail

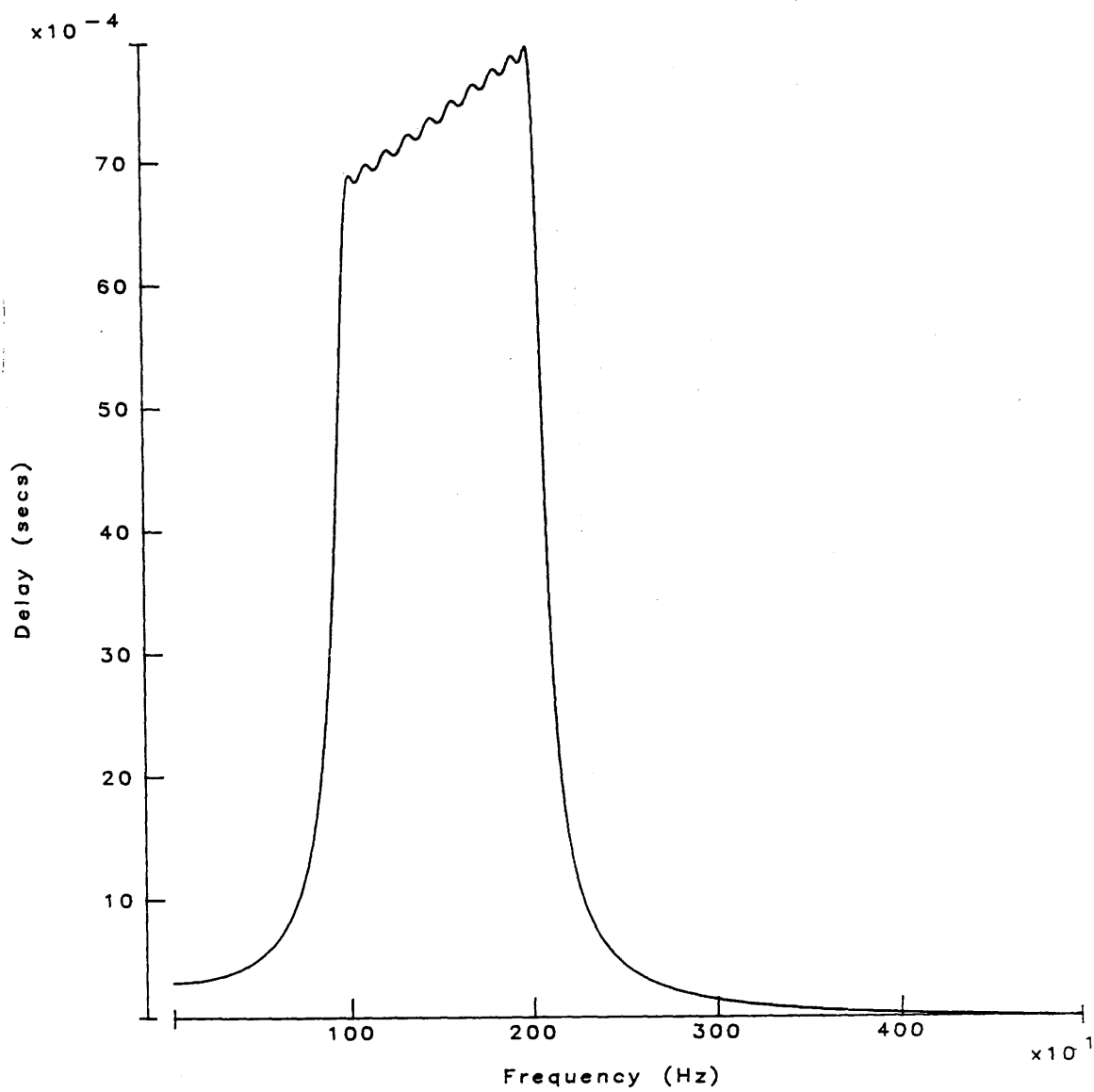


Fig. 3.3 20th order sloping allpass group delay approximation

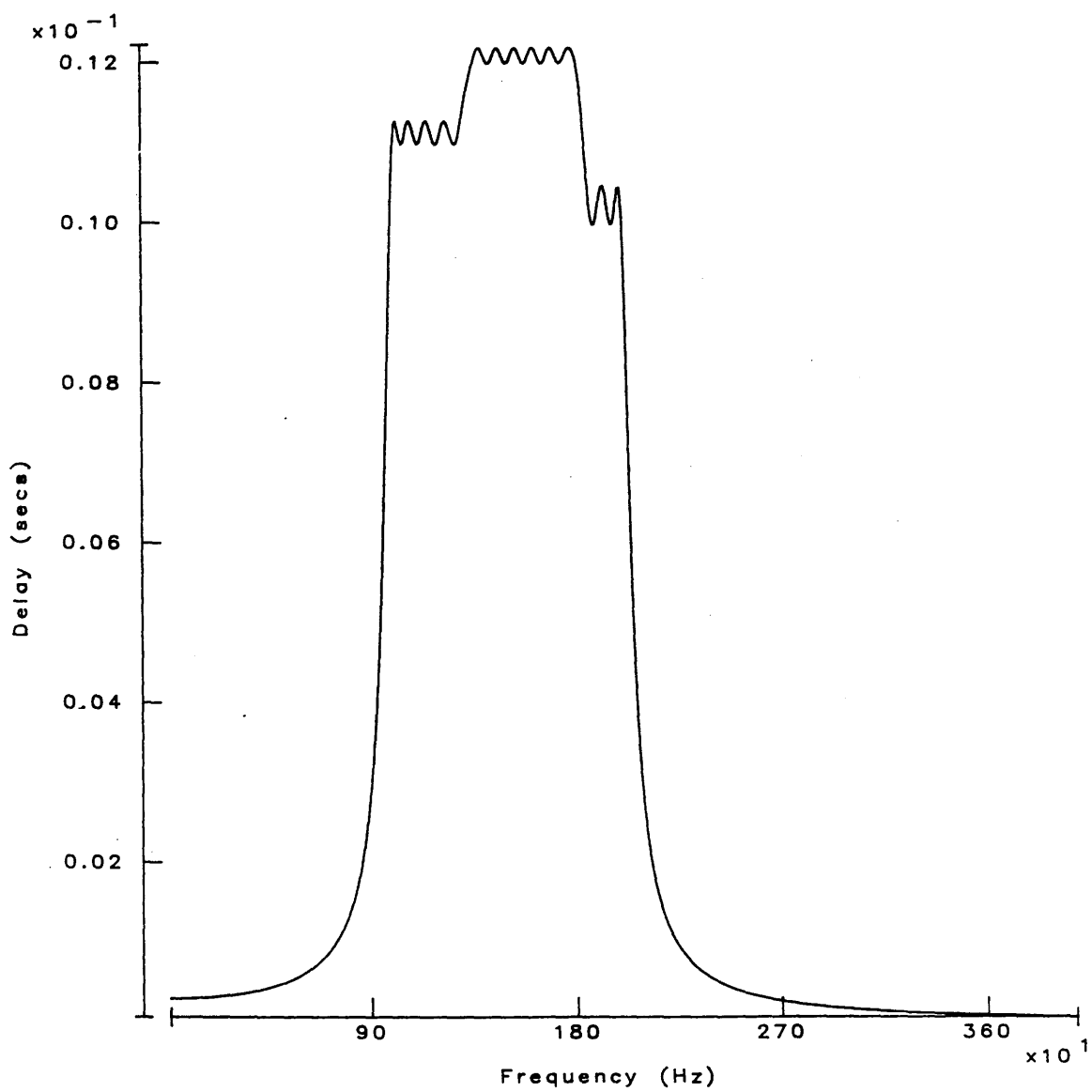


Fig. 3.4 28th order stepped allpass group delay approximation

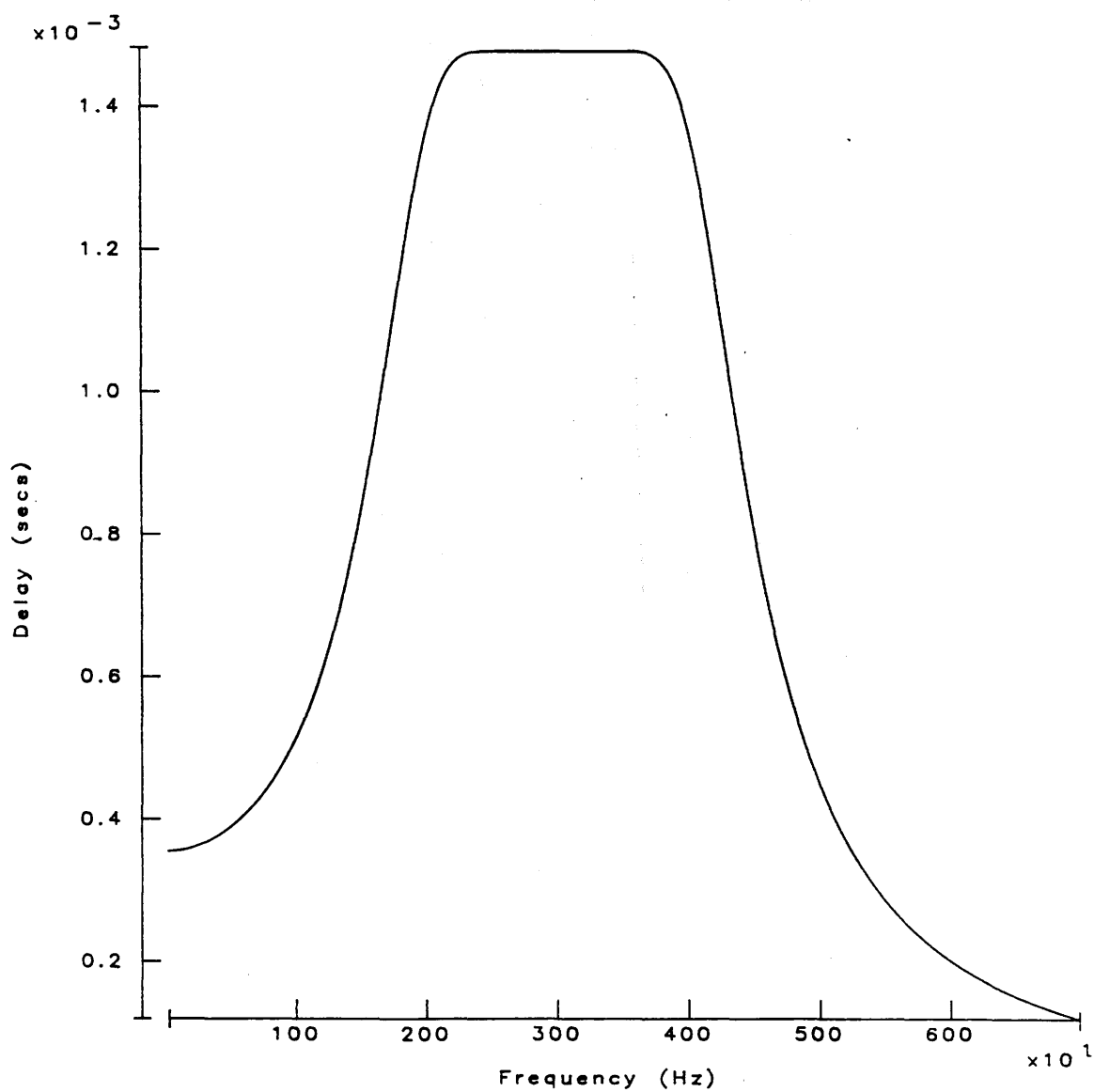


Fig. 3.5 12th order maximally flat allpass group delay approximation

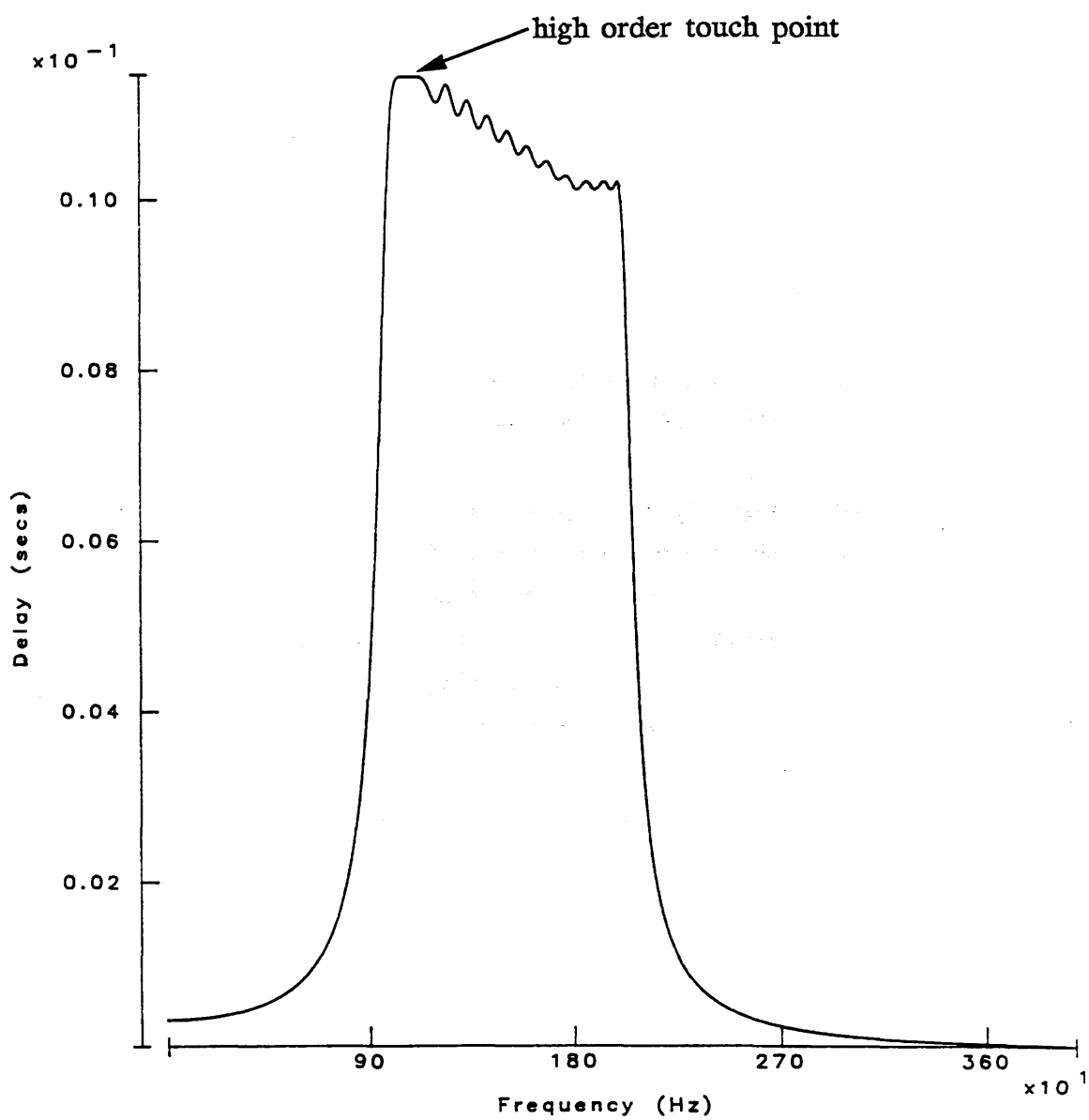


Fig. 3.6 28th order allpass group delay approximation  
with high order touch point

### 3.4 SUMMARY

An iterative design procedure which works on the group delay function and employs Remez-type approximation has been proposed. Advantages of this algorithm are:

1. Good initial guesses of parameters are not required for convergence. As with the Remez approximation the interpolation ordinates can be arbitrarily spaced on the approximation region (normally equi-distantly).

2. The algorithm is well-conditioned. Accuracy is maintained by representing the design polynomials in either Newton or factored form instead of the ill-conditioned coefficient form. High orders ( $> 40$ ) and narrow band design can be obtained. High order designs are of some interest for digital filters where a very selective linear-phase filter is required and would be too expensive in non-recursive form.

3. Stability of the solution is guaranteed at all stages of the algorithm. The roots of the denominator of the all-pass function must lie in the left-half plane because of the Hurwitz factorisation step.

4. Computational requirements are light. The process only involves the fast Remez exchange and a factorisation steps.

5. The convergence of the algorithm is good.

In computer terms, this algorithm can be conveniently combined with amplitude approximation software, since it draws on the same numerical methods of interpolation and factorisation.

### REFERENCES

[1] G. Cortelazzo and M. R. Lightner, "Simultaneous design in both magnitude and group delay of IIR and FIR filters based on multiple criterion optimisation", IEEE Trans. Acoustics, Speech and Signal Processing, Vol. ASSP-32, No.5, pp.949-967, Oct. 1984.

[2] R. K. Kwan and G. G. Bach, "Simultaneous approximations in filter design", IEEE Trans. Circuit Theory, Vol. CT-16, pp. 117-121, Feb. 1969.

[3] I. H. Zalabawi, "Design of flat group delay IIR filters with prescribed amplitude characteristics", Proc. ISCAS, pp.2493-2496, Helsinki, Finland, 1988.

[4] H. J. Orchard and D. M. Tragoff, "Image-parameter approximations for designing linear-phase filters", IEEE Trans. on Circuits and Systems, Vol.

CAS- 25, No.6, pp.325- 333, June 1978.

[5] J. D. Rhodes and I. H. Zalabawi, "Design of selective linear-phase filters with equiripple amplitude characteristics", Trans. on Circuits and Systems, Vol. CAS- 25, No.12, pp. 989- 1000, Dec. 1978.

[6] P. Jarry and H. Abdalla, "Arbitrary phase and group delay polynomials", Proc. ISCAS, pp. 1117- 1119, Rome, Italy, 1982.

[7] J. D. Rhodes, "Filters approximating ideal amplitude and phase characteristics", IEEE Trans. on Circuit Theory, Vol. CT- 20, No. 2, pp. 120- 124, March 1973.

[8] H. Baher and M. O'Malley, "FIR transfer functions with arbitrary amplitude and phase with application to the design of quasi-all-pass delay equalisers", Proc. ISCAS, pp. 2489- 2492, Helsinki, Finland, 1988.

[9] B. Nowrouzian and L. S. Lee, "Minimal multiplier realisation of bilinear-LDI digital all-pass networks", Proc. IEE, Pt. G, No. 3, pp. 114- 117, June 1989.

[10] Li Ping and J. I. Sewell, "Switched-capacitor and active-RC all-pass ladder realisation", submitted for publication.

[11] R. Gregorian and G. C. Temes, "Design techniques for digital and analog all-pass circuits", IEEE Trans. Circuits and Systems, Vol. CAS- 25, No. 12, pp. 981- 988, Dec. 1978.

[12] A. G. Deczky, "Equiripple and minimax (Chebyshev) approximations for recursive digital filters", IEEE Trans. on Acoustics, Speech and Signal Processing, Vol. ASSP- 22, No. 2, pp. 98- 111, April 1974.

[13] C. Charalambous, A. Antoniou, "Equalisation of recursive digital filters", IEE Proc., Vol. 127, Pt.- G, No. 5, pp. 219- 225, Oct. 1980.

[14] Zhongqi Jing, "A new method for digital all-pass filter design", IEEE Trans. on Acoustics, Speech and Signal Processing, ", Vol. ASSP- 35, No. 11, Nov. 1987.

[15] R. K. Henderson and J. I. Sewell, "A design algorithm for all-pass delay equalisers", Digest of IEE Saraga Colloquium on Electronic Filters, pp.11/1- 11/8, London, 1989.

[16] E. Ya. Remez, "General computation methods of Tchebysheff approximation", Kiev USSR, Atomic Energy Translation 4491, pp. 1- 85, 1957.

[17] B. R. Smith and G. C. Temes, "An iterative approximation procedure for automatic filter synthesis", IEEE Trans. Circ. Theory, Vol. CT- 12, No.1, pp.107- 112, March 1967.

[18] Muller D. E., "A method for solving algebraic equations using an automatic computer", Mathematical Tables and other Aids for Computation, vol. 10, pp. 208- 215, 1985.



## **CHAPTER 4**

### **FILTER PROTOTYPE DESIGN**

#### **4.1 INTRODUCTION**

#### **4.2 PASSIVE LADDER PROTOTYPE DESIGN**

- 4.2.1 Passive ladder synthesis
- 4.2.2 Computational issues in synthesis
- 4.2.3 Iterative design of passive ladder networks
- 4.2.4 Computational issues

#### **4.3 COUPLED ITERATIVE DESIGN METHOD**

- 4.3.1 Computer method
- 4.3.2 Computational issues
- 4.3.3 High order ladder design

#### **4.4 DESIGN OF LADDER PROTOTYPES FOR SC SIMULATION**

- 4.4.1 Special topologies
- 4.4.2 Negative element values
- 4.4.3 Zeros at  $\pm 2fs$  by bilinear transformation
- 4.4.4 Realisation of zeros at  $\pm 2fs$
- 4.4.5 Synthesis for exact-LDI type SC ladder filters
- 4.4.6 Special transfer functions

#### **4.5 CONCLUSIONS**

#### **REFERENCES**

## 4.1 INTRODUCTION

Computer methods for the approximation of a transfer function within given amplitude and group delay tolerance schemes have been presented in previous chapters. However, a transfer function designed in this way will not be immediately realisable in circuit form and it must be decomposed algebraically into simple operators describing basic circuit elements [1]. This procedure is known as prototype design and forms the basis of circuit implementation in a variety of technologies. There are two principal means of decomposition; factorisation into second order terms and expansion as a continued fraction, representing biquad and ladder circuit topologies respectively. This chapter will concern itself with the numerical methods involved in prototype design. Since many reliable methods are known for polynomial factorisation, the emphasis will be on the accuracy-critical ladder design methods [2]. A unified approximation and iterative ladder design algorithm will be presented which avoids the ill-conditioned Hurwitz factorisation step [3–4].

Design of passive ladders purposely for further simulation by active circuits will be considered. Passive ladders make good quality prototypes because their low-sensitivity properties are usually inherited by corresponding active circuits [5]. However, the advantages of simulating passive ladders have always been compromised by their complicated design procedures and associated implementation cost [6]. Biquadratic cascade filters are popular because they have a very regular structure which grows by a uniform progression with increasing filter order, regardless of the type of transfer function. Design techniques for ladder structures are strongly dependent on the type of the transfer function and no simple progression with order is known at present [1,7].

A series of methods is proposed for the design of special passive ladder prototypes for simulation by active circuits. The simulating active network will be of a regular form with a minimum number of components. Canonic simulation in terms of the number of operational amplifiers can be guaranteed for all transfer function classes with imaginary zeros. Negative element values are employed to design special prototypes which unify LDI and bilinear SC ladder filter structures. The distortion introduced by approximate LDI filter design can also be removed [8–9].

## 4.2 PASSIVE LADDER PROTOTYPE DESIGN

### 4.2.1 Passive ladder synthesis

A brief review of the computational steps involved in the synthesis of a doubly-terminated passive ladder network will be given [1]. Synthesis begins from a rational transfer function in the  $s$ -domain

$$T(s) = \frac{P(s)}{E(s)} \quad (4.1)$$

where the standard naming convention is used for  $E(s)$  and  $P(s)$  as the numerator and denominator polynomials of the transfer function.

*Step 1* : The characteristic function  $K(s)$  must be obtained. It is related to  $T(s)$  by *Feldtkeller's equation* :

$$T(s)T(-s) = 1 + K(s)K(-s) \quad (4.2)$$

and this introduces an additional polynomial  $F(s)$  which must be determined from

$$F(s)F(-s) = E(s)E(-s) - P(s)P(-s) \quad (4.3)$$

For classical functions  $K(s)$  has purely imaginary roots and can be determined analytically. However, for general transfer functions which do not necessarily have maximum transmission points a Hurwitz factorisation step is involved.

*Step 2* : Construct the intermediate polynomials

$$E_{ev}(s) = \text{Even}(E(s)) \quad F_{ev}(s) = \text{Even}(F(s)) \quad (4.4)$$

$$E_{od}(s) = \text{Odd}(E(s)) \quad F_{od}(s) = \text{Odd}(F(s))$$

$$EPF_{ev}(s) = E_{ev}(s) + F_{ev}(s) \quad EPF_{od}(s) = E_{od}(s) + F_{od}(s)$$

$$EMF_{ev}(s) = E_{ev}(s) - F_{ev}(s) \quad EMF_{od}(s) = E_{od}(s) - F_{od}(s) \quad (4.5)$$

*Step 3* : According to the order of  $P(s)$  construct short or open circuit impedance polynomials. For the case of even  $P(s)$  then

$$\begin{aligned} Z_{1O}(s) &= R_1 \frac{EMF_{ev}(s)}{EPF_{od}(s)} & Z_{2O}(s) &= R_2 \frac{EPF_{ev}(s)}{EPF_{od}(s)} \\ Z_{1S}(s) &= R_1 \frac{EMF_{od}(s)}{EPF_{ev}(s)} & Z_{2S}(s) &= R_2 \frac{EMF_{od}(s)}{EPF_{ev}(s)} \end{aligned} \quad (4.6)$$

For the case of odd  $P(s)$  then

$$\begin{aligned} Z_{1O}(s) &= R_1 \frac{EMF_{od}(s)}{EPF_{ev}(s)} & Z_{2O}(s) &= R_2 \frac{EPF_{od}(s)}{EPF_{ev}(s)} \\ Z_{1S}(s) &= R_1 \frac{EMF_{ev}(s)}{EPF_{od}(s)} & Z_{2S}(s) &= R_2 \frac{EMF_{ev}(s)}{EMF_{od}(s)} \end{aligned} \quad (4.7)$$

*Step 4* : Select highest order impedance polynomial and extract from it a series of two port networks by *pole removal operations*. This is the forward synthesis step.

*Step 5* : Perform a reverse synthesis using the highest order impedance seen from port 2. Determine the terminating resistor value  $R_2$  by ratio of corresponding elements to the forward synthesis.

#### Pole Removal Operations

A passive ladder network can be viewed as a cascade connection of two-port networks, each realising a loss pole (or a zero of  $P(s)$ ). The pole removal operations at *Step 4* of the synthesis procedure involve decomposing an impedance polynomial into a succession of these two-port impedances.

Starting from a given driving point resistance  $Z_1(s)$  can be decomposed as a connection of a two-port network to an unknown network impedance of lower order  $Z_2(s)$ . The type of two-port section that may be removed depends on the position of the loss poles of the impedance polynomial. In minimum phase transfer functions there are three main types of loss pole,

*Pole at zero* : can be realised by a series capacitor or a shunt inductor. For the former case (Fig. 4.1)

$$Z_1(s) = \frac{1}{sC} + Z_2(s) \quad (4.8)$$

where  $C$  is the value of the capacitor. It can be seen that

$$\lim_{s \rightarrow 0} Z_1(s) = \lim_{s \rightarrow 0} \frac{1}{sC} \quad (4.9)$$

and so  $C$  can be determined from

$$C = \lim_{s \rightarrow 0} \left[ \frac{1}{sZ_1(s)} \right] \quad (4.10)$$

where the remaining unknown impedance may be calculated from

$$Z_2(s) = Z_1(s) - \frac{1}{sC} \quad (4.11)$$

Further pole removal steps may proceed from  $Z_2(s)$ . Note that for a finite value of  $C$  to be obtained from (4.10)  $Z_1(s)$  must have a single pole at  $s=0$ . Thus certain conditions are imposed on the form of  $Z_1(s)$  for a given pole removal operation to be appropriate.

*Pole at infinity* : appropriate two-ports are a shunt capacitor or a series inductor. For example, the value of a shunt capacitor (Fig. 4.2) may be established by examining the behaviour of the reactance function  $Z_1(s)$  at  $s \rightarrow \infty$ .

$$C = \lim_{s \rightarrow \infty} \left[ \frac{1}{sZ_1(s)} \right] \quad (4.12)$$

and the remainder reactance is

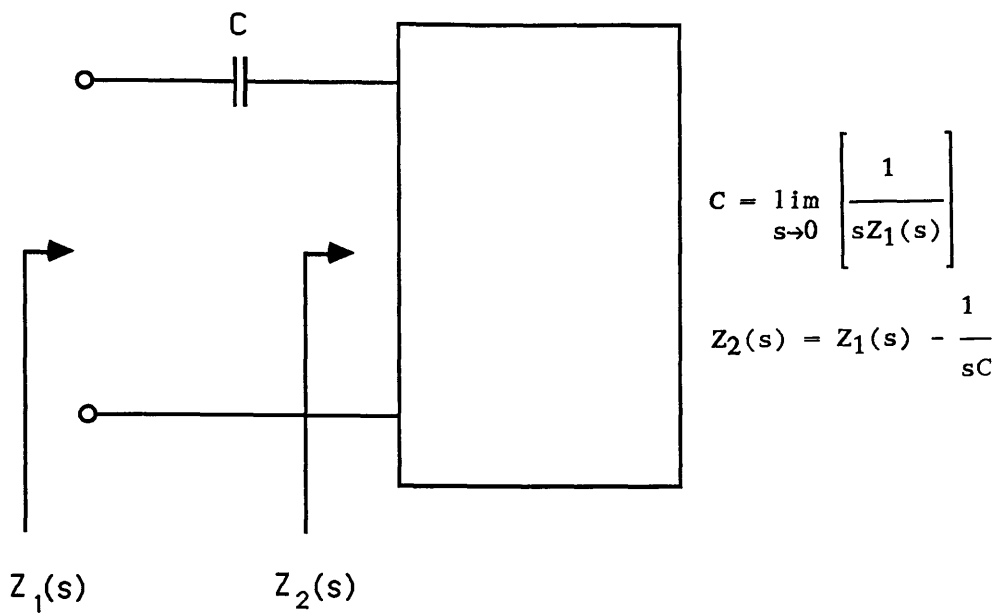


Fig. 4.1 Removal of a pole of impedance at  $s=0$

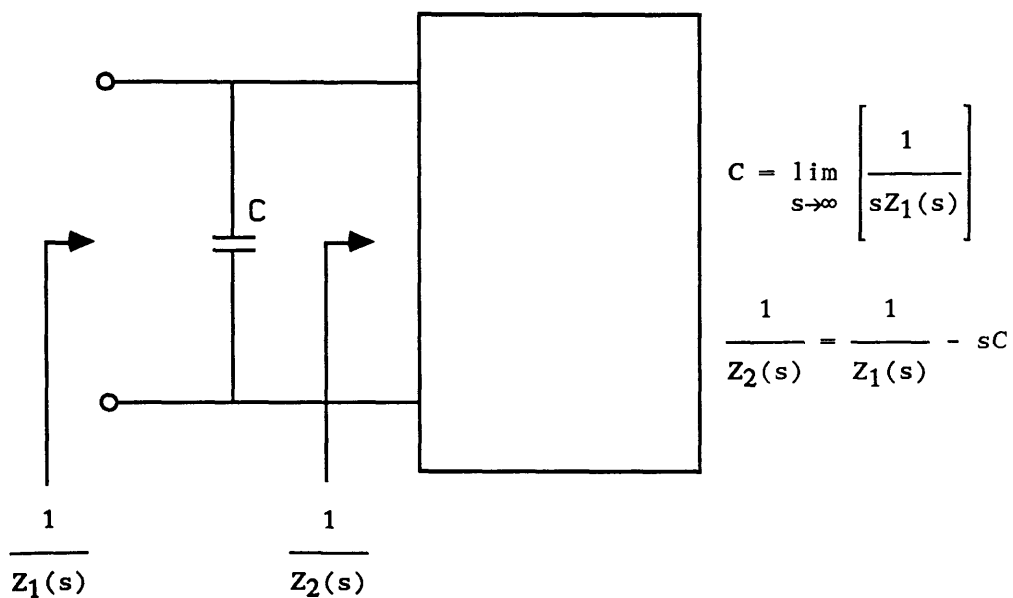


Fig. 4.2 Removal of a pole of admittance at  $s=\infty$

$$\frac{1}{Z_2(s)} = \frac{1}{Z_1(s)} - sC \quad (4.13)$$

*Pole at  $s=j\omega_n$*  : an appropriate two-port section is a shunt capacitor with a series resonant LC branch (several others are also possible). This two-port is composed of a shunt and series branch. The shunt capacitance branch is removed first. Its value can be determined by supposing that the series resonant network to follow will produce an open circuit (infinite impedance) at the required pole frequency  $\omega_n$ . At this frequency the network reduces simply to the single shunt capacitor. Thus

$$C = \lim_{s \rightarrow j\omega_n} \left[ \frac{1}{sZ_1(s)} \right] \quad (4.14)$$

and the remainder impedance is

$$\frac{1}{Z_2(s)} = \frac{1}{Z_1(s)} - sC \quad (4.15)$$

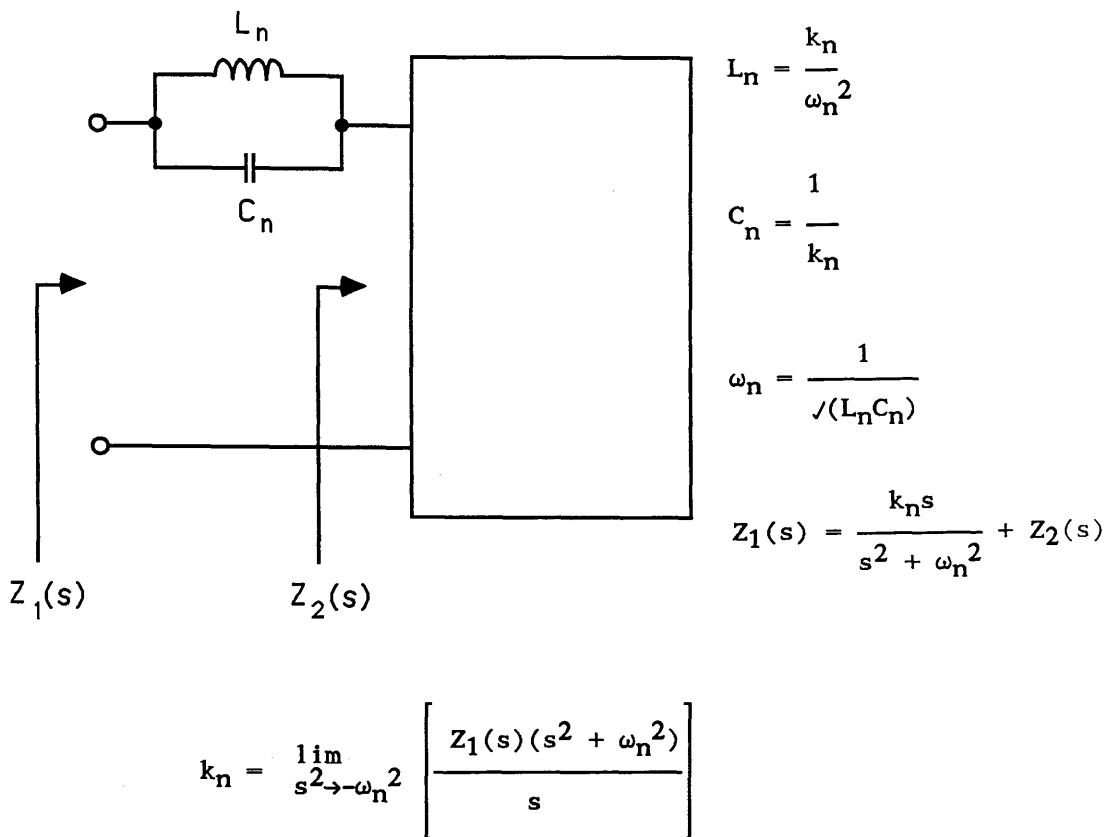
This operation is called a partial pole removal since the effect of the shunt capacitor is to prepare for a full pole removal by the series resonant branch (Fig. 4.3). The element values may be obtained from (re-assign  $Z_1(s)=Z_2(s)$ )

$$C_n = \left[ \frac{s}{(s^2 + \omega_n^2)Z_1(s)} \right]_{s^2 = -\omega_n^2} \quad L_n = \frac{1}{\omega_n^2 C_n} \quad (4.16)$$

and the final remainder impedance  $Z_2(s)$  is

$$Z_2(s) = Z_1(s) - \frac{s}{C_n(s^2 + \omega_n^2)} \quad (4.17)$$

There are various other two-port sections which can be removed. For a full treatment see [1-4].



**Fig. 4.3 Removal of a pole of impedance at  $s = j\omega_n$**



#### 4.2.2 Computational issues in synthesis

The pole removal operations involved in synthesis are numerically ill-conditioned [2]. They involve many subtractions of nearly equal numbers causing cancellation errors. Sources of inaccuracy can be seen to arise from

##### 1. Representation of polynomials in coefficient form e.g.

$$a_0 s^{-n} + a_1 s^{-(n-1)} + a_2 s^{-(n-2)} + \dots + a_{n-1} s + a_n$$

The loss of accuracy due to this polynomial form may be illustrated by means of a simple example: if the factor  $(s + 1.010)$  is multiplied by  $(s + 1.020)$  the result is (rounded to four decimal digits),

$$s^2 + 2.030s + 1.030$$

If this function is now re-factored the factors are calculated to be  $(s + 1.000)$  and  $(s + 1.030)$ . Thus information has been lost about the variation of the function around the root positions by the coefficient representation.

An improved method is to store the roots of the polynomial directly (factored form) and never to multiply out into coefficient form [10]. The multiplication of polynomials involves simply adding lists of root positions, whereas addition must be done by root finding of the combined polynomial. This is not inconvenient since a factorisation of a similar kind must be undertaken at *Step 2*.

2. The poles of the transfer function tend to cluster tightly around the passband region of the imaginary axis [11]. The finite precision of numbers on a digital computer means that there is insufficient resolution for the accurate representation of these pole positions. A loss of accuracy in the position of these roots causes a distortion of the designed passband response of the filter. The numerical conditioning may be improved by increasing the separation of the root positions by a bilinear transformation,

$$z^2 = \frac{1-s^2}{1+s^2} \quad (4.18)$$

All calculations must be done in terms of the transformed variable  $z$ , to benefit from the improved relative spacing of roots in the  $z$ -plane. Methods have been presented to perform both filter approximation and ladder synthesis in the  $z$  variable [11]. However certain complications are also introduced into the software, associated with the need to manipulate surds. In addition, the transforms involved must vary according to the class of filter making it difficult to write a comprehensive program. The technique is particularly successful for the design of maximum transmission filters of the classical types.

The quality of the element values can be further improved by synthesising from all four ABCD parameters, and taking average values from a forward and reverse synthesis [12].

#### 4.2.3 Iterative design of passive ladder networks

Orchard has proposed a very simple but efficient algorithm to design an RLC ladder from a given reflection function  $\rho(\omega)$  [13]. The structure of the ladder is prescribed and only the component values remain to be determined. A set of real and imaginary parts,  $\{\text{Re}[\rho(\omega_{tk})], \text{Im}[\rho(\omega_{tk})]\}$  are used to set up the objective function vector,  $F$ , for Newton type iteration and component values,  $\{y_k\}$ , form a vector of variables  $Y$  [14]. The core of Orchard's algorithm is an elegant, well conditioned method to compute  $F$  and the Jacobian matrix of derivatives

$$\text{Re} \left[ \frac{\partial \rho(j\omega_{tk})}{\partial y_i} \right] \quad \text{and} \quad \text{Im} \left[ \frac{\partial \rho(j\omega_{tk})}{\partial y_i} \right]$$

by chain matrix calculations.

#### 4.2.4 Computational issues

Unlike synthesis, an analysis of a ladder network can be done with great precision. Orchard's method therefore offers excellent accuracy of final component values (comparable to those obtainable from explicit formulae). In addition the program required is simple and concise. Execution time is greater than for a synthesis approach and the convergence can be unreliable from poor initial guesses.

## 4.3 COUPLED ITERATIVE DESIGN METHOD

### 4.3.1 Computer method

In the case of certain classical approximations, where the points of maximum or minimum transmission ( $\rho(j\omega)=0$  or  $\rho(j\omega)=1$ ) are known, the explicit calculation of  $\rho(j\omega)$  is not necessary for Orchard's algorithm. However in general, Orchard's method requires the formation of  $\rho(j\omega)$  by Hurwitz factorisation of  $|\rho|^2$  as in classical synthesis, which is an ill-conditioned procedure [2]. In the following an extension of Orchard's method is described which works with more general forms of  $|\rho|^2$  but eliminates any root finding requirement [15].

The value of  $|\rho|^2$  and its derivatives at the touch points  $\{x_{ti}\}$  can be chosen as the objective function for the Newton's scheme. The derivatives of  $|\rho|^2$  with respect to the element values,  $\{y_k\}$ , are required for the construction of the Jacobian matrix and are given by (let  $x_{ti} = -\omega_{ti}^2$ )

$$\frac{\partial}{\partial y_k} \left( \frac{d^r |\rho(\omega_{ti})|^2}{dx^r} \right) = 2 \frac{d^r}{d\omega^r} \left\{ \text{Re} [\bar{\rho}(j\omega_{ti}) \frac{\partial \rho(j\omega_{ti})}{\partial y_k}] \right\} \quad (4.19)$$

for  $r = 0, \dots, \mu_i$  and  $i = 1, 2, \dots, M$

Notice that here  $\bar{\rho}$  (the conjugate of  $\rho$ ) and  $\partial \rho / \partial y_k$  are obtained from the approximate network with guessed component values, which can be generated by Orchard's algorithm and then the remaining part of (4.19) can be calculated by a numerical differentiation. Here it is also found efficient to use 'cluster' method mentioned earlier in Section 2.4.2. The objective function  $|\rho(\omega_{ti})|^2$  and derivatives are obtainable from a unilateral passband approximation of Section 2.3.6. This provides a direct link between approximation and ladder design procedures, bypassing the traditional Hurwitz factorisation step.

### 4.3.2 Computational issues

No additional programming effort or computation cost is incurred by the extended algorithm. Both the original and extended Orchard's algorithms have good convergency for lowpass functions.

The advantages of both iterative design and classical synthesis methods can be usefully combined. A synthesis program, can be used to decide the structure

of the ladder and can provide initial guesses of component values. An iterative algorithm can then be used for accuracy refinement. The synthesis program may be much simplified by dropping the use of complicated accuracy preservation measures.

Continuation methods [14] are particularly useful in this problem to maintain the convergency of Newton iteration. It is important that the values of the components obtained are realisable i.e. positive and not too large or small. Continuation methods ensure that if the iteration is started with a set reasonable initial values, then it usually terminates with a set of reasonable solution values.

#### **4.3.3 High order ladder design**

In the case of very high order design (above 50) where ordinary synthesis programs would meet severe numerical difficulties a special approach may be taken. Observation of standard filter tables [16] reveals that there is some pattern of progression in element values of filters having similar ripple specifications for different orders. This raises the possibility of predicting the element values for higher order ladders from lower order ones. The procedure starts with a relaxed specification and a low order ladder, ( $n = 5, 6, 7, \dots$ ) is produced by any conventional method. The component values for high order ladders are predicted by a third order extrapolation technique. Because the structures of even and odd order ladders differ topologically, it is better to increment the order by 2 at each step to retain the even or odd property. As the orders increase, the specifications also approach their prescribed state. Filters up to 100th order have been designed in this way without loss of accuracy.

### **4.4 DESIGN OF LADDER PROTOTYPES FOR SC SIMULATION**

#### **4.4.1 Special topologies**

Ladder networks which are designed for the purpose of simulation by active or switched-capacitor circuits must conform to certain rules to ensure efficient implementation. An unsuitable structure of ladder can, depending on the simulation method, result in a circuit with an excess number of op-amps, switches and capacitors. In this thesis, operational simulation methods are employed which choose the node voltages of the ladder as internal variables of the SC filter. The efficiency of the simulation is directly dependent on the number of nodes in the prototype. Therefore, ladder networks are sought with a

minimum number of nodes (normally half the order of the transfer function). Synthesis operations must be restricted to a set of two-port sections without unnecessary internal nodes (Fig. 4.4). Note that the dual two-ports have more nodes but fewer loops and would be suitable if loop currents were the simulated variables.

#### 4.4.2 Negative element values

Certain sequences of pole removal operations may cause negative element values to occur in the passive prototype. Their occurrence can be predicted from the Fujisawa conditions [17]. Although negative elements cannot be realised by strictly passive RLC circuits, they can be easily simulated by active circuits. In fact, it will be seen that provided

$$\sum_j C_{ij} + \sum_j \frac{1}{L_{ij}} + \sum_j G_{ij} > 0$$

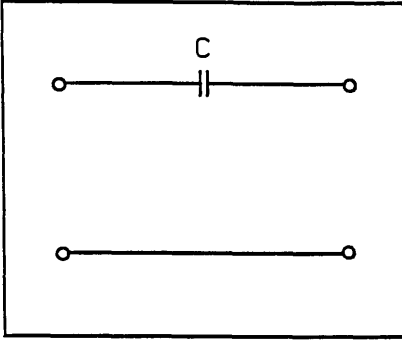
then the passive prototype can be simulated by switched-capacitor circuits without the need for inverted signals. No ladder derived from a stable, passive transfer function has been observed to disobey this rule. It has also been proven [18] that the presence of a negative element does not influence the inherent stability or sensitivity properties. The ladder synthesis program can be further simplified by relaxing the criterion that all element values be positive.

#### 4.4.3 Zeros at $\pm 2fs$ by bilinear transformation

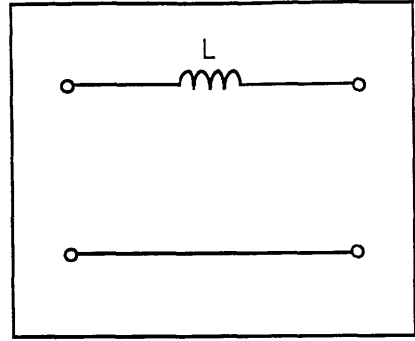
It can be shown that transfer function zeros at  $\pm 2fs$  ( $fs$  is the sampling frequency) on the real axis of the  $s$ -domain can be efficiently realised by switched-capacitor ladder filters [18]. There is no need for capacitor loops or special feed-in branches which are required for realisation of imaginary axis zeros.

Real axis zeros at  $\pm 2fs$  can be introduced by bilinear transformation of a transfer function approximated in the  $z$ -domain. The transfer function can be linearised in terms of  $\cos(\omega T)$  by working with a magnitude squared function;

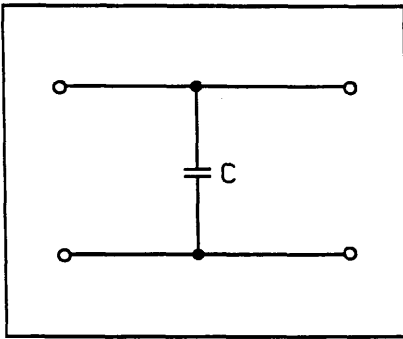
$$T(z)T(z^{-1}) = \frac{N(\cos(\omega T))}{D(\cos(\omega T))} \quad (4.20)$$



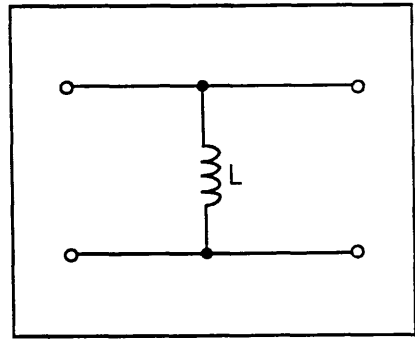
SERIES C



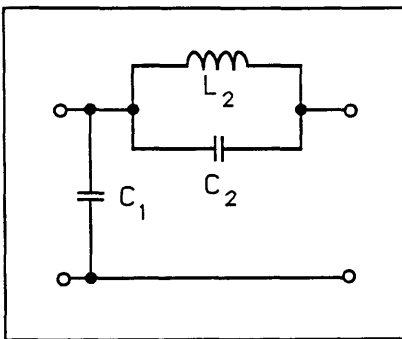
SERIES L



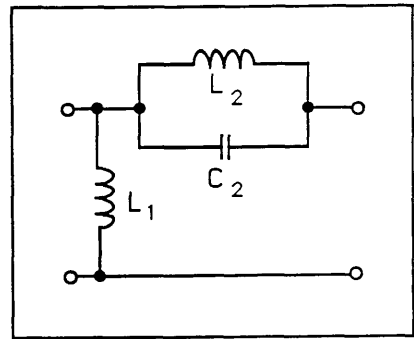
SHUNT C



SHUNT L



SHUNT C SERIES L C



SHUNT L SERIES L C

Fig. 4.4 Set of minimum node two-ports

where the numerator order is NN and the denominator order is ND. The bilinear transformation is

$$s = \frac{2}{T} \frac{1 - z^{-1}}{1 + z^{-1}} \quad (4.21)$$

and

$$\cos(\omega T) = \frac{z + z^{-1}}{2} \bigg|_{s=j\omega} \quad (4.22)$$

$$\cos(\omega T) = \frac{1 + \left[ \frac{s}{2fs} \right]^2}{1 - \left[ \frac{s}{2fs} \right]^2} \bigg|_{s=j\omega} \quad (4.23)$$

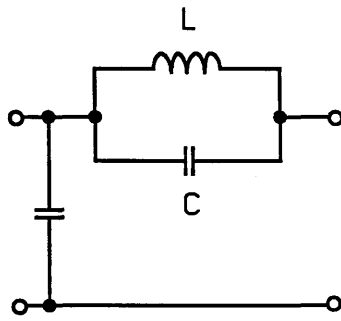
If (4.23) is substituted into the magnitude squared function (4.20) and  $NN < ND$  then the result is

$$T(s)T(-s) = \frac{N(s)N(-s)}{D(s)D(-s)} \left[ 1 - \left[ \frac{s}{2fs} \right]^2 \right]^{(ND-NN)} \quad (4.24)$$

Thus  $(ND - NN)$  zeros at infinity in the  $z$ -domain are transformed to  $\pm 2fs$  on the real axis of the  $s$ -domain in  $T(s)$ . Zeros at  $z = -1$  are transformed to infinity.

#### 4.4.4 Realisation of zeros at $\pm 2fs$

When the order of numerator and denominator polynomials differs by even degree pairs of zeros at  $+2fs$  and  $-2fs$  are introduced into the  $s$ -domain transfer function. The transfer function is now of non-minimum phase type and hence does not have a strictly positive RLC prototype realisation. In fact a single negative element must be synthesised as part of a parallel tuned circuit (Fig 4.5).



$$s^2 = -\frac{1}{LC} = -\frac{4}{T^2}$$

**Fig.4.5 Two-port realisation of zeros at  $+2f_s$  and  $-2f_s$**



A simple modification to the classical synthesis program can be made to permit these negative tuned circuits to be realised. A sign must be associated with the square of the resonant transmission zero frequencies. If the sign is negative a negative component value must be synthesised.

#### 4.4.5 Synthesis for exact—LDI type SC ladder filters

The synthesis of prototype ladders for exact simulation by LDI switched—capacitor filter structures has received much attention [19–23]. Unfortunately, the resistive termination of classical ladder prototypes cannot be simulated properly by LDI—type integrators and the approximate simulation introduces a distortion of the desired frequency response (Fig. 4.6) [8–9]. Classical synthesis procedures can be modified to take this distortion into account, producing a special prototype which can be simulated exactly by replacement of LDI—type integrators. However, the prototype must be synthesised in terms of LDI—type frequency variables, requiring complex, special—purpose synthesis and Hurwitz factorisation software rather than re—using existing, well—tested programs [24–25].

A method is now proposed which can produce prototypes for LDI—type SC ladder filter structures using mainstream s—domain synthesis methods. The expected LDI—type distortion is removed, resulting in SC filters with exact frequency response. The approximation and instability problem inherent in the use of the LDI transform is avoided. Only the exact bilinear transform is employed.

It has been shown [26] that an approximate realisation of a passive ladder by an LDI—type SC filter structure introduces a distortion factor into the frequency response of

$$|T'(j\omega)| = \frac{1}{\cos(\omega T/2)} |T(j\omega)| \quad (4.25)$$

This produces an upward weighting which becomes worse as the signal—to—sampling frequency ratio is reduced. If instead a transfer function with an inverse weighting is designed

$$\cos(\omega T/2) |T(j\omega)|$$

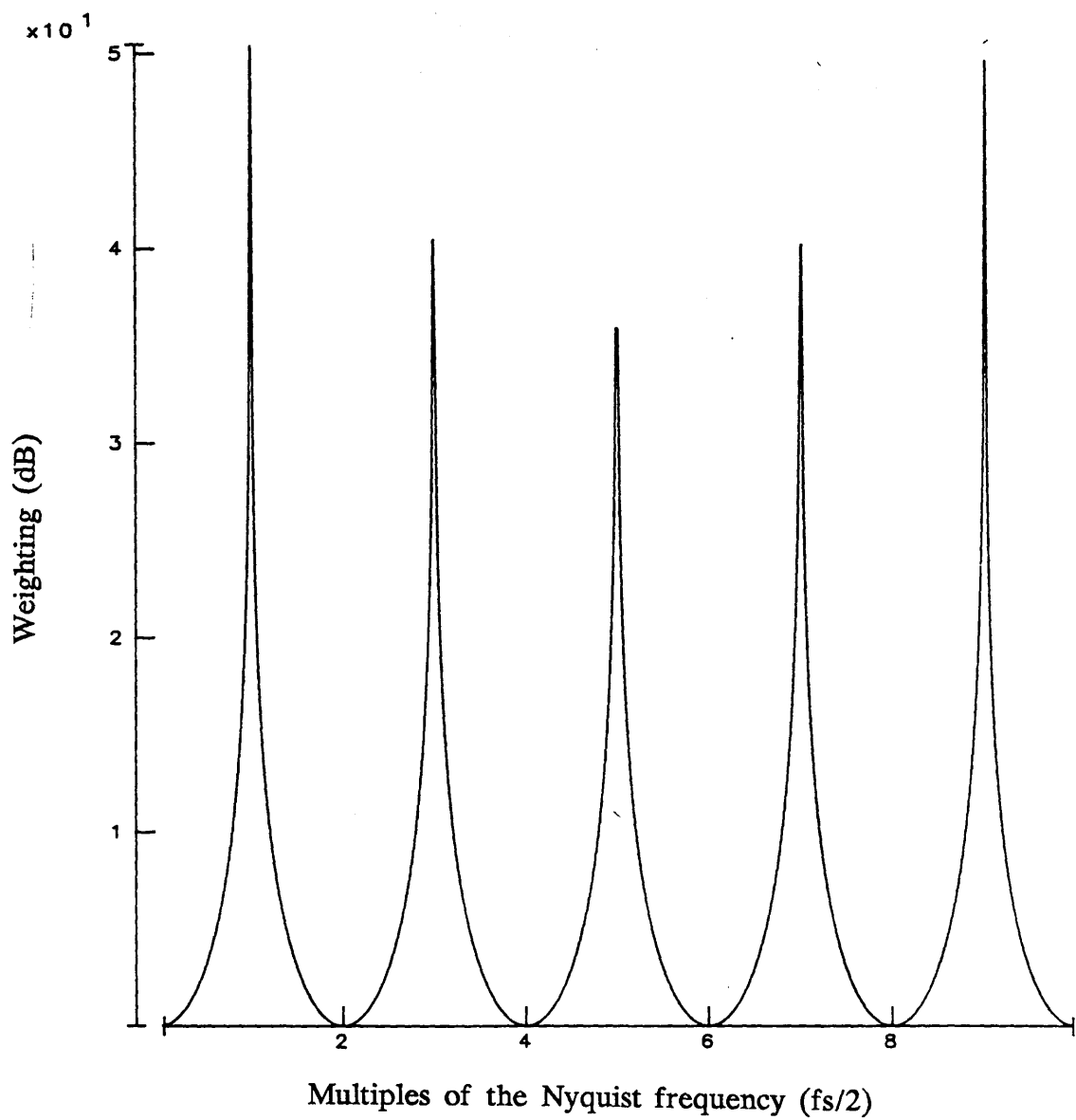


Fig. 4.6 Distortion due to termination error in LDI ladder simulation

the resulting approximate realisation will have the original intended frequency response.

There are two ways of weighting the transfer function,

1. The filter amplitude specifications can be weighted by the factor  $|\cos(\omega T/2)|$  in the passband. The general approximation methods of the previous chapter can be applied to design a pre-distorted transfer function.

2. If the difference between the orders of the numerator and denominator of the approximated transfer function is an odd number then an unpaired numerator factor  $(1 - s/(2fs))$  will occur after bilinear transformation to the  $s$ -domain. If this term is deleted from the transfer function this is equivalent to scaling by a factor  $\cos(\omega T/2)$  and introducing an additional zero at infinity. The same effect can be obtained by multiplying the transfer function by a factor

$$\frac{1}{\left[ 1 - \frac{s}{2fs} \right]}$$

However this has the effect of increasing the order of the transfer function by 1.

Synthesis of the prototype proceeds as normal from the  $s$ -domain transfer function. Simulation of the prototype is done using the bilinear transform. Special considerations are presented in the next chapter.

#### 4.4.6 Special transfer functions

Transfer functions with finite (non-zero) transmission at high frequency are difficult to realise efficiently by integrated ladder filters. A common example of this problem occurs in the realisation of even order elliptic functions. Passive ladder networks must have open or short circuit characteristics (implying full or zero transmission) at zero or infinite frequency respectively [27]. Therefore, lowpass or bandpass functions with finite (non-zero) stopband transmission at these extreme frequencies cannot be synthesised as passive ladders. 'Pure' even order elliptic functions and their frequency-transformed versions belong to this category (Fig. 4.7). To obtain a realisable function, a finite transmission zero must be shifted to infinite frequency [28]. This has the dual penalty of degraded

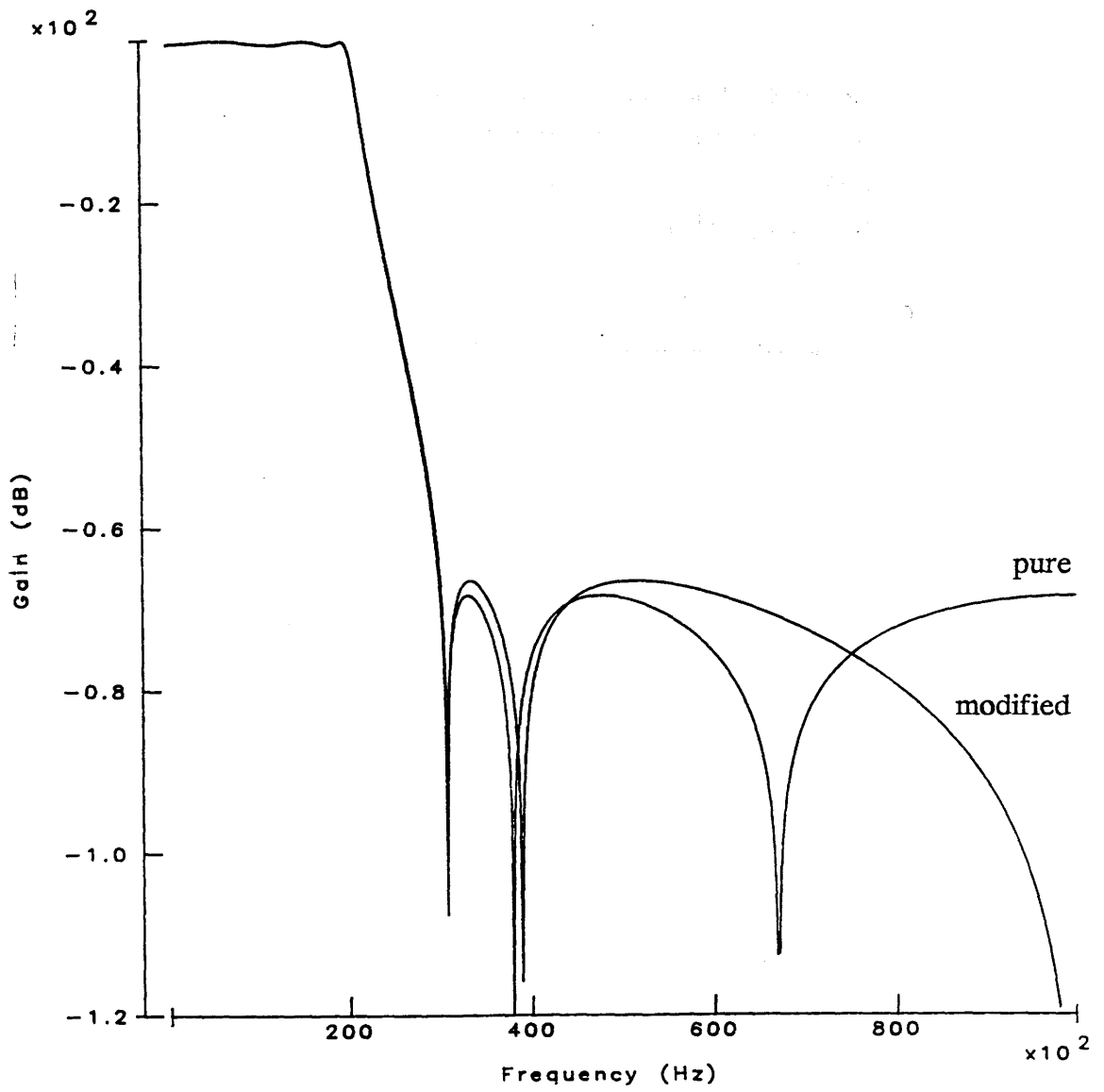


Fig. 4.7 Pure and modified 6th order lowpass elliptic functions

filter performance and non-uniform passive ladder structure between odd and even order design (Fig. 4.8), reflected also in the simulation by integrated circuits. For this reason, such transfer functions are practically undesirable for ladder simulation, since they are so close in cost to their related higher odd order function.

Another difficulty occurs in the realisation of bandstop or highpass transfer functions. Circuits obtained by straightforward operational simulation of bandstop or highpass ladder prototypes are found to be unstable [8]. Various methods have been presented to overcome this problem [29] but these further increase the complexity of design procedure.

Filter transfer functions with finite transmission at infinite frequency are taken to be of the following form

$$H(s) = \frac{A \prod_{j=1}^N (s^2 + \omega_j^2)}{\prod_{i=1}^N (s^2 + \frac{\omega_i}{Q_i} s + \omega_i^2)} \quad (4.26)$$

Where the order of numerator and denominator polynomials are identical. The function can be partitioned in the following way

$$H(s) = \frac{As \prod_{j=1}^{N-1} (s^2 + \omega_j^2)}{\prod_{i=1}^N (s^2 + \frac{\omega_i}{Q_i} s + \omega_i^2)} \times (s + \frac{\omega_N^2}{s}) \quad (4.27)$$

Define a new subsidiary transfer function as

$$H'(s) = H(s)/F(s) \quad (4.28)$$

where

$$F(s) = s + \frac{\omega_N^2}{s} \quad (4.29)$$

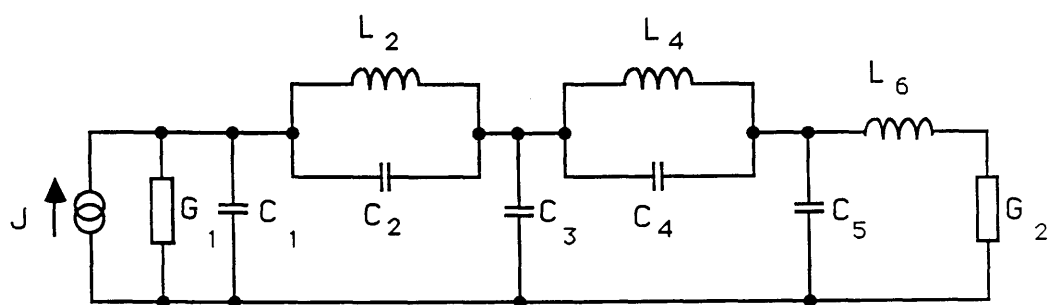


Fig. 4.8a Passive ladder realisation of modified 6th order elliptic function

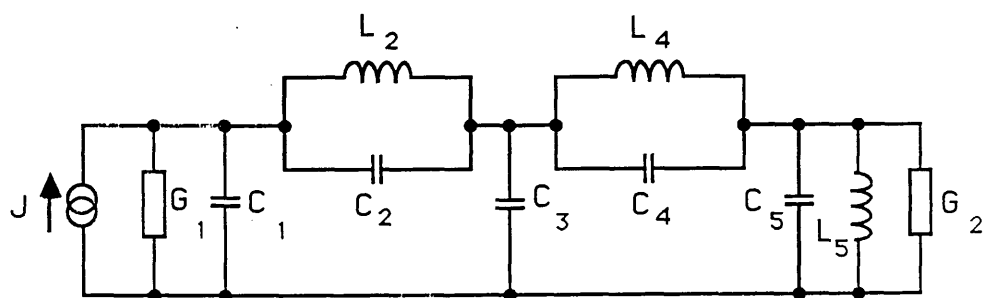


Fig. 4.8b Passive ladder realisation of pure 6th order elliptic function

$H'(s)$  now possesses zero transmission at both zero and infinite frequency and can be synthesised as a passive prototype of a minimum node form (Fig. 4.8b). It should be re-scaled to have a maximum transmission at a point in the passband to ensure optimal passive sensitivity. A canonical active simulation can now be designed with an altered input stage to realise  $F(s)$  [30].

## 4.5 CONCLUSIONS

The difficult problem of the design of passive ladder prototypes for SC simulation has been considered. It has been shown that an iterative ladder design method can be linked directly to the results of the approximation algorithm and can assist classical synthesis methods toward greater accuracy. A combination of classical synthesis methods and an iterative approach would seem to offer the best compromise in terms of accuracy and low software complexity. Transformed variable methods can be avoided greatly simplifying the synthesis part. Good initial values are then obtainable which can be further refined by a simple iterative algorithm. Very high order ladder networks have been obtained by a repeated prediction scheme.

Aside from the numerical problems of passive prototype synthesis, there is the technological one of how to design a prototype for efficient simulation by active circuits. Negative element values in the prototype can be simulated without stability or sensitivity problems. They are then employed to design LDI-type SC filter structures without the need for special synthesis software. These filters are simpler than corresponding bilinear structures but will usually have some frequency response distortion due to approximations inherent in the simulation method. However by incorporating the distortion at the approximation stage a unified 'exact' synthesis approach is obtained. Only the exact bilinear transform is employed. A major objection to ladder simulations is that it is difficult to obtain regular, canonic filter structures. By restricting the prototypes to a minimum node form of prototype regular structures can be guaranteed, without loss of generality. Furthermore, by modifying transfer functions with highpass transmission or even numerator order a prototype can always be synthesised and simulated by a stable, canonic active network.

## REFERENCES

- [1] A. S. Sedra and P. O. Brackett, "Filter Theory and Design: Active and Passive", Pitman, London, 1979.
- [2] J. A. C. Bingham, "A new method of solving the accuracy problem in filter design", IEEE Trans. on Circuit Theory, Vol. CT-11, pp. 327-341, Sept. 1964.
- [3] R. Saal and E. Ulbrich, "On the design of filters by synthesis", IRE Trans. Circuit Theory, vol. CT-5, pp.284-317, Dec. 1958.
- [4] G. Szentirmai, "Computer-aided Filter Design", IEEE Press, New York, 1973.
- [5] H.J. Orchard, "Inductorless filters", Electron. Lett., vol. 2, pp. 224-225, June, 1966.
- [6] Li Ping and J. I. Sewell, "Filter realisation by passive ladder simulation", IEE Proc., part G. vol. 135, no. 4, pp 167-176, August 1988.
- [7] A. Kaelin, R. Sigg and G. S. Moschytz, "Designing cellular parasitic-insensitive SC-ladder filters suitable for mask-programmable manufacture", Electronics Letters, Vol. 22, No. 23, pp. 1250-1252, Nov. 1986.
- [8] R. Gregorian, K. W. Martin and G. C. Temes, "Switched-capacitor circuit design", Proc. IEEE, Vol. 71, No. 8, pp941-966, Aug. 1983.
- [9] T. Choi and R. W. Broderson, "Considerations for high-frequency switched-capacitor ladder filters", IEEE Trans. Circ. and Syst., Vol. CAS-27, pp.545-552. June 1980.
- [10] C. Norek, "Product method for the calculation of the effective loss of LC filters", Proc. Int. Symp. Circ. Theory (Belgrade, Yugoslavia), pp. 353-363, 1968.
- [11] H. J. Orchard and G. C. Temes, "Filter design using transformed variables", IEEE Trans. on Circuit Theory, Vol. CT-15, No. 4, pp. 385-408, Dec. 1968.
- [12] L. F. Lind, "Accurate cascade synthesis", IEEE Trans. on Circuits and Systems, Vol. CAS-25, No. 12, pp.1012-1014, Dec. 1978.
- [13] H. J. Orchard, "Filter design by iterated analysis", IEEE Trans., Circuits and Syst., Vol. CAS-3d, No. 11, pp. 1089-1096, Nov. 1985.
- [14] S. D. Conte and C. de Boor, "Elementary numerical analysis", McGraw-Hill, pp. 120-125, 1980.
- [15] Li Ping, R. K. Henderson and J. I. Sewell, "A new filter approximation and design algorithm", Proc. ISCAS, pp. 1063-1066, Portland, Oregon, 1989.
- [16] R. Saal, "Handbook of filter design", Telefunken, W. Berlin, 1979.



- [17] T. Fujisawa, "Realizability theorem for mid-series or mid-shunt low-pass ladders without mutual induction", IRE Trans. Circuit Theory, Vol. CT-2, No. 4, pp. 320-325, Dec. 1965.
- [18] Li Ping and J. I. Sewell, "High performance filter networks and symmetric matrix systems", to be published in Proc. IEE Pt.-G.
- [19] A. Kaelin, G. S. Moschytz, "Exact design of arbitrary parasitic-insensitive elliptic SC-ladder filters in the z-domain", Proc. ISCAS, pp. 2485-2488, Helsinki, Finland, 1988.
- [20] S. O. Scanlan, "Analysis and synthesis of switched-capacitor state variable ladder filters", IEEE Trans. Circ. and Syst., vol. CAS-28, pp. 85-93, Feb. 1981.
- [21] J. Taylor, "Exact design of elliptic switched-capacitor filters by synthesis", Electronics Letters, Vol. 18, No. 19, pp. 807-809, Sept. 1982.
- [22] J. Taylor, "Stability analysis and exact design of switched-capacitor filters of the lossless discrete integrator type", PhD Thesis, University of London, 1985.
- [23] D. M. Gee, "An intentionally approximate bilinear based transform", Digest of IEE Saraga Colloquium on Electronic Filters, pp. 12/1-12/4, London 1989.
- [24] J. T. Taylor, L. F. Lind, D. G. Haigh, "An interactive technique for polynomial factorisation", Proc. IEEE ISCAS, pp. 139-142, Helsinki, Finland, 1988.
- [25] L. F. Lind, "A polynomial splitting algorithm", Digest of IEE Saraga Colloquium on Electronic Filters, pp. 1/1-1/4, London, 1987.
- [26] Li Ping, R. K. Henderson and J. I. Sewell, "Matrix methods for switched-capacitor filter design", Proc. ISCAS, pp.1044-1048, Helsinki 1988.
- [27] J. L. Herrero and G. Willoner, "Synthesis of filters", Prentice-Hall Inc., Englewood Cliffs, N.J., 1966, chap.6.
- [28] R. W. Daniels, "Approximation methods for electronic filter design", McGraw-Hill, New York, 1974, chap.6.
- [29] Li Ping and J. I. Sewell, "The TWINTOR in bandstop switched-capacitor ladder filter realisation", IEEE Trans. Circuits and Systems, Vol. CAS-36, No.7, pp.1041-1044, July 1989.
- [30] R. K. Henderson and J. I. Sewell, "A unified approach to the design of canonic integrated ladder filters", submitted for publication.
- [31] B.D. Rakovich and V.D. Pavlovic, "Method of designing doubly terminated lossy ladder filters with increased element tolerances", Proc. IEE. Part G, Vol. 134, No. 6, pp. 285-291, Dec. 1987

## **CHAPTER 5**

### **FILTER REALISATION**

#### **5.1 INTRODUCTION**

#### **5.2 SWITCHED—CAPACITOR FILTER DESIGN METHODS**

- 5.2.1 Cascade biquad design
- 5.2.2 Passive ladder simulation
- 5.2.3 Overview

#### **5.3 SYSTEMATIC DESIGN METHODS**

- 5.3.1 A general matrix form
- 5.3.2 Matrix description for SC filters
- 5.3.3 Bilinear ladder design
- 5.3.4 Ladders with finite transmission at high frequency
- 5.3.5 Bilinear/LDI ladder design
- 5.3.6 Biquad design
- 5.3.7 Analysis and scaling
- 5.3.8 Network realisation from matrix form
- 5.3.9 Computational issues

#### **5.4 CAPACITANCE SPREAD REDUCTION TECHNIQUES**

- 5.4.1 Dynamic range tradeoff
- 5.4.2 Pole removal permutations for ladders
- 5.4.3 Pole—zero pairing for biquads

#### **5.5 SUMMARY**

#### **REFERENCES**

## 5.1 INTRODUCTION

Filter realisation is concerned with producing a realisable circuit description from a given prototype expansion of a filter transfer function. Just as there are a number of different ways to expand a given transfer function into a prototype, there are many filter networks possible to realise a given prototype [1]. Chapter 5 concerns itself with computer techniques for filter network design from a pre-computed prototype. Due to the diverse nature of the procedures involved, it has been difficult in the past for software to handle more than a single filter structure, restricting the choice of filter architectures to a user [2–3]. To illustrate this point, the most popular stray-insensitive SC filter design methods, biquad and leapfrog ladder simulation are first reviewed [4–5].

A unified approach to circuit description and processing is then presented. Matrix methods, which have been so successfully applied in circuit analysis, are shown also to be an excellent vehicle for the processing of linear equations involved in circuit design [6]. A variety of design methods, both new and old can now be brought together within a single program. Various filter implementations can also be treated in a uniform manner e.g. switched-capacitor, active-RC and digital. Scaling for maximum dynamic range and minimum capacitance spread is accomplished by performing very simple matrix operations. Large component spreads can sometimes make a filter realisation not feasible due to circuit area and sensitivity. A set of computer methods are considered to ease this problem.

## 5.2 SWITCHED-CAPACITOR FILTER DESIGN METHODS

A review of the current procedures involved in realising a filter prototype as a switched-capacitor circuit is now undertaken. Only the most successful, stray capacitance insensitive filter structures are examined. There are two main architectures; cascade biquad and passive ladder simulation filters.

### 5.2.1 Cascade biquad design

A brief summary of the design steps involved in the design of a general parasitic-insensitive biquadratic filter section is given [7–10].

*Step 1* : Select a single second order rational term from the factorised transfer function in the  $z$ -domain. It will have the following general form;

$$H(z) = \frac{\gamma + \epsilon z^{-1} + \delta z^{-2}}{1 + \alpha z^{-1} + \beta z^{-2}} \quad (5.1)$$

**Step 2 :** By nodal analysis of the general second order SC filter section in Fig. 5.1 the following transfer function is obtained;

$$T(z) = - \frac{DI + (AG - DI - DJ)z^{-1} + (DJ - AH)z^{-2}}{D(F + B) + (AC + AE - DF - 2DB)z^{-1} + (DB - AE)z^{-2}} \quad (5.2)$$

**Step 3 :** Compare coefficients of (5.1) and (5.2) to obtain the following set of overdetermined, nonlinear equations

$$\begin{aligned} \gamma &= DI \\ \epsilon &= AG - DI - DJ \\ \delta &= DJ - AH \\ 1 &= D(F + B) \\ \alpha &= AC + AE - DF - 2DB \\ \beta &= DB - AE \end{aligned} \quad (5.3a-f)$$

**Step 4 :** Set  $A=B=D=1$  to yield the simplified equations

$$\begin{aligned} \gamma &= I \\ \epsilon &= G - I - J \\ \delta &= J - H \\ F &= 0 \\ \alpha &= C + E - 2 \\ \beta &= 1 + E \end{aligned} \quad (5.4a-f)$$

**Step 5 :** Assign the values of the feedback capacitors to position the poles of  $T(z)$

$$\begin{aligned} E &= 1 - \beta \\ C &= 1 + \beta + \alpha \\ F &= 0 \end{aligned} \quad (5.5a-c)$$

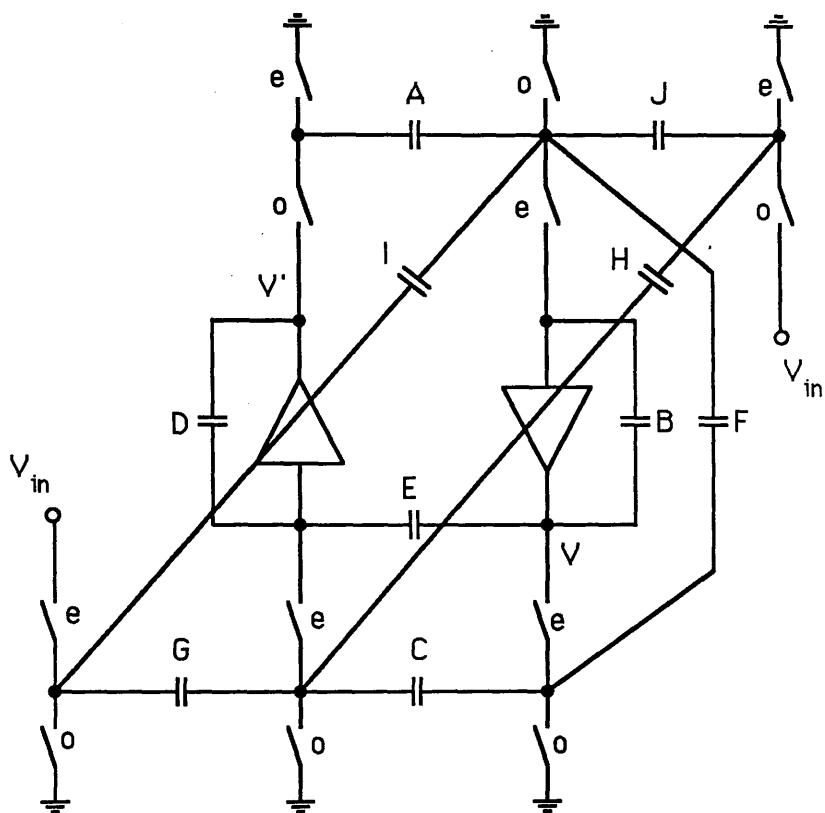


Fig. 5.1 General parasitic-insensitive biquad

and assign the values of the feedforward capacitors to position the zeros of  $T(z)$

$$\begin{aligned} I &= \gamma \\ J &= \delta + x \\ G &= \gamma + \delta + \epsilon + x \\ H &= x \geq 0 \end{aligned} \quad (5.6a-d)$$

*Step 6* : According to the type of zero being realised, attempt to cancel one or more of the feedforward capacitors e.g. often  $H=0$ .

Note that the above circuit automatically dispenses with the need for the F capacitor, using instead the E capacitor (Fig. 5.2a). It is therefore named the E-type biquad. An F-type biquad is also possible when  $E=0$ , and uses the F capacitor as feedback (Fig. 5.2b). The design equations at steps 4 and 5 are then

$$\begin{aligned} \gamma/\beta &= I \\ \epsilon/\beta &= G - I - J \\ \delta/\beta &= J - H \\ 1/\beta &= F + 1 \\ \alpha/\beta &= C - F - 2 \\ E &= 0 \end{aligned} \quad (5.7a-f)$$

leading to feedback capacitors

$$\begin{aligned} F &= (1 - \beta)/\beta \\ C &= (1 + \alpha + \beta)/\beta \\ E &= 0 \end{aligned} \quad (5.8a-c)$$

and feedforward capacitors

$$\begin{aligned} I &= \gamma/\beta \\ J &= (\delta + x)/\beta \\ G &= (\gamma + \delta + \epsilon + x)/\beta \\ H &= x/\beta \geq 0 \end{aligned} \quad (5.9a-d)$$

The biquad section must be arranged in a cascade and scaled for optimum capacitance spread and dynamic range.

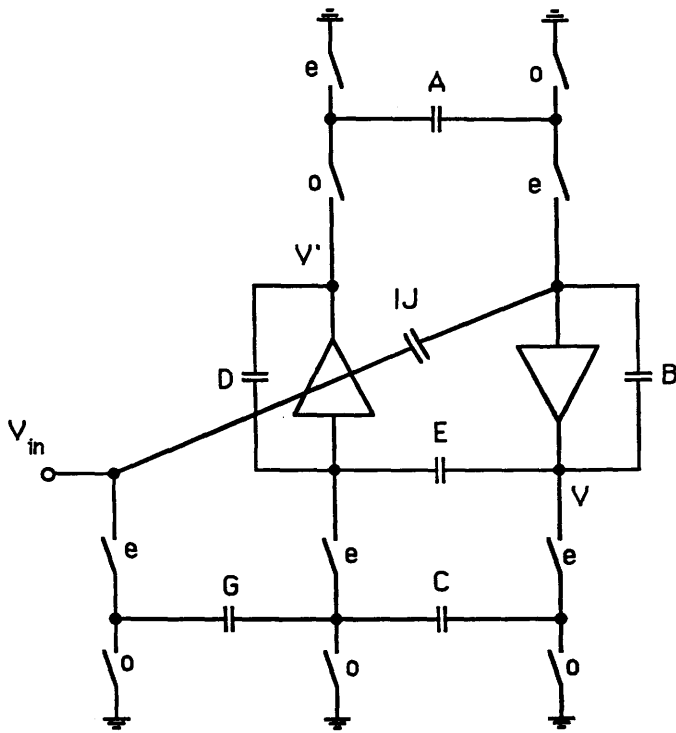


Fig. 5.2a E-type biquad

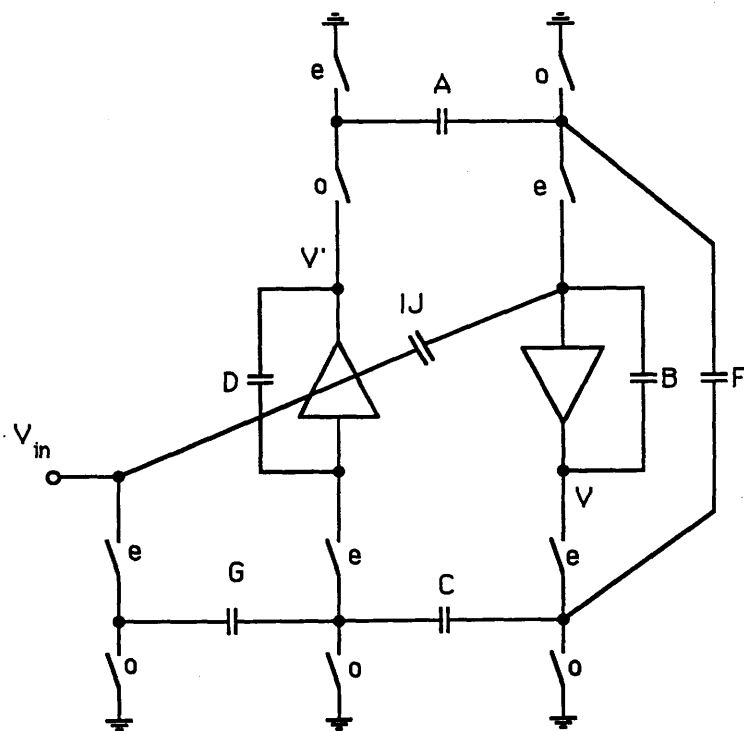


Fig. 5.2b F-type biquad

### 5.2.2 Passive ladder simulation

#### LDI leap-frog simulation

The design of a SC circuit to simulate the operation of a passive ladder prototype will now be illustrated [11–12]. Consider the 5th order all-pole doubly-terminated LC low-pass filter shown in Fig. 5.3a.

*Step 1* : Write a complete set of integral voltage/current relations for the ladder as follows

$$V_1 = (1/sC_1)(J_{in} - G_1V_1 - I_2)$$

$$I_2 = (1/sL_2)(V_1 - V_3)$$

$$V_3 = (1/sC_3)(I_2 - I_4)$$

$$I_4 = (1/sL_4)(V_3 - V_5)$$

$$V_5 = (1/sC_5)(I_4 - G_2V_5) \quad (5.10a-e)$$

*Step 2* : Draw a signal flow graph to represent these relations (Fig. 5.3b) and invert the signs of alternate variables.

*Step 3* : Realise the integration branches by alternately phased inverting and non-inverting LDI integrators (Fig. 5.3c). The capacitor ratios can be obtained by comparing the integrator coefficients and denormalising to the cut-off frequency  $\omega_c$  in radians (the LHS capacitors refer to the SC network of Fig. 5.3c).

$$\frac{C_1}{C_2} = \frac{C_{20}}{C_2} = \frac{C_{21}}{C_2} = \frac{T\omega_c}{C_1}$$

$$\frac{C_4}{C_6} = \frac{C_8}{C_6} = \frac{T\omega_c}{L_2}$$



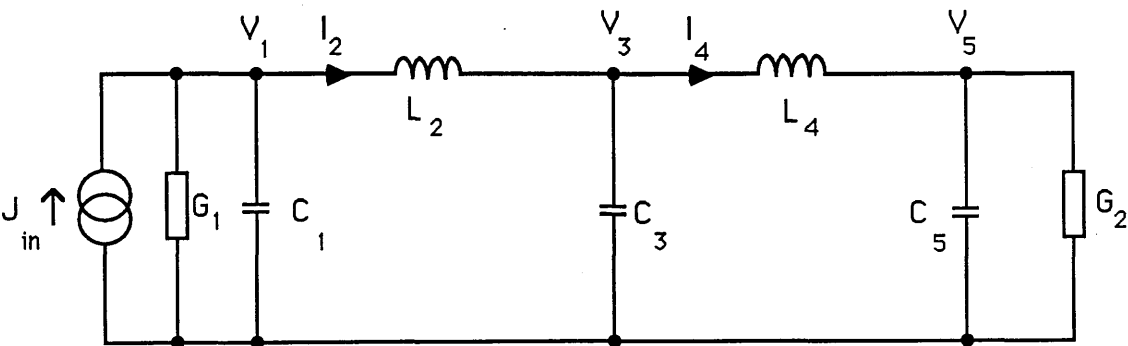


Fig. 5.3a 5th order all-pole lowpass prototype

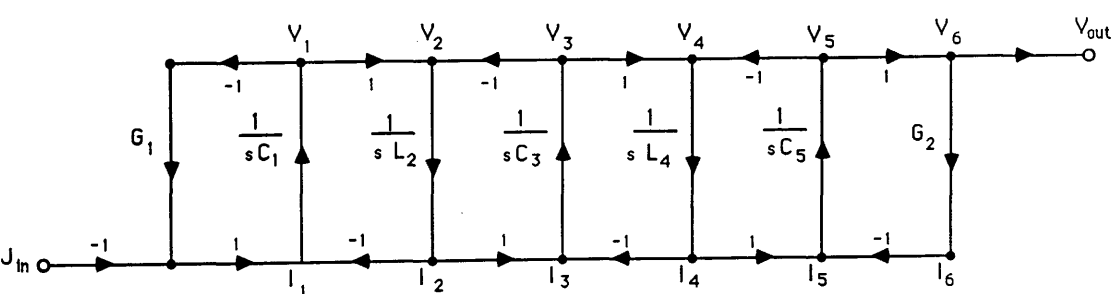


Fig. 5.3b Signal flow graph

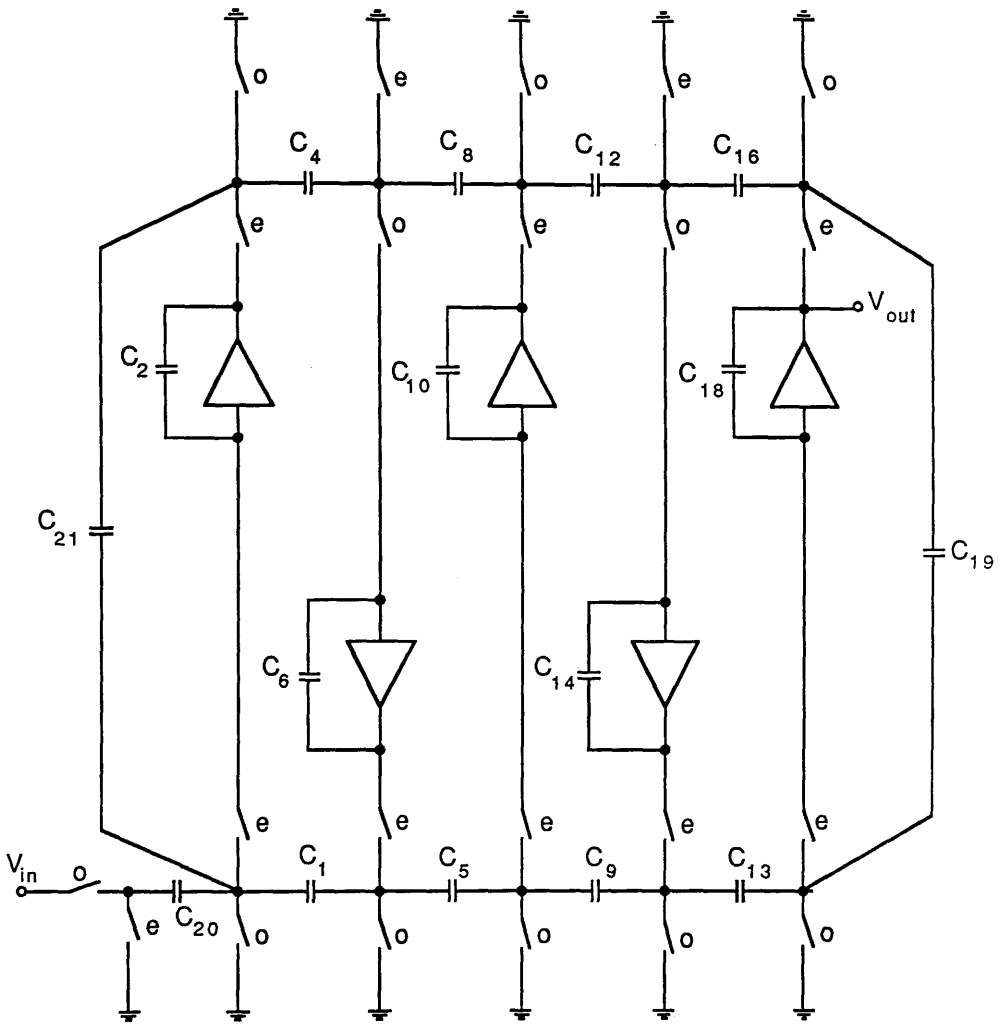


Fig. 5.3c LDI leapfrog simulation

$$\begin{aligned}
\frac{C_5}{C_{10}} &= \frac{C_9}{C_{10}} = \frac{T\omega_c}{C_3} \\
\frac{C_{12}}{C_{14}} &= \frac{C_{16}}{C_{14}} = \frac{T\omega_c}{L_4} \\
\frac{C_{13}}{C_{18}} &= \frac{C_{19}}{C_{18}} = \frac{T\omega_c}{C_5}
\end{aligned} \tag{5.11a-e}$$

Note that the terminating loop in the signal flow graph is not realised exactly by the SC circuitry, giving rise to the so-called LDI termination error distortion of the frequency response [4,13]. Thus the SC filter is only an approximate simulation of the prototype.

The ladder prototype may have a different structure, such as where an LC series tank circuit is used to realise a finite transmission zero. In this case the design process is more complicated. The prototype of Fig. 5.4a is transformed into an equivalent form with voltage-controlled voltage sources in Fig. 5.4b. Equations (5.10a), (5.10c) and (5.10e) are now rewritten as

$$V_1 = (1/sC_{12})(J_{in} - G_2V_1 - I_2) + K_{13}V_3 \tag{5.12a}$$

$$V_3 = (1/sC_{234})(I_2 - I_4) + K_{31}V_1 + K_{53}V_5 \tag{5.12b}$$

$$V_5 = (1/sC_{34})(I_4 - G_2V_5) + K_{35}V_3 \tag{5.12c}$$

defining

$$\begin{aligned}
C_{12} &= C_1 + C_2 \\
C_{234} &= C_2 + C_3 + C_4 \\
C_{45} &= C_4 + C_5 \\
K_{13} &= C_2/C_{12} \\
K_{31} &= C_2/C_{234} \\
K_{53} &= C_4/C_{234} \\
K_{35} &= C_4/C_{34}
\end{aligned} \tag{5.13a-g}$$

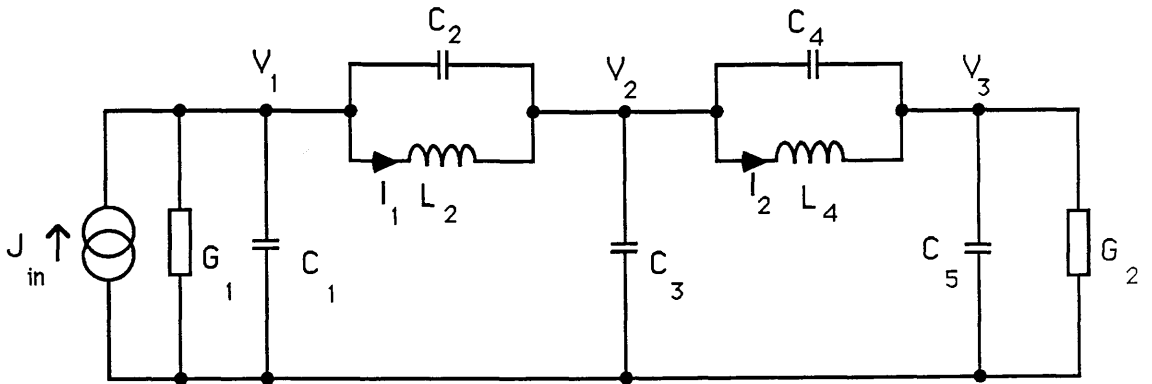


Fig. 5.4a 5th order elliptic lowpass prototype

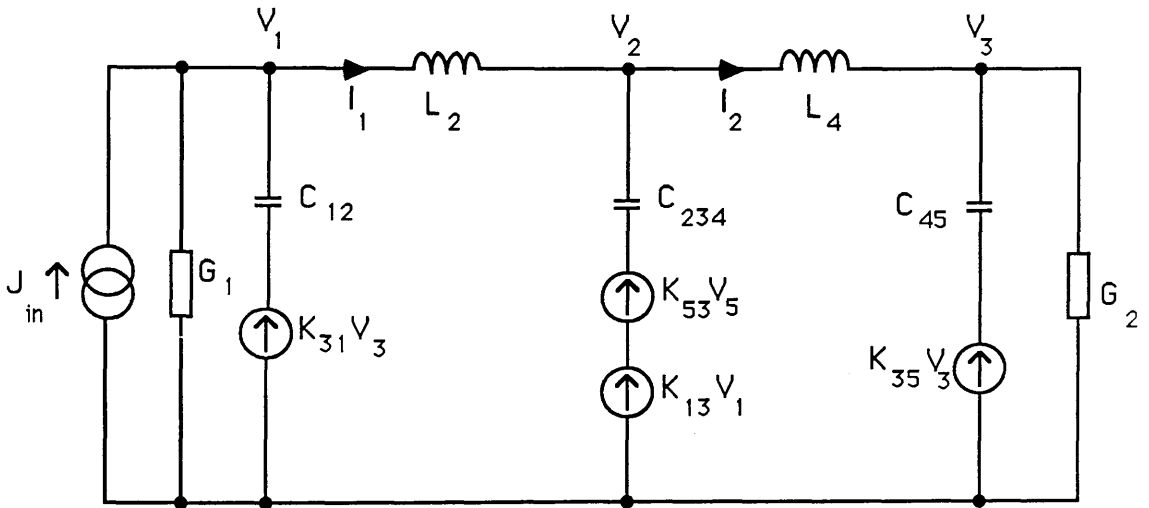


Fig. 5.4b Equivalent circuit

Apart from the integration terms, there are now multiplications and additions to be performed. Pairs of capacitive feed-through branches linking voltages  $V_1$  to  $V_3$  and  $V_3$  to  $V_5$  can be used to realise these terms (Fig. 5.4c). The integrator time constants are changed accordingly. Note that the realisation of a finite transmission zero, generally requires a pair of cross-coupled integrators in SC implementation (Fig. 5.4d).

The above method yields only an approximate simulation of the ladder prototype. Direct realisation of the continuous-time integrations by backward Euler sampled-data integrators introduces two distortions of the filter response. The first is a straightforward warping of the frequency scale which can be easily taken into account in the design process. The second is an error introduced by improper realisation of the recursive integral relationships of (5.10a) and (5.10b) representing the resistive terminations of the prototype. This so-called LDI termination error can be removed by synthesising a special ladder prototype [14–18]. In this case, the ladder involves only the LDI variables  $\gamma = \sin(\omega T/2)$  and  $\mu = \cos(\omega T/2)$ . Direct replacement by LDI integrators which automatically realise  $\gamma$  and  $\mu$  transfer functions at the termination yields an exact simulation. The design procedure is essentially the same, although the ladder synthesis is complicated.

#### Bilinear leapfrog simulation

The bilinear transform may also be used to yield an exact simulation of a passive prototype. Lee and Chang [19–20] found that a ladder, bilinearly transformed from the continuous-time domain, could be exactly simulated by the LDI design process above. Their process requires that each inductor in the prototype be compensated by adding a negative valued capacitor of appropriate value in parallel. The resulting LDI filter realises the exact bilinearly transformed transfer function. A special stray-capacitance insensitive input stage is necessary [21].

#### Coupled-biquad simulation

The internal operation of the ladder prototype was simulated in the leapfrog method by a series of current-voltage integral relations. Another technique is to simulate a set of voltage-voltage relations [22]. In this case the method is only suitable for even order prototypes such as the sixth order bandpass ladder of Fig. 5.5a. The following set of equations describe the voltage coupling relationships

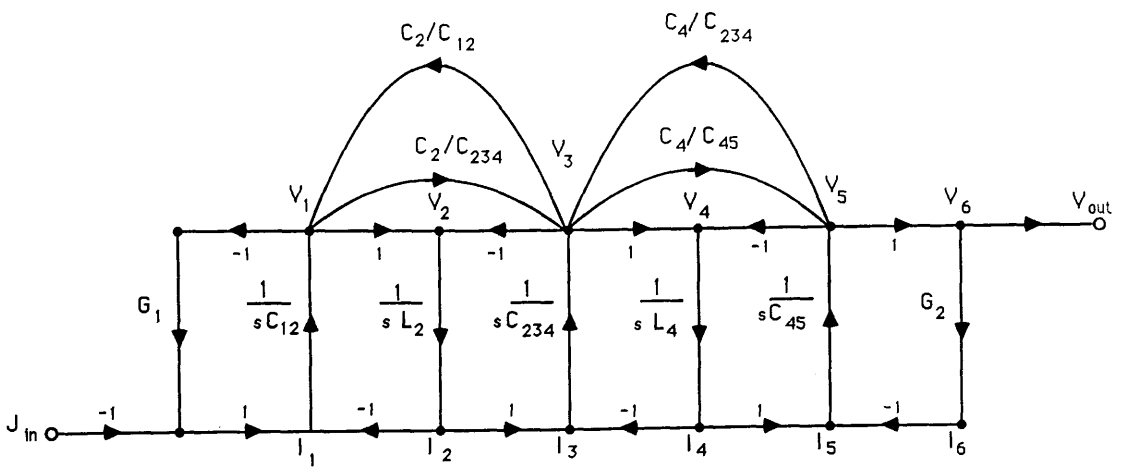


Fig. 5.4c Signal flow graph

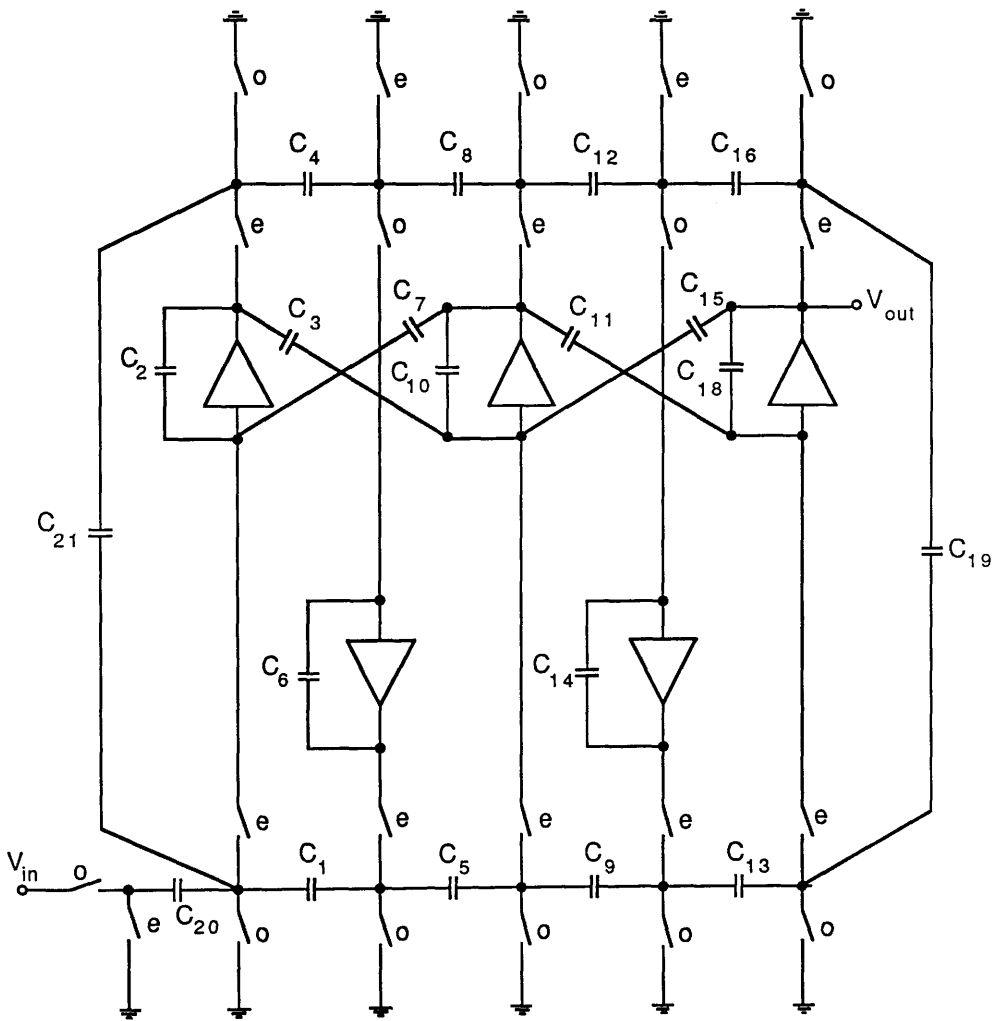


Fig. 5.4d LDI leapfrog simulation

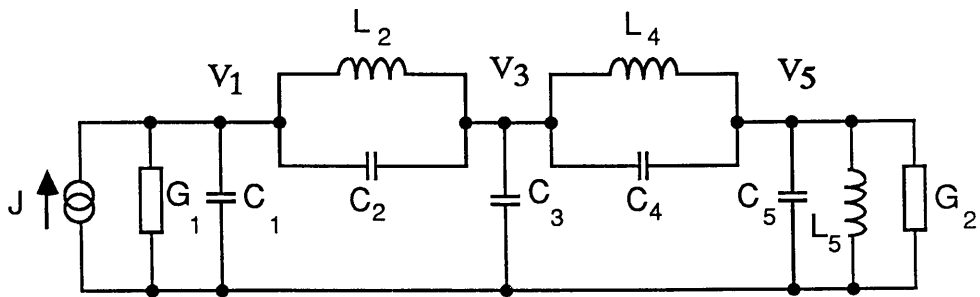


Fig. 5.5a 6th order bandpass prototype

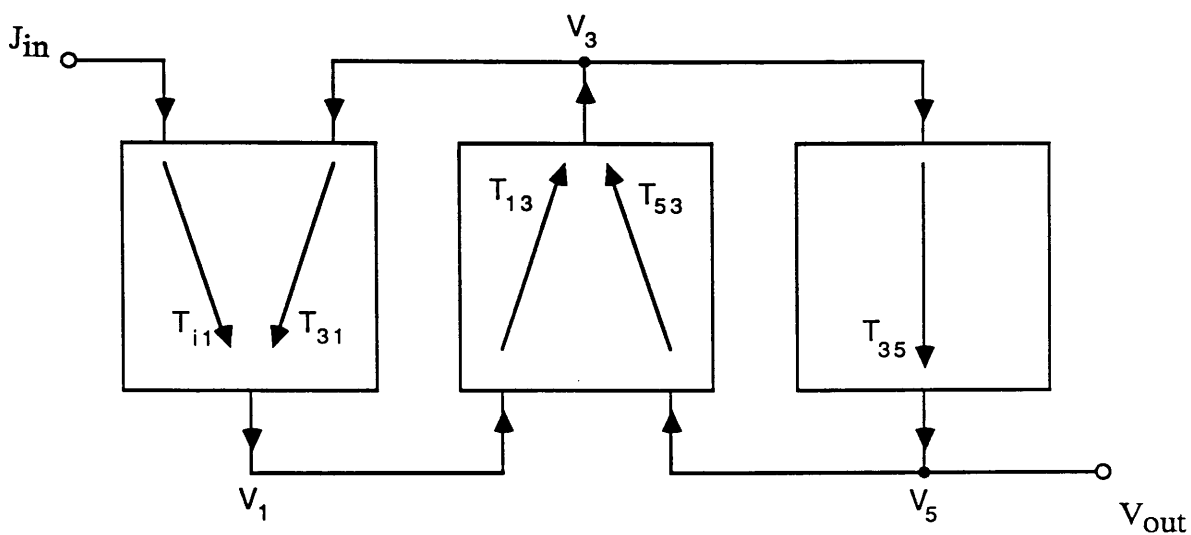


Fig. 5.5b Interconnection of biquadratic blocks

$$V_1 = T_{i1}J_{in} + T_{31}V_3$$

$$V_3 = T_{13}V_1 + T_{53}V_5$$

$$V_5 = T_{35}V_3 \quad (5.14a-c)$$

where the transfer functions are defined as

$$\begin{aligned} T_{i1} &= \left. \frac{V_1}{J_{in}} \right|_{V_3=0} & T_{31} &= \left. \frac{V_1}{V_3} \right|_{J_{in}=0} \\ T_{13} &= \left. \frac{V_3}{V_1} \right|_{V_5=0} & T_{53} &= \left. \frac{V_3}{V_5} \right|_{V_1=0} \\ T_{35} &= \frac{V_5}{V_3} \end{aligned} \quad (5.15)$$

The transfer functions can be calculated as second order rational terms of the form e.g.

$$T_{i1} = \frac{1}{C_1+C_2} \frac{s}{s^2 + s \frac{1}{R_1(C_1+C_2)} + \frac{1}{L_2(C_1+C_2)}} \quad (5.16)$$

or

$$T_{31} = \frac{C_2}{C_1+C_2} \frac{s^2 + \frac{1}{L_2 C_2}}{s^2 + s \frac{1}{R_1(C_1+C_2)} + \frac{1}{L_2(C_1+C_2)}} \quad (5.17)$$

Each second order term can be bilinearly transformed and realised by a biquad section. The interconnection of the biquads is done according to the signal flow graph of Fig. 5.5b. resulting in the circuit structure of Fig. 5.5c.



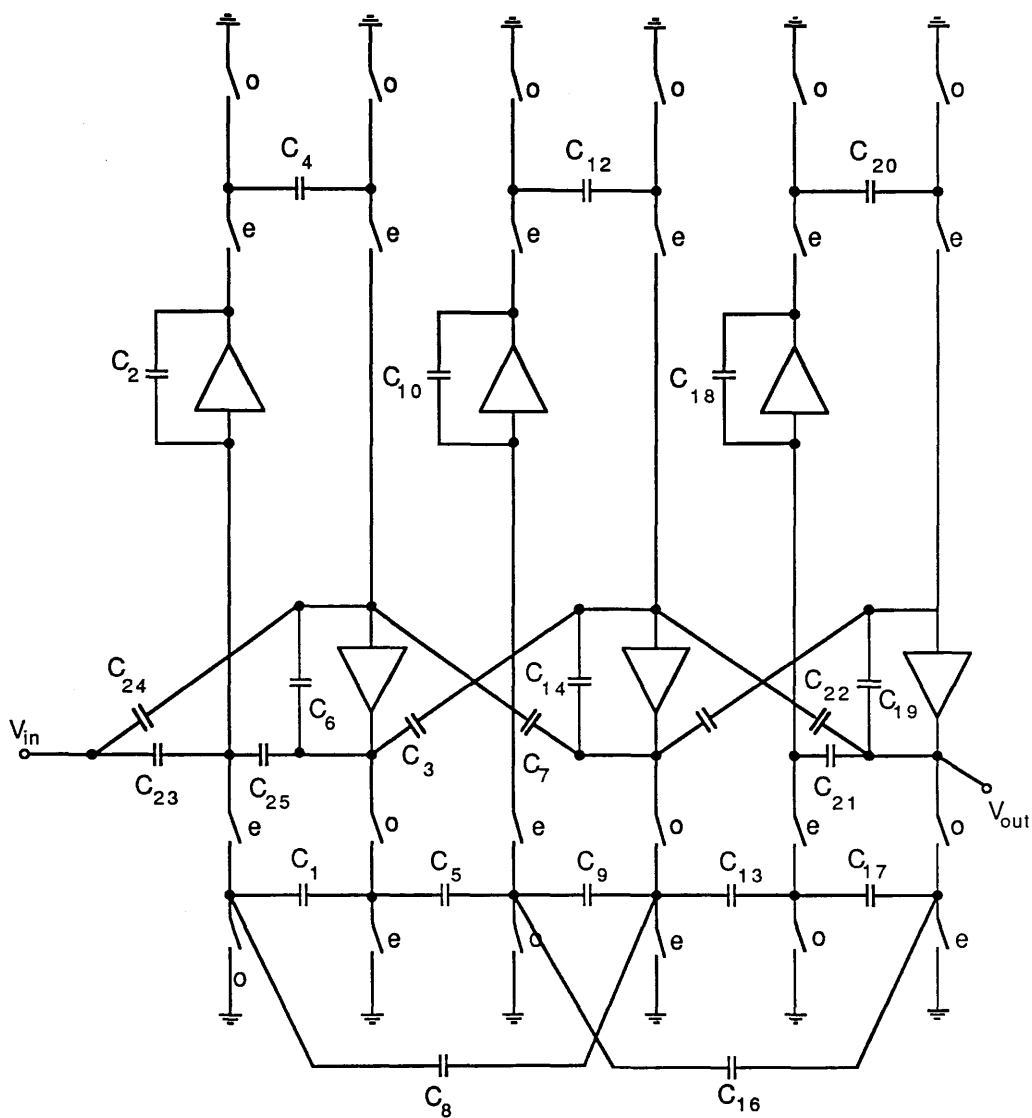


Fig. 5.5c Coupled-biquad simulation

### 5.2.3 Overview

The design methods above are now examined for suitability for computer implementation. Biquad and ladder simulation methods differ greatly and do not seem amenable to a unified treatment. The latter suffer from a lack of consistency when simulating different ladder topologies. The formulation of the set of voltage—current relations must be changed according to the position and type of elements in the ladder. In addition, there is no simple progression in ladder structure with increasing order of transfer function. Certain types of transfer function cannot at present be simulated at all by ladder structures due to instability problems or unrealisability of the passive prototype. Biquadratic filters however have no such constraints and have achieved popularity because of their flexibility and ease of design. Increases in filter order simply require additional biquad stages to be added to the cascade. Any non—minimum phase transfer function can be simulated by the general biquad section. These factors have contributed greatly to the popularity of biquad implementations over ladders.

A lack of unity exists for different ladder simulation strategies. Ladder design is inherently more complicated than biquad design due to the multi—feedback nature of the ladder structure. Different simulations appear to involve entirely different processing steps to set up their characteristic equations. Special design techniques are required depending on whether the bilinear, approximate LDI or exact LDI transformation methods are employed. Dynamic range scaling will generally require a full network frequency analysis for both filter structures, costing a great deal of computation.

## 5.3 SYSTEMATIC DESIGN METHODS

### 5.3.1 A general matrix form

A matrix description is introduced, suitable for the description and processing of both biquad and ladder filter structures. A multi—input multi—output filter network can be described by the equation,

$$MX = J \quad (5.18)$$

where  $M$  is the system matrix

$X$  is a vector of internal filter variables

$J$  is a vector of input variables

It is convenient to regard  $M$  as composed of submatrices, defining coupling relationships between sets of internal variables within  $X$ .

$$\begin{bmatrix} M_{11} & | & \cdot & \cdot & \cdot & | & M_{1n} \\ \hline \cdot & & & & & & \cdot \\ \cdot & & & & & & \cdot \\ \cdot & & & & & & \cdot \\ \hline M_{n1} & | & \cdot & \cdot & \cdot & | & M_{nn} \end{bmatrix} \begin{bmatrix} X_1 \\ \hline \cdot \\ \cdot \\ \cdot \\ \hline X_n \end{bmatrix} = \begin{bmatrix} J_1 \\ \hline \cdot \\ \cdot \\ \cdot \\ \hline J_n \end{bmatrix} \quad (5.19)$$

where  $X_i$  is the  $i^{\text{th}}$  vector of internal filter variables,

$M_{ij}$  is the submatrix relating variables  $X_i$  to  $X_j$ ,

$J_i$  is the input vector to the  $i^{\text{th}}$  variable set

Furthermore each sub-matrix can be expressed as;

$$M_{ij} = \sum_{k=1}^m \Theta_k M_{ijk} \quad (5.20)$$

where  $M_{ijk}$  is a matrix of same dimension as  $M_{ij}$ , defining connection of the  $k^{\text{th}}$  building block,

$\Theta_k$  is the transfer function of the  $k^{\text{th}}$  realisable block,

$m$  is the number of distinct types of block used in the system

The input vector is defined similarly,

$$J_i = \sum_{k=1}^m \Theta_k J_{ik} \quad (5.21)$$

where  $J_{ik}$  is a vector of same dimension as  $J_i$ , defining connection of the  $k^{\text{th}}$  input block,

$\Theta_k$  is the transfer function of the  $k^{\text{th}}$  realisable block,

$m$  is the number of distinct types of block used in the system

A non-zero entry  $m_{pq}$  of matrix  $M_{ijk}$  represents the connection of a block with transfer function  $\Theta_k$  between the  $p^{\text{th}}$  variable of set  $X_i$  to the  $q^{\text{th}}$  variable

of set  $X_j$ . The block has parameter value  $m_{pq}$ . A zero entry marks the absence of such a connection.

A non-zero entry  $j_p$  of vector  $J_{ik}$  represents the connection of an input block with transfer function  $\Theta_k$  to the  $p^{\text{th}}$  variable of set  $X_i$ . A zero entry marks the absence of such a connection. In fact, this matrix form describes a general signal flow graph in terms of a set of constituent building blocks.

### 5.3.2 Matrix description for SC filters

The type of stray-insensitive SC filters which are considered here can be constructed from the first order branch shown in Fig. 5.6. The building blocks that are used are the inverting and non-inverting integrator and capacitive feed-through gain element. They have special transfer functions which are denoted as

$$\Psi = \frac{z^{-1}}{1 - z^{-1}} \quad \Phi = \frac{-1}{1 - z^{-1}} \quad (5.22)$$

Two blocks are used solely as filter input stages, one for bilinear ladders and the other for LDI ladders and biquads.

Although we shall deal mainly with SC circuits, the matrix methods can easily be extended to active RC circuits, by the identification of  $\Psi = -\Phi = 1/s$ . The basic building blocks in active-RC are damped and lossless integrators. The design of digital circuits using matrix descriptions has been discussed elsewhere [23].

### 5.3.3 Bilinear ladder design

A ladder network can be described by a matrix nodal equation [24],

$$\left(sC + \frac{1}{s}\Gamma + G\right)V = J \quad (5.23)$$

where  $C$ ,  $\Gamma$  and  $G$  are nodal matrices formed by contributions of capacitors, inductors and resistors in the prototype.  $V$  is a vector of node voltages and  $J$  is a vector of input currents.

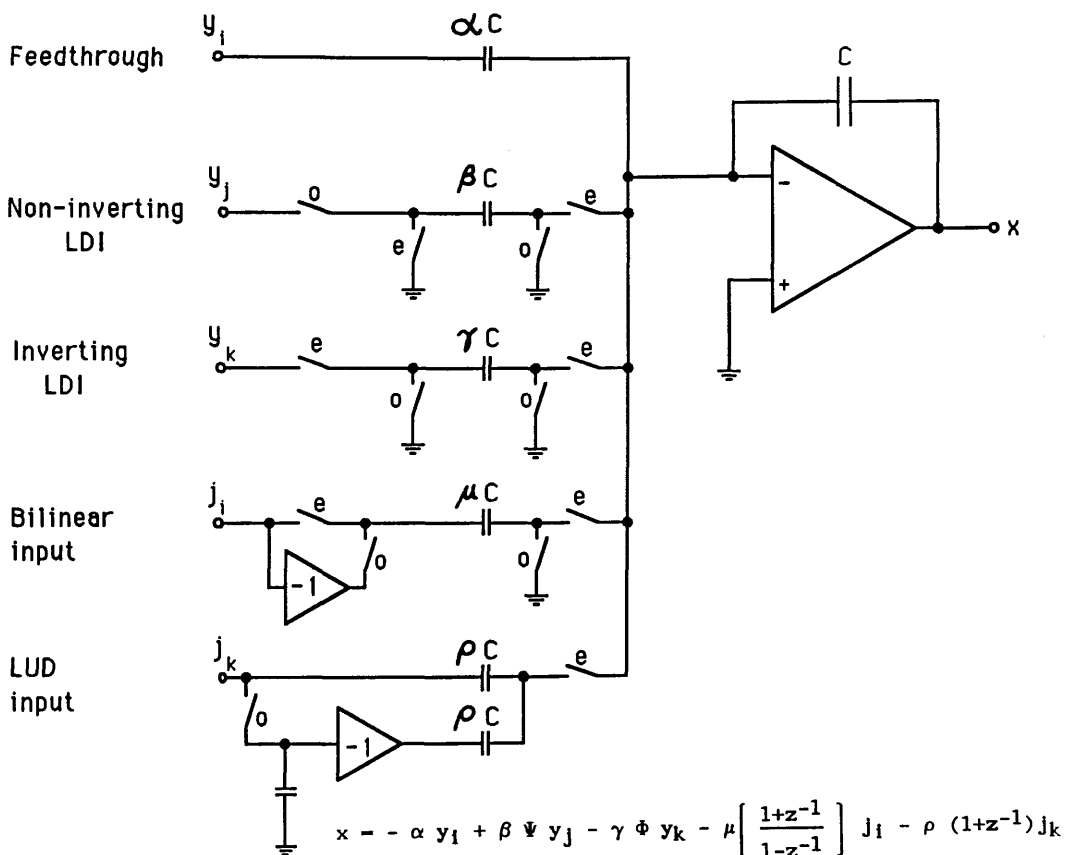


Fig. 5.6 Stray-insensitive SC first order building blocks

Li [25] describes how this equation can be bilinearly transformed and decomposed into realisable form. This is done by introducing a set of intermediate variables, and partitioning the system into two linear equations in terms of the simple realisable building blocks. Decomposition of the right and left hand sides of the original system yields two families of circuits. The type of decomposition can be varied to yield structures with different op-amp coupling. The derivations are not of concern here, merely the computational procedure. An admittance matrix composed of entries of all the elements in the ladder must be set up,

$$\mathbf{A} = \mathbf{C} + \mathbf{\Gamma} + \mathbf{G} \quad (5.24)$$

#### LUD ladder design

LUD ladder simulations result from a left-hand decomposition of  $\mathbf{A}$  by LU factorisation [25–26].

$$\mathbf{A} = \mathbf{LU} \quad (5.25)$$

The matrix system is

$$\left[ \begin{array}{c|c} \mathbf{L} & 4\Phi\mathbf{\Gamma} + 2\mathbf{G} \\ \hline \Psi\mathbf{I} & \mathbf{U} \end{array} \right] \begin{bmatrix} \mathbf{x}_1 \\ \mathbf{x}_2 \end{bmatrix} = \begin{bmatrix} (1+z)\mathbf{J} \\ 0 \\ 0 \end{bmatrix} \quad (5.26)$$

#### Type-E coupled biquad design

Coupled-biquad designs can also be expressed in matrix form. They result from the direct decomposition of  $\mathbf{A} = \mathbf{AI}$  or  $\mathbf{A} = \mathbf{IA}$ . These give rise to two dual forms using E-type biquads,

$$\left[ \begin{array}{c|c} \mathbf{A} & 4\Phi\mathbf{\Gamma} + 2\mathbf{G} \\ \hline \Psi\mathbf{I} & \mathbf{I} \end{array} \right] \begin{bmatrix} \mathbf{x}_1 \\ \mathbf{x}_2 \end{bmatrix} = \begin{bmatrix} (1+z)\mathbf{J} \\ 0 \\ 0 \end{bmatrix} \quad (5.27)$$

$$\left[ \begin{array}{c|c} \mathbf{I} & 4\Phi\mathbf{\Gamma} + 2\mathbf{G} \\ \hline \Psi\mathbf{I} & \mathbf{A} \end{array} \right] \begin{bmatrix} \mathbf{x}_1 \\ \mathbf{x}_2 \end{bmatrix} = \begin{bmatrix} (1+z)\mathbf{J} \\ 0 \\ 0 \end{bmatrix} \quad (5.28)$$

### Leapfrog design

Leapfrog simulation results from a right hand decomposition of  $\Gamma$  by LU decomposition.

$$4\Gamma = LU \quad (5.29)$$

$$\left[ \begin{array}{c|c} \Phi L & A + 2\Psi G \\ \hline I & \Psi U \end{array} \right] \begin{bmatrix} X_1 \\ X_2 \end{bmatrix} = \begin{bmatrix} (\Psi - \Phi) J \\ 0 \\ 0 \end{bmatrix} \quad (5.30)$$

### F-type coupled biquad design

Coupled biquad simulation by type-F biquad blocks results from direct factorisation of  $\Gamma$  as

$$\Gamma = I\Gamma \quad (5.31)$$

$$\left[ \begin{array}{c|c} \Phi I & A + 2\Psi G \\ \hline I & \Psi 4\Gamma \end{array} \right] \begin{bmatrix} X_1 \\ X_2 \end{bmatrix} = \begin{bmatrix} (\Psi - \Phi) J \\ 0 \\ 0 \end{bmatrix} \quad (5.32)$$

$$\left[ \begin{array}{c|c} \Phi 4\Gamma & A + 2\Psi G \\ \hline I & \Psi I \end{array} \right] \begin{bmatrix} X_1 \\ X_2 \end{bmatrix} = \begin{bmatrix} (\Psi - \Phi) J \\ 0 \\ 0 \end{bmatrix} \quad (5.33)$$

These four design methods are used to simulate the prototype of Fig. 5.5a yielding the circuits in Fig. 5.7. The procedure for the design of a ladder simulation in this matrix form are as follows,

*Step 1: Form the C,  $\Gamma$  and G nodal matrices of the prototype by adding an appropriate stamp for each component in the ladder [24].*

*Step 2: Form the A matrix.*

*Step 3: Perform a factorisation of either A or  $\Gamma$ , depending on whether a left or right simulation is desired. There are then two possibilities; LU factorisation or straightforward separation using the identity matrix.*

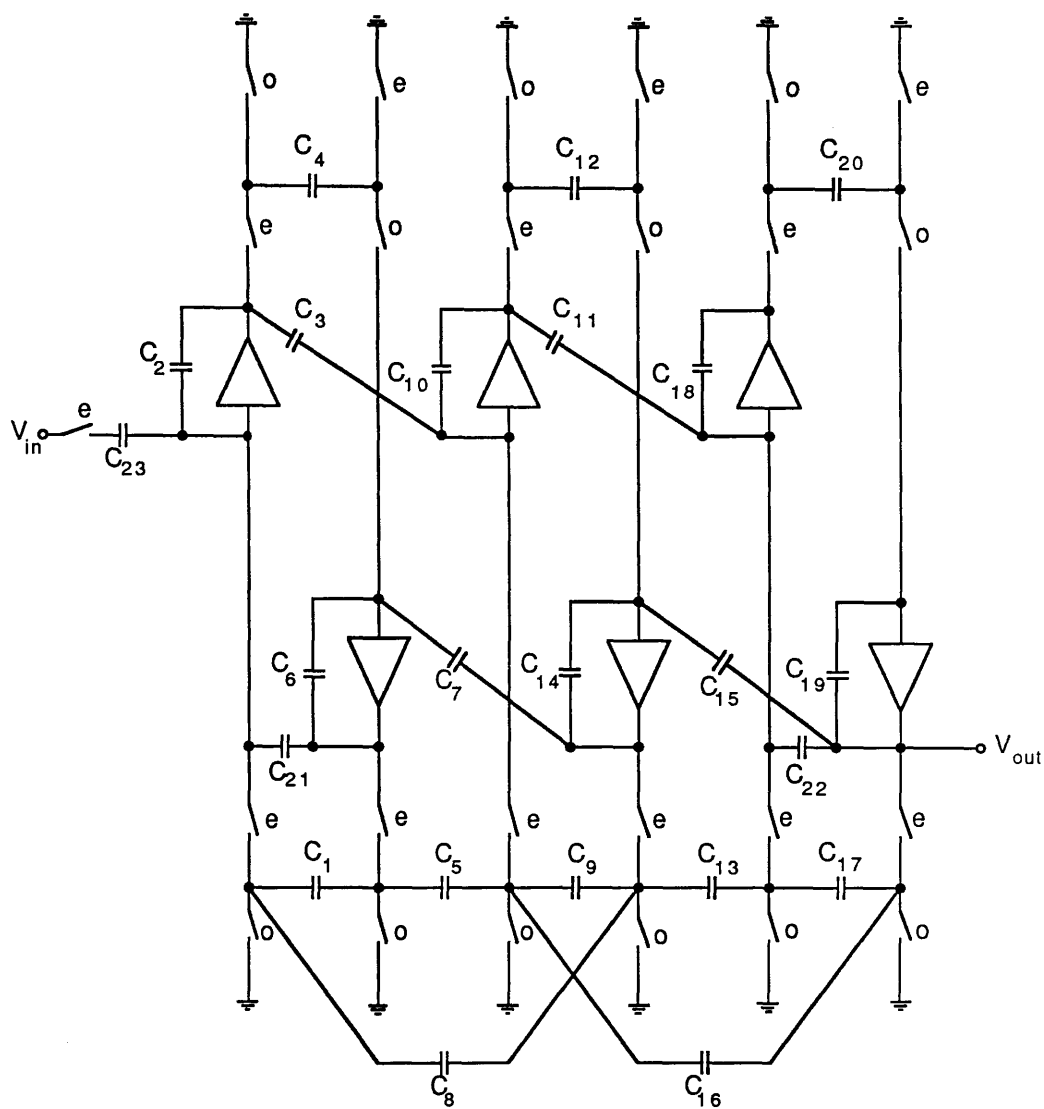


Fig. 5.7a Left-LUD design

Fig. 5.7 Alternative realisations of 6th order bandpass filter



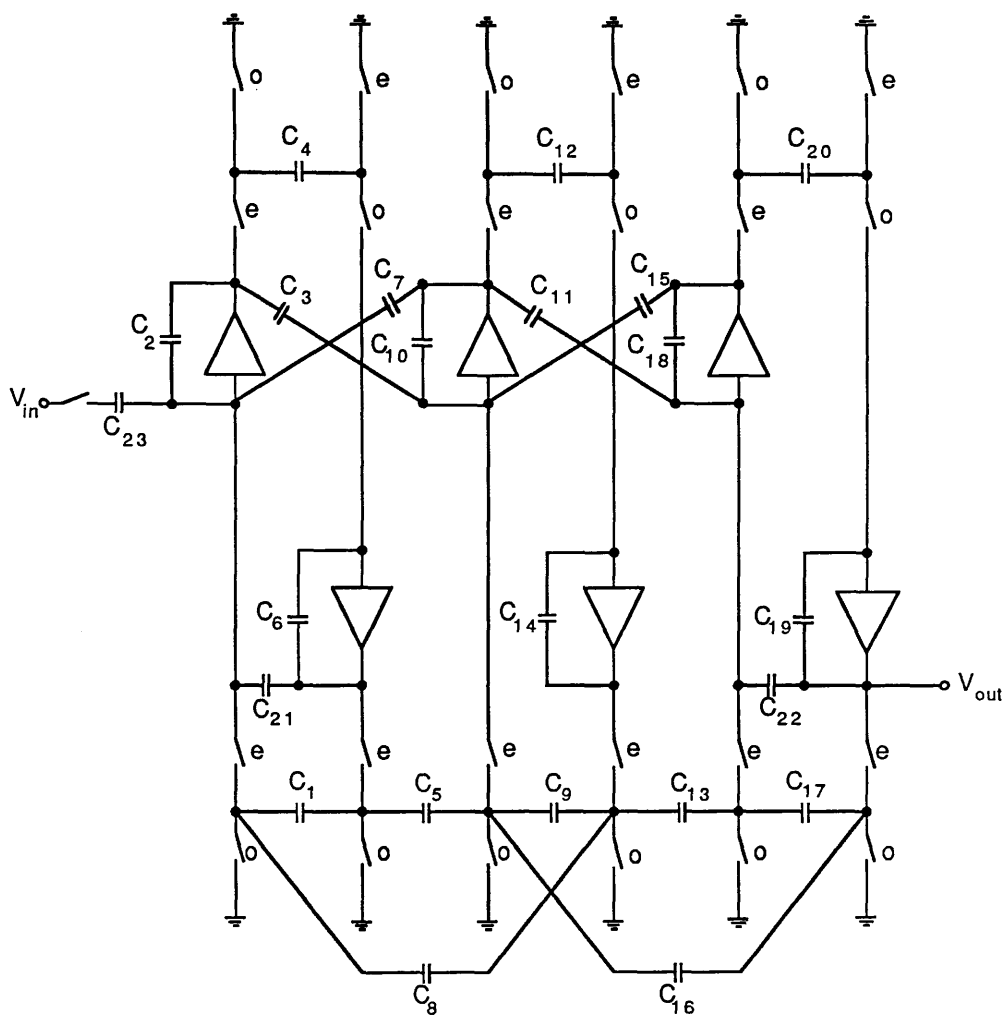


Fig. 5.7b Left-direct design (type-E coupled-biquad)

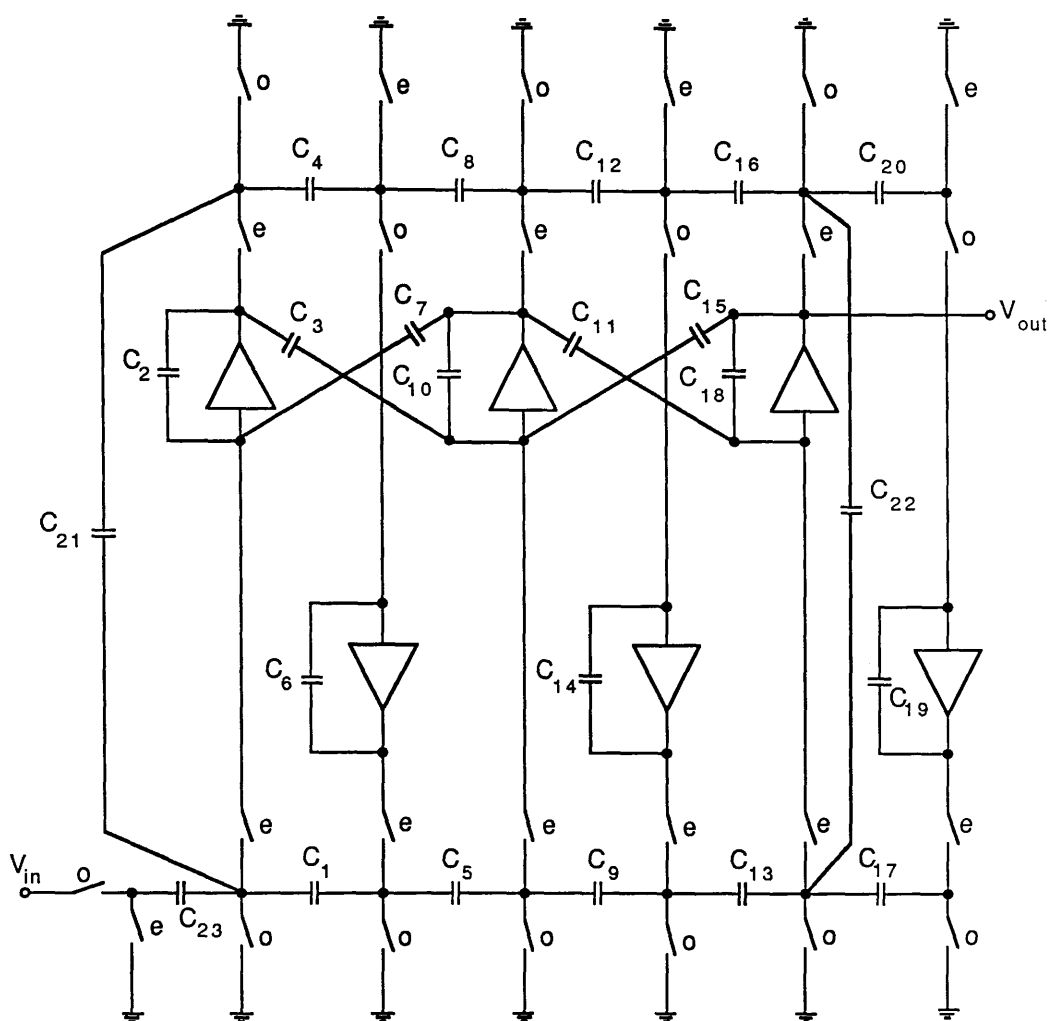


Fig. 5.7c Right-LUD design (leapfrog)

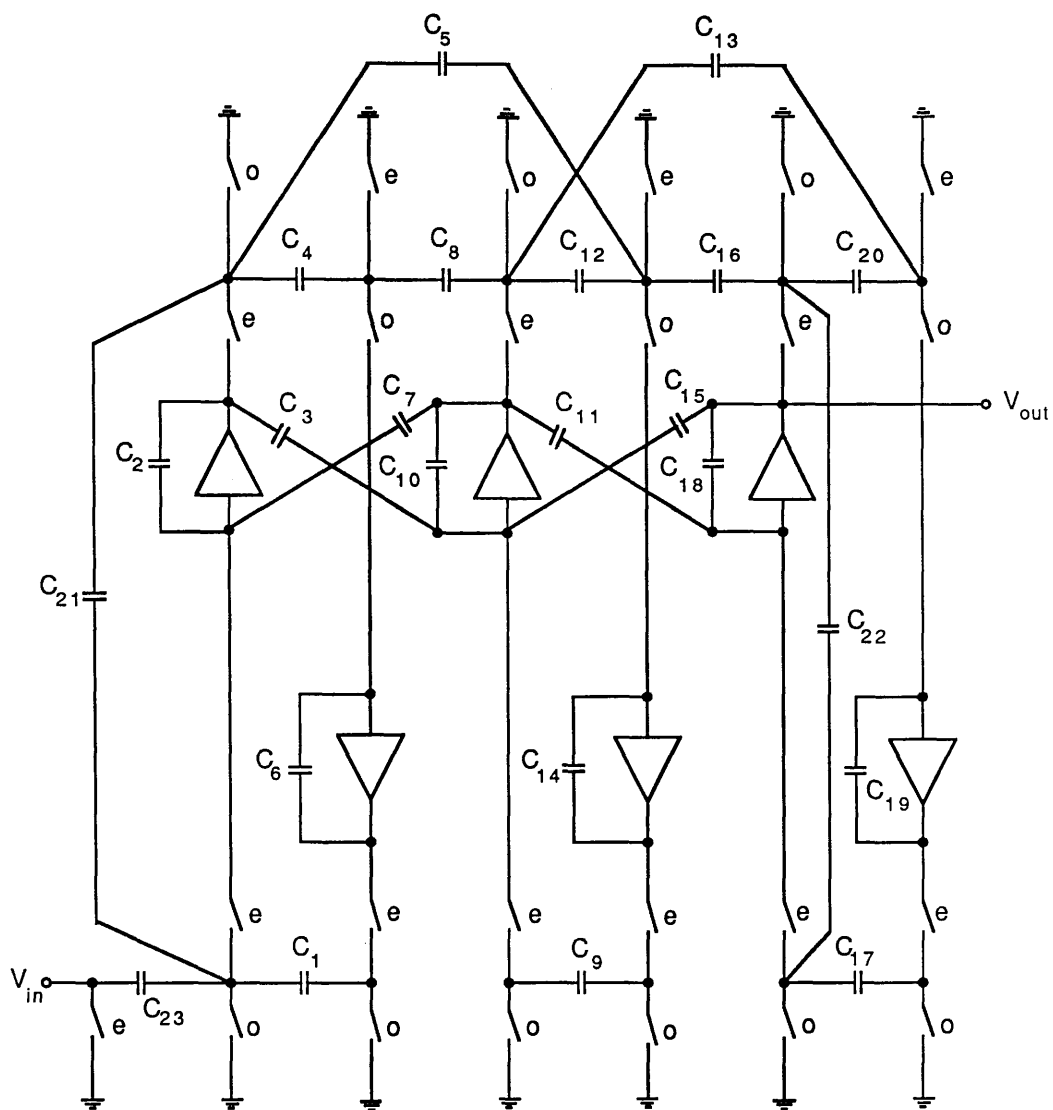


Fig. 5.7d Right-direct design (type-F coupled-biquad)

*Step 4: Enter the relevant matrices into the general matrix form.*

Any form of ladder prototype filter can be simulated by the above procedure regardless of its internal structure.

#### 5.3.4 Ladders with finite transmission at high frequency

Design and simulation of prototypes with finite (non-zero) transmission at high frequency presents various special problems. Straightforward bilinear simulation of highpass or bandstop prototypes will result in unstable circuits [4]. Lowpass or bandpass transfer functions with finite transmission at high frequency (e.g. pure even order elliptic functions) must first be modified before they can be realised. Simulation of the resulting ladder (which possesses an extra node) will yield an inefficient circuit unless a special technique is applied [25]. These drawbacks have been a contributory factor in hindering the application of ladder simulation circuits.

However by the methods of Sections 4.4.3 and 4.4.5 a minimum node prototype can be synthesised for such transfer functions. The input term  $F(s)$  remains to be realised by adjusting the input branches of the filter. There is now an input to each of the two variable sets. The filter system matrices of Section 5.3.3 become

#### LUD ladder simulation

LUD ladder simulations result from a left-hand decomposition of  $A$  by UL factorisation.

$$A = UL \quad (5.34)$$

The matrix system is

$$\left[ \begin{array}{c|c} U & 4\Phi\Gamma + 2G \\ \hline \Psi I & L \end{array} \right] \begin{bmatrix} X_1 \\ X_2 \end{bmatrix} = \begin{bmatrix} 4\omega_N^2 \Phi J \\ 0 \\ \hline (\omega_N^2 + 1) J \\ 0 \end{bmatrix} \quad (5.35)$$

### Type-E coupled biquad design

$$\left[ \begin{array}{c|c} I & 4\Phi\Gamma + 2G \\ \hline \Psi I & A \end{array} \right] \begin{bmatrix} X_1 \\ X_2 \end{bmatrix} = \begin{bmatrix} 4\omega_N^2\Phi J \\ 0 \\ \hline (\omega_N^{2+1})J \\ 0 \end{bmatrix} \quad (5.36)$$

### Leapfrog design

Leapfrog simulation results from a right hand decomposition of  $\Gamma$  by UL decomposition.

$$4\Gamma = UL \quad (5.37)$$

$$\left[ \begin{array}{c|c} \Phi U & A + 2\Psi G \\ \hline I & \Psi L \end{array} \right] \begin{bmatrix} X_2 \\ X_1 \end{bmatrix} = \begin{bmatrix} (\omega_N^{2+1})J \\ 0 \\ \hline 4\omega_N^2J \\ 0 \end{bmatrix} \quad (5.38)$$

### F-type coupled biquad design

Coupled biquad simulation by type-F blocks results from direct factorisation of  $\Gamma$ .

$$\Gamma = I\Gamma \quad (5.39)$$

$$\left[ \begin{array}{c|c} \Phi I & A + 2\Psi G \\ \hline I & \Psi 4\Gamma \end{array} \right] \begin{bmatrix} X_2 \\ X_1 \end{bmatrix} = \begin{bmatrix} (\omega_N^{2+1})J \\ 0 \\ \hline 4\omega_N^2J \\ 0 \end{bmatrix} \quad (5.40)$$

The prototype of Fig 5.5a can also realise the pure sixth order elliptic function of Fig. 4.5 by the methods of Sections 4.4.6 and 4.4.1. Four circuits can then be designed to simulate this prototype (Fig. 5.8). These structures, together with those of Section 5.3.3 are sufficient to realise all transfer functions with purely imaginary axis zeros with canonical numbers of op-amps. Notice the similarities with E and F biquads in Fig 5.2, to which these circuits reduce for second order transfer functions.

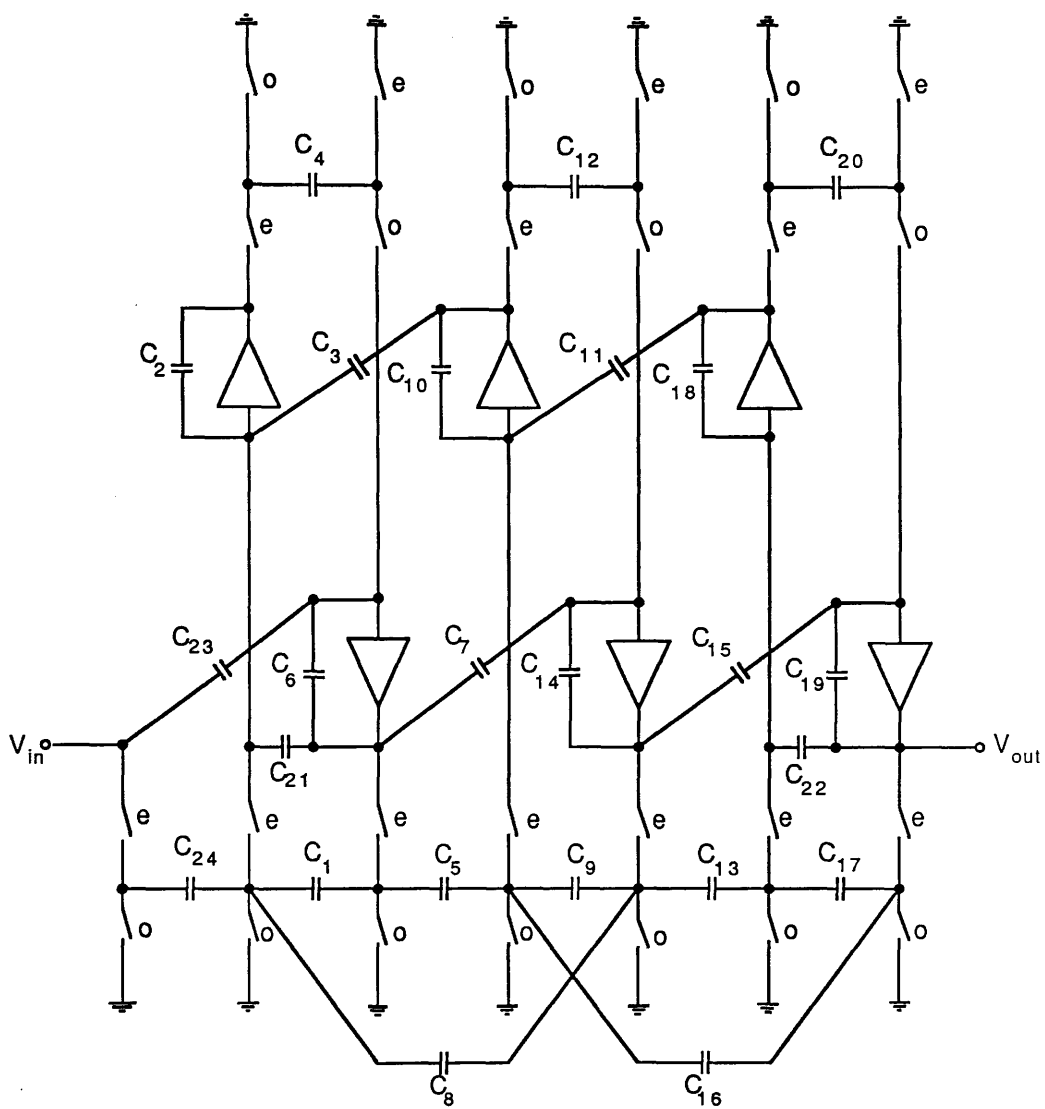


Fig. 5.8a Canonic left-LUD design

Fig. 5.8 Alternative realisations of pure 6th order lowpass elliptic filter

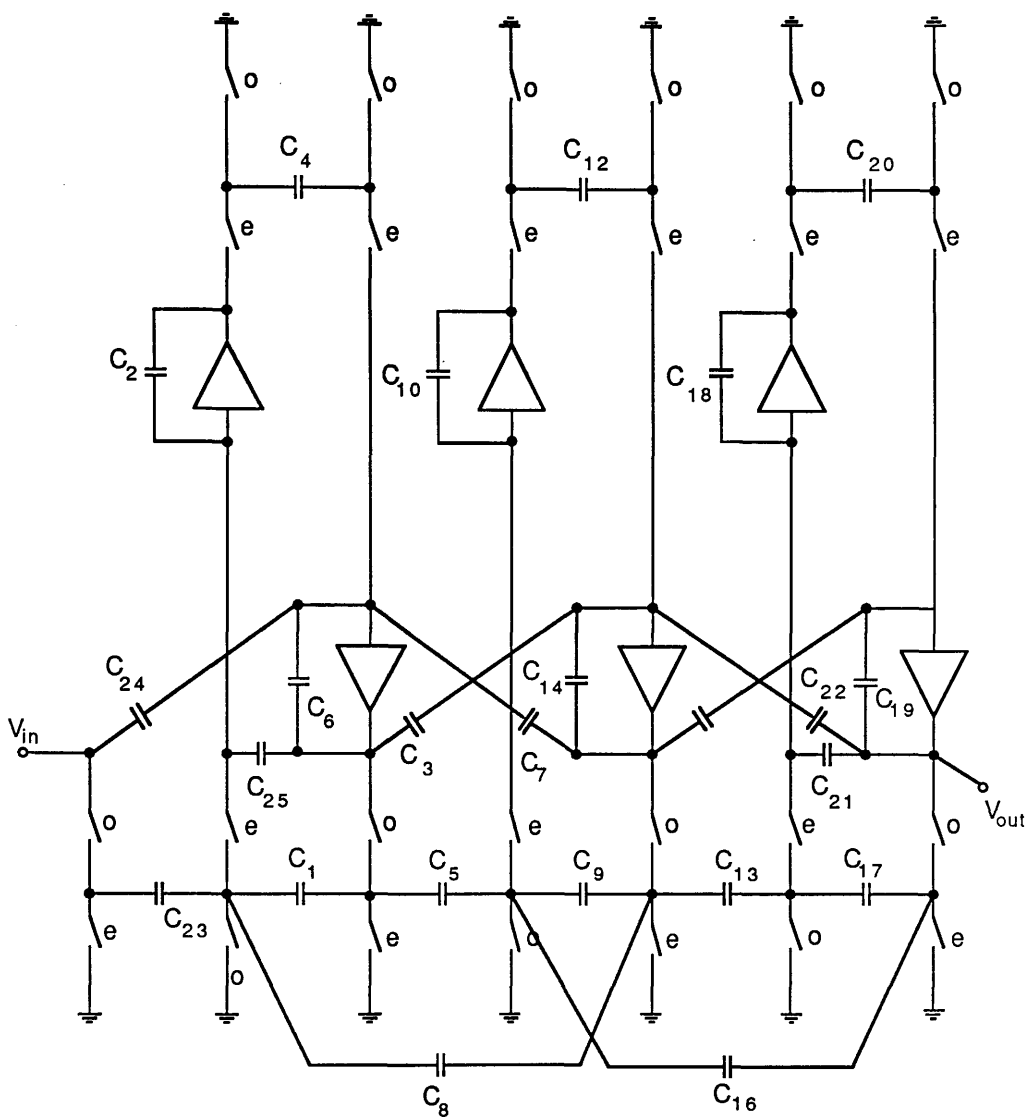


Fig. 5.8b Canonic left-direct design (type-E coupled-biquad)

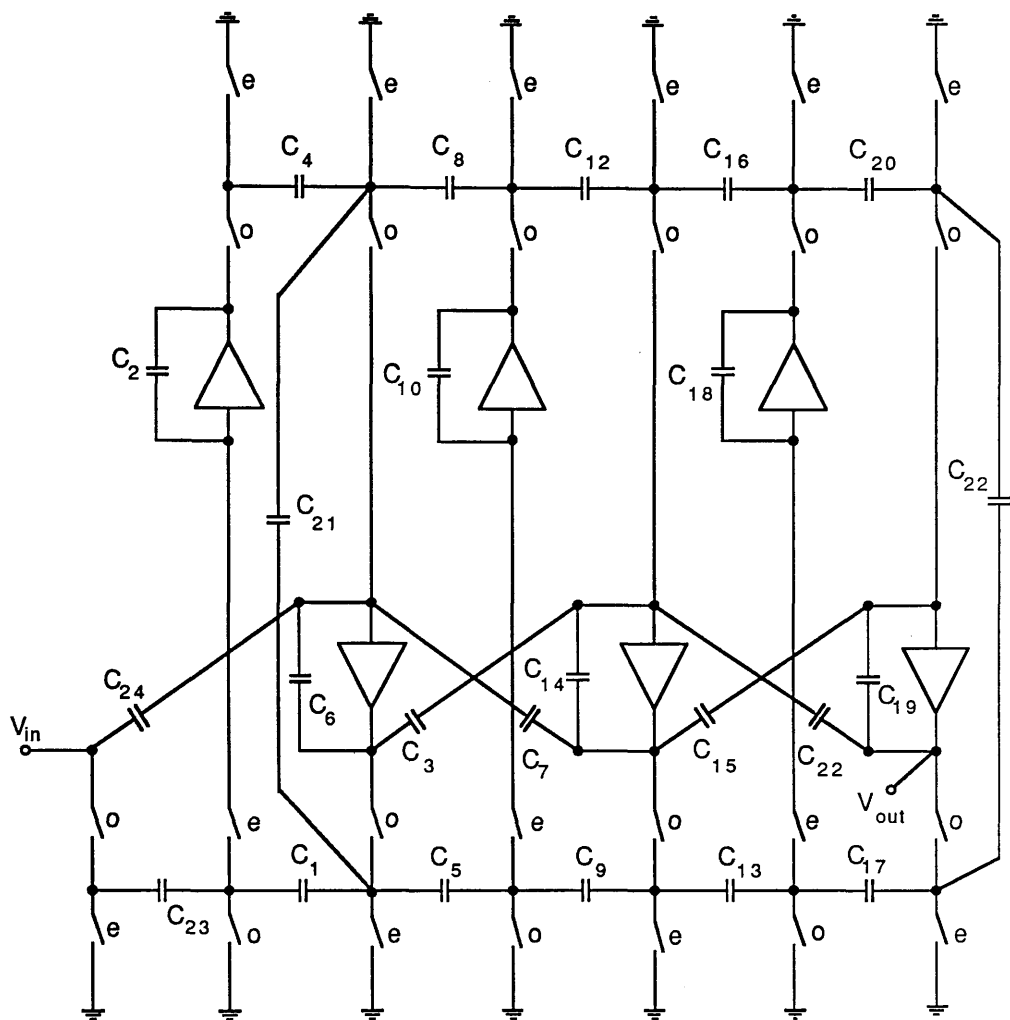


Fig. 5.8c Canonic right-LUD design (leapfrog)



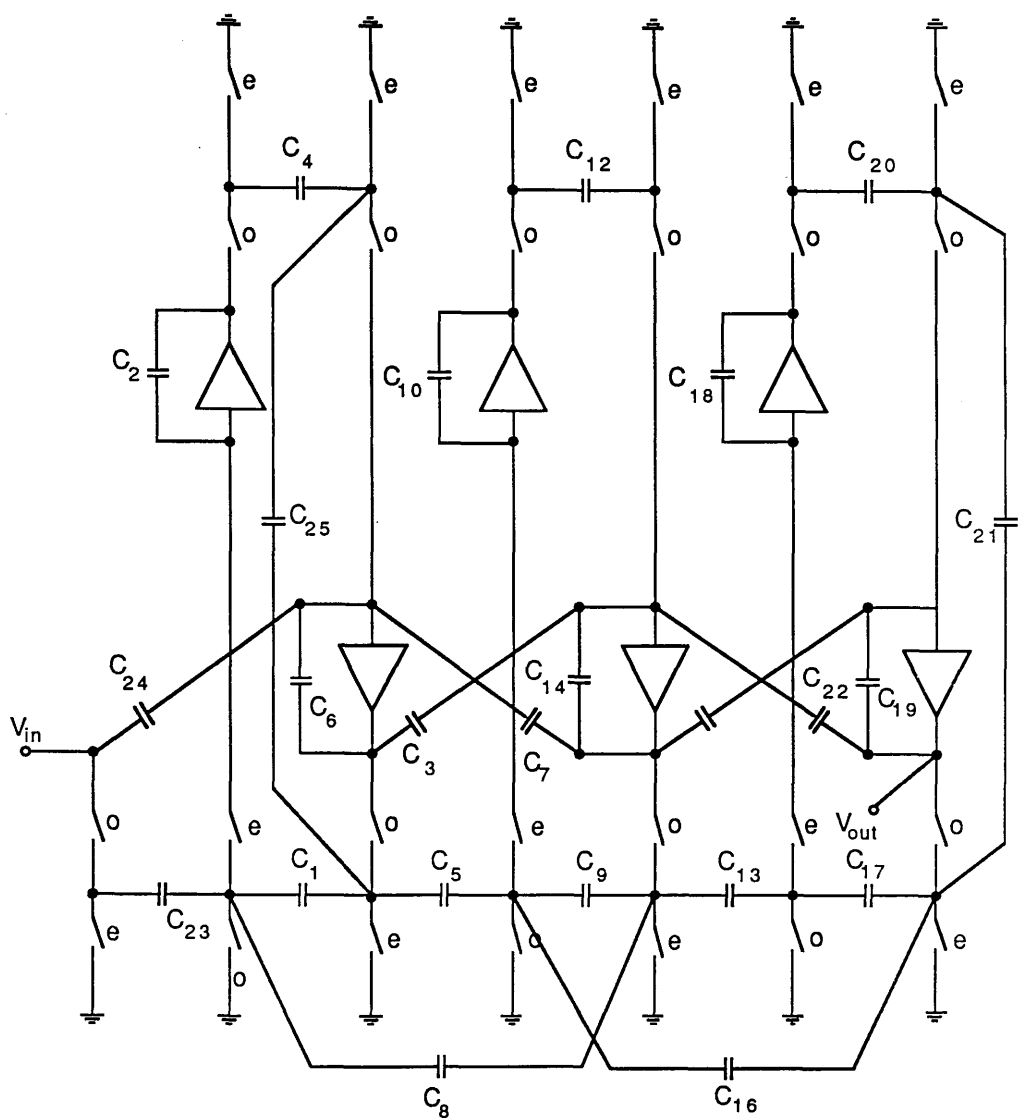


Fig. 5.8d Canonic right-direct design (type-F coupled-biquad)

Alternative methods to realise highpass or bandstop transfer functions also exist and can be expressed in the matrix form. Ladder simulations based on Twintor circuits for bandstop filter realisation have been derived by matrix methods [26]. Highpass filters can be designed by the modulation method of Montecchi [27] can also be easily written in this way.

All-pass ladders have recently been described in SC implementation [25,29–30]. Once again the derivation of these circuits has been achieved by matrix methods and can quite simply be described in the general matrix system. A special singly-terminated prototype must be synthesised from the all-pass transfer function. Negative element values are used to cancel excess components in the SC simulation. The leapfrog, LUD and coupled-biquad systems can be set up in a similar manner as above.

### 5.3.5 Bilinear/LDI ladder design

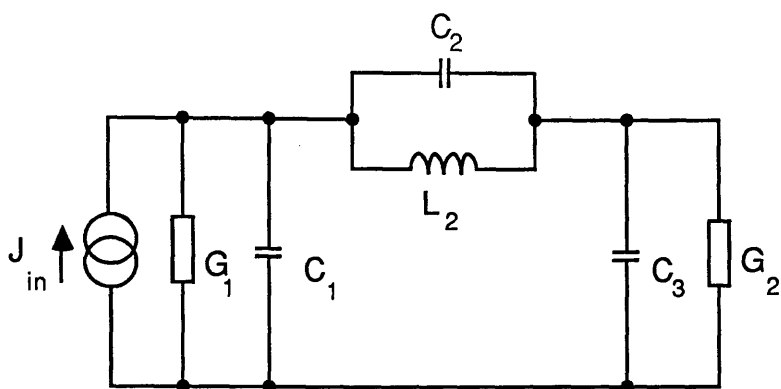
The ladder prototype realised directly by LDI integrators often results in a simplified SC circuit. Cross-over capacitors are not required to realise bilinear zeros and the bilinear input stage can be reduced in complexity, dispensing with a sample-and-hold circuit [31]. LDI ladders can be designed by simulating a special LDI-transformed prototype, entailing a complicated exact synthesis procedure or by an approximate procedure with a distorted transfer function.

An alternative method which yields identical circuit structures using the bilinear transform is now proposed. Bilinear zeros are introduced by transforming zeros at infinity in an  $s$ -domain function. However, transformation of zeros at infinity in a  $z$ -domain function has been shown to yield  $s$ -domain zeros at  $\pm 2fs$  on the real axis. These can be realised by using negative elements in shunt LC tank sections (Fig 5.9a). The element values are given by the formula

$$L_i C_i = -4fs^2 \quad (5.41)$$

when the  $A$  matrix is formed these elements cause cancellation of off-diagonal elements which remove cross-over capacitors from the SC circuit. A single off-diagonal element in the  $A$  matrix is formed by the calculation

$$a_{ij} = -\frac{C_i}{T} + \frac{T}{2L_i} \quad (5.42)$$



$$s^2 = -\frac{1}{L_2 C_2} = -\frac{4}{T^2}$$

Fig. 5.9a 3rd order passive prototype with zeros at  $\pm 2fs$

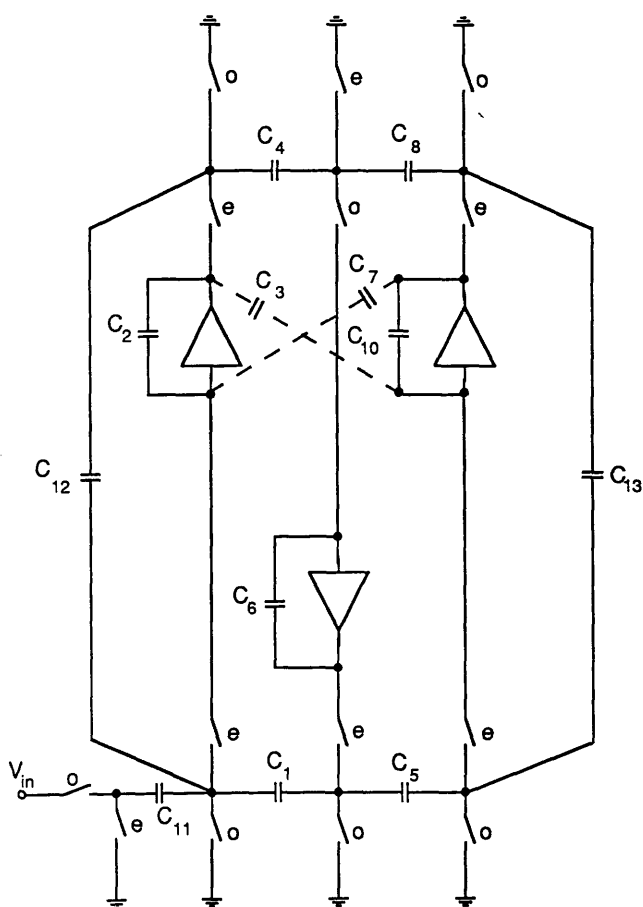


Fig. 5.9b Simulation of 3rd order prototype showing cancellation of feedthrough capacitors

and when (5.41) is true then  $a_{ij}$  becomes zero. An example of this cancellation is given in Fig. 5.9b.

The replacement of the bilinear input stage by an LDI input results in a failure to realise a single bilinear zero at half the sampling frequency [6]. This is equivalent to an upward warping function on the exact filter response of

$$W(\omega) = 1/\cos(\omega T) \tag{5.43}$$

The pre-distortion scheme of Section 4.4.5 can be used to cancel this effect.

### 5.3.6 Biquad design

Biquad circuits may also be described in matrix form. Consider the signal flow graph of Fig. 5.10 in which the branch relations of single biquad section have been expressed in terms of the SC building block functions. This signal flow graph can be entered as a stamp into a matrix description. A single variable set  $X_1$  is chosen as successive output voltages in the cascade of biquads. Let the system be formed as

$$M_{11}X_1 = J_1 \tag{5.44}$$

where  $X_1=(V_1,V_2,V_3,...V_n)^T$  and

$$M_{11} = \Psi M_{111} + \Phi M_{112} - M_{113} \tag{5.45}$$

An input voltage  $V_i$  from a previous stage enters a biquad with outputs  $V_{i+1}$  and  $V_{i+2}$ . The three submatrices in the system, can be formed from additions of contributions of successive biquad sections. The stamp for  $M_{111}$  (inverting switched-capacitors) is

$$\begin{matrix} & & V_i & V_{i+2} \\ & & V_{i+1} & \\ & & | & | & | \\ & & | & | & | \\ V_i & - & - & 0 & 0 & 0 & - & - \\ V_{i+1} & - & - & H & 0 & 0 & - & - \\ V_{i+2} & - & - & J & A & 0 & - & - \\ & & | & | & | \\ & & | & | & | \end{matrix} \left[ \begin{matrix} \\ \\ \\ \\ \\ \\ \\ \\ \end{matrix} \right]$$

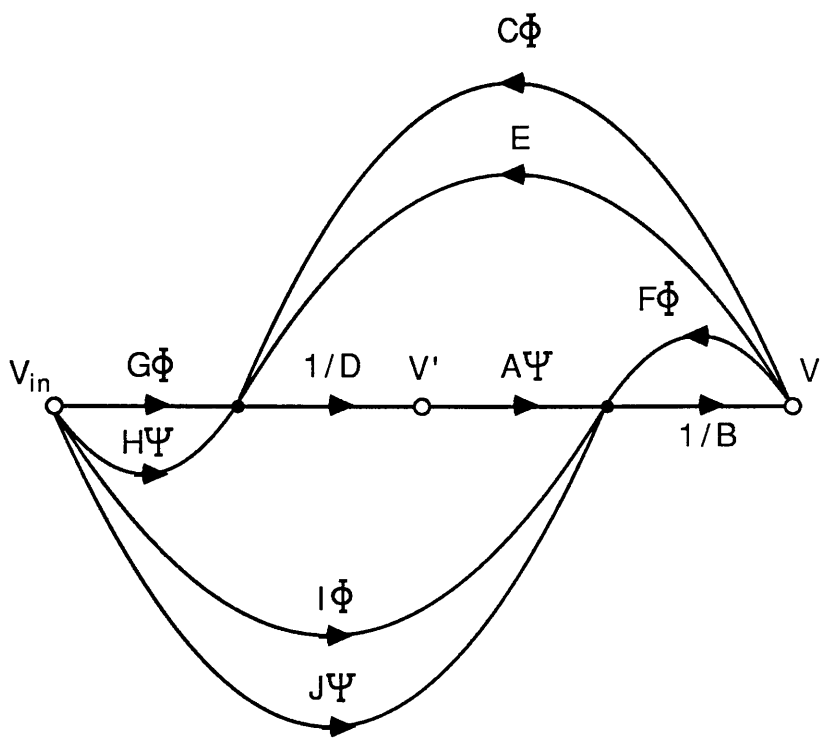


Fig. 5.10 Signal flow graph of general parasitic-insensitive biquad



Step 3 : Calculate the input vector  $J$  similarly.

Step 4 : Assemble submatrices into  $M$  and  $J$ .

Step 5 : By Gauss elimination solve the system

$$MX = J \quad (5.46)$$

for the internal voltage levels  $\{x_i\}$ .

To reduce the amount of computation, the known sparse structure of the component submatrices can be used to advantage. System solution can usually be done with linear efficiency.

A frequency sweep analysis of the filter passband is performed during dynamic range scaling, to determine the maximum signal levels of the internal voltages. To avoid amplifier saturation and to optimise the signal-to-noise ratio the voltage levels must be scaled to a single maximum level. Scaling can be done by multiplying column  $j$  of  $M$  by the maximum value of the variable  $x_j$  for all variables in  $X$ . This is equivalent to creating a new variable  $x_j/\hat{x}_j$ , where  $\hat{x}_j$  is the maximum value attained by  $x_j$ . Clearly the maximum value that the new variable can attain is unity. This is performed for all variables. The following matrix operation can be employed,

$$\hat{M} = M\hat{S} \quad (5.47)$$

where

$$\hat{S} = \begin{bmatrix} \hat{x}_1 & 0 & 0 & \dots & 0 \\ 0 & \hat{x}_2 & 0 & \dots & 0 \\ 0 & 0 & \hat{x}_3 & \dots & 0 \\ \vdots & \vdots & \vdots & \ddots & \vdots \\ 0 & 0 & 0 & \dots & \hat{x}_n \end{bmatrix} \quad (5.48)$$

Scaling for minimum capacitance spread is done to normalise all capacitors to a basic unit capacitor. The minimum non-zero entry  $\check{m}_i$  in the  $i^{\text{th}}$  row of the  $M$  matrix must be determined, and then all the entries in the  $i^{\text{th}}$  row of  $M$  are divided by  $\check{m}_i$ . This operation does not change the poles of the system. It merely

scales each linear relationship at a given operational amplifier to some elementary unit capacitance value. This is equivalent to the following matrix operation.

$$\check{M} = \check{S} \check{M} \tag{5.49}$$

where

$$\check{S} = \begin{bmatrix} \frac{1}{\check{m}_1} & 0 & 0 & \dots & 0 \\ 0 & \frac{1}{\check{m}_2} & 0 & \dots & 0 \\ 0 & 0 & \frac{1}{\check{m}_3} & \dots & 0 \\ \vdots & \vdots & \vdots & \ddots & \vdots \\ 0 & 0 & 0 & \dots & \frac{1}{\check{m}_n} \end{bmatrix} \tag{5.50}$$

### 5.3.8 Network realisation from matrix form

The matrix system can be seen to represent a signal flow graph of the filter by the following rules

To illustrate the principle consider a single row equation,

$$a_{22}x_2 = -(a_{21}x_1 + a_{23}x_3) + \Psi(b_{21}y_1 + e_{21}x_1) + \Phi(c_{21}y_1 + f_{21}x_1) + \Psi(b_{22}y_2 + d_{21}y_1) + \dots \tag{5.51}$$

The terms appearing in this equation can be represented by the signal flow graph (SFG) of Fig. 5.11 which can be implemented with branches of the SC circuit in Fig. 5.6. The following principles for construction of the SFG from a matrix equation are applied:

*For the i-th row of (5.51) the variable  $x_i$  is selected as the nodal variable in the SFG. The i-th row equation is just the linear relationship at this node.*



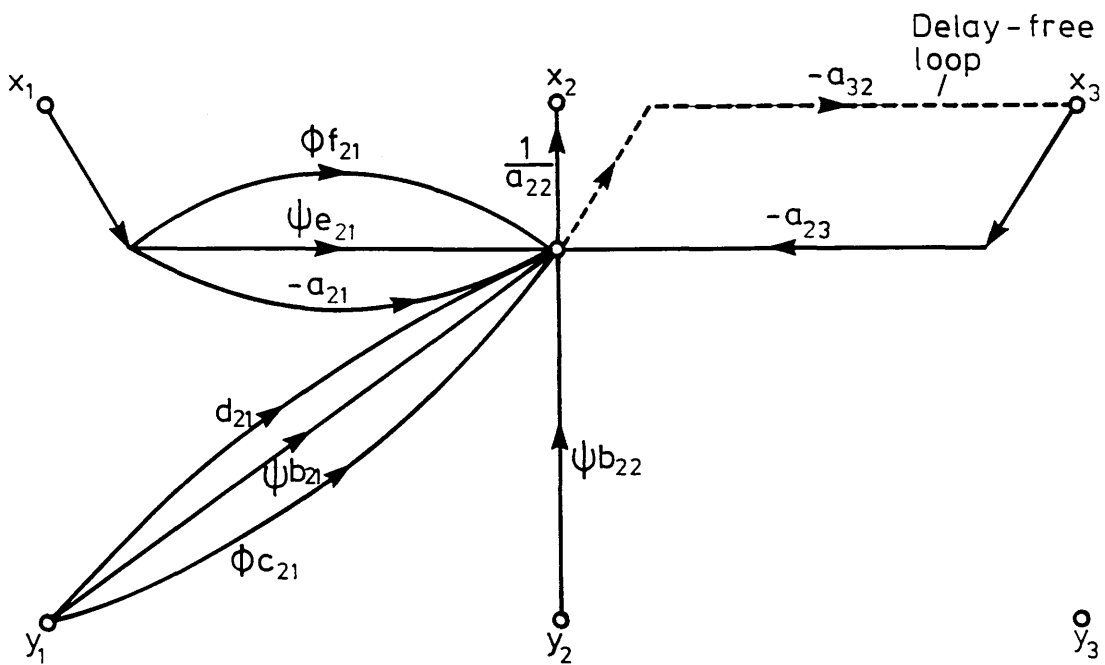


Fig. 5.11 Elementary signal flow graph of single row equation

The following rules are used for the SC replacement of the SFG:

*Each variable in  $X$  represents the voltage of an opamp output node and each feedthrough diagonal entry of  $M$  is realised by a damping capacitor. Every other non-zero entry in a matrix represents the connection of a circuit element between opamps.*

The one-to-one correspondence between the circuit elements and the matrix entries indicates that the efficiency of the SC implementation in terms of numbers of capacitors is related to the sparsity of the system matrices.

These rules can be used to form a netlist of the SC filter.

*Step 1 : Create a series of operational amplifiers for each of the variables within  $X$ . The output of each op-amp simulates the variable in  $X$  and the input is a summing junction.*

*Step 2 : Consider entry  $m_{pq}$  in submatrix  $M_{ijk}$ . If  $m_{pq}$  is non-zero then create a block of type  $\Theta_k$  connected from the output of the op-amp simulating the  $q^{th}$  variable in set  $X_i$  to the input of the op-amp simulating the  $p^{th}$  variable in set  $X_j$ . The block has parameter value  $m_{pq}$ . No connection is present if  $m_{pq}$  is zero.*

*Step 3 : Repeat Step 2 for all entries in all submatrices in  $M$ .*

*Step 4 : Consider entry  $j_p$  in subvector  $J_{ik}$ . If  $j_p$  is non-zero then create an input block of type  $\Theta_k$  between the input source and the input of the op-amp simulating the  $p^{th}$  variable in set  $X_i$ .*

*Step 5 : Repeat Step 3 for all entries in all subvectors in  $J$ .*

The network realised by the above scheme will normally be inefficient in terms of hardware, since the block description of the network prevents sharing of components. A further processing stage can be undertaken to remove redundant components.

### 5.3.9 Computational issues

The cost of the design process is very small. Once the component matrices have been set up by a summation of stamps, only a well known LU decomposition algorithm need be applied. The known sparse structure (tridiagonal or banded) of the matrices can be used to greatly improve the efficiency of this operation ( $O(n)$ ). This knowledge can be further employed in the solution of the

full matrix system during the frequency sweep of the passband for dynamic range scaling. The pre-computed block transfer functions  $\Psi$  and  $\Phi$  already provide a significant improvement in computational efficiency by avoiding repetitive analysis of common blocks in the structure.

The netlist output step only involves a traverse of the matrix system. A special sparse matrix storage scheme could be adopted to avoid unnecessary testing of zero entries at all stages of the processing. In this case the storage cost would be  $O(n)$  rather than  $O(n^2)$  for full matrices.

## 5.4 CAPACITANCE SPREAD REDUCTION TECHNIQUES

### 5.4.1 Dynamic range tradeoff

A filter which has been scaled for optimal dynamic range will have good noise rejection and will assure maximum signal handling capability of the amplifiers [4,21]. However this scaling does not take into account sensitivity of the filter response to random component value errors in fabrication. Often, a capacitor will have attained a particularly large value during scaling to ensure maximum dynamic range, particularly in narrow band filters. Large capacitor ratios ( $>40$ ) are particularly prone to fabrication errors and so the filter sensitivity becomes poor.

However it is always possible to tradeoff between the capacitance spread and the dynamic range of the filter. Rather than scale voltages to a common maximum level, certain ones can be scaled to some lower value to relax the size of large capacitors. The loss in dynamic range can be kept bounded. A multivariable quasi-Newton algorithm has been implemented to adjust the voltage levels within this bounded space to obtain the optimal capacitance spread.

Fig. 5.12a shows a 10th order bandpass LUD SC filter scaled for maximum dynamic range. In Fig. 5.12b a 6dB loss of dynamic range is allowed, causing a slight spread of the peak levels of the internal voltages. By this measure, a saving of 12% of the total capacitance is obtained. A loss of 6dB will half the largest capacitor value. Ladder networks are more tolerant of this adjustment than biquads as their signal levels are very often bounded throughout the passband within some small range.

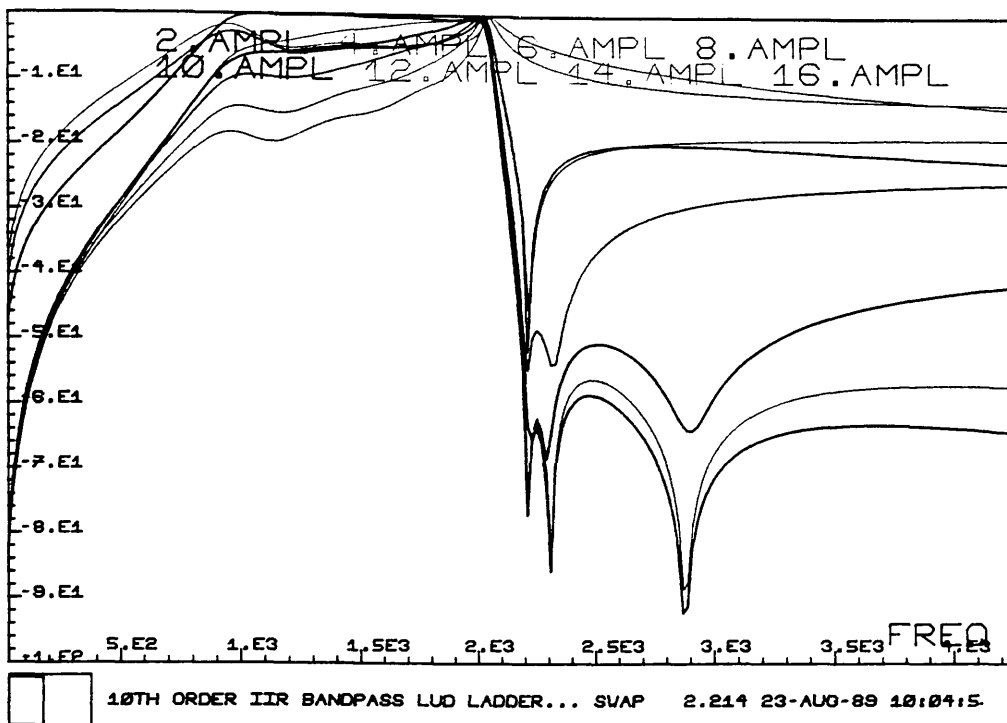


Fig. 5.12a Internal voltages of 10th order SC LUD filter showing dynamic range scaling

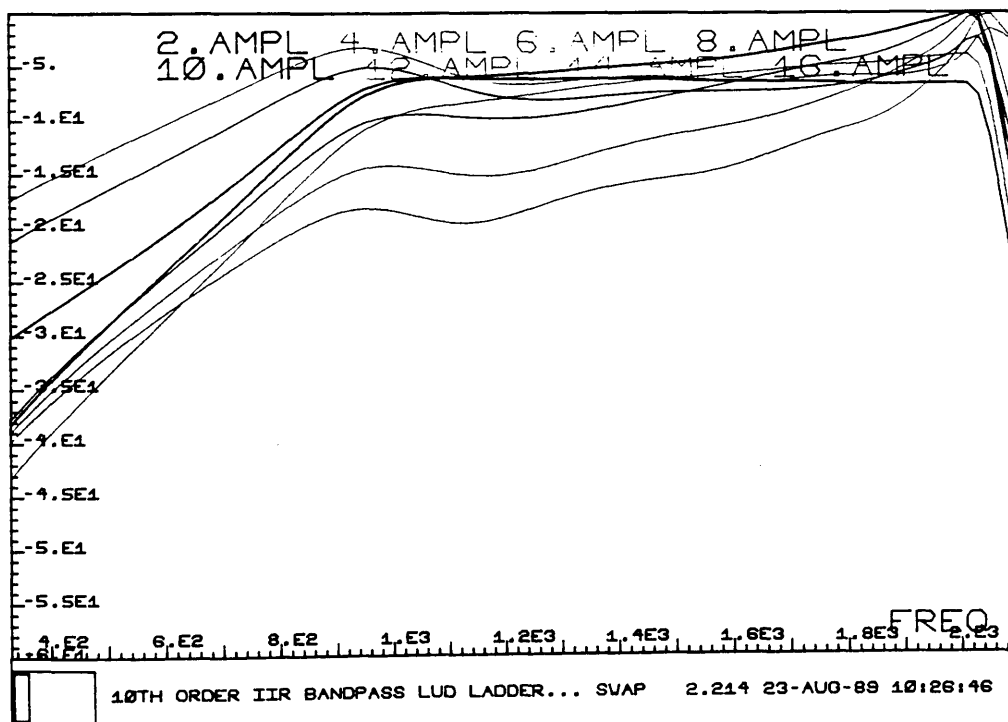


Fig. 5.12b 6dB trade-off between dynamic range and capacitance spread

### 5.4.2 Pole removal permutations for ladders

The structure of a typical 7th order lowpass passive ladder network is shown in Fig. 5.13a with response in Fig. 5.13b. Each parallel resonant LC branch realises a single loss pole. By choosing the sequence of poles optimally, a significant reduction in the component spread may be achieved, Table 5.1. When the passive prototype is simulated by a leapfrog switched-capacitor network similar savings in capacitance spread are observed, Table 5.2. For low order filters an exhaustive check of all pole sequences can be made. It is expected that the dynamic-range properties may also be improved.

### 5.4.3 Pole-zero pairing for biquads

In the design of biquad prototypes there is great freedom in the sequence of realisation of the second-order pole and zero terms. The pairing of a pole term with a zero-term can greatly influence the capacitance spread and dynamic range properties of the filter [1]. To determine the optimal sequence often requires as many permutations to be tested as possible. Since this is of factorial efficiency the computational cost becomes exorbitant after a certain point (e.g. 12th order). Thus efficient scaling and spread cost calculations are necessary to test as many sequences as possible. Sparse analysis and scaling of the biquad matrix system becomes essential. Various 'rule of thumb' sequences can be examined when exhaustive testing becomes too costly [32].

Another effective method of reducing the size of large capacitors in a SCF is to adopt a low-spread structure [33–36]. This will often entail some sensitivity to stray capacitance or loss of dynamic range.

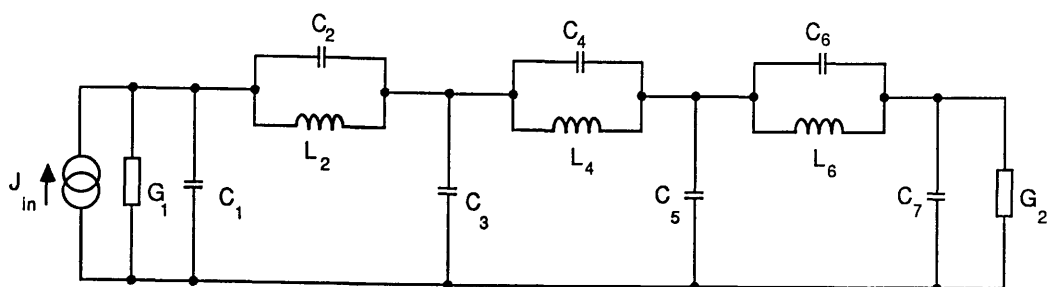


Fig. 5.13a Seventh order lowpass elliptic LC prototype

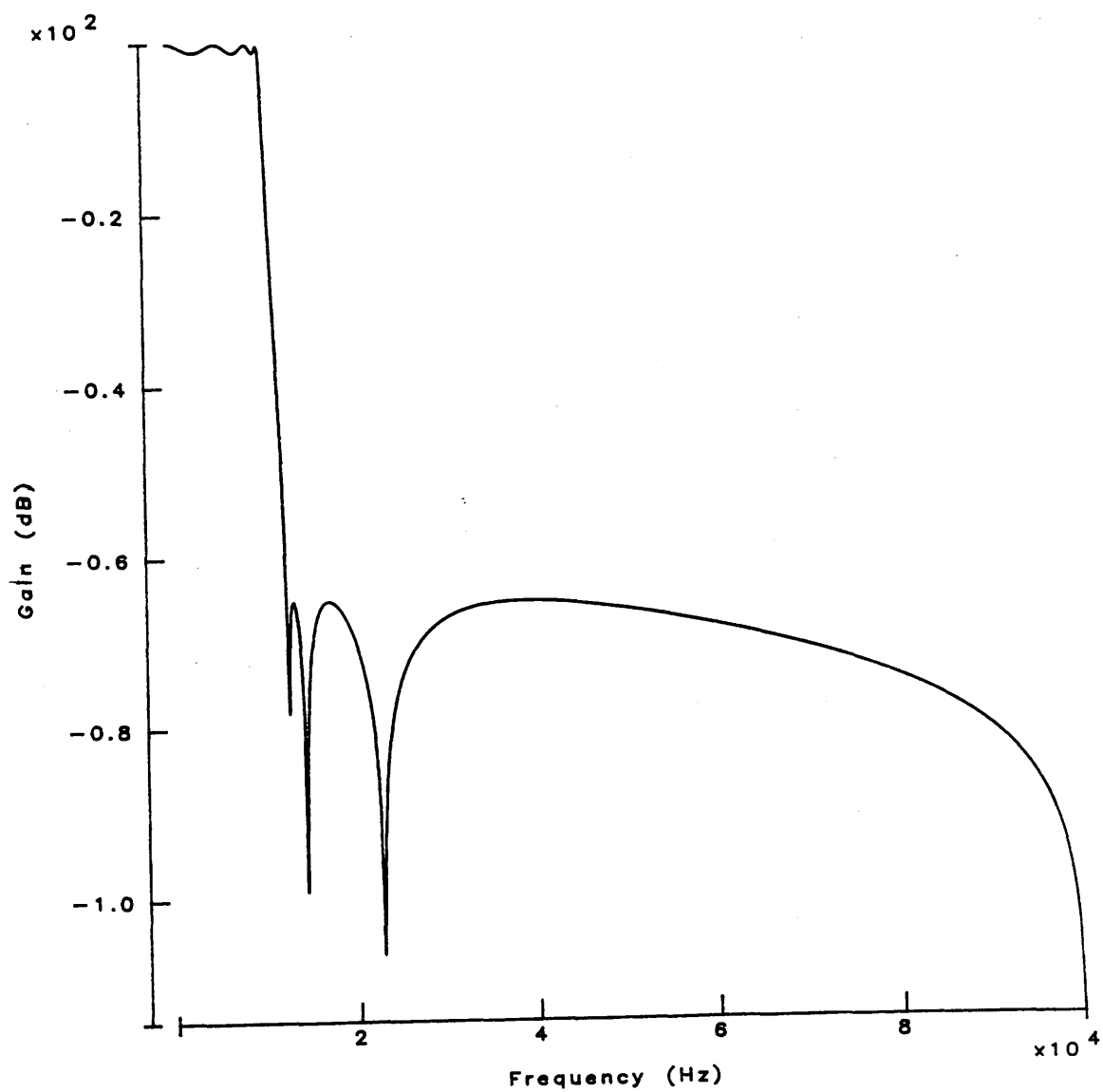


Fig. 5.13b Seventh order elliptic response

Pole order	C spread	Total C	Average C
1-2-3	23.75	104.6	3.74
1-3-2	16.68	99.38	3.55
2-1-3	24.85	108.1	3.86
2-3-1	15.17	98.20	3.51
3-2-1	15.93	92.36	3.30
3-1-2	16.67	101.4	3.62

**Table 5.1 Variation of capacitance statistics with pole sequence for 7th order LC prototype realised by LDI leapfrog SC filter**

lower passband edge      20kHz      lower stopband edge      25KHz passband ripple          < 1.0dB      stopband attenuation      > 65dB sampling frequency      200KHz      G1 = 1.0      G2 = 1.2										
Pole order	C1	C2	L2	C3	C4	L2	C5	C6	L6	C7
1-2-3	1.63	1.07	0.58	2.30	0.59	0.78	2.81	0.19	0.91	2.22
1-3-2	1.63	1.06	0.58	2.63	0.17	0.98	2.84	0.66	0.70	1.86
2-1-3	1.88	0.64	0.71	2.28	0.96	0.64	2.59	0.19	0.91	2.22
2-3-1	1.88	0.64	0.71	2.83	0.17	0.98	2.65	1.09	0.56	1.61
3-2-1	2.23	0.18	0.92	2.80	0.59	0.78	2.32	1.09	0.56	1.61
3-1-2	2.23	0.18	0.92	2.58	0.96	0.64	2.29	0.66	0.70	1.86

**Table 5.2 Various pole orderings of 7th order lowpass LC ladder**

## 5.5 SUMMARY

A matrix description suitable for computer description, analysis, scaling and realisation of filter networks has been introduced. Both biquadratic cascade and ladder simulations can be constructed within unified framework. The design of ladder simulations is treated in a very systematic manner, which does not vary according of the form of the prototype or type of transfer function. A variety of ladder simulation structures can be produced by simply altering the matrix operations used to set up the filter system. The procedures are further unified by the bilinear transform which maps filters between digital and analogue domains. Indeed, filters in entirely different implementations such as active-RC, MOSFET-C or digital can be produced with very little change to the methods. The sparse properties of the matrices permit efficient computer processing and storage. A number of techniques to reduce large capacitance spreads have been proposed for both ladder and biquad filters.

## REFERENCES

- [1] A. S. Sedra and P. O. Brackett, "Filter Theory and Design: Active and Passive", Pitman, London, 1979.
- [2] E. Sanchez-Sinencio and J. Ramirez-Angulo, "AROMA : An area optimised CAD program for cascade SC filter design", IEEE Trans. CAD, Vol. CAD-4, No. 3, pp.296-303, July 1985.
- [3] J. Assael, P. Senn and M. S. Tawfik, "A switched-capacitor filter compiler", IEEE Journal of Solid-State Circuits, Vol. SC-23, pp. 166-174, Feb. 1988.
- [4] G. S. Moschytz, ed., "MOS switched-capacitor filters : analysis and design", IEEE Press, New York, 1984.
- [5] R. Gregorian, K. W. Martin and G. C. Temes, "Switched-capacitor circuit design", Proc. IEEE, Vol. 71, No. 8, pp941-966, Aug. 1983.
- [6] Li Ping, R. K. Henderson and J. I. Sewell, "Matrix methods for switched-capacitor filter design", Proc. ISCAS, pp.1044-1048, Helsinki 1988.
- [7] R. Gregorian, "Switched capacitor filter design using cascaded sections", IEEE Trans. Circs and Syst., vol. CAS-27, pp. 515-521, June 1980.
- [8] E. Sanchez-Sinencio, "Switched-capacitor circuits", Van-Nostrand Reinhold, 1985.
- [9] M. S. Ghausi and K. R. Laker, "Modern filter design : active RC and switched-capacitor", Prentice-Hall, Englewood Cliffs, New Jersey, 1981.



- [10] E. Sanchez-Sinencio, J. Silvia-Martinez and R. L. Geiger, "Biquadratic switched-capacitor filters with small GB effects", IEEE Trans. CAS, Vol. CAS-31, pp. 876-884, Oct. 1984.
- [11] R. Gregorian and G. C. Temes, "Analog MOS Integrated Circuits for Signal Processing", Wiley, 1986.
- [12] Y. Tsididis and P. Antognetti, eds, "Design of MOS VLSI circuits for telecommunications", Prentice-Hall, Englewood Cliffs, NJ, 1985.
- [13] T. Choi and R. W. Broderson, "Considerations for high-frequency switched-capacitor ladder filters", IEEE Trans. Circ. and Syst., Vol. CAS-27, pp.545-552. June 1980.
- [14] A. Kaelin, G. S. Moschytz, "Exact design of arbitrary parasitic-insensitive elliptic SC-ladder filters in the  $z$ -domain", Proc. ISCAS, pp. 2485-2488, Helsinki, Finland, 1988.
- [15] A. Kaelin, R. Sigg and G. S. Moschytz, "A programmable design technique for cellular LDI-equivalent switched capacitor ladder filters", pp.1-4,
- [16] S. O. Scanlan, "Analysis and synthesis of switched-capacitor state variable ladder filters", IEEE Trans. Circ. and Syst., vol. CAS-28, pp. 85-93, Feb. 1981.
- [17] J. Taylor, "Stability analysis and exact design of switched-capacitor filters of the lossless discrete integrator type", PhD Thesis, University of London, 1985.
- [18] J. Taylor, "Exact design of elliptic switched-capacitor filters by synthesis", Electronics Letters, Vol. 18, No. 19, pp. 807-809, Sept. 1982.
- [19] M. S. Lee and C. Chang, "Switched-capacitor filters using the LDI and bilinear transformations", IEEE Trans. Circuits and Systems, Vol. CAS-30, No. 12, pp. 873-887.
- [20] M. S. Lee, G. Temes, C. Chang and M. Ghaderi, "Bilinear switched capacitor ladder filters", IEEE Trans. on Circuits and Systems, Vol. CAS-28, pp.811-821, Aug. 1981
- [21] Teng-Hsien Hsu and G. C. Temes, "Improved input stage for bilinear switched-capacitor ladder filters", IEEE Trans. on Circuits and Systems, vol. CAS-30, no. 10, pp.758-760, Oct. 1983.
- [22] K. Martin and A. S. Sedra, "Exact design of switched-capacitor bandpass filters using coupled biquad structures", IEEE Trans. Circuits and Systems, vol. CAS-27, pp.469-474, June 1980.
- [23] Li Ping and J. I. Sewell, "Filter realisation by passive ladder simulation", IEE Proc., Pt.-G. Vol. 135, No. 4, pp 167-176, August 1988.
- [24] K. Singhal and J. Vlach, "Computer methods for circuit analysis and design", Van Nostrand Reinhold, 1983

- [25] Li Ping, "Theory and methodology for integrated ladder filter design", PhD thesis, University of Glasgow, 1990.
- [26] Li Ping and J. I. Sewell, "The LUD approach to switched-capacitor filter design", IEEE Trans. Circuits Syst., vol. CAS-34, no. 12, pp 1611-1614 Dec. 1987.
- [27] Li Ping and J. I. Sewell, "The TWINTOR in bandstop switched-capacitor ladder filter realisation", IEEE Trans. Circuits and Systems, Vol. CAS-36, No.7, pp.1041-1044, July 1989.
- [28] F. Montecchi, "Bilinear design of high-pass switched-capacitor ladder filters", IEEE ISCAS, pp. 547-550, Kyoto, Japan 1985.
- [29] B. Nowrouzian and L. S. Lee, "Minimal multiplier realisation of bilinear-LDI digital all-pass networks", Proc. IEE, Pt. G, No. 3, pp. 114-117, June 1989.
- [30] Li Ping and J. I. Sewell, "Switched-capacitor and active-RC all-pass ladder realisation", submitted for publication.
- [31] D. M. Gee, "An intentionally approximate bilinear based transform", Digest of IEE Saraga Colloquium on Electronic Filters, pp. 12/1-12/4, London 1989.
- [32] C. Xuexiang, E. Sanchez-Sinencio and R. L. Geiger, "Pole-zero pairing strategy for area and sensitivity reduction in cascade SC filters", IEEE ISCAS, pp. 609-611, 1986.
- [33] K. Nagaraj, "A parasitic-insensitive area-efficient approach to realizing very large time constants in switched-capacitor circuits", IEEE Trans. Circuits and Systems, Vol. CAS-36, No. 9, pp. 1210-1216, Sept. 1989.
- [34] P. Van Peteghem and W. Sansen, "T-cell integrator synthesizes very large capacitance ratios", Electron. Lett., Vol. 19, pp. 541-544, July, 1983.
- [35] W. Sansen and P. Van Peteghem, "An area-efficient approach to the design of very large time-constants in switched-capacitor integrators", IEEE J. Solid-State Circuits, Vol. SC-19, pp. 772-779, Oct. 1984.
- [36] Q. Huang, "A novel technique for the reduction of capacitance spread in high-Q SC circuits", Proc. ISCAS, pp. 1249-1253, Helsinki, Finland, 1988.

## **CHAPTER 6**

### **A COMPUTER-AIDED FILTER DESIGN SYSTEM**

#### **6.1 INTRODUCTION**

#### **6.2 AN INTEGRATED FILTER COMPILER : PANDDA**

- 6.2.1 Design philosophy
- 6.2.2 Internal structure
- 6.2.3 Specifications
- 6.2.4 Filter approximation
- 6.2.5 Prototype design
- 6.2.6 Circuit design and scaling
- 6.2.7 Optimisation

#### **6.3 DESIGN OF A FM RADIO FILTER**

#### **6.4 DESIGN OF A TELECOMMUNICATIONS FILTER**

#### **6.5 A SWITCHED-CAPACITOR FILTER ASIC**

#### **6.6 SUMMARY**

#### **REFERENCES**

## 6.1 INTRODUCTION

Previous chapters have seen the development of a set of fast, accurate, flexible computer methods for the various stages of filter design; approximation, prototype design and realisation. In the present Chapter, the assembly of these design tools into a practical filter CAD package called PANDDA is reported. The philosophy of the program is explained and its internal structure is examined. PANDDA is then applied to various practical design problems.

The use of specialised transfer functions is illustrated. High order touch points are shown to produce compromises between the classical approximations elliptic and Chebyshev, with respect to their amplitude, group delay and passive sensitivity properties. By employing sloping and asymmetric approximations the transfer function can be tailored to difficult yet realistic filter specifications. In particular, correction of systematic weighting of the amplitude response is possible by inverse-weighting the original specifications. Important examples of weightings for SCFs are those due to  $\text{sinc}(x)$ , LDI termination error and telephone line transmission characteristics. The group delay response of the amplitude filter is equalised in a similar manner; by designing an all-pass function to inverse-weighted group delay boundaries.

A simple, effective optimisation algorithm is proposed, using the design facilities in an iterative loop with an analysis program. Distortions induced by non-ideal circuit parameters such as op-amp gain-bandwidth and switch resistance can be corrected. Various practical examples are given.

As an illustration of the combined use of all PANDDA's facilities, the process of design of several practical SCFs is traced from specification to fabrication on silicon. PANDDA is applied to two commercial filter specifications which pose special difficulties for standard design techniques. The program is shown to produce efficient, practical realisations of the SCFs. Finally, PANDDA was used to design a group of filters for a speech processing chip by engineers in the AMSYS group of GEC Research. Test results of the fabricated ASIC (application specific integrated circuit) are presented. This demonstrates the speed and ease with which good quality, straightforward SCF designs can be obtained.

## 6.2 AN INTEGRATED FILTER COMPILER : PANDDA

### 6.2.1 Design philosophy

The key aims in the construction of the PANDDA filter design system are as follows;

1. Modularity. The program has been arranged as an array of distinct software tools with simple interfaces. This permits easy intervention in the design process at intermediate stages. Often a designer will concentrate on a single phase of a design at a time, rather than proceed from start to finish. Thus several runs of an approximation program to find the 'best' transfer function, may be followed by a few trial syntheses of passive ladder prototypes.

2. Flexibility. A design program should not present a set of irregular restrictions to the user. This statement is difficult to realise if there is insufficient unity in the underlying design methods. PANDDA presents a series of unified filter design algorithms which can approximate arbitrary filter functions and can guarantee efficient realisation by an array of different filter structures.

3. Rapid evaluation of results. A set of fast analysis programs are provided internally to PANDDA. These make use of the internal knowledge of the filter to speed up analysis. Quick feedback of results is essential for iterative refinement of the design. External analysis programs need only be used as a final check.

4. Simplicity. Complex methods should be restricted to difficult, nonlinear problems. Most of the computational tasks in filter design can be tackled by general optimisation methods. However, they do not take sufficient account of the linearity of filter design, at a cost of long computation times and slower convergency. Furthermore, special transformations which complicate present software have been avoided, e.g. LDI transform, symmetrical frequency transforms, accuracy preservation transforms.

PANDDA is distinguished particularly by the following features,

1. the design of general forms of amplitude and group delay response,
2. easy construction and comparison of the many different filter structures, especially to allow new structures to compete with the popular, well-tested ones,
3. optimisation methods to improve the performance of circuits within physical constraints.

### 6.2.2 Internal structure

The software package PANDDA [1–2], has been constructed as a comprehensive SC filter design tool. Its internal structure is illustrated in Fig. 6.1. Further details are to be found in Appendix A.

PANDDA has been structured in levels, matching the conceptual stages in the filter design process as discussed in this thesis. Each level has a well-defined series of inputs and outputs allowing them to be developed and run independently. Following sections describe the facilities offered within each level with examples illustrating practical applications.

### 6.2.3 Specifications

The frequency response is defined either by parameters of a classical approximation or as a piece-wise linear tolerance plot of filter attenuation and group delay.

Filter options require selection of design method (biquad, LUD, coupled-biquad, leapfrog etc.), circuit implementation (switched-capacitor, active-RC, digital), non-ideal circuit parameters (unit capacitance, switch resistances, op-amp parameters, wordlength) and scaling directives.

### 6.2.4 Filter approximation

Classical approximation methods have been implemented, most notably elliptic approximation by Darlington's method [3–4].

Specialised amplitude responses may be designed by a combination of the Remez-exchange [5] and Newton [6] approximation algorithms. The latter is a new approach which permits the order of tangency of certain extreme points (touch points) of the amplitude response to attenuation boundaries to be specified. The designer has the freedom to specify the sequence of passbands and stopbands and the distribution of touch points in each. A sequence of high order touch points placed in the passband of a filter approximation will yield a discrete sequence of functions, between Butterworth and Elliptic. Fig. 6.2 illustrates a set of 14th order bandpass functions with various sequences of touch points, together with their associated group delay. Note that as the touch points smooth the

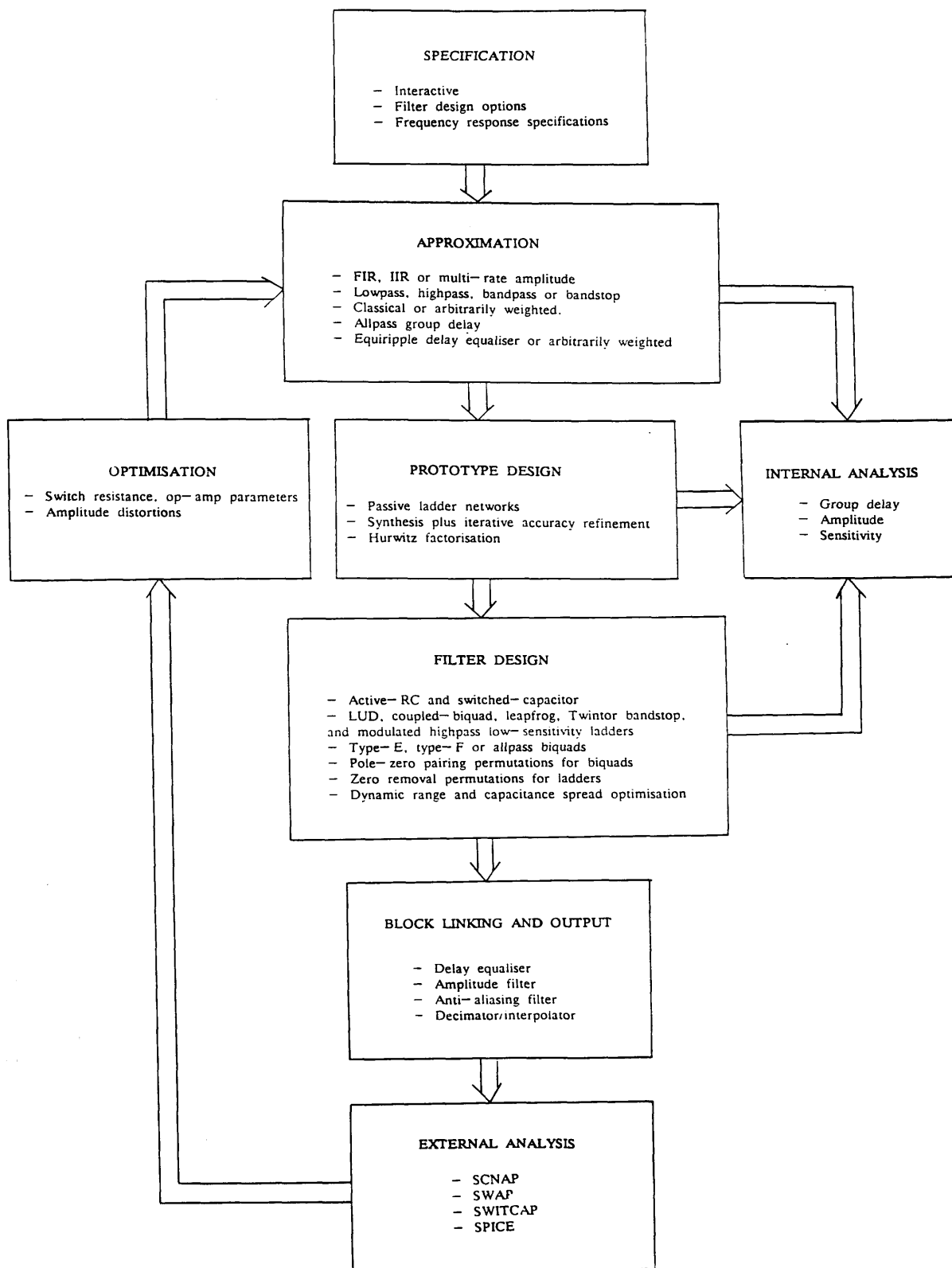


Fig. 6.1 Internal structure of PANDDA filter design system

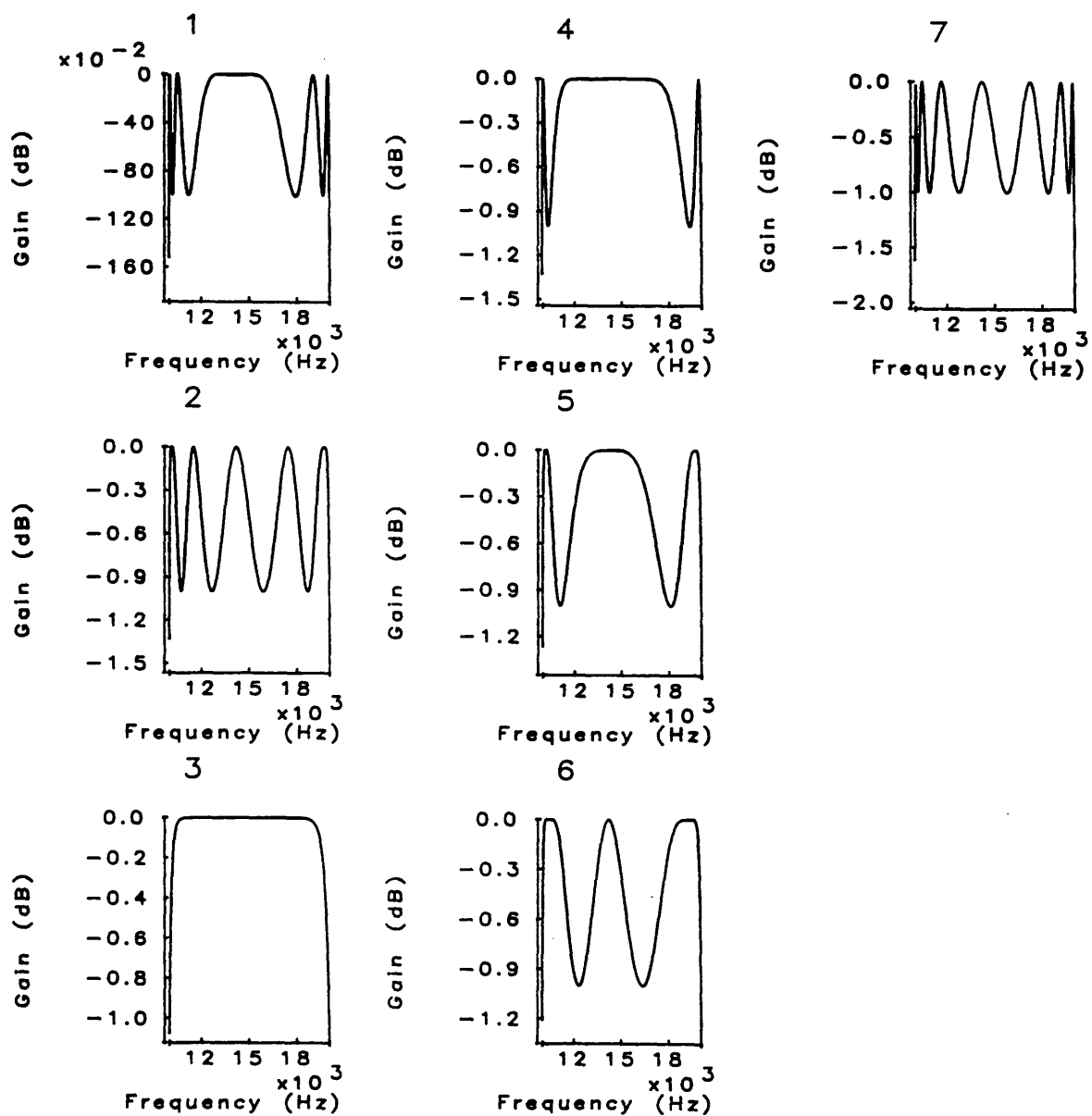


Fig. 6.2a Passbands of various 14th order bandpass filters employing high order touch points



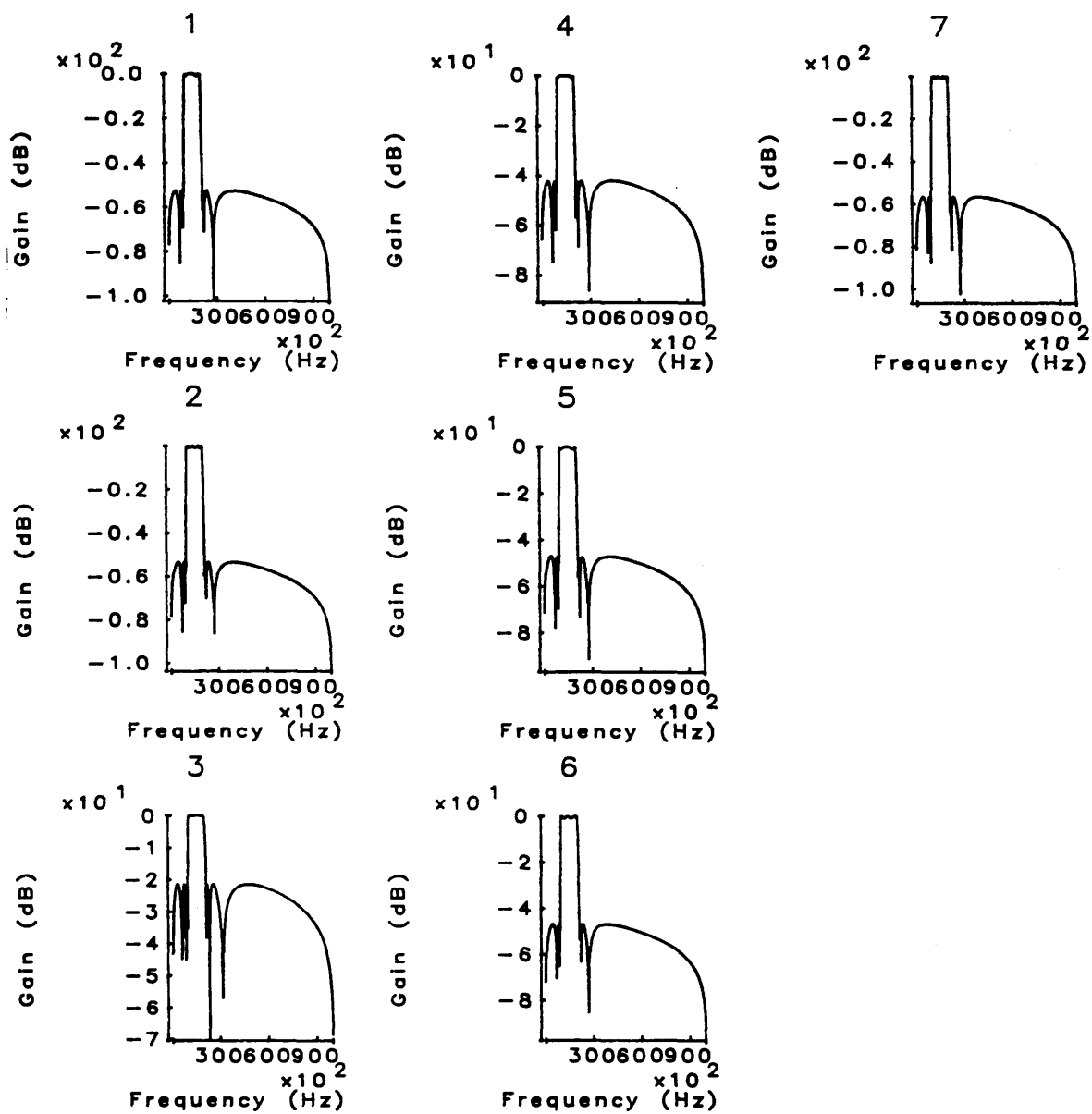


Fig. 6.2b Overall filter responses showing variation in stopband attenuation

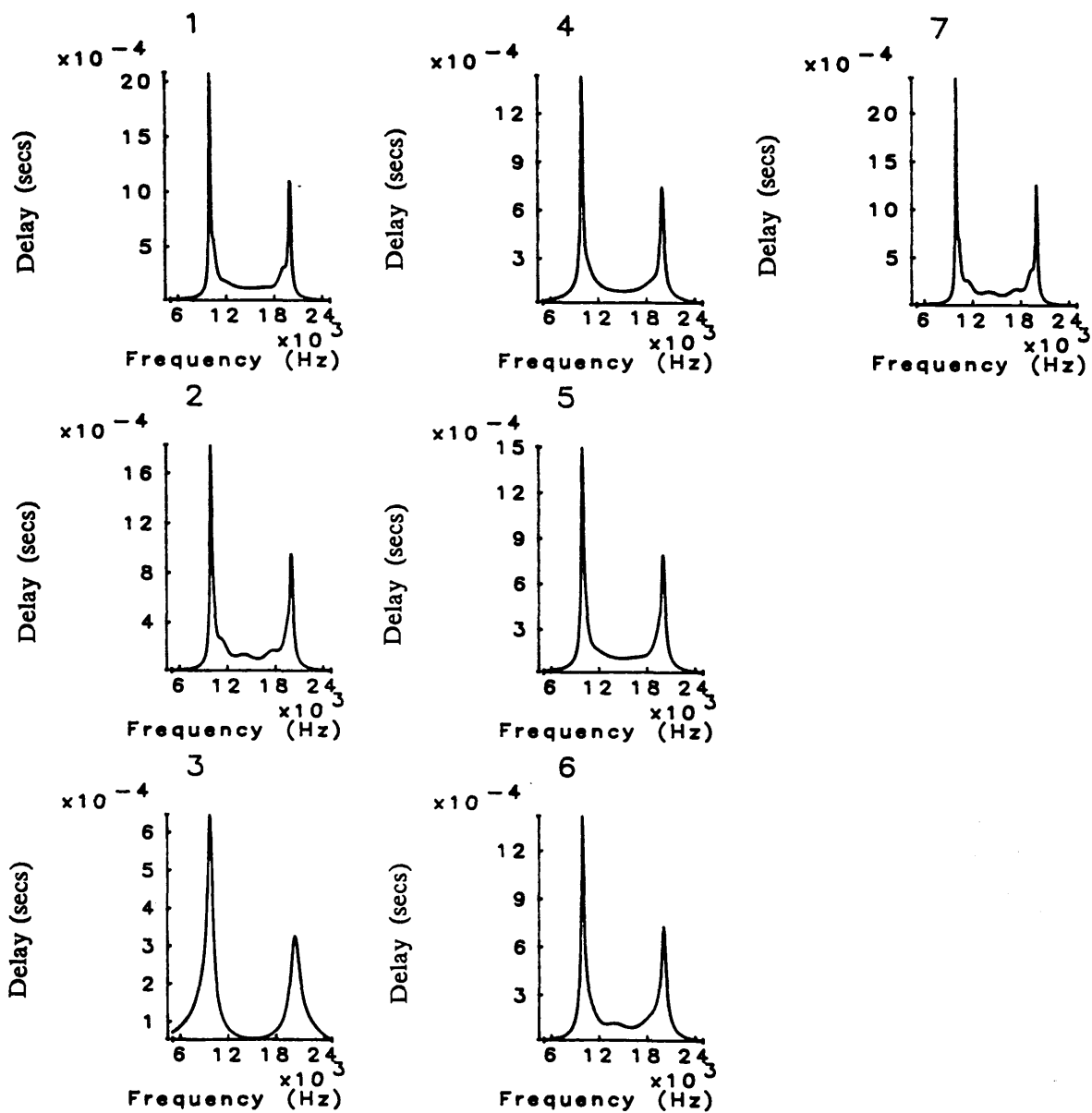


Fig. 6.2c Group delay variation

amplitude function, the delay peaking near the passband edge lessens, at the expense of poorer stopband rejection. The two extreme cases are the elliptic and inverse Chebyshev responses, formed by selecting seven 1st order or a single 13th order touch point respectively. Thus a family of responses are available which lie between classical forms offering a greater trade-off between their properties. Fig. 6.3 further emphasises this point; a series of 9th order lowpass functions have been designed to fixed passband and stopband edge frequencies and stopband attenuation of 65dB. Normally there are only two classical approximations with finite zeros. However by utilising various high order touch points, a series of responses can be obtained with associated progression of group delay. Some special methods have been presented for the design of such compromise functions e.g. transitional elliptic-inverse Chebyshev filters (Fig. 6.4) and transitional Butterworth-Chebyshev filters (Fig.6.5) [7]. They can be easily designed by selecting a single high order touch point at the band edge.

High order touch points in the filter stopband create deep, multiple notches for single frequency rejection. These notches are realisable by filters with greater symmetry and hence improved sensitivity [8-9]. A filter response with single ripple in passband and stopband created by high order touch points is shown in Fig. 6.6.

A further application of high order touch points is in the design of FIR differentiators with improved linearity at low frequency [10]. This can be done quite simply by specifying linearly sloping boundaries and by selecting a single high order touch point at 0Hz (Fig. 6.7). FIR transfer functions with specified degree of flatness are also required in the design of decimators [11], in order to introduce as little amplitude distortion into succeeding filtering as possible. A single high order touch point incident to a flat upper frequency boundary has the same effect (Fig. 6.8).

The attenuation function in each band is specified by a pair of arbitrary piece-wise linear boundaries between which a linear-phase FIR, IIR or multi-rate transfer function will be fitted. This means that the response can be weighted or shaped arbitrarily in passband or stopband. Weighting of the amplitude response in the passband can be of use in a number of ways. Equalisation of the  $\text{sinc}(x)$  effect is done by approximating to boundaries warped by the upward sloping  $1/\text{sinc}(x)$  function. Weighting to correct LDI termination error distortion requires a warping of the boundaries by  $\cos(\omega T/2)$  function; a downward sloping function. It is normally convenient to combine this with the

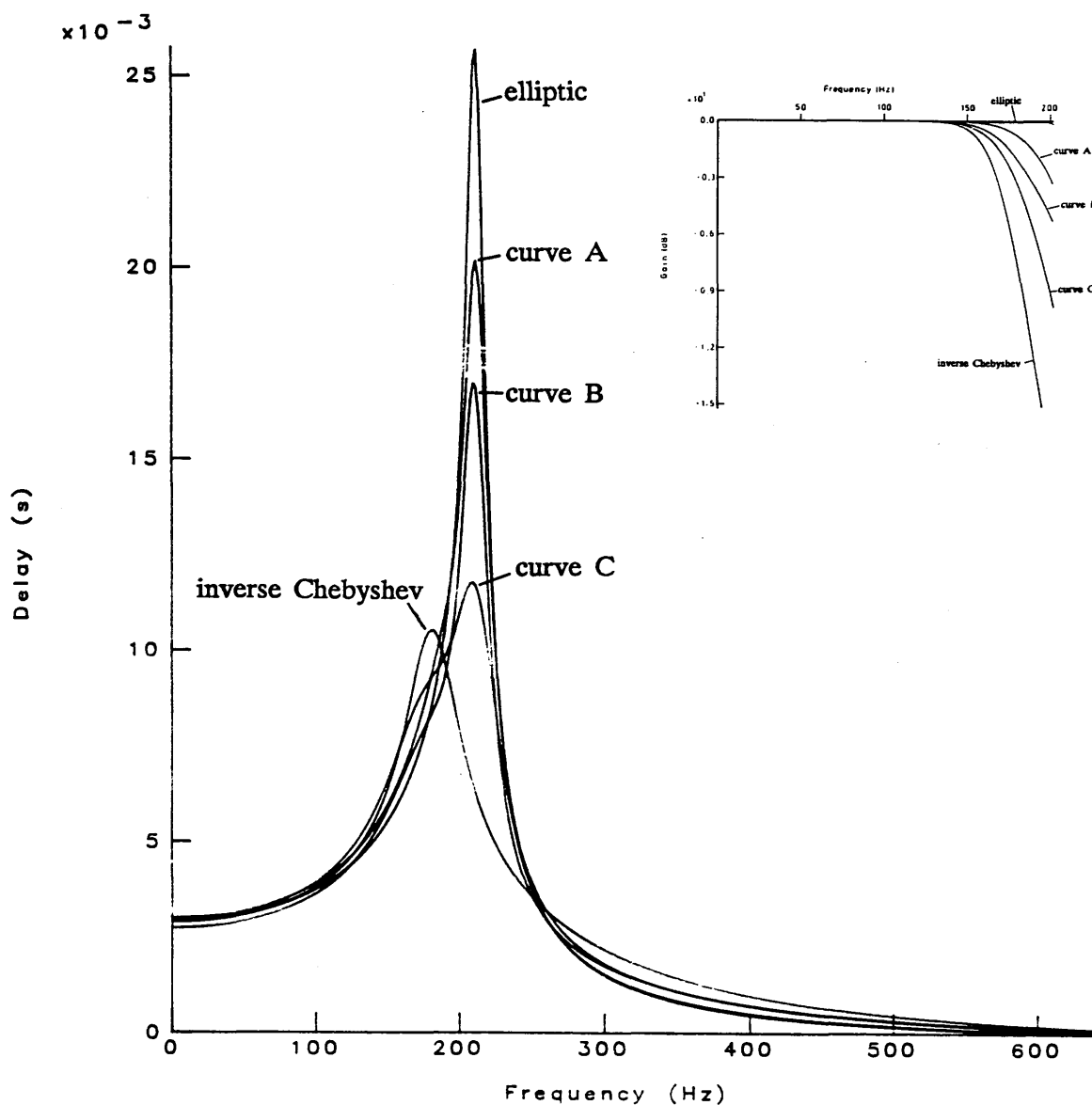


Fig. 6.3 Group delay variation of 9th order bandpass filters employing high order touch points (passband amplitude response shown inset)

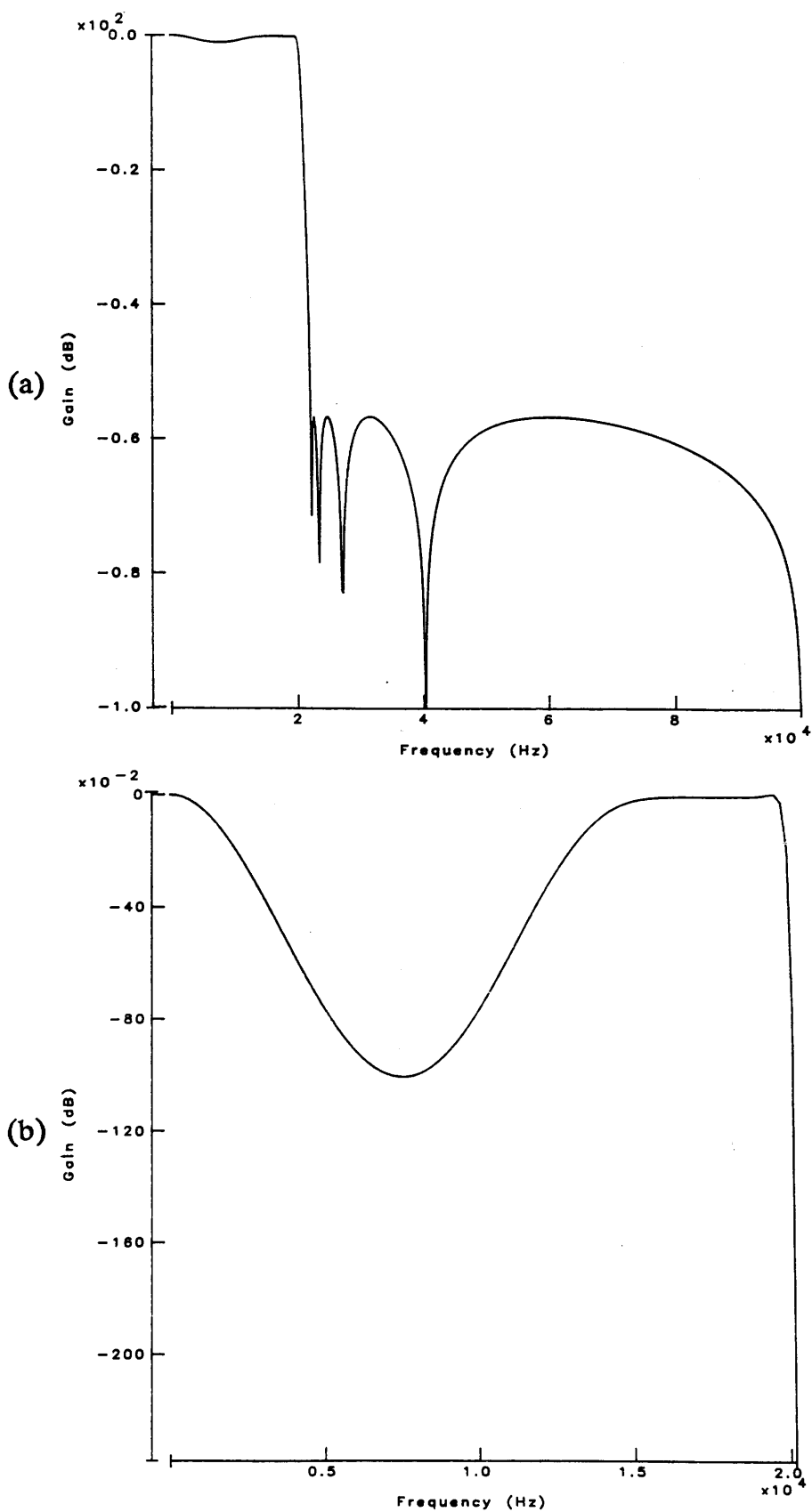


Fig. 6.4 (a) 9th order transitional elliptic/inverse Chebyshev lowpass filter  
 (b) Passband detail

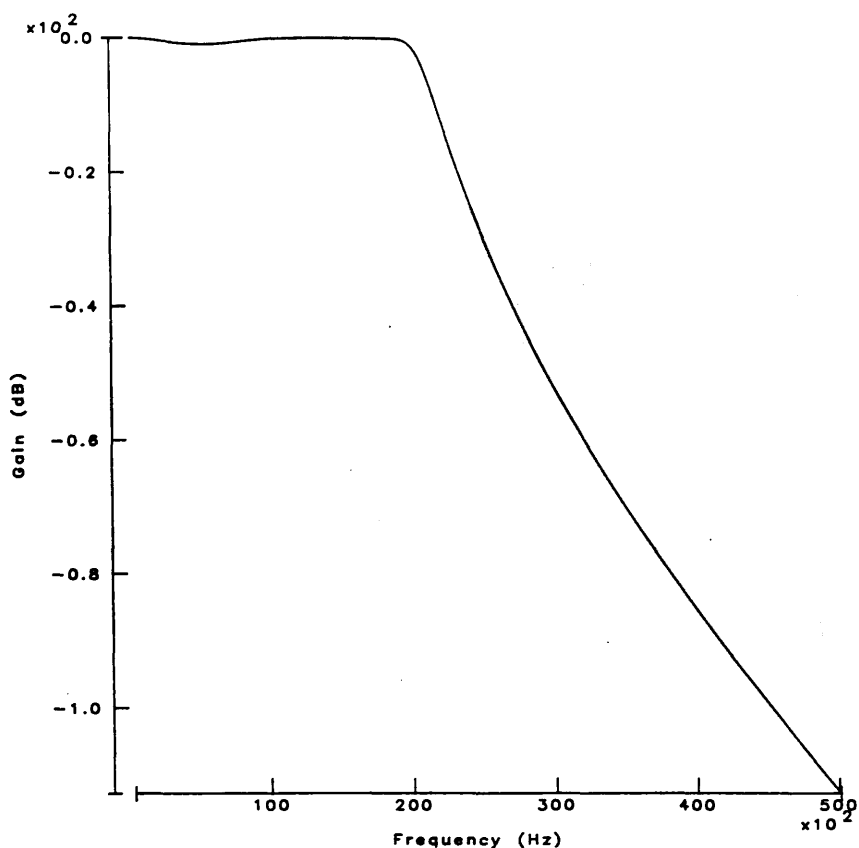


Fig. 6.5 9th order transitional Butterworth/Chebyshev lowpass filter

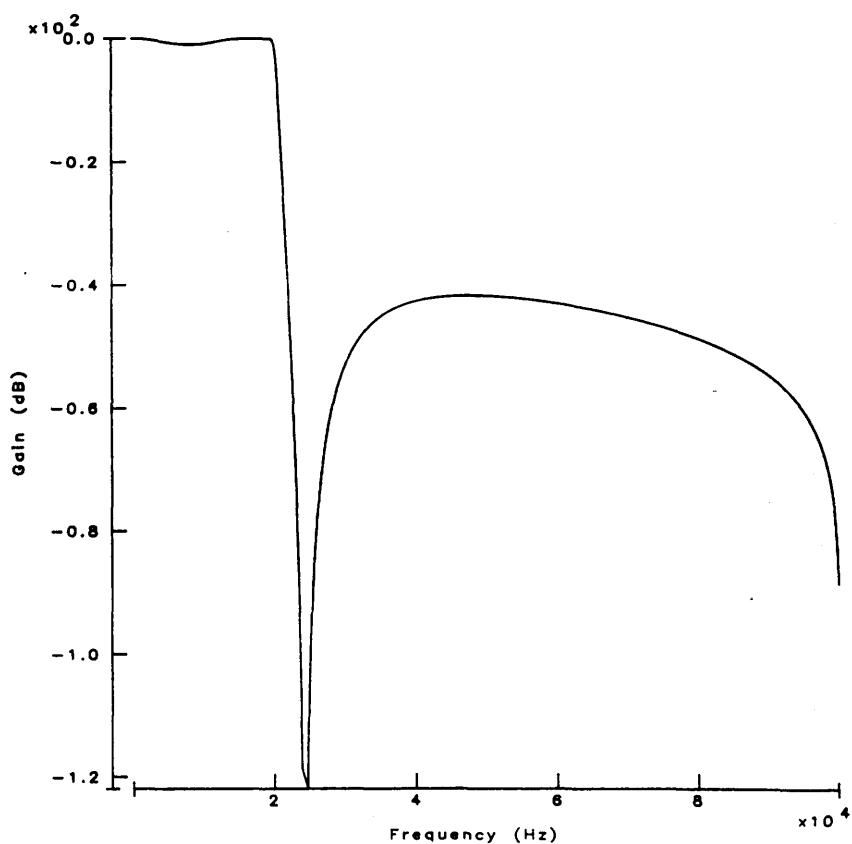


Fig. 6.6 9th order lowpass filter with single ripple in both passband and stopband

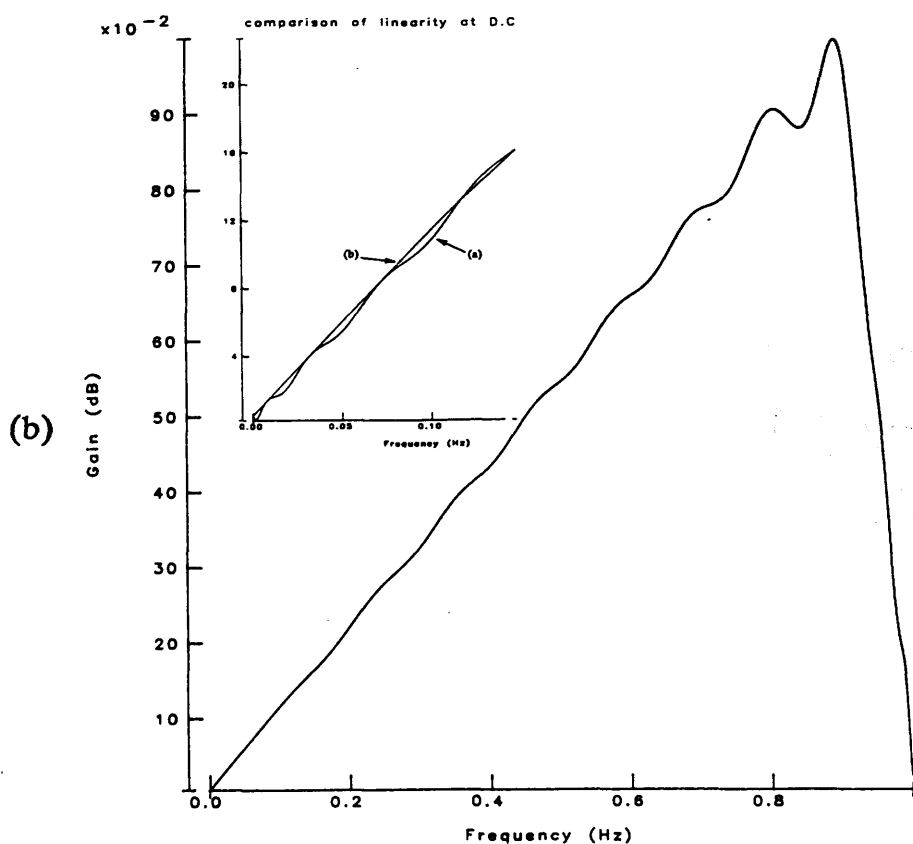
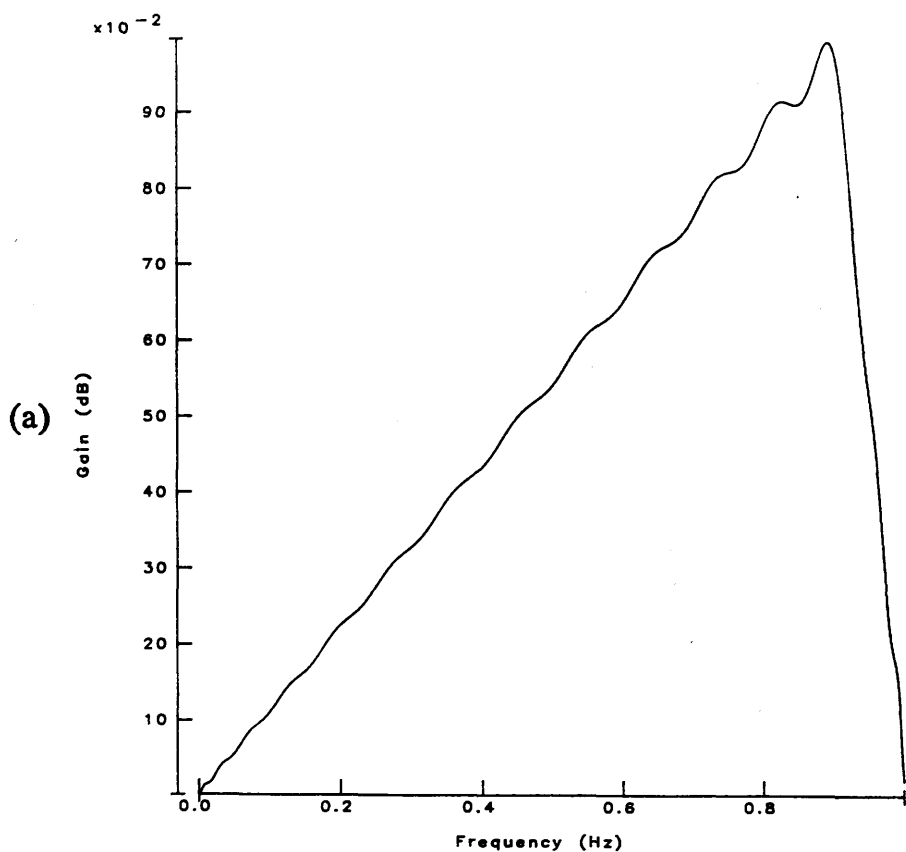


Fig. 6.7 (a) Length 69 FIR differentiator

(b) Length 69 FIR differentiator with 13th order touch point at 0Hz (linearity comparison shown inset)

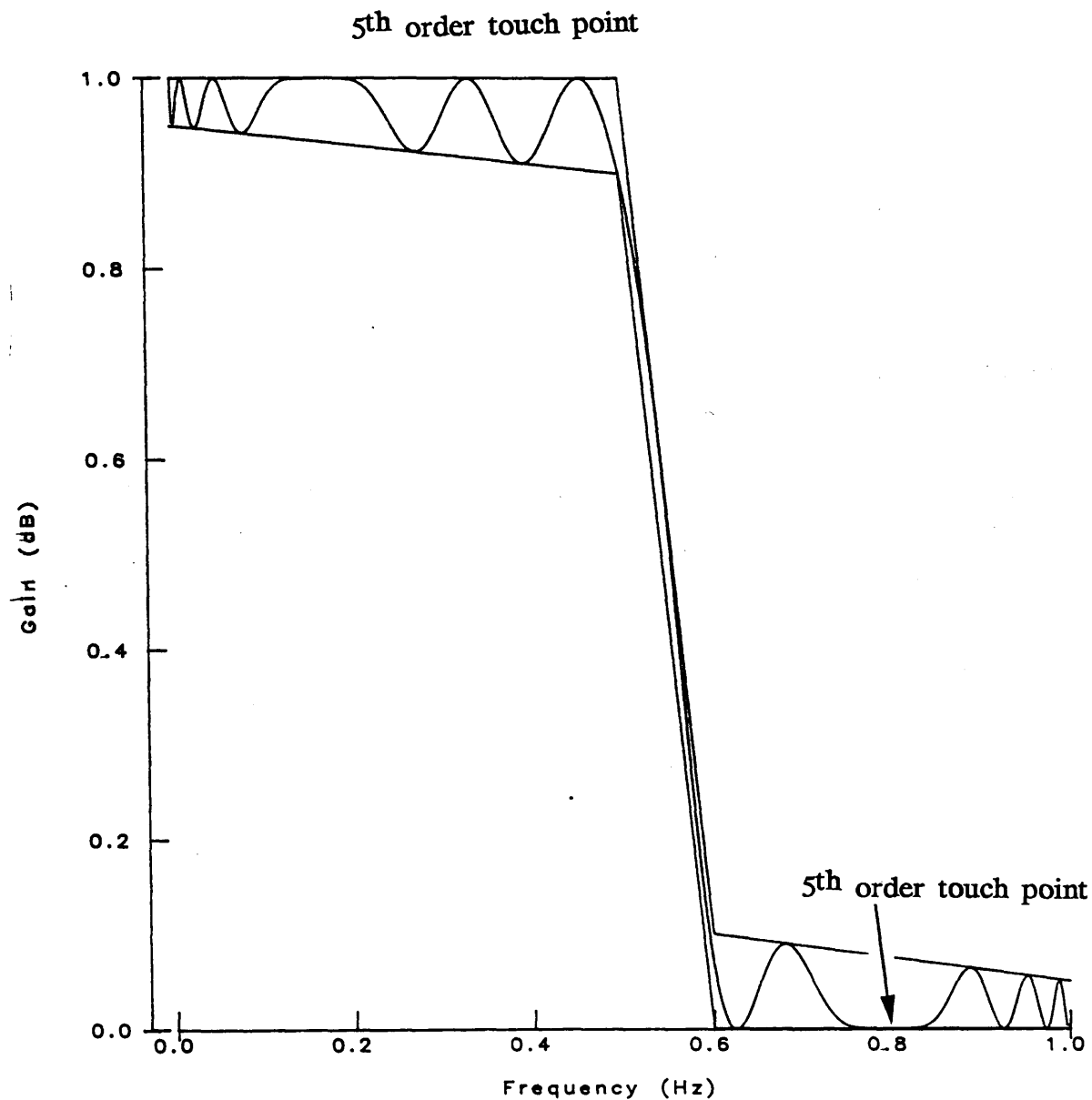


Fig. 6.8 Length 61 FIR lowpass approximation with high order touch point in passband and stopband



$\text{sinc}(x)$  weighting to produce a  $\text{tanc}(\omega T/2)$  warping, which is a flatter function because of the tendencies of the distortions to cancel (Fig. 6.9). An example of  $\text{sinc}(x)$  correction of a wideband 14th order bandpass filter is shown in Fig. 6.10.  $\text{Tanc}(x)$  correction is shown for the same filter in Fig. 6.11.

Local loop telephone lines have a transmission characteristic which exhibits a monotonous roll-off over the voice band (Fig. 6.12a). Correction of this function can be done by inverting the loss function over the filter passband. Modem filters often require this kind of equalisation (Fig. 6.12b). The roll-off of anti-aliasing filters can also disturb the ideal passband response (Fig. 6.13). In this case, a distributed-RC anti-aliasing filter has been chosen because it has certain advantages over lumped implementations [12]. Analysis of this distributed circuit has been done by a special program (Appendix B). Correction of this distortion is achieved by sloping the passband in a contrary direction (Fig. 6.14). The filter is a 14th order asymmetric bandpass with 200kHz sampling frequency. Note that, unlike other techniques of amplitude correction, this method will result in a bounded minimax function [13–15].

Tapering of the filter passband ripple is of use to decrease the sensitivity of passive filter realisations [16]. This can be achieved by weighting the lower passband boundary suitably (Fig. 6.15a). Combined with high order touch points (Fig. 6.15b) the sensitivity improvement is even more marked (Fig. 6.15d) at the expense of poorer stopband rejection (Fig. 6.15c).

Weighting of the filter stopband is sometimes also required. For example, in a transmitter system it is required to attenuate the harmonics of the carrier frequency. These harmonics are progressively smaller in amplitude as the frequency increases and so an efficient filter will attenuate those at low frequency most and those at higher frequency less [17–18]. This amounts to an upward sloping gain specification (Fig. 6.16).

Bandpass filters with unequal stopband attenuation requirements are most efficiently approximated by functions with unequal numbers of zeros in either band. Asymmetric functions, as they are known, can be designed by PANDDA. High order touch points, weighted passband and stopband and asymmetry may all be combined in a single approximation to create a very specialised transfer function.

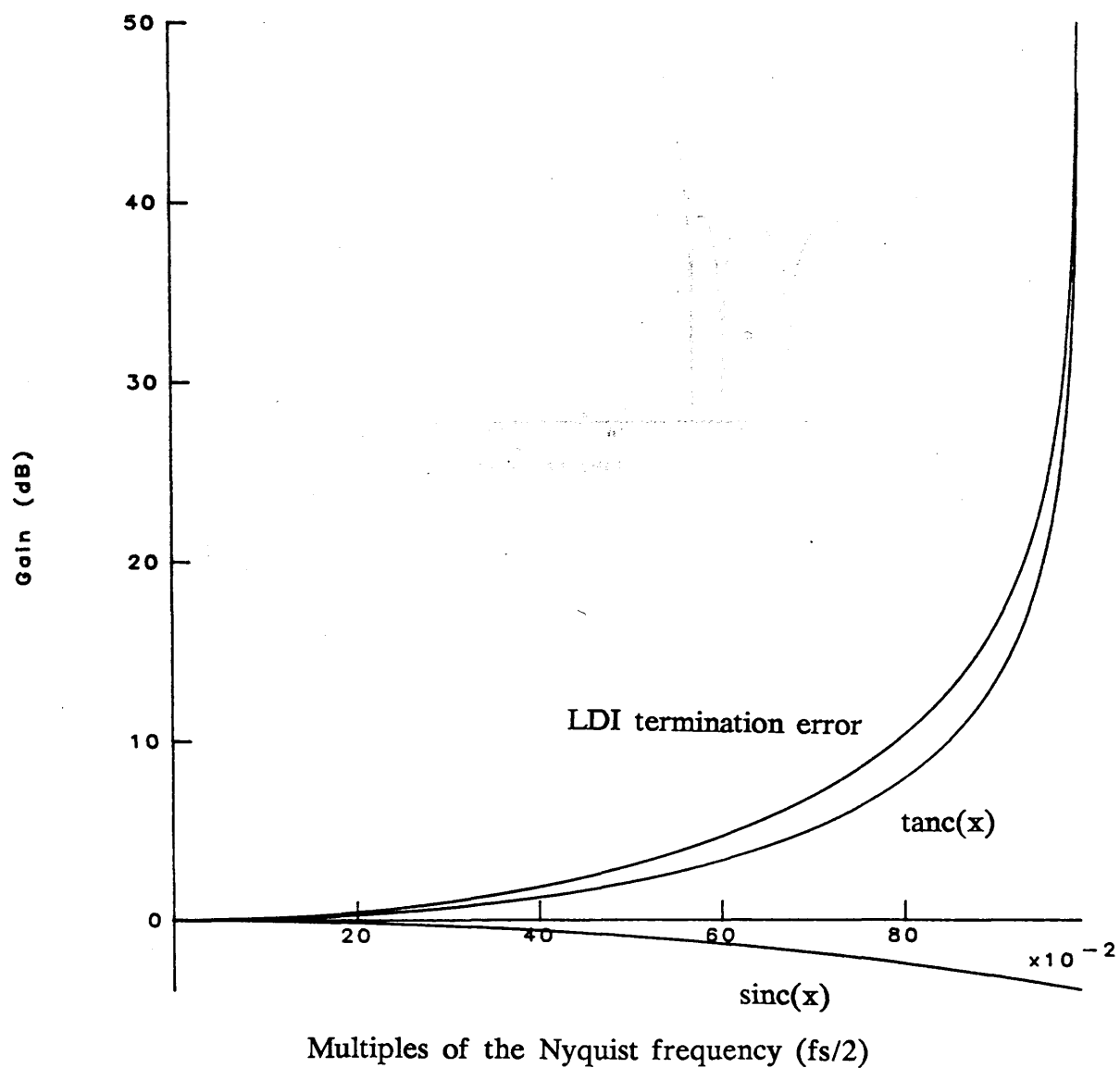


Fig. 6.9 Relative influence of  $\text{sinc}(x)$ , LDI termination error distortion and their combination ( $\text{tanc}(x)$ )

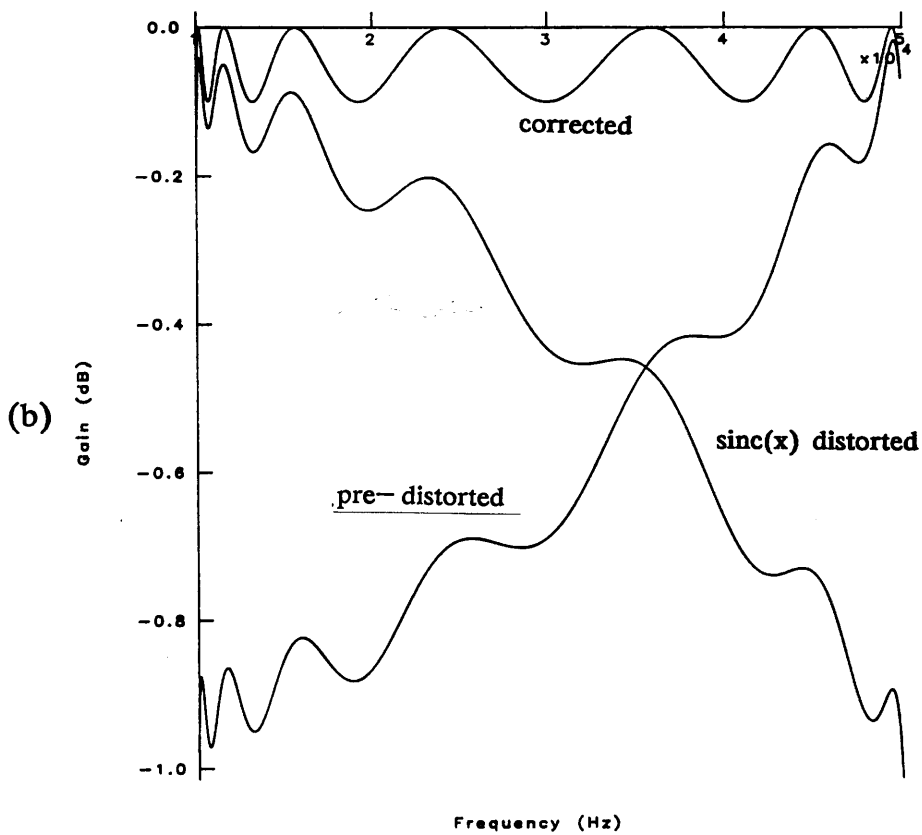
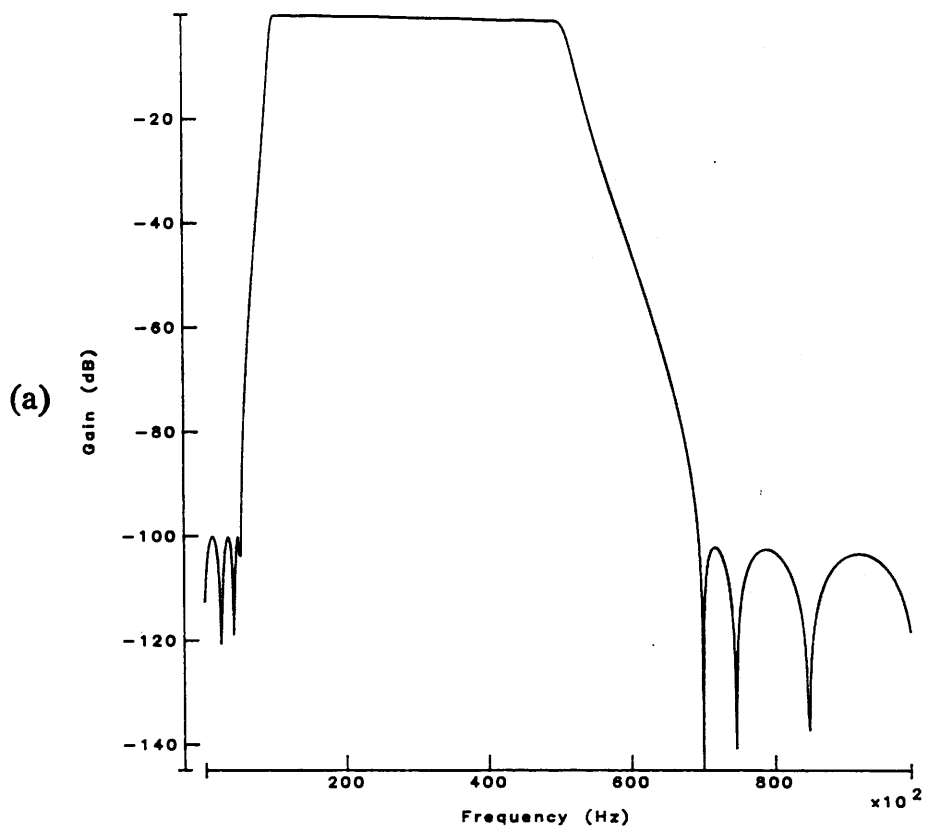


Fig. 6.10 (a) Effect of sinc(x) distortion on wideband bandpass SC filter  
(b) Sinc(x) correction

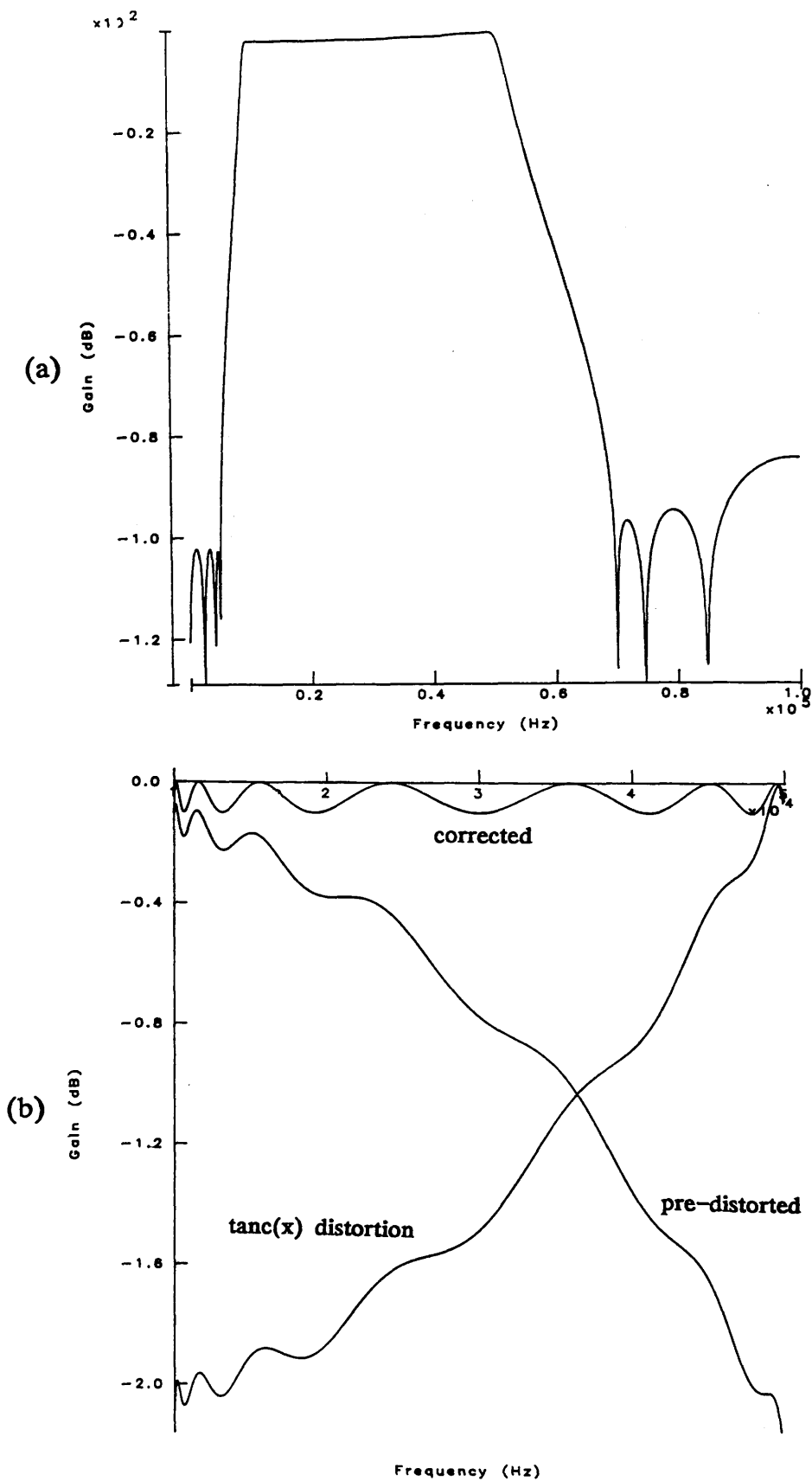


Fig. 6.11 (a) Effect of sinc(x) and LDI termination error on wideband bandpass SC filter  
(b) Tanc(x) correction

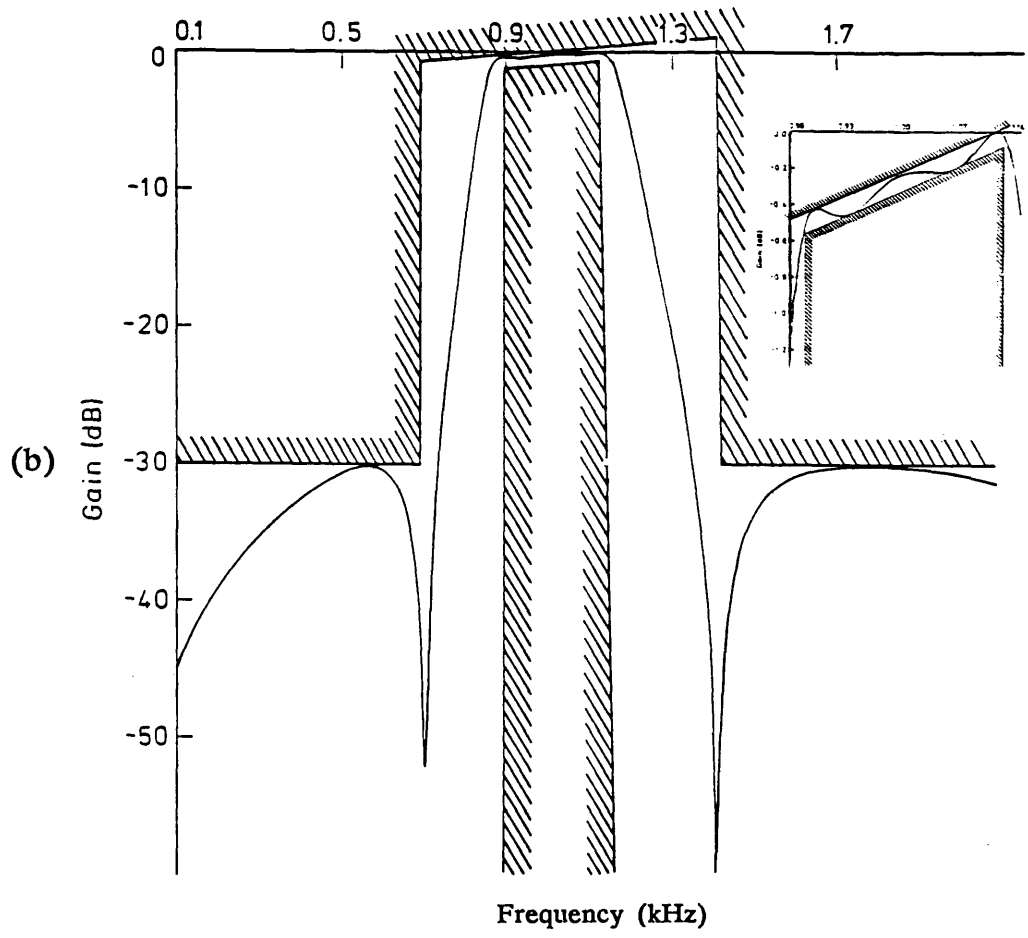
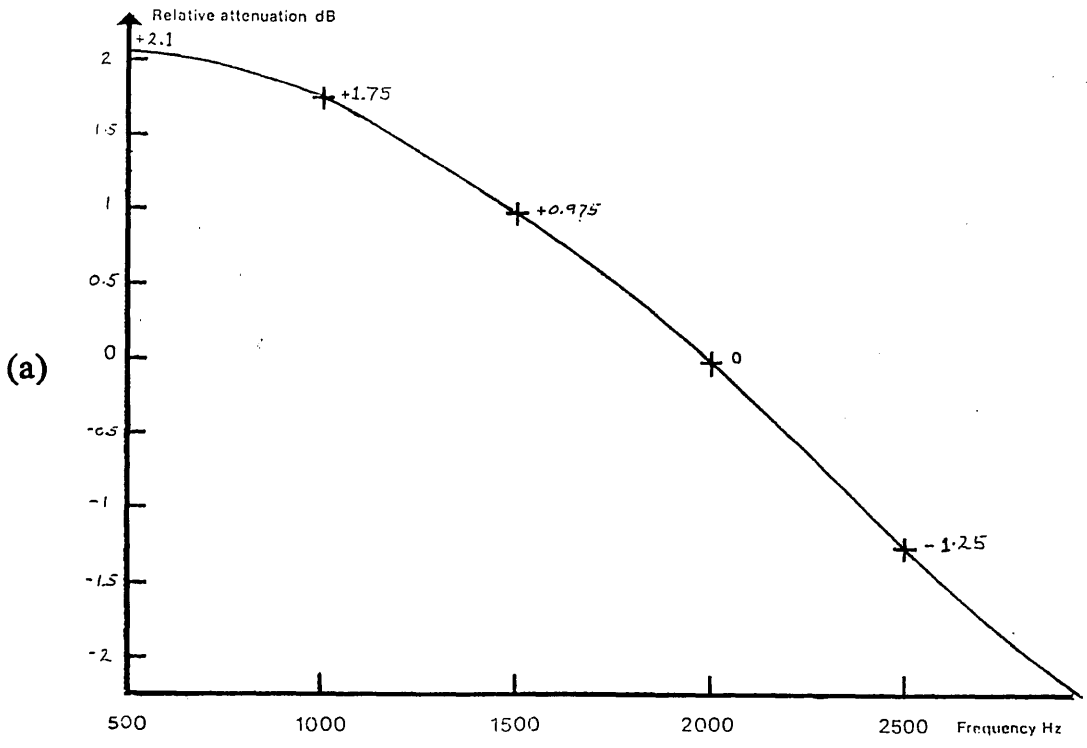
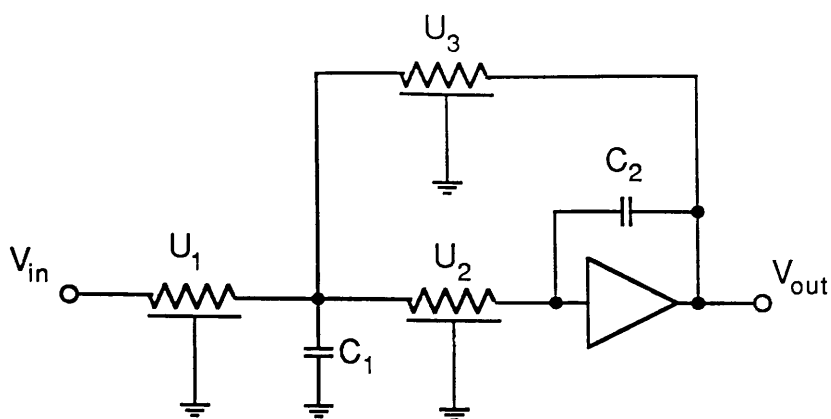


Fig. 6.12 (a) Telephone line transmission characteristics  
(b) 6th order equalised modem filter response



$$U_1 = U_3 = 190\text{k}\Omega, \quad 1\text{pF} \quad C_1 = 64\text{pF}$$

$$U_2 = 82.5\text{k}\Omega, \quad 1\text{pF} \quad C_2 = 24\text{pF}$$

Fig. 6.13 (a) URC anti-aliasing filter

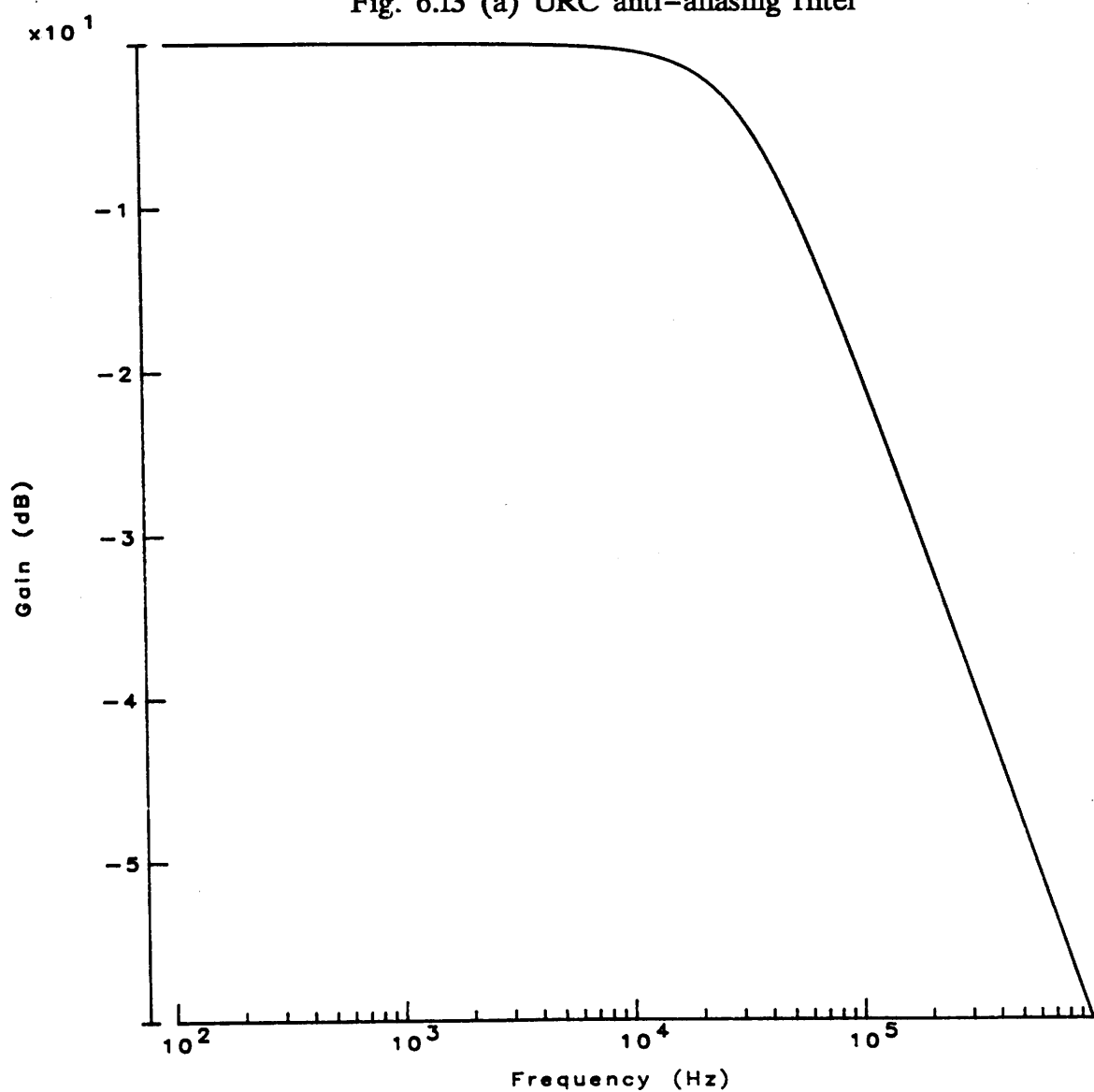


Fig. 6.13 (b) frequency response

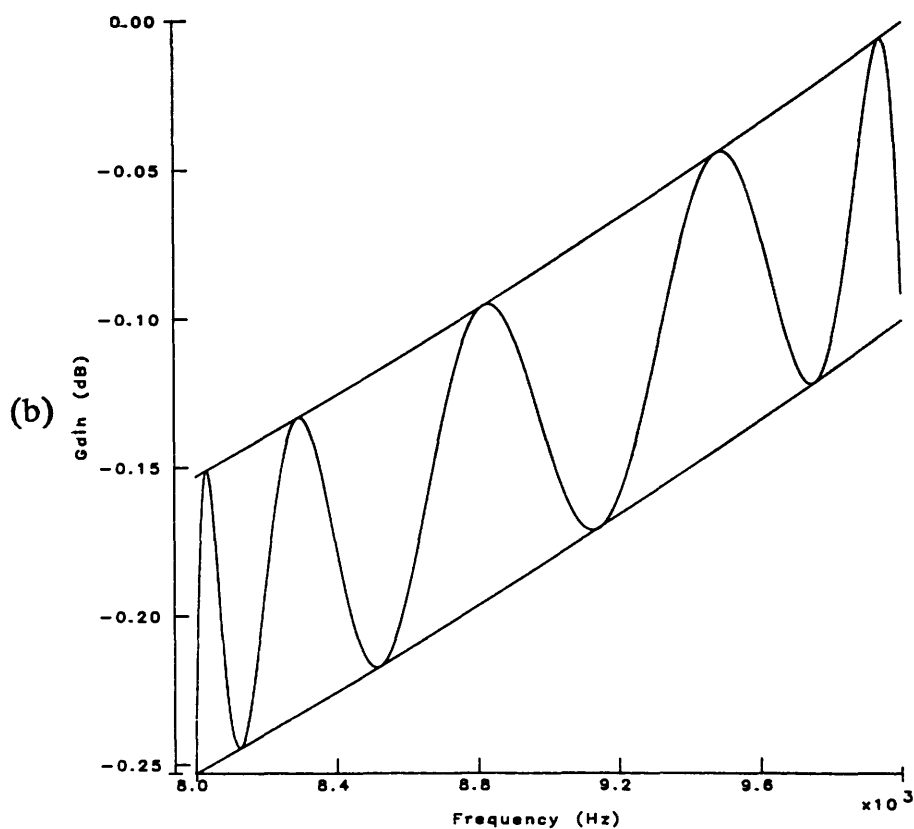
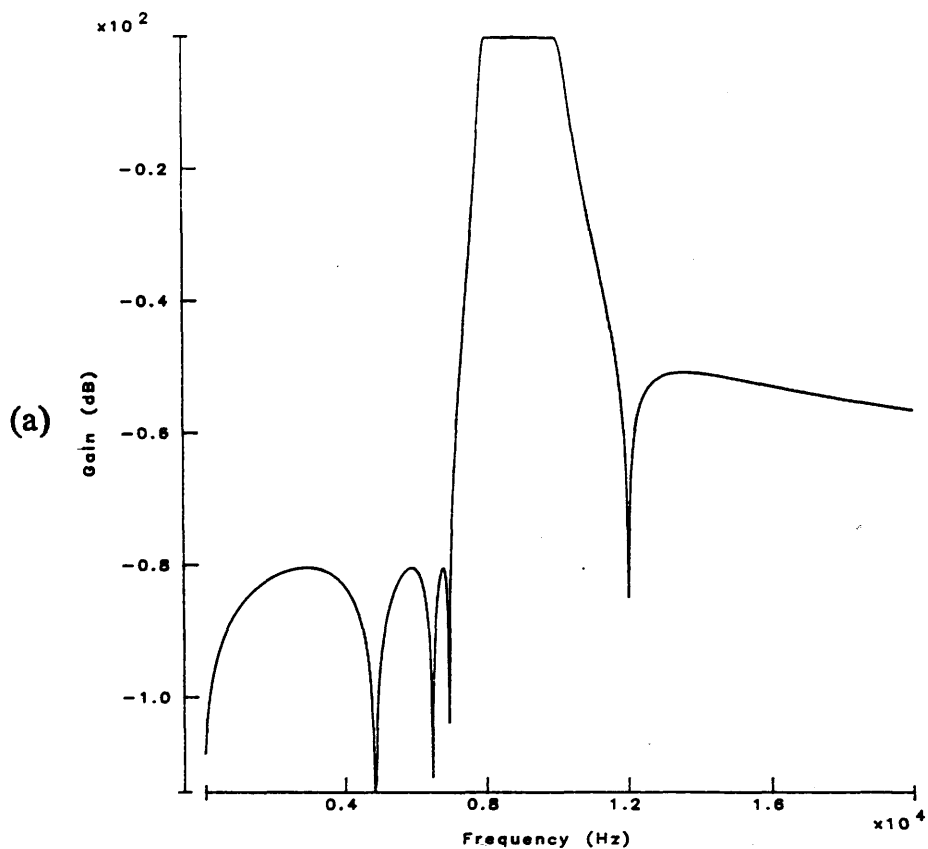


Fig. 6.14 (a) 10th order asymmetric bandpass filter pre-distorted for anti-aliasing filter roll-off

(b) Passband detail

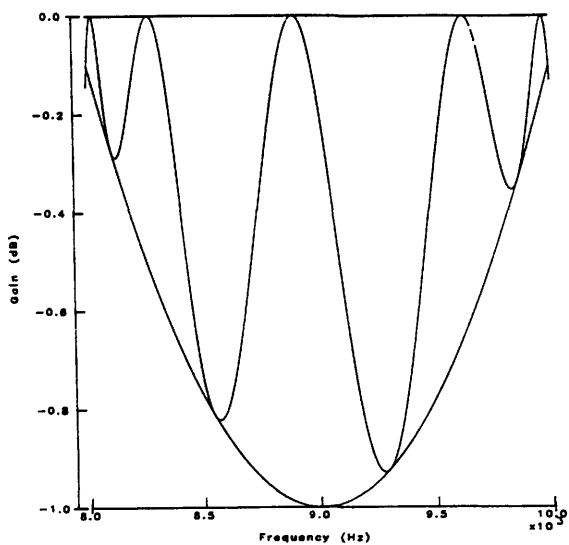


Fig. 6.15 (a) 10th order bandpass filter with tapered passband ripple

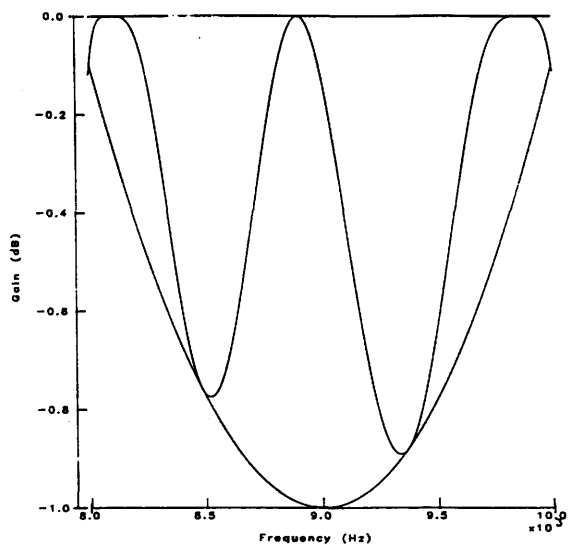


Fig. 6.15 (b) 10th order bandpass filter with taper and high order touch points

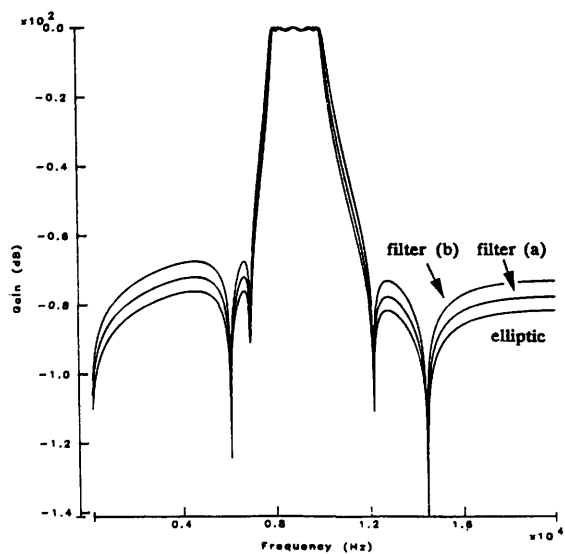


Fig. 6.15 (c) Comparison of stopbands of filters (a) and (b) with elliptic filter

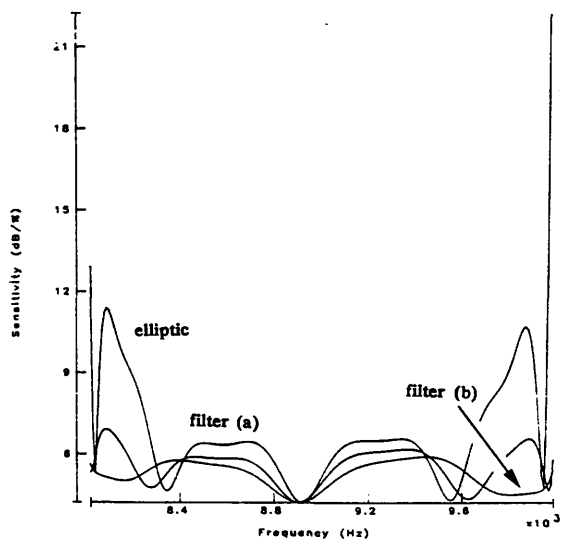


Fig. 6.15 (d) Sensitivity comparison of leapfrog SC realisations of filters (a) and (b) with elliptic



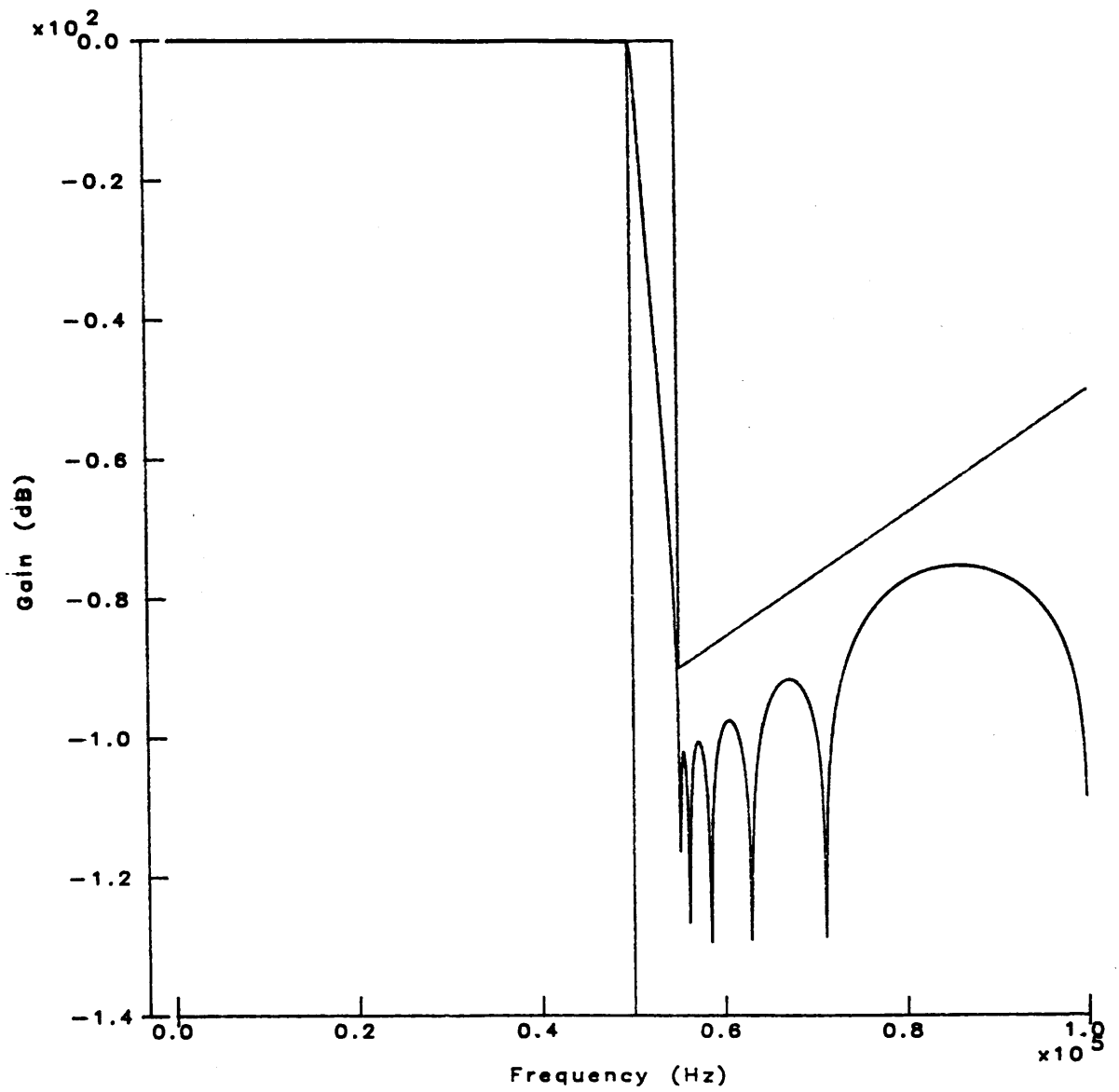


Fig. 6.16 12th order lowpass filter with sloping stopband to attenuate FM transmitter harmonics

All-pass transfer functions can be designed to equalise the amplitude filter delay response by a new algorithm [19]. In general, the group delay can be fitted between a pair of piece-wise linear boundaries. Often the required order of the all-pass function will be large if full equalisation over the whole passband is required. A 28th order equalisation of a 10th order elliptic function with passband from 2kHz to 4kHz is illustrated in Fig. 6.17.

### 6.2.5 Prototype design

The basis of the succeeding filter design stage is either a normalised doubly-terminated LC ladder or a transfer function in factorised form.

Design of passive ladder networks is accomplished by an extension of an iterative design method due to Orchard [20] in conjunction with a simplified insertion-loss synthesis [21] program. The latter is used to set up the structure and provide initial component values for the iterative part. Features of the iterative algorithm are very good accuracy and the ability to design high order networks (up to 100th). It is therefore useful for accuracy refinement and order augmentation.

Passive networks are of particular interest for operational simulation by active and digital circuits. The low-sensitivity properties of an original passive ladder is usually inherited by its simulation. Ladders with minimum node configurations can be most efficiently simulated. Negative element values are permissible and are even useful to eliminate certain excess components in the filter.

### 6.2.6 Circuit design and scaling

A variety of filter designs are available, including general biquads (including all-pass) [22] and coupled-biquad, LUD or leapfrog bilinear ladders [23–25]. Among several new ladder simulations [26], LUD structures are notable because of the absence of unswitched capacitor loops and good capacitance spread for narrow bandpass applications. Simulation of highpass ladders is achieved by the modulation method of [27] and bandstop ladders by the new twintor circuits [28]. All-pass functions can also be realised as low-sensitivity ladder networks using newly-developed circuits [29]. SCFs which are canonic in terms of numbers of op-amps are guaranteed for both ladder and biquad topologies. Interesting comparisons of the sensitivities, component value spreads and size of the different structures can be quickly made.

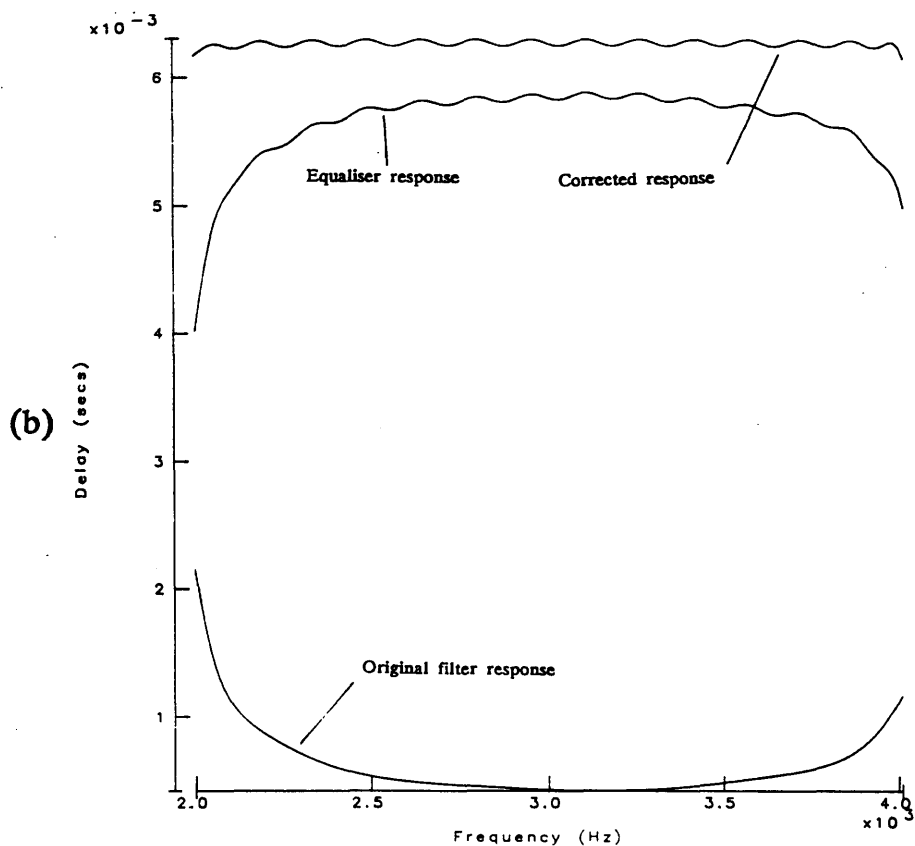
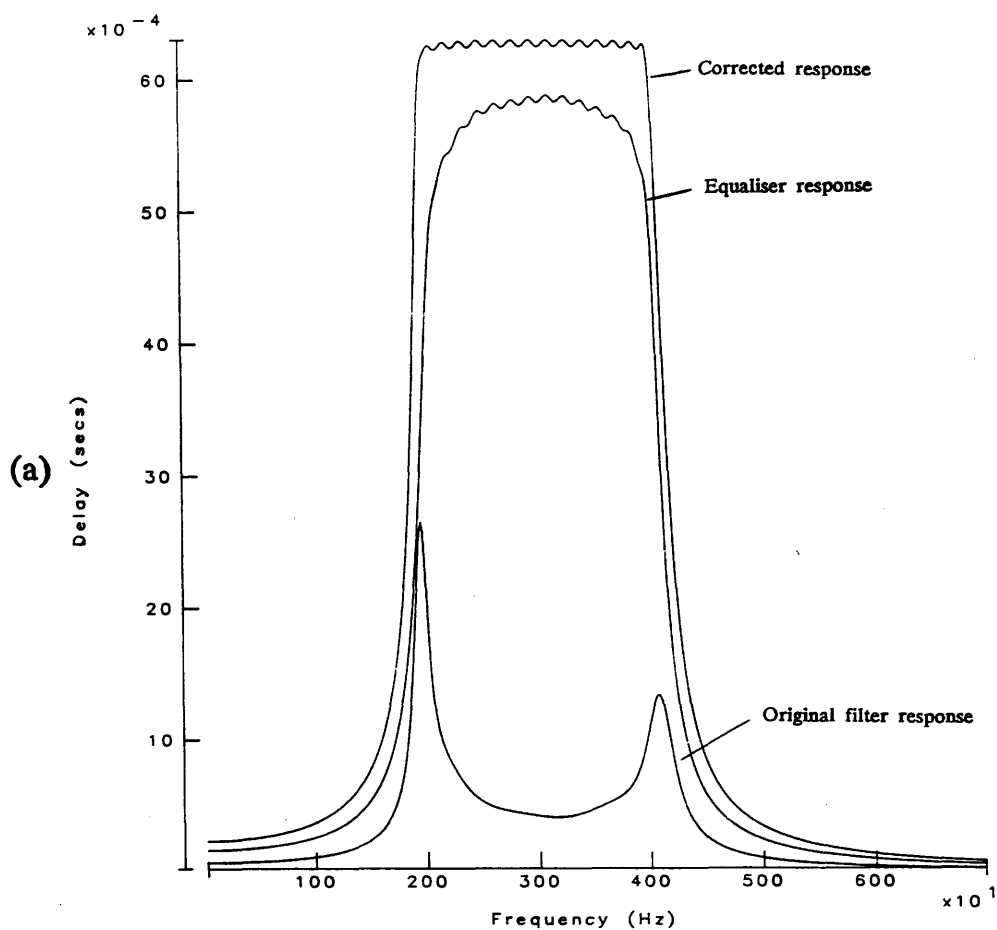


Fig. 6.17 (a) Equalisation of 10th order elliptic filter delay response by 28th order all-pass function  
(b) Passband detail

All filter structures are designed by a matrix methods [26]. A matrix system is a very concise and flexible means of representation of a wide variety of networks. Each non-zero entry in a matrix represents the connection of a building-block between nodes. Building-blocks may belong to a variety of different technologies e.g. Miller integrator in active-RC, LDI integrator in switched-capacitor (SC) and delay element in digital. The sparse structure of the matrices is known at the design stage and this information is used to provide a fast internal analysis for dynamic range and capacitance spread scaling. Some tradeoff between these two factors is available to reduce any large capacitors.

Various permutation strategies for pairing the poles and zeros of biquad cascade networks are available to improve their total capacitance. Similarly for ladder simulations where the sequence of zero removals is significant.

An internal network description may be translated into an external format suitable for layout or analysis by standard programs SWAP, SWITCAP, SCNAP or SPICE.

### 6.2.7 Optimisation

Fast frequency analysis of non-ideal switched-capacitor circuits is available from the QUICKSCNAP program [30]. Results of a passband analysis of a filter with realistic switch resistance and op-amp parameters will reveal some deviation from the designed frequency response. Correction of the error is achieved by pre-distorting the attenuation specifications and re-designing the filter.

*Step 1* : Design filter to meet ideal amplitude specifications

*Step 2* : Analyse under non-ideal circuit conditions

*Step 3* : Create error function between distorted passband function and ideal passband function.

*Step 4* : Pre-distort the original amplitude specifications by the error function.

*Step 5* : Re-design the filter to meet the pre-distorted specifications and repeat from *Step 2* until converged.

Note that it is only likely to be useful, provided that the degree of distortion is such that ripples are still recognisable.

This simple optimisation scheme has certain advantages over a full SC network optimisation [31];

1. The problem on the order of the original filter, not on the number of components in the SC circuit. This represents a considerable saving in computation (a typical 10th order filter will have as many as 40 capacitors).
2. No special derivatives are necessary.
3. Provided a suitable analysis program is available, any distortion can be eliminated.
4. Ease of designer intervention in the optimisation process.
5. Re-design is very fast compared to analysis.

An example illustrates the use of the design algorithms within the PANDDA filter design program. A sixth order bandpass filter is designed to typical modem specifications, with sloping passband amplitude response to correct transmission line attenuation (Fig. 6.18). A left-LUD SC realisation is simulated with non-ideal circuit parameters (Fig. 6.19) and the ideal response is distorted. By pre-distorting the specifications to compensate for the error and re-designing the RLC ladder prototype the original response can be restored after only a few iterations. In this case, the optimisation converged in 5 iterations with 5 minutes of CPU time on a MicroVAX II computer. The optimised component values are given in Table 6.1.

### 6.3 DESIGN OF A FM RADIO FILTER

The specifications of an FM radio filter are shown in Table. 6.2 and the amplitude template of Fig. 6.20. The filter requires a  $-20\text{dB/decade}$  slope over the passband range which cannot be met by the classical approximations Butterworth, Chebyshev or elliptic. The general IIR approximation capability must be employed. Various stopband schemes of a sixth order filter function are tested, the passband specifications being exactly satisfied (Fig. 6.21). Only two of these meet the specifications, one with a low frequency notch in the lower stopband (Fig. 6.21b) and the other with a triple notch at zero frequency (Fig. 6.21c). After designing a suitable ladder prototype various realisations of this transfer functions are viewed. The component spreads of the first filter are exorbitantly high (Table 6.3). This a problem caused by the low time constant introduced by the notch at 80Hz. However, the second transfer function reduces the implementation cost to practical levels by placing the notches at zero frequency (Table 6.4).

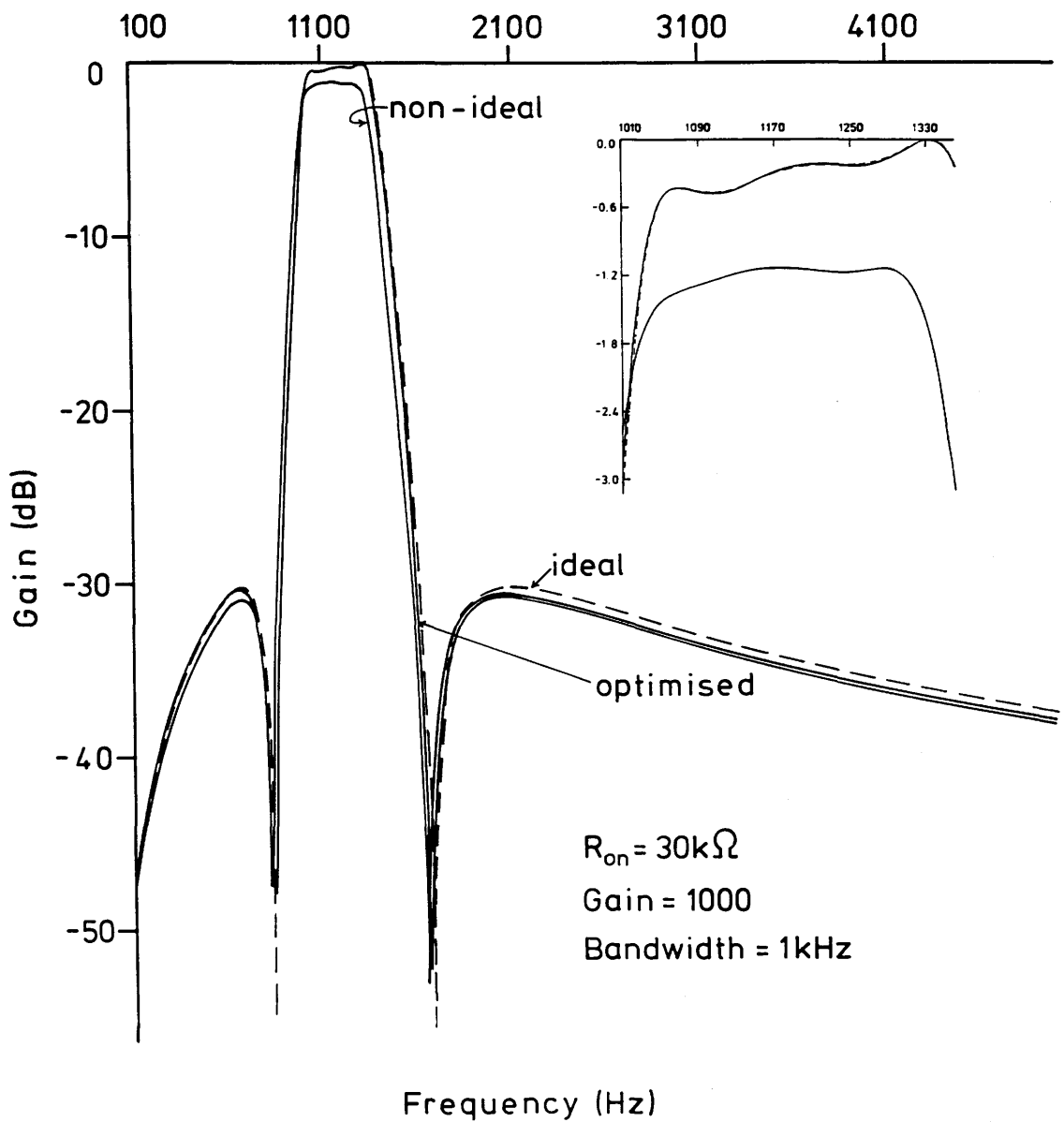


Fig. 6.18 (a) Optimisation of a 6th order SC modem channel filter for switch and op-amp non-idealities

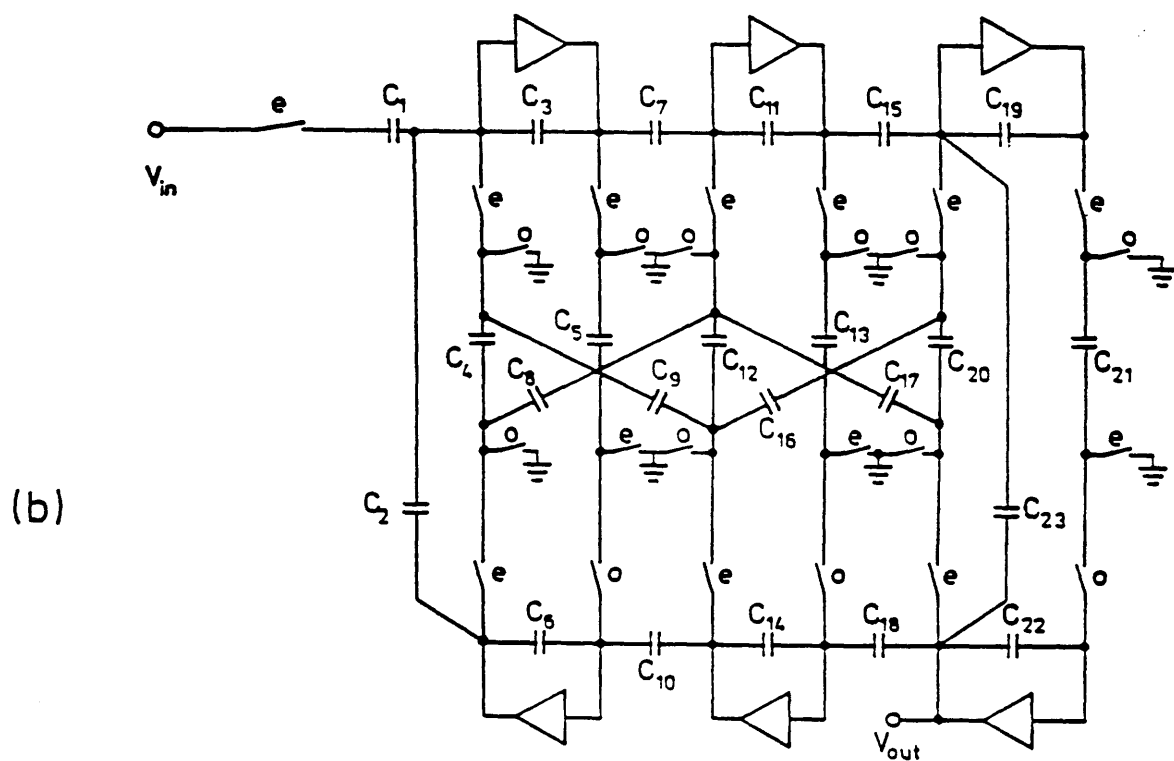
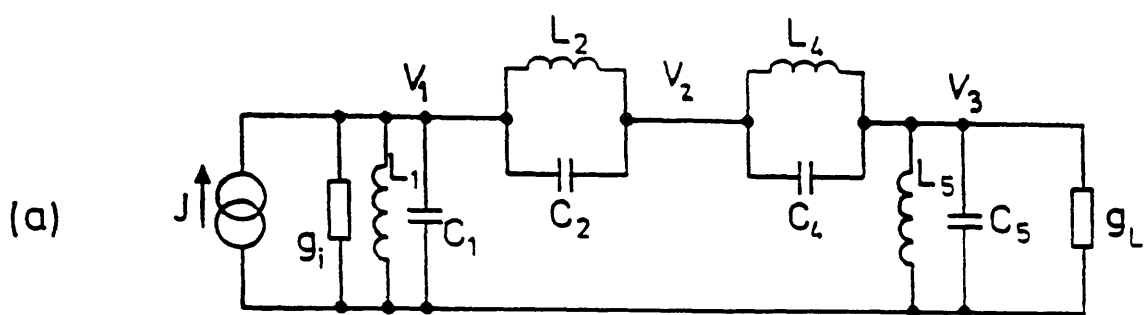


Fig. 6.19 (a) 6th order bandpass RLC prototype  
(b) 6th order LUD SC filter

Normalised data for LC ladder of Fig. 6.19a					
upper passband edge		1.1342	lower passband edge		0.8817
upper stopband edge		1.3570	lower stopband edge		0.7369
passband ripple		< 0.1dB	stopband attenuation		> 30dB
G1	1.0	G2	1.63638	C1	4.01347
L2	1.08867	C4	0.94039	L4	0.53119
				C5	5.70643
				L1	0.25806
				C2	1.83882
				L5	0.16995

Component values for ideal SCF of Fig. 6.19b					
C1	7.3567	C2	6.0431	C3	38.648
C5	1.0	C6	7.9198	C7	18.978
C9	1.0	C10	3.7889	C11	40.347
C13	1.0986	C14	7.5087	C15	5.3223
C17	1.0	C18	1.0	C19	10.023
C21	1.0	C22	7.6061	C23	2.2936
total capacitance		173.515	capacitance spread		40.347

Component values for optimised SCF of Fig. 6.19b					
C1	7.1491	C2	4.8066	C3	41.475
C5	1.0	C6	7.7376	C7	19.978
C9	1.0	C10	3.3754	C11	40.721
C13	1.14	C14	7.7278	C15	5.2695
C17	1.0	C18	1.0	C19	9.9422
C21	1.0	C22	7.3943	C23	2.1483
total capacitance		175.918	capacitance spread		41.475

number of capacitors	23	number of switches	25
number of op-amps	6	clock frequency	64kHz
lower passband edge	1050Hz	upper passband edge	1350Hz
unit capacitance	1pF		

Table 6.1 Specifications and component values for Fig. 6.18 and Fig. 6.19



Design example

FM radio filter:

Filter class = BANDPASS

Clock frequency = 200kHz

Lower passband edge = 300Hz

Upper passband edge = 3kHz

Lower stopband edge = 100Hz

Upper stopband edge = 7kHz

Passband ripple = 0.5dB

-20dB/decade slope over passband for integration

Table 6.2 FM radio filter specifications

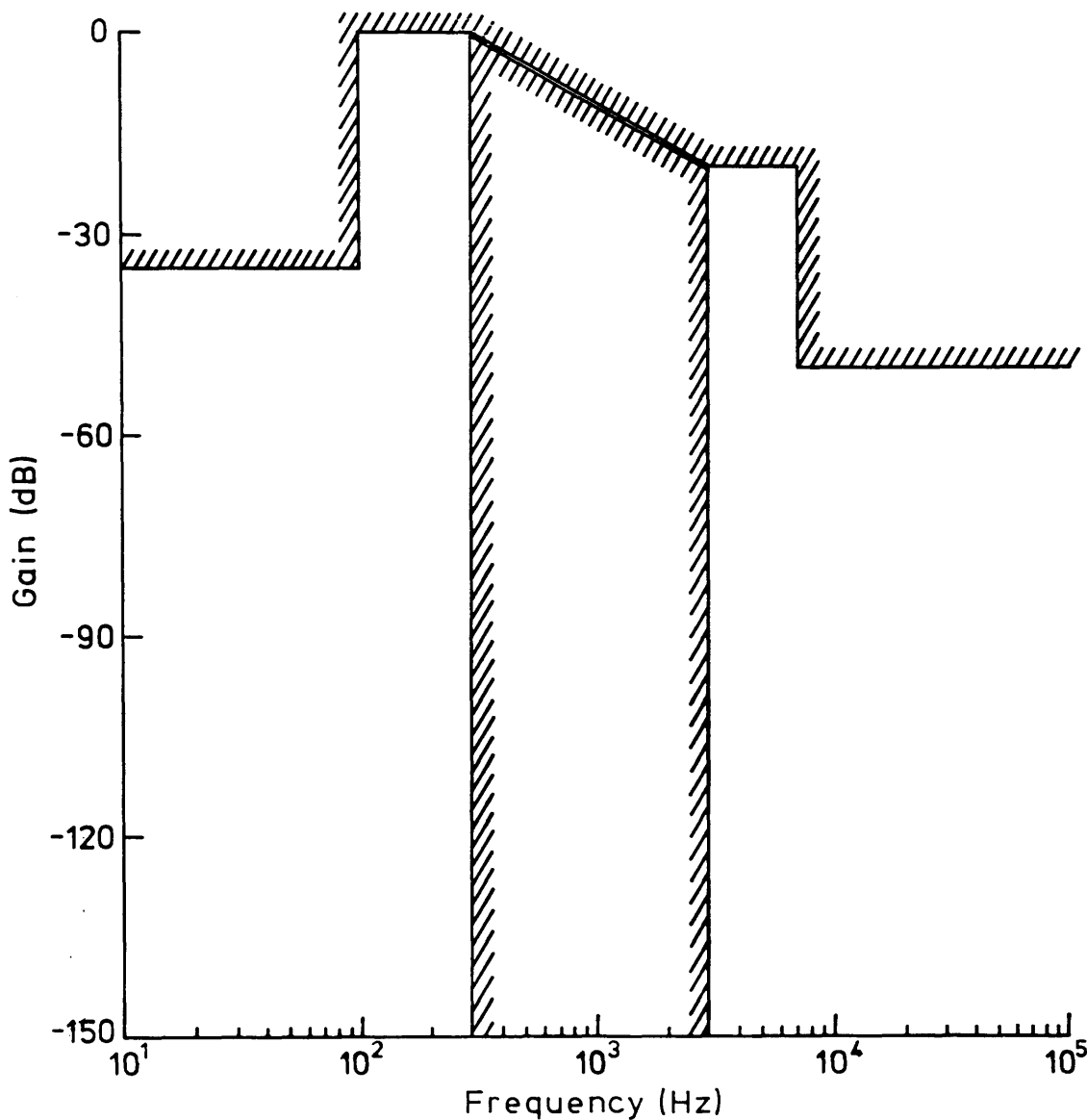


Fig. 6.20 Amplitude template for FM radio filter

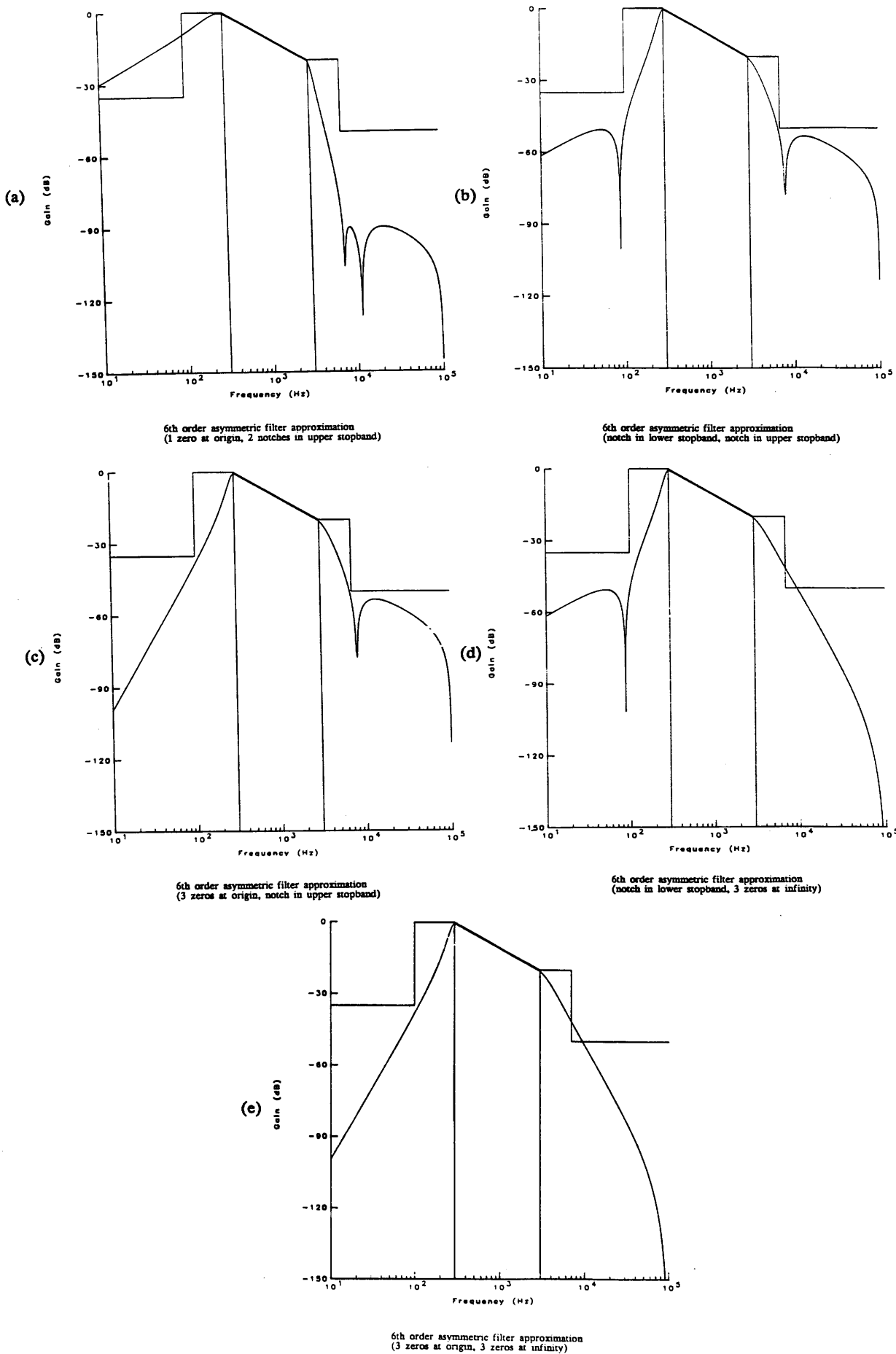


Fig. 6.21 Various 6th order filter approximations

Design method	Total C	C Spread	Average C	No. Switch	No. Caps	No. Op-amps
LUD	10484	5387.4	419.4	27	25	6
Leapfrog	8999.6	5664.9	359.9	32	25	6
Coupled-biquad	10252	5387.4	410.4	27	25	6
Biquad	2099.1	1436.5	91.3	28	23	6

Table 6.3 Statistics of various SC realisations of filter in Fig. 6.21b

Design method	Total C	C Spread	Average C	No. Switch	No. Caps	No. Op-amps
LUD	573.9	102.8	24.9	27	25	6
Leapfrog	1334.9	757.8	58.0	32	25	6
Coupled-biquad	556.6	107.6	24.2	27	25	6
Biquad	523.7	111.4	23.8	28	23	6

Table 6.4 Statistics of various SC realisations of filter in Fig. 6.21c

## 6.4 DESIGN OF A TELECOMMUNICATIONS FILTER

The specifications of a bandpass telecommunications filter are shown in Table 6.5 and the template of Fig. 6.22. Note that this filter has an asymmetric amplitude requirement and a group delay tolerance in the passband.

The simplest design approach is to meet the amplitude specifications by a classical approximation. However as seen from Fig. 6.23 the order of these functions is rather high, clearly due to the fact that they do not make efficient use of the freedom in the stopbands. The general IIR approximation methods can therefore be applied in order to tailor the response more closely to the irregular specifications (Fig. 6.24). A 10th order function is estimated as the improvement over the best classical approximation, the 14th order elliptic. A 3rd order lower stopband, and a 7th order upper stopband are guessed initially to reflect the asymmetry of the specifications. After various alterations to the stopband zero distributions much of the remaining stopband freedom can be used up. Remaining room can be taken up by adjusting the passband form. By adopting high order touch points in the stopband the group delay peaking is also improved over the equiripple form. Furthermore the passive filter sensitivity can be lessened by tapering the ripple towards the passband edge and introducing a high order touch point (Fig. 6.25). The final approximation appears in Fig. 6.24e with passband as in Fig. 6.25c.

Having obtained a suitable minimum-order transfer function to meet the amplitude specifications various circuit realisations must be considered. Table 6.6 shows the cost of both ladder and biquad implementations. It appears that the biquad and left-LUD circuits have the most favourable implementation cost in terms of capacitance. All the filters are canonical in number of op-amps and very similar in the number of other components. The designer should also study the mean sensitivity to capacitance value deviations before making the final selection of filter structure (Fig. 6.26). As expected the ladder structures offer better sensitivity than the biquad. If it is desired to further reduce the total capacitance some trade-off in the dynamic range can be allowed, in this case 6dB (see Fig. 5.19). Some 10–20% saving is typically obtained as shown in Table. 6.7. A LUD filter is then selected as the best choice. A netlist can then be produced and the response checked by an external analysis program. Often, at this stage, some non-ideal deviation of the designed frequency response will be observed. This may take the form of sinc(x) weighting or LDI termination error or more generally some distortion due to non-ideal realisation of components.

Design Example 1

Telecommunications filter:

Filter class = BANDPASS	Clock frequency = 100kHz
Lower passband edge = 1kHz	Upper passband edge = 2kHz
Lower stopband edge = 250Hz	Upper stopband edge = 2.2kHz
Passband ripple = 0.2dB	
Group delay variation = $\pm 50\mu\text{s}$ within 10% of passband edges	

Table 6.5 Specifications of a telecommunications filter

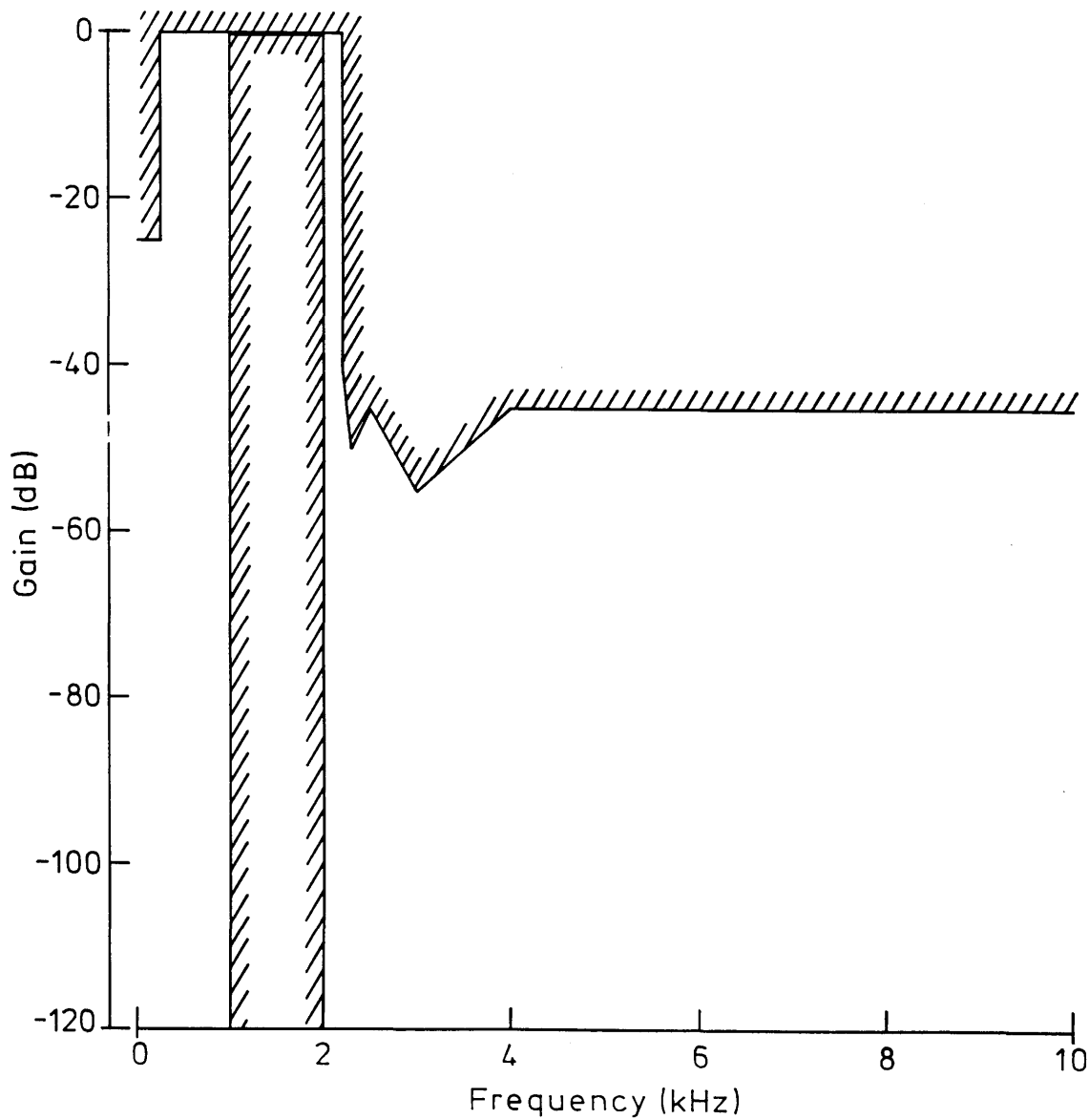
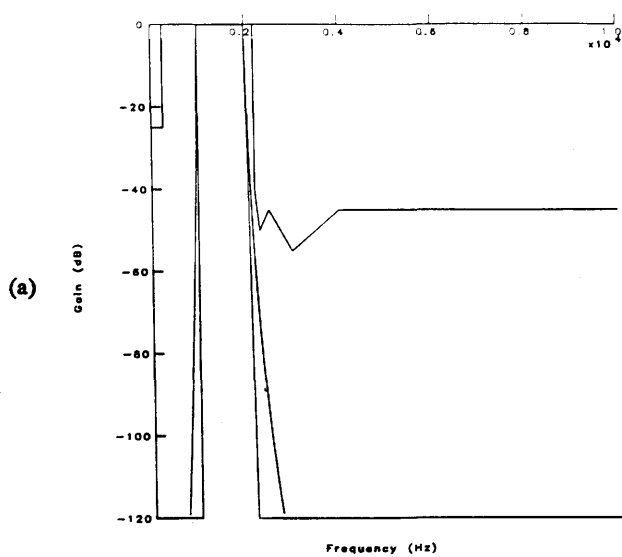
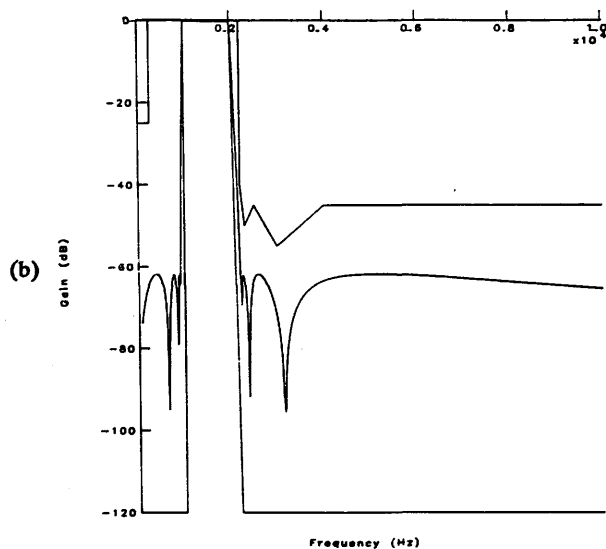


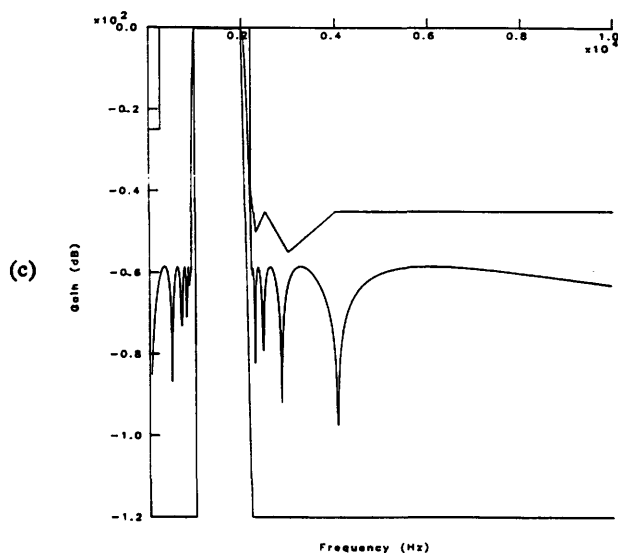
Fig. 6.22 Amplitude template for a telecommunications filter



24th order Chebyshev approximation



14th order elliptic approximation



24th order inverse Chebyshev approximation

Fig. 6.23 Various classical filter approximations

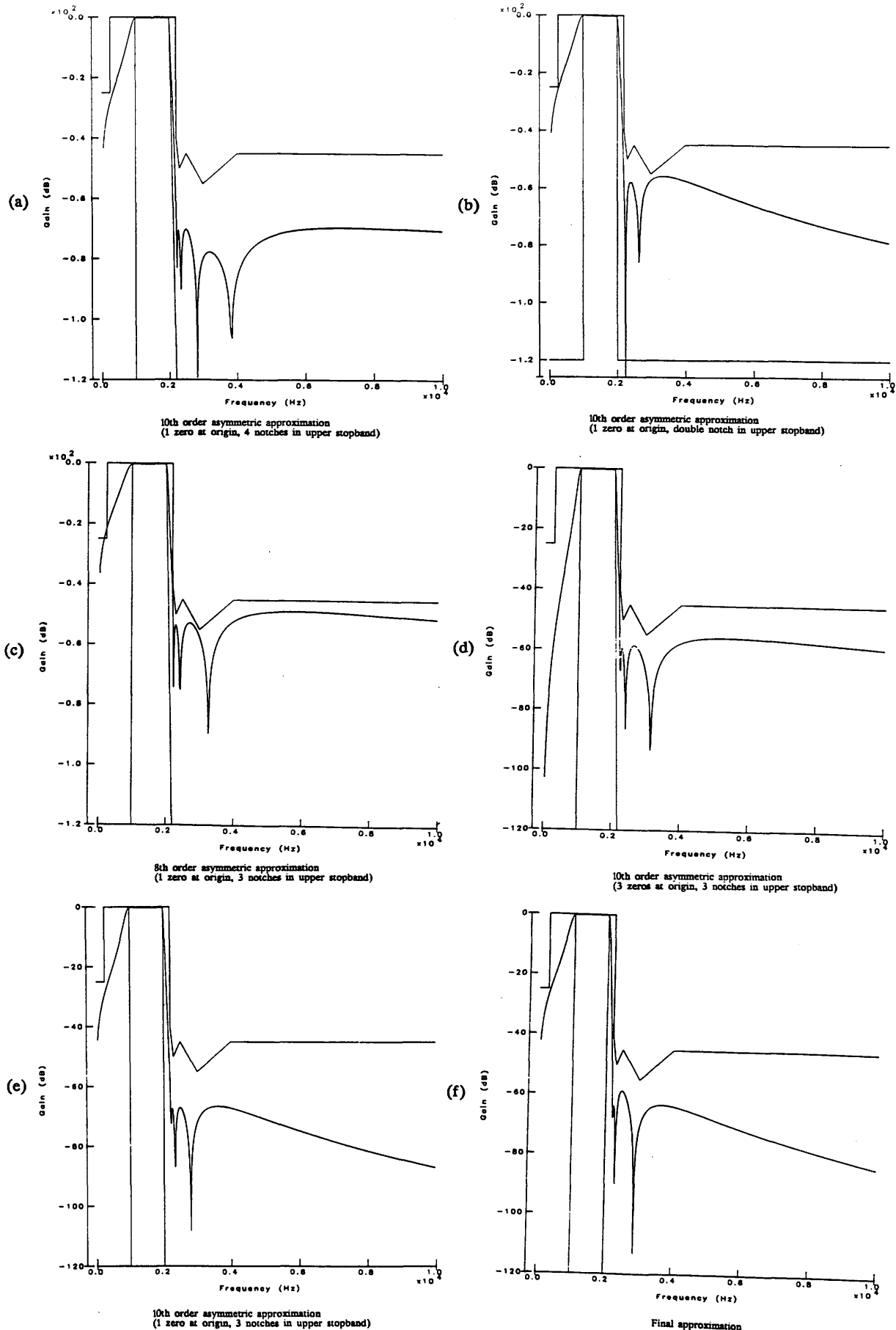


Fig. 6.24 Various asymmetric filter approximations

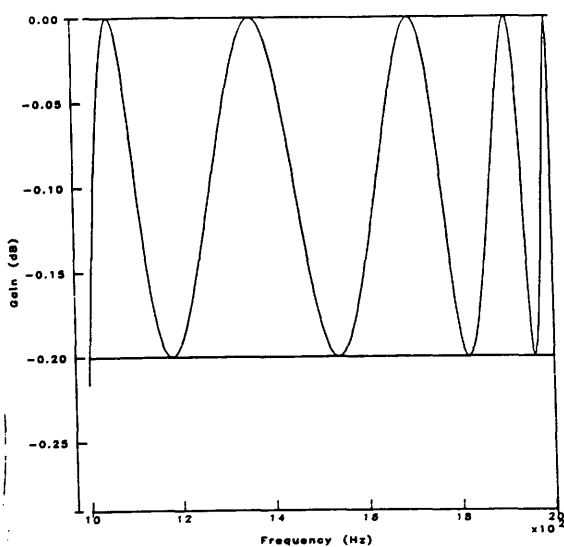


Fig. 6.25 (a) Elliptic-type passband

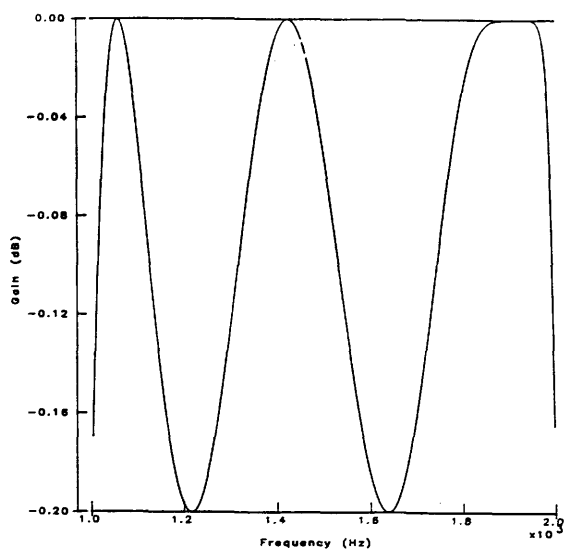


Fig. 6.25 (b) High order touch point at band edge

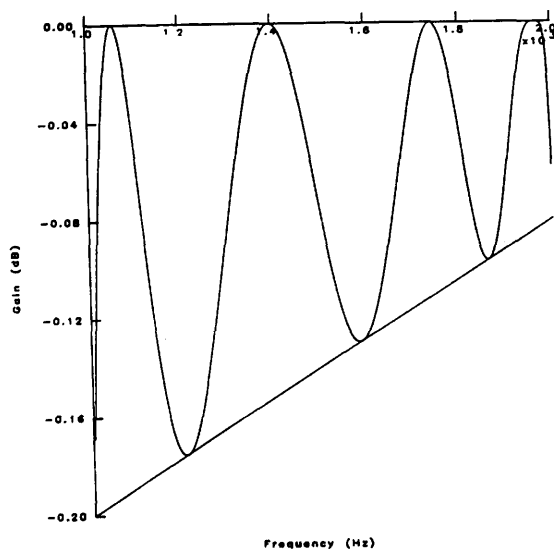


Fig. 6.25 (c) Taper plus high order touch point

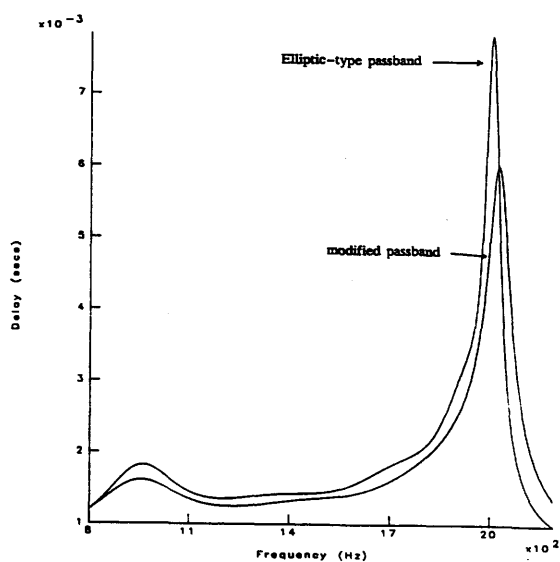


Fig. 6.25 (d) Comparison of group delays of (a) and (b)



Design method	Total C	C Spread	Average C	No. Switch	No. Caps	No. Op-amps
LUD	203.8	21.7	5.2	43	39	10
Leapfrog	321.7	55.7	8.3	48	39	10
Coupled-biquad	269.6	51.8	6.9	43	39	10
Biquad	218.4	28.2	6.1	44	36	10

Table 6.6 Statistics of various SC realisations of filter in Fig. 6.24e

Design method	Total C	C Spread	Average C	No. Switch	No. Caps	No. Op-amps
LUD	194.8	17.9	5.0	43	39	10
Leapfrog	298.1	55.7	7.6	48	39	10
Coupled-biquad	199.6	26.0	5.1	43	39	10
Biquad	188.6	24.5	5.2	44	36	10

Table 6.7 Statistics of various SC realisations of filter in Fig. 6.24e after capacitance spread optimisation

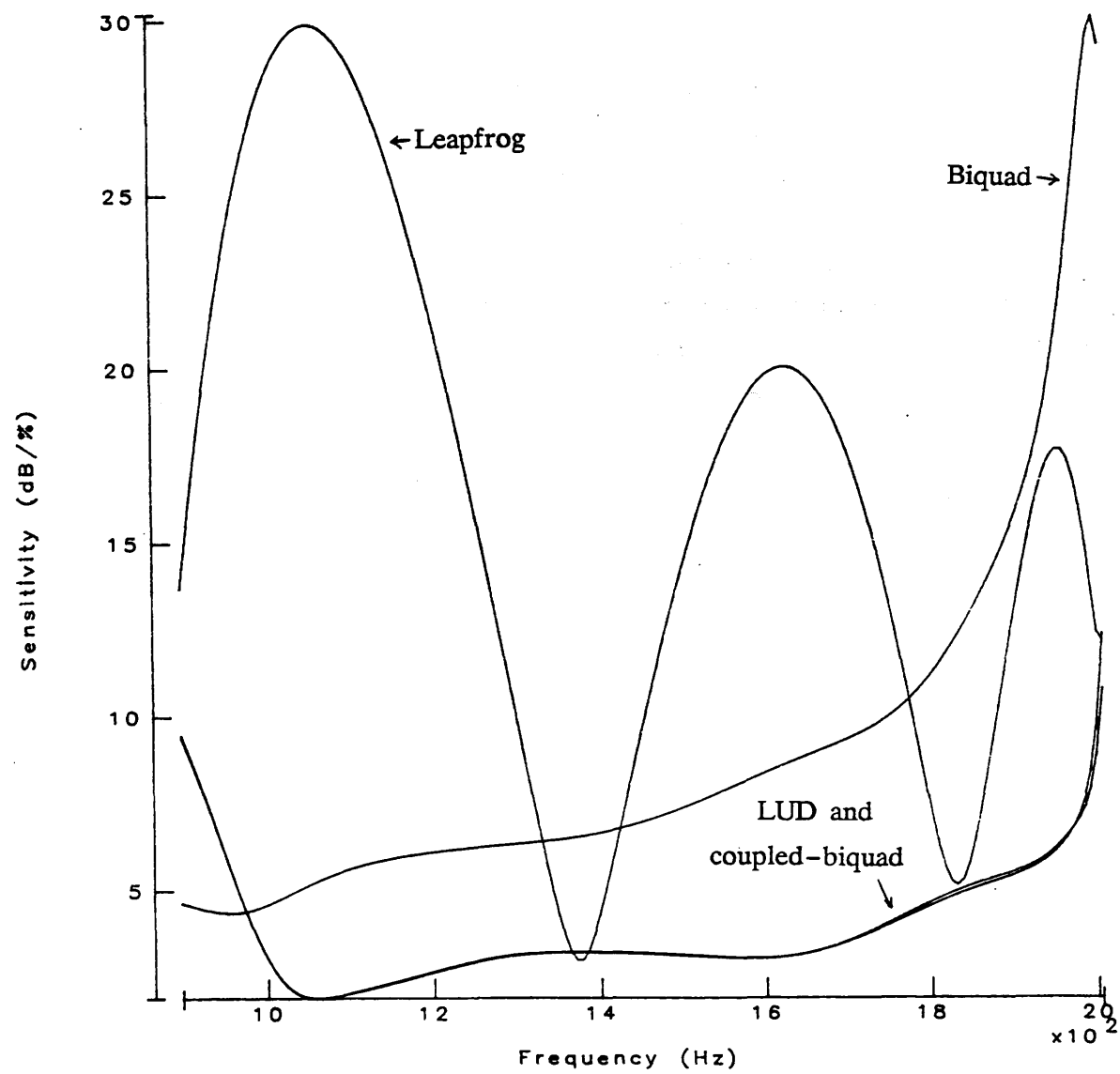


Fig. 6.26 Sensitivity comparison of various 10th order filter realisations

In a SC filter the switches can have finite resistances and the op-amps finite gain-bandwidth product. This will cause a typical distortion as shown in Fig. 6.27. The optimisation method of Section 6.2.7 can be applied to remove this effect after a few re-design iterations.

Once the design of the amplitude filter has been satisfactorily completed, the group-delay equaliser can be designed. In this case a 10th order equaliser must be approximated to meet the specifications (Fig. 6.28). It can be realised by both ladder and biquad topologies with the implementation cost shown in Fig. 6.8. In this case the ladder and biquad have much lower total capacitance than the biquad. Comparing sensitivities reveals that the structures have relatively similar properties (Fig. 6.29). The final filter implementation is shown in Fig. 6.30. It is a cascade of a 10th order LUD ladder with a 10th order allpass group delay equaliser. Notice, that a pair of capacitors have been cancelled in the ladder filter, realising a notch at  $\pm 2f_s$ .

## 6.5 A SWITCHED-CAPACITOR FILTER ASIC

Table 6.9 shows the specifications of a group of filters of lowpass, bandpass and bandstop (notch) classes. They form the main part of a dual-channel speech processing chip. Engineers in the AMSYS group of GEC research running PANDDA, were able to produce acceptable designs of these filters in a period of 6 weeks, and fully working silicon ASIC in 12 weeks. They obtained elliptic approximations of 7th, 6th and 6th order respectively and chose leapfrog and two biquad cascades as their SC realisations. Layouts of the filters were then produced (Fig. 6.30). At that time (June 1987) this was done manually, though it has now been fully automated (see Appendix A). The filters were subsequently fabricated using a 3 micron double-poly process with a die size of  $20\text{mm}^2$  (Fig. 6.31). Each filter has two channels, making a total of 50 orders of filtering on a single chip. Test results of the filters are shown in Figs 6.32–6.34.

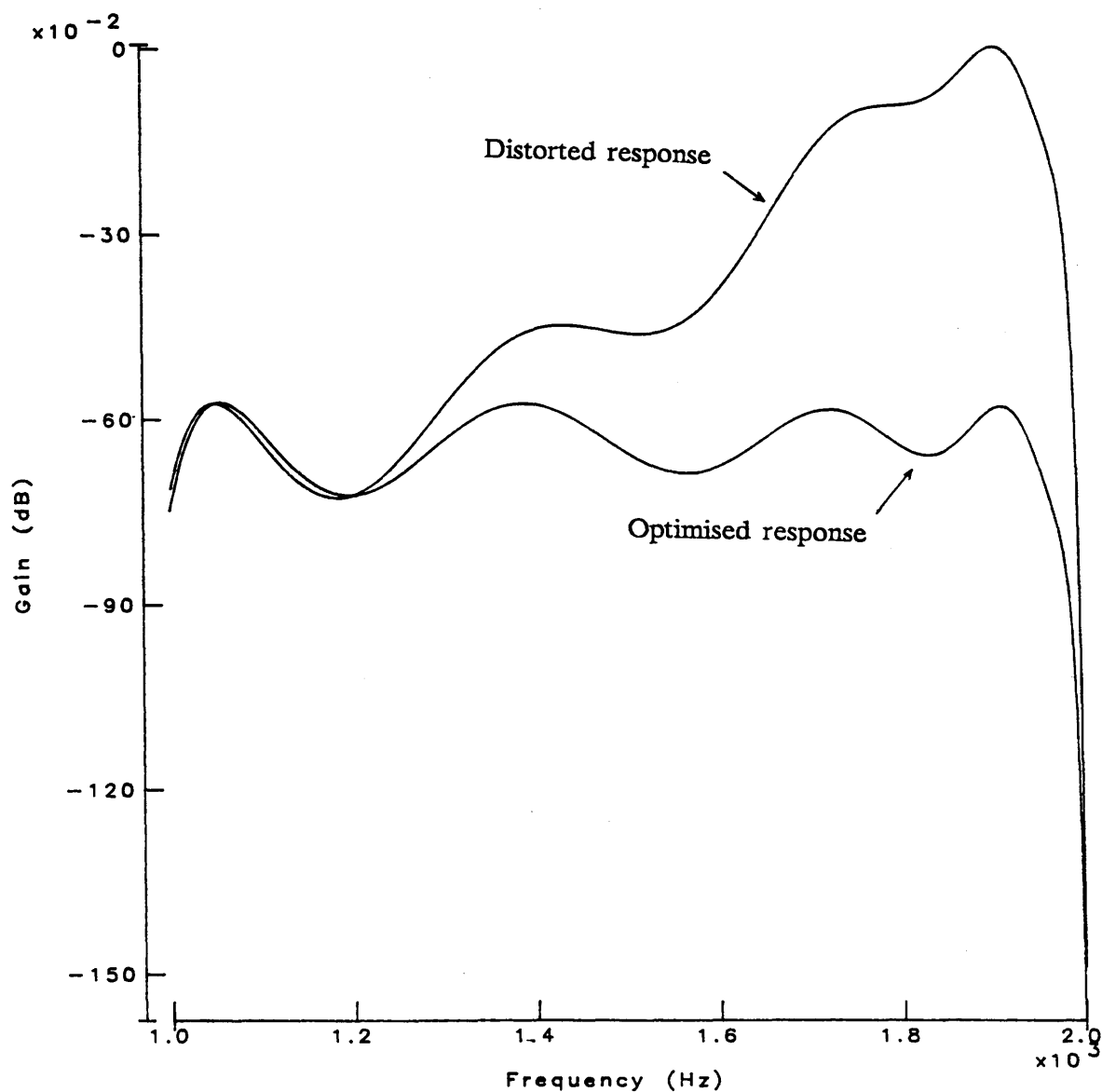


Fig. 6.27 Optimisation of filter response for non-ideal op-amp and switch parameters

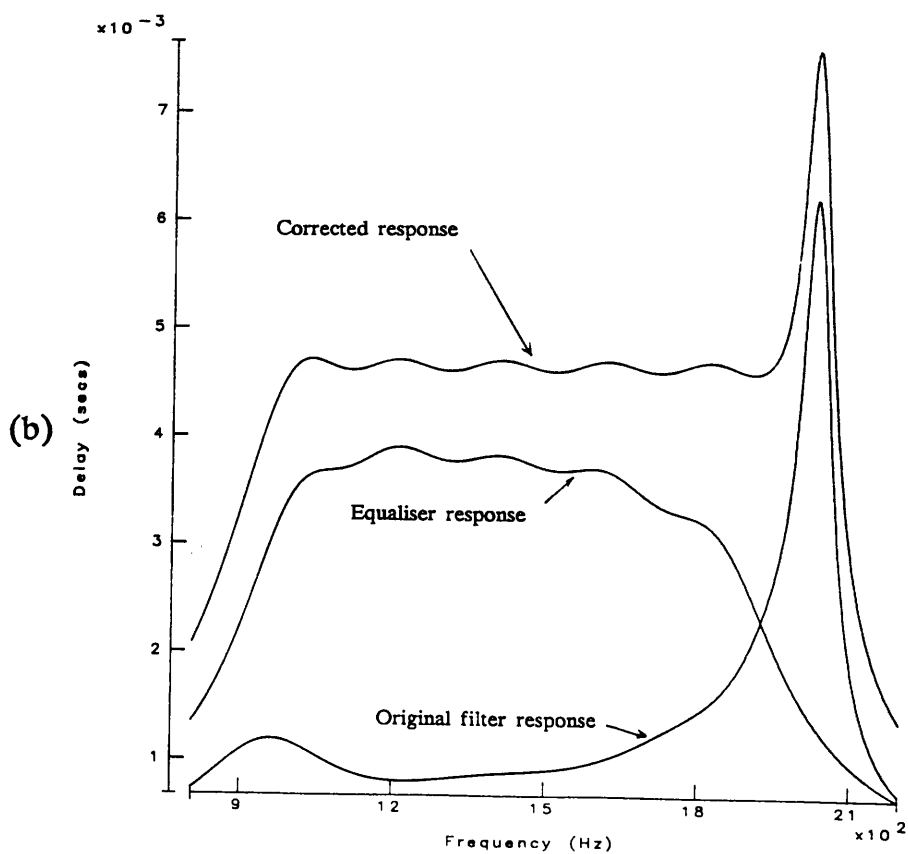
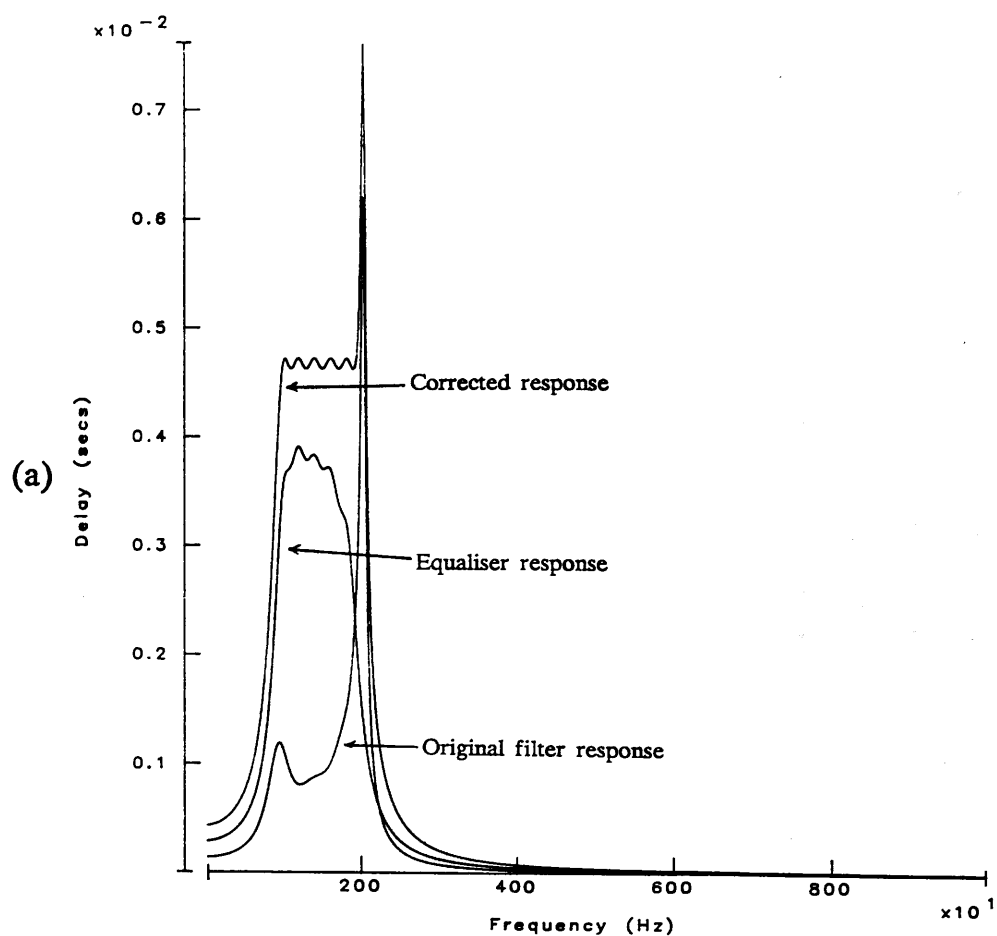


Fig. 6.28 (a) Group delay equalisation of 10th order bandpass filter  
(b) Passband detail

Design method	Total C	C Spread	Average C	No. Switch	No. Caps	No. Op-amps
LUD	286.9	50.7	8.4	45	34	10
Leapfrog	313.7	50.6	9.2	47	34	10
Biquad	677.7	54.7	16.1	54	42	10

**Table 6.8 Statistics of various SC realisations of 10th order group delay equaliser**

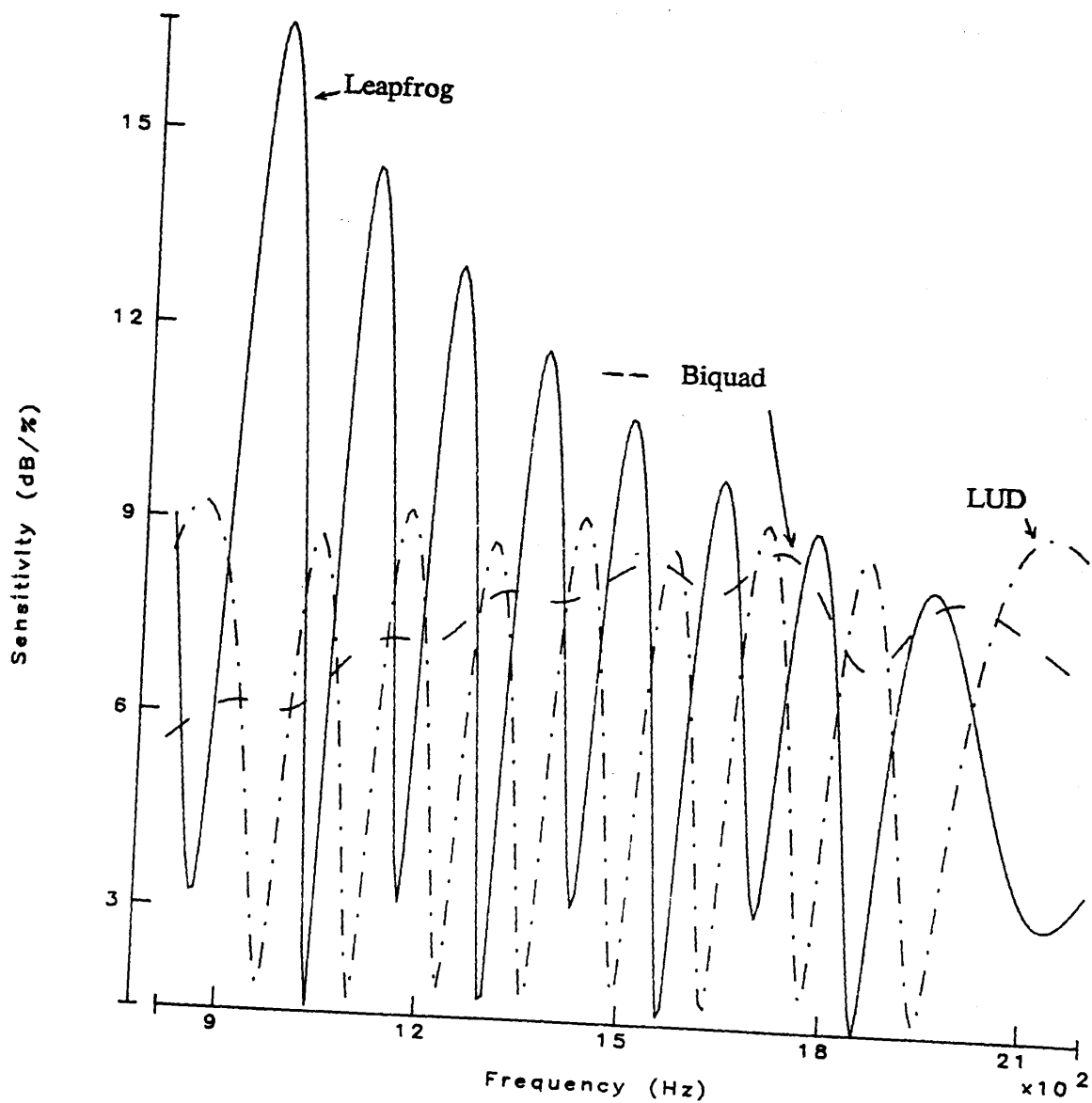


Fig. 6.29 Sensitivity comparison of various SC realisations of group delay equaliser

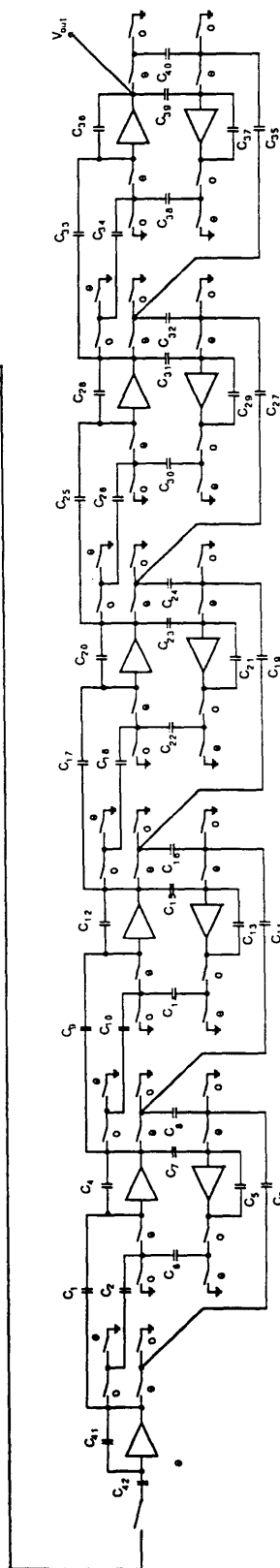
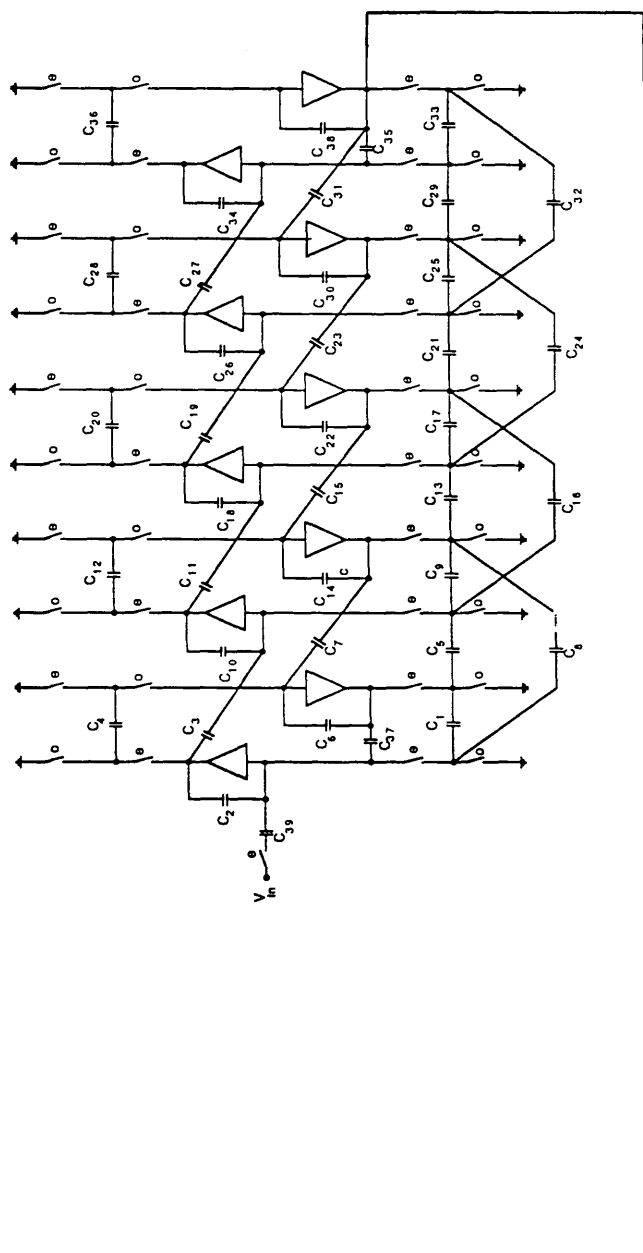


Fig. 6.30 Final design as a cascade of a 10th order LUD filter with a 10th order biquad group delay equaliser



Lowpass filter

Clock frequency	= 106.7kHz	
Upper passband edge	= 3.4kHz	Lower stopband edge = 8kHz
Passband ripple	< 0.5dB	Stopband attenuation > 80dB
Passband gain	= 6dB	

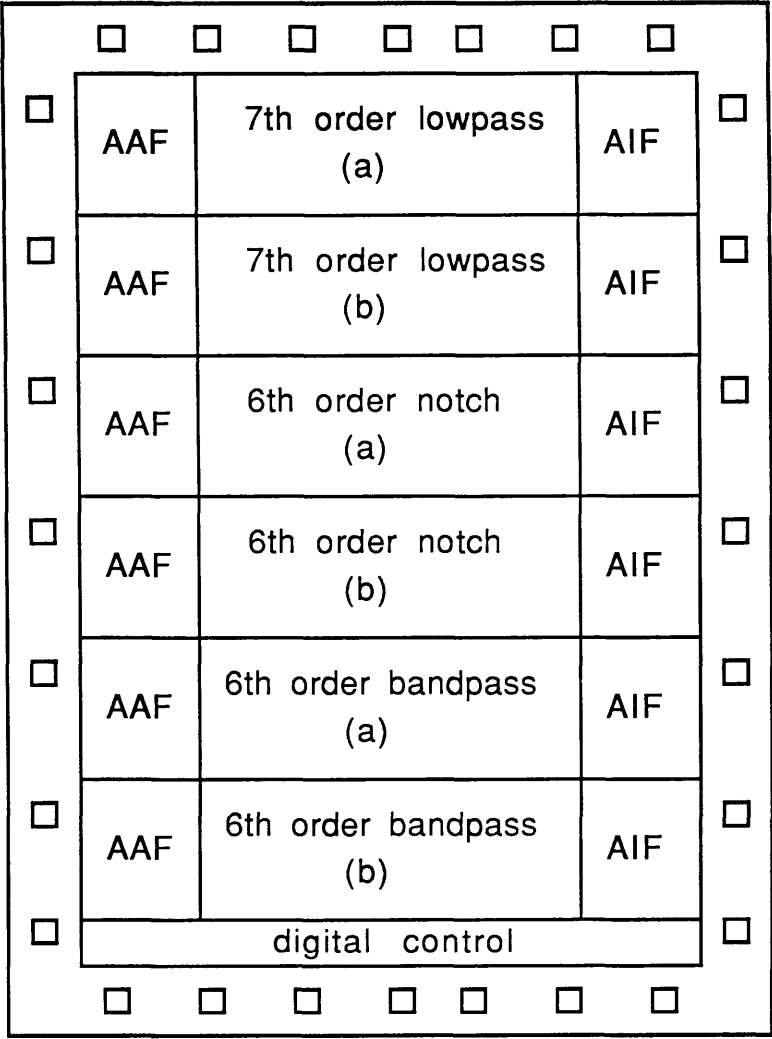
Bandpass filter

Clock frequency	= 53.3kHz	
Lower passband edge	= 642Hz	Upper passband edge = 710Hz
Passband ripple	< 0.1dB	Stopband attenuation > 40dB
Passband gain	= 6dB	

Bandstop filter

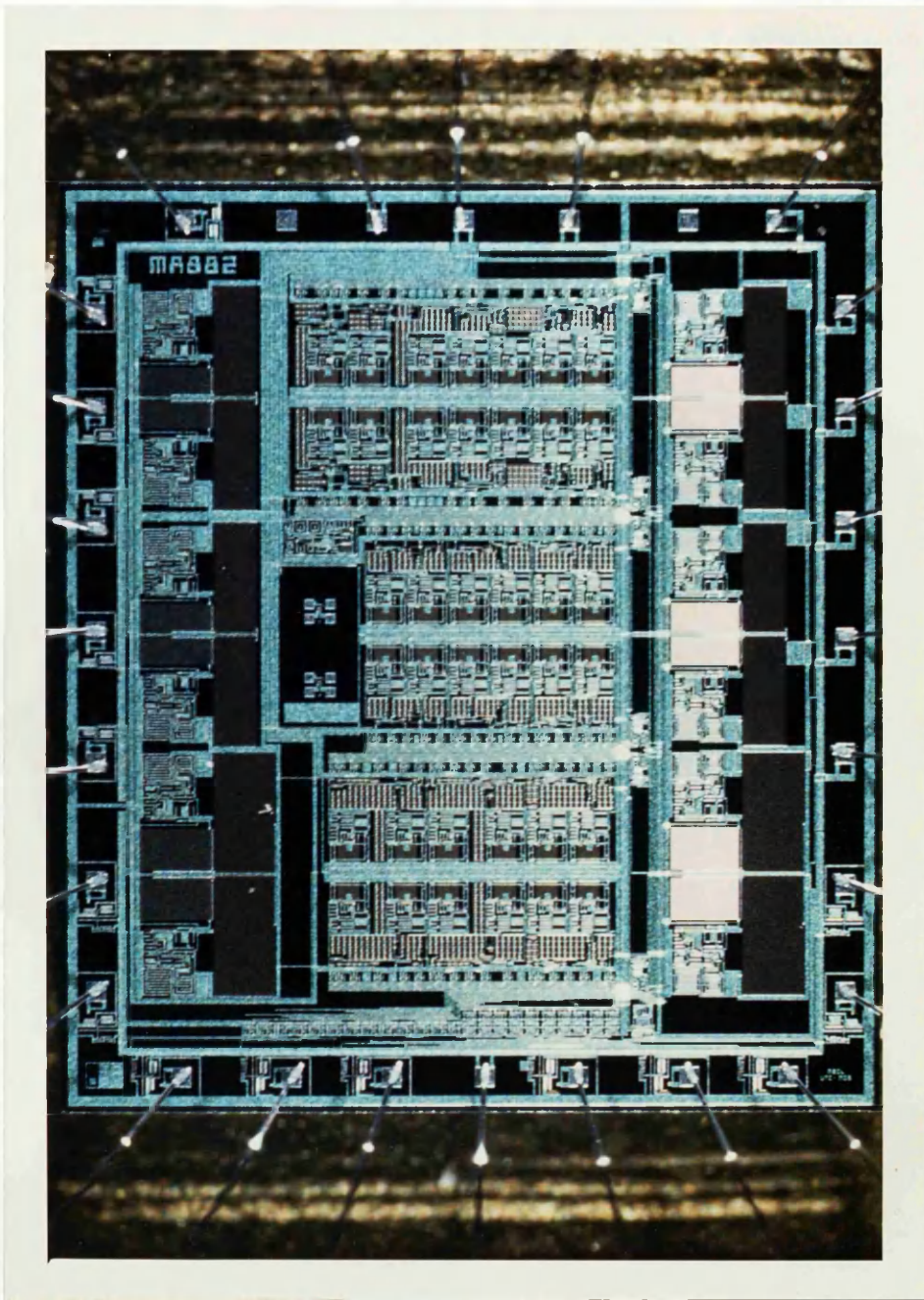
Clock frequency	= 53.3kHz	
Lower passband edge	= 500Hz	Upper passband edge = 800Hz
Passband ripple	< 0.1dB	Stopband attenuation > 60dB
Attenuation of 2dB at 150kHz		

Table 6.9 Specifications of lowpass, bandpass and bandstop filters



(AAF - Anti-Aliasing Filter, AIF - Anti-Imaging Filter)

Fig. 6.30 Floorplan of SC filter ASIC



© General Electric Company PLC, 1989

Fig. 6.31 Photograph of SC filter ASIC

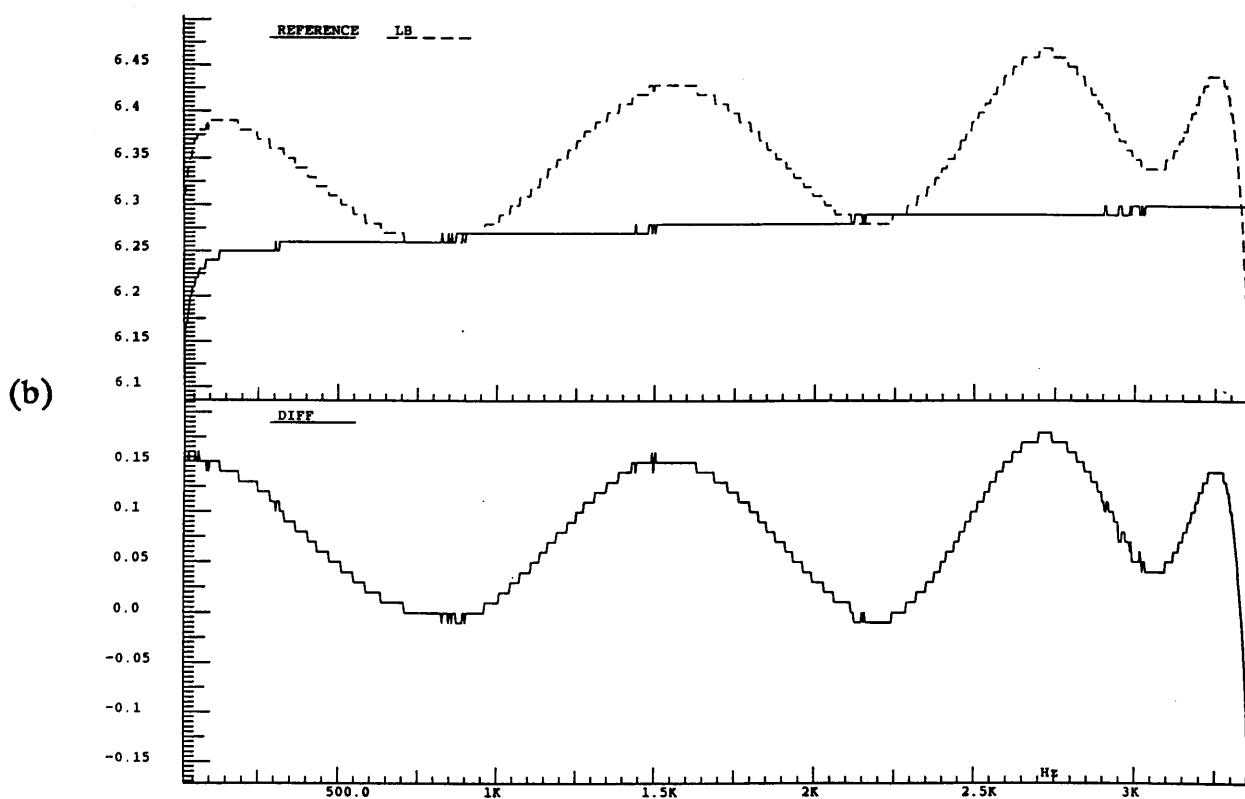
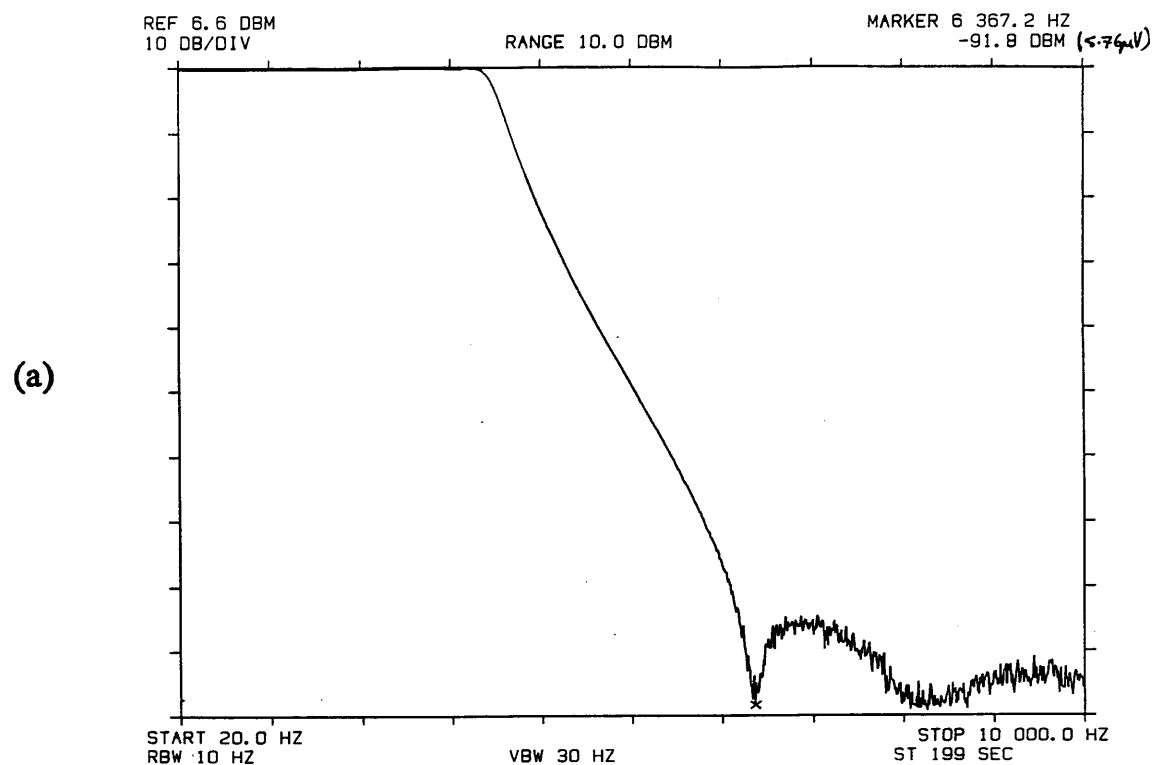


Fig. 6.32 (a) Frequency response of 7th order lowpass filter  
(b) Passband detail

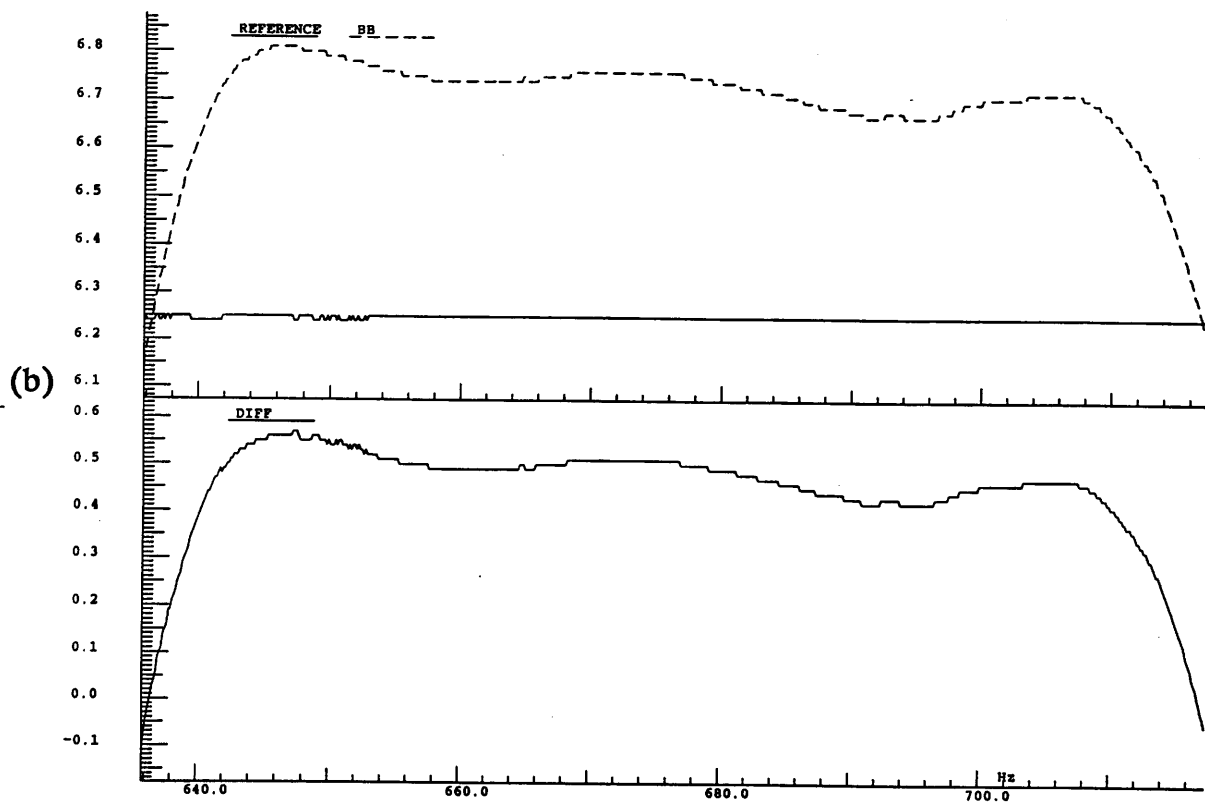
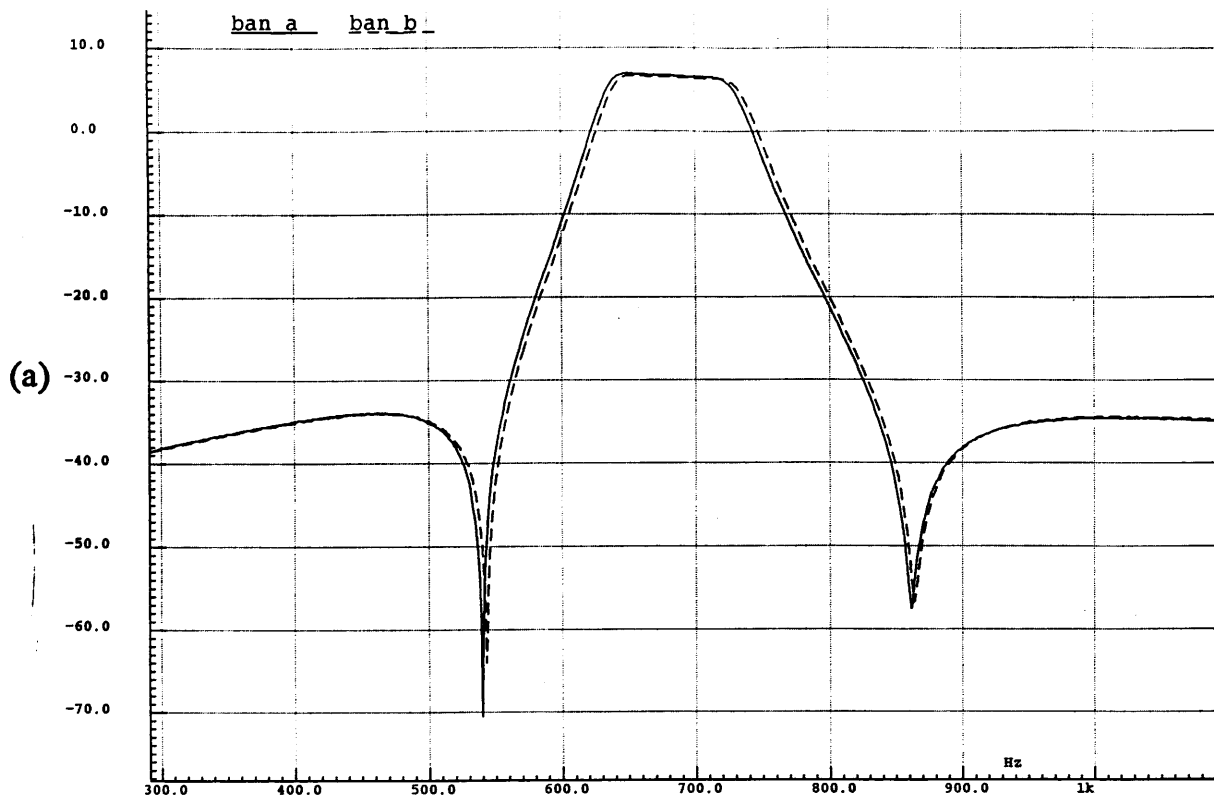


Fig. 6.33 (a) Frequency response of 6th order bandpass filter  
(b) Passband detail

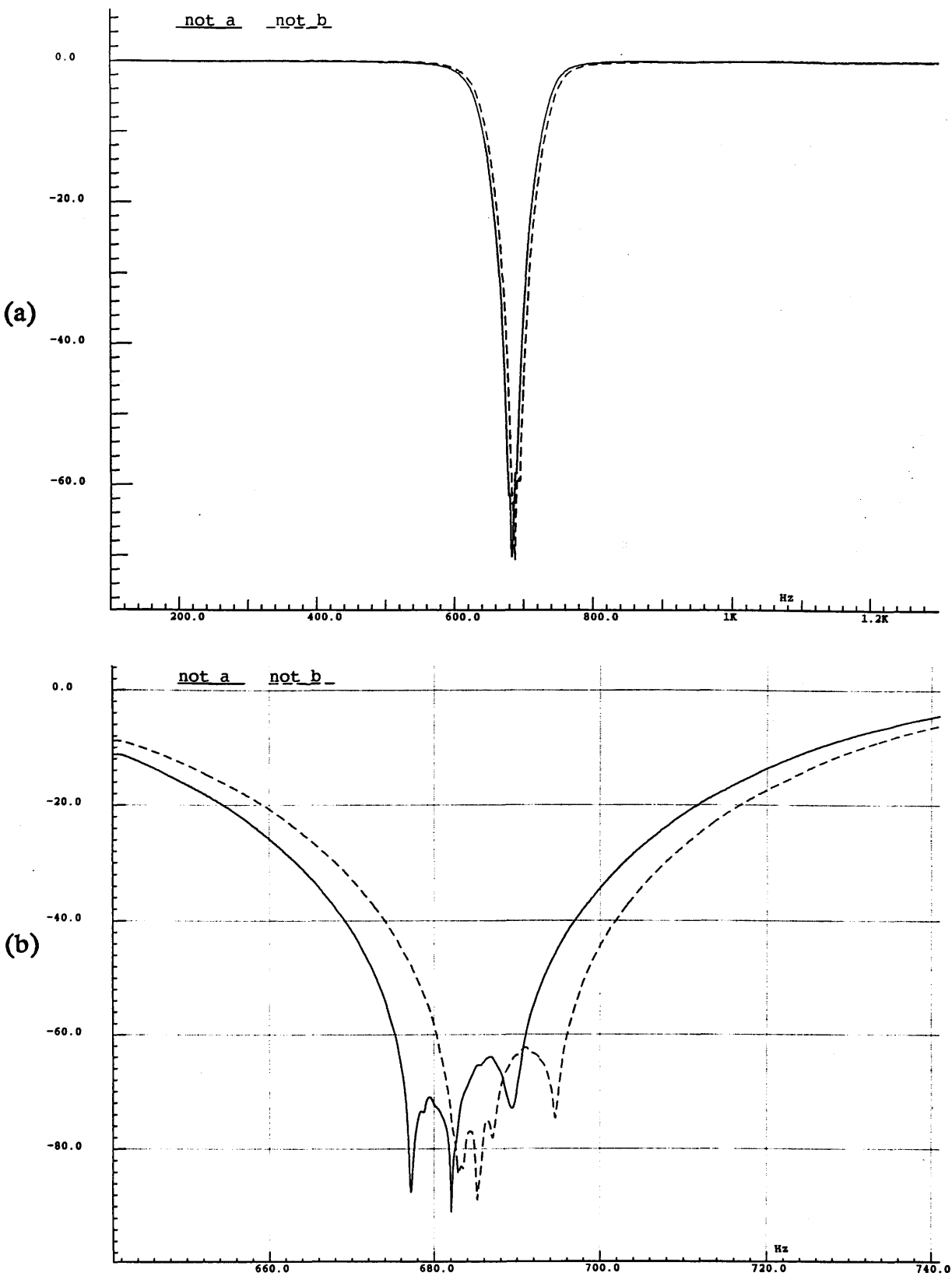


Fig. 6.34 (a) Frequency response of 6th order bandstop filter  
(b) Stopband detail

## 6.6 SUMMARY

Chapter 6 concerns the assembly of the computer design methods of this thesis into a software package for integrated filter design (PANDDA). The program attempts to unify the diverse methods of approximation, synthesis and realisation to provide a structured design tool with simple interfaces and few restrictions. The modularity of the program and its wide range of design options are described.

Section 6.2 shows how filter specifications can be approximated very closely by specialised transfer functions. Departure of filter approximations from their well-known classical forms can be done in a progression of metamorphoses. First, the equiripple passband can be evolved towards maximally flat to trade-off group-delay and amplitude. Second, the constant passband and stopband tolerances can be relaxed to arbitrarily taper the filter ripple. Third, the specifications may be arbitrarily weighted or sloped. A series of practical problems illustrate the usefulness of the unorthodox filter responses obtainable by these transformations. A further application of pre-warping functions is to correct amplitude distortion due to non-ideal circuit parameters.

The program is applied in Sections 6.3–5 to practical filter designs. They are traced from specification to network, and network to silicon. Test results of filters fabricated for GEC research are given.

## REFERENCES

- [1] R. K. Henderson, Li Ping and J. I. Sewell, "PANDDA : A Program for Advanced Network Design : Digital and Analogue", IEE Saraga Colloquium on Electronic Filters, pp. 4/1–4/8, London 1988.
- [2] R.K.Henderson, Li Ping and J.I.Sewell, "A design program for digital and analogue filters : PANDDA", Proc. ECCTD '89, pp. 289–293, Brighton, U.K., Sept. 1989.
- [3] S. Darlington, "Simple algorithms for elliptic filters and generalisations thereof", IEEE Trans. Circuits and Systems, Vol. CAS–25, No. 12, pp. 975–980, Dec. 1978.
- [4] L. F. Lind, "Simple computation of elliptic function filters", Digest of IEE Saraga Colloquium on Electronic Filters, London, 1984.
- [5] M. T. McCallig and B. J. Leon, "Constrained ripple design of FIR

- digital filters", Trans. on Circuits and Systems, Vol. CAS-25, No. 11, pp. 893-901, Nov. 1978.
- [6] Li Ping, R. K. Henderson and J. I. Sewell, "A new filter approximation and design algorithm", Proc. ISCAS, pp. 1063-1066, Portland, Oregon, 1989.
- [7] R. W. Daniels, "Approximation methods for electronic filter design", McGraw-Hill, New York, 1974.
- [8] A. C. M. de Queiroz and L. P. Caloba, "Physically symmetrical and antimetrical ladder filters with finite transmission zeros", Proc. 30th Midwest Symposium on Circuits and Systems, pp. 639-643, 1987.
- [9] Che-Ho Wei and Shyue-Win Wei, "Lowpass filters with single ripple in both passband and stopband", Proc. ISCAS, pp. 1632-1635, Portland, U.S.A., 1989.
- [10] G. W. Medlin, "A new design technique for maximally linear differentiators", Proc. ICASSP, pp. 825-828, Glasgow, Scotland, 1989.
- [11] P. P. Vaidyanathan, "Optimal design of linear-phase FIR digital filters with very flat passbands and equiripple stopbands", IEEE Trans. on Circuits and Systems, Vol. CAS-32, No. 9, pp. 904-917, Sept. 1985.
- [12] B. K. Ahuja, "Implementation of active distributed RC anti-aliasing/smoothing filters", IEEE J. Solid-State Circs, vol. SC-17, no. 6, Dec. 1982.
- [13] M. S. Nakhla, "Approximation of lowpass filters with frequency dependent input gain characteristic", IEEE Trans., vol. CAS-26, pp. 198-202, 1979.
- [14] J. Taylor, "Stability analysis and exact design of switched-capacitor filters of the lossless discrete integrator type", PhD Thesis, University of London, 1985.
- [15] S. N. Filho, R. Seara and J. C. M. Bermudez, "A new method for the compensation of the  $\sin(x)/x$  distortion in discrete time to continuous time signal conversions", Proc. ISCAS, pp. 1668-1671, Portland, Oregon, 1989.
- [16] B.D. Rakovich and V.D. Pavlovic, "Method of designing doubly terminated lossy ladder filters with increased element tolerances", Proc. IEE. Part G, Vol. 134, No. 6, pp. 285-291, Dec. 1987
- [17] N. O. Sokal, "Unsolved theoretical problem in design of optimal low-pass filter for harmonic suppression in radio-transmitter output", IEEE Trans. on Circuits and Systems, Vol. CAS-27, No. 3, p235, March 1980.
- [18] M. Markiewicz-Wrzeciono and N. O. Sokal, "Filters with unequal ripples in the passband for class-E power amplifiers", Proc. ISCAS, pp. 1628-1631, Portland, U.S.A., 1989.
- [19] R. K. Henderson and J. I. Sewell, "A design algorithm for all-pass



delay equalisers", Digest of IEE Saraga Colloquium on Electronic Filters, pp.11/1–11/8, London, 1989.

[20] H. J. Orchard, "Filter design by iterated analysis", IEEE Trans., Circuits and Syst., Vol. CAS–3d, No. 11, pp. 1089–1096, Nov. 1985.

[21] G. Szentirmai, "FILSYN – A general purpose filter synthesis program", Proc. IEEE, Vol. 65, No. 10, pp.1443–1458, Oct. 1977.

[22] M. S. Ghausi and K. R. Laker, "Modern filter design : active RC and switched–capacitor", Prentice–Hall, Englewood Cliffs, New Jersey, 1981.

[23] K. Martin and A. S. Sedra, "Exact design of switched–capacitor bandpass filters using coupled biquad structures", IEEE Trans. Circuits and Systems, vol. CAS–27, pp.469–474, June 1980.

[24] Li Ping and J. I. Sewell, "The LUD approach to switched–capacitor filter design", IEEE Trans. Circuits Syst., vol. CAS–34, no. 12, pp 1611–1614 Dec. 1987.

[25] M. S. Lee and C. Chang, "Switched–capacitor filters using the LDI and bilinear transformations", IEEE Trans. Circuits and Systems, Vol. CAS–30, No. 12, pp. 873–887.

[26] Li Ping, R. K. Henderson and J. I. Sewell, "Matrix methods for switched–capacitor filter design", Proc. ISCAS, pp.1044–1048, Helsinki 1988.

[27] F. Montecchi, "Bilinear design of high–pass switched–capacitor ladder filters", IEEE ISCAS, pp. 547–550, Kyoto, Japan 1985.

[28] Li Ping and J. I. Sewell, "The TWINTOR in bandstop switched–capacitor ladder filter realisation", IEEE Trans. Circuits and Systems, Vol. CAS–36, No.7, pp.1041–1044, July 1989.

[29] Li Ping and J. I. Sewell, "Switched–capacitor and active–RC all–pass ladder realisation", submitted for publication.

[30] L. B. Wolovitz and J. I. Sewell, "General analysis of large linear switched–capacitor networks, Proc. IEE, Part G, Vol. 135, No. 3, pp. 119–124, June 1988.

[31] G. C. Temes and D. A. Calahan, "Computer–aided network optimisation : the state–of–the–art", Proc. IEEE, Vol. 53, pp. 1832–1863, Nov. 1967.

## **CHAPTER 7**

### **CONCLUSIONS**

#### **7.1 DISCUSSION OF RESULTS**

#### **7.2 PROPOSALS FOR FUTURE WORK**

#### **REFERENCES**

## 7.1 DISCUSSION OF RESULTS

The objective of this work was to study computer techniques for SC filter design. In many cases, current techniques were developed by manual derivation and, because of the effort involved, only special examples were considered. However, in developing a computer program, the aim is that it should be as flexible as possible and present as few conceptual restrictions to a designer as possible. For example, if a 7th order elliptic transfer function can be designed as a canonical leapfrog circuit, so should an 8th order one. If a bandpass function can be designed by a ladder circuit, so should a bandstop function. If the passband response can be made flat or equiripple, why not forms between these? If the response can be made flat why not sloping as well? A design capability, say, in the approximation of the transfer function should not exclude a capability in circuit realisation. All this necessitates a uniform treatment of the various stages of filter design. In many cases, the current approaches must be extended and regularised to make them suitable for a computer-aided design. Contributions towards this objective have formed the main achievement of this thesis.

A summary of the main results now follows. Methods for the approximation of ideal filter characteristics were reviewed. It was observed that although these function were optimal approximations in various senses and were easy and quick to compute, they were unsuitable for many practical filtering tasks. This is largely due to the departure of real filter systems specifications from ideal forms. In particular, the properties of symmetry and flatness rarely conform closely to required performance. For example, sampled-data filters suffer from inherent amplitude response distortions due to  $\text{sinc}(x)$  effect which make flat passbands unsuitable. Asymmetric filters often occur in modem channels. Thus the ideal role of the filter must be partially reconsidered. Rather than purely passing or stopping signals in certain bands the filter must additionally be considered as requiring to shape the input spectrum in some arbitrary manner. Thus the filter frequency response must be matched as closely as possible to some template defining this shaping. This is the task approached in Chapter 2, in which some general computer algorithms are advanced to fit polynomial functions in a minimax sense to shaped boundaries of attenuation. A relationship to the Remez algorithm was discovered. A generalisation is introduced, allowing the transmission characteristic to vary continuously between equiripple and maximally flat forms. So-called high order touch points can be introduced at which the approximated function matches the boundary functions to a certain number of derivatives. A

subsidiary result is the generation of a whole family of intermediate ideal filter approximations between elliptic and inverse Chebyshev. The approximation was done in the discrete time domain and bilinearly transformed to the continuous time domain. In this way, both continuous and sampled-data filters could be designed from a common basis. Special accuracy preservation measures were considered to remove order limitation problems, successfully raising the design orders to practical levels.

The dual filter characteristic to amplitude response is the group delay response. Both are of concern in the design of filters which must often transmit signals with uniform delay in the passband. In minimum phase types of transfer function, employed to effect the amplitude response the two are directly inter-related [1]. It is commonly observed that where the amplitude response varies most rapidly there are peaks in the group delay. Accordingly, by tailoring the amplitude response to the specifications the disturbance in the group delay can also be minimised. In this respect, high-order touch points are of particular interest since they smooth the amplitude, using up excess stopband-rejection towards more uniform group delay. This represents a further advantage of the arbitrary amplitude approximation capability.

The two filter characteristics can also be treated independently by adopting an all-pass function to equalise the group delay of the minimum phase function, without disturbing its amplitude response. The design of arbitrary group delay equalisers is considered in Chapter 3. The aim of this work was to unify the treatment of group delay with that of amplitude. As before, the group delay specifications should be allowed to be of arbitrary forms, not simply flat, as defined by two bounding functions. The similarity of the allpass group delay function with an amplitude function was observed. An algorithm was developed whereby the same approximation techniques for amplitude could be re-used for group delay equalisation. Although group delay equalisation by all-pass functions is known to be a non-optimal solution to a filter problem, it has become more attractive by the recent development of low-sensitivity all-pass integrated ladder filter realisations. Both amplitude and delay filtering can now be performed by low-sensitivity circuits, an option not yet available for non-minimum phase transfer functions.

The next stage is the synthesis of a ladder prototype. Traditionally this has been done by a Hurwitz factorisation of the transfer function followed by a pole

removal synthesis step. Both stages are extremely sensitive to round-off and cancellation errors caused by implementation in finite wordlength computer arithmetic. This severely limits the order of the ladder prototype that can be synthesised without crippling loss of accuracy. To avoid this problem, transformed variable methods can be applied, but these greatly complicate the software and require different transformations for different transfer functions. An extension of Orchard's iterative algorithm was proposed, offering the compromises of high accuracy and simple software but slower computation times and the need for initial values. The novel feature of the method is that it works directly from the touch point information from the amplitude approximation steps without requiring ill-conditioned Hurwitz factorisation. The iterative method was used to design very high order ladder prototypes in full double precision accuracy (up to 100th). A combination of the synthesis method and the iterative method was suggested as the best compromise, the former providing approximate initial values and the latter refining the accuracy of the solution.

The design of passive ladders as prototypes for simulation by SC circuits was given special consideration. Here, the concerns are whether the ladder can be simulated by an SC circuit with a minimum cost in components (principally op-amps) and with an exact transfer function. Some ladder prototypes entail extra op-amps or feedthrough branches in the SC simulation unless special steps are taken. As in the case of approximate LDI simulation, it is possible that the SC circuit will realise the transfer function with some distortion. In certain cases, a passive prototype cannot be realised at all or when simulated will cause an unstable SC circuit. However, it shown that by anticipating these problems at the prototype design stage they can be avoided. The first development is to permit negative element values in the prototype. Although disallowed by strictly passive realisations, they can easily be simulated by active circuits. The removal of this constraint also eases the development of software. The negative element values are also shown to be of use in design of bilinear/LDI filter structures. A negative component can be synthesised in the prototype, which when simulated by a bilinear SC circuit will cause cancellation of capacitive feedthrough branches. This in fact, produces a circuit structure akin to that obtained by LDI simulation methods. Normally LDI simulation will cause a distortion of the designed transfer function. This can also be avoided by introducing certain pole positions into the transfer function or pre-warping the response. This allows the ladder simulation to be unified solely under the use of the bilinear transform. In order to assure canonic ladder simulations and regular SC circuits, a simple rule is introduced into the prototype synthesis whereby only minimum node configurations are

permitted. The class of transfer functions with finite attenuation at high frequency cannot normally be realised as a passive ladder would cause instability when straightforwardly simulated by bilinear circuits. A common example, is the pure even order elliptic function or bandstop or highpass functions. By a modification of the transfer function a suitable minimum node prototype can always be designed. This uniform treatment of prototype design ensures that stable, canonic SC simulations can be produced with exact frequency response.

The final stage in the filter design process is circuit realisation from a suitable prototype. Only stray-capacitance insensitive SC circuits are examined. They belong to either biquadratic cascade or ladder simulation architectures. Until now, the treatment of the two approaches has differed greatly. Particularly within the latter, the design techniques vary widely according to form of prototype, type of transformation, class of transfer function and simulation method. Ladder simulation is inherently more difficult than biquad design because of the highly coupled form of the circuit, which makes the equations harder to manipulate. These problems have made it very difficult for any single computer program to produce more than a few standard filter types. In Chapter 5, the use of a matrix scheme to regularise the processing of linear equations involved in the design, scaling and realisation of SC filters is presented. The methods are centrally based on the bilinear transform avoiding the specialised problems with the LDI transform. Both biquad and ladder filters can be set up by adding stamps into a general matrix scheme. The derivation of different filter types can then be accomplished in a uniform manner by a series of matrix decompositions which do not alter according to the form of the prototype. LUD, coupled-biquad and leapfrog topologies are easily provided. The interconnection pattern of the filter circuit can be seen from the non-zero structure of the matrix, and the canonic properties can be seen from the order of the system. The known sparse structure of the matrix means that the computer processing and storage of the filter can be made very efficient. A canonic SC filter is guaranteed for both architectures of filter, biquad or ladder, regardless of the type or order of transfer function. This assurance can normally only be given for biquad filters. Dynamic range and capacitance spread scaling can be performed by simple matrix operations. A variety of techniques have been investigated for capacitance spread reduction.

The filter design program PANDDA has been written, encompassing all the theoretical developments above. An optimisation loop, making use of the various design stages in this program was discussed. This algorithm makes use of the fast re-design and general approximation capabilities to pre-distort the original

frequency specifications for non-ideal effects. In Chapter 6, PANDDA was applied to a set of difficult filtering problems illustrating how its facilities can be applied to produce improved design solutions. It was demonstrated that high order touch points can be introduced into the transfer function to ease the group delay peaking near the passband edges. The asymmetric responses can be employed to tailor the responses closely to the specifications, offering reductions in the order of the transfer function. The sloping properties are used to correct  $\text{sinc}(x)$  and LDI termination error distortion. The cost of implementing the transfer functions in a variety of networks is then investigated. The uniform design strategy in PANDDA ensures that biquad and ladder now compete very fairly in terms of silicon area and numbers of components. The same conclusions are true for delay equalisation by all-pass functions.

To summarise, the results of the present research and that of Li Ping [2] have contributed towards a powerful CAD tool for integrated filters, PANDDA. It presents the user with a conceptually uniform, flexible set of design features which remove traditional limitations. The program is actively being used by the AMSYS group at GEC Hirst Research and has been successfully used to produce fabricated SC filters.

## 7.2 PROPOSALS FOR FUTURE WORK

Certain extensions of the approximation methods of Chapter 2 would be worthwhile. The standard filter classes lowpass, bandpass, bandstop and highpass were considered in detail. However, there is occasionally a need to design filters with multiple bands, e.g. filter banks, comb filters, in which case a formalisation of the techniques to multi-band cases is necessary. An extra degree of freedom is introduced by each additional band which must be assigned in some useful way to a designer, e.g. variable passband edge, passband ripple. The problem is then to re-express the design algorithms suitably to take into account these extra parameters.

The approximation methods at present generate minimum phase functions with imaginary transmission zeros. This means that zero transmission will occur at certain points in the stopband. However, in certain applications it is undesirable to completely suppress signals e.g. hearing-aid design. In fact, the absence of a stopband implies that the concept of a filter must be reconsidered. The filter must be generalised to become a spectrum shaping device. The design of non-minimum phase transfer functions with complex zero positions is necessary.

They are also known to offer better combined amplitude and group-delay properties than a minimum phase amplitude stage with a group delay equaliser. At present, there is no simple, uniform algorithm to compute these functions. It would seem possible to extend the Newton approximation methods to this task and to apply the techniques of the all-pass group delay algorithm. A greater insight into the operating principle and proof of convergence of the latter would seem necessary pre-requisites.

Further research into low-sensitivity integrated ladder realisations of the non-minimum phase transfer functions would therefore be valuable. It seems likely that the filter structures could be easily designed in terms of the matrix scheme presented in Chapter 5. However, some extension in filter synthesis methods must be made to develop special ladder prototypes. These would no longer be singly or doubly-terminated ladders, but lossy, multi-resistor structures. Complex transmission zeros would be realised by LC tank circuits shunted by a resistor. In this case, the traditional insertion-loss synthesis method is no longer valid. However, the iterative methods of Chapter 4 could be applied quite straightforwardly. Convergency is likely to be the main problem.

At present, canonical filter realisations with arbitrary amplitude response can be designed with good reliability. The ability to design the different stages in a complete SC filter system has not been fully integrated into the PANDDA software. Although simple decimators and interpolators have already been designed, more sophisticated structures should be investigated [3]. This will demand an extension of the approximation methods to multi-phase transfer functions and description of the structures in matrix form. In addition, the trade-off between the responses of the decimator/interpolators and SCF should be incorporated automatically at the approximation stage. Furthermore, since continuous-time anti-aliasing/ imaging filters must accompany the sampled-data parts of the system, it would be desirable to couple the design of these stages together. An analysis package for active distributed-RC anti-aliasing filters has been written and awaits incorporation (Appendix B). Eventually, this will allow the filter to be designed as one system, with an automatic trade-off of one stage against another.

Indeed, the view of the filter as a system poses the next challenge for CAD software for analogue circuits. At present, a set of reliable basic tools exist for the design of the building blocks of the system; SCF, group-delay equaliser, decimator. The filter designer must use his expert knowledge to drive the



software, knowing for example how to obtain the most efficient transfer function, how to choose the best filter realisation for a given type of filtering and how to trade-off between the influences of the different blocks in the system. This knowledge must now be incorporated into a higher level expert-system shell which will control the basic facilities and guide the designer towards a good-quality system. Ultimately, the different filter implementations, active-RC, digital and continuous-time should be comparable within the one package. An overall filter design tool can then join other CAD systems for signal processing such as D/A converters, phase locked loops, modulators etc.

## REFERENCES

- [1] M. L. Liou and C. F. Kurth, "Computation of group delay from attenuation characteristics via Hilbert transformation and spline function and its application to filter design", IEEE Trans. on Circuits and Systems, Vol. CAS-22, No. 9, pp. 729-734, Sept. 1985.
- [2] Li Ping, "Theory and methodology of integrated ladder filter design", Ph.D. Thesis, University of Glasgow, 1989.
- [3] J. DeFranca, "Switched Capacitor Systems for Narrow Bandpass Filtering", PhD Thesis, University of London, 1985.

## APPENDIX A : DESCRIPTION OF PANDDA FILTER DESIGN SOFTWARE

### A.1 FUNCTIONAL SPECIFICATIONS

The internal structure of the PANDDA filter design program is shown in Fig. A.1. A brief summary of the function of each stage is now given with examples.

#### A.1.1 Filter specification (USER)

This program allows of a valid filter design to be specified a user. The outputs are a series of files defining the current filter design to all succeeding stages of PANDDA. In the version being run by the AMSYS group of GEC Research on Apollo workstations, the program has been given a menu-driven front-end (Fig. A.2). The specification of a filter to PANDDA is divided conceptually into two parts:

- (S) set the desired type of frequency response required of the filter,
- (O) define the physical implementation of the filter as a circuit.

Option (S) is then subdivided into

- (A) define the amplitude characteristics of the filter response,
- (D) define the group delay characteristics of the filter response.

When non-classical filters are required, option (A) is again subdivided into

- (PB) define the passband amplitude characteristics,
- (SB) define the stopband amplitude characteristics.

The options offered to the user are now examined under each of these categories

#### Frequency Response Parameters

Filter class : [LOWPASS, BANDPASS, HIGHPASS, BANDSTOP]

Passband and stopband edge frequencies must be defined when the filter class is specified. Highpass

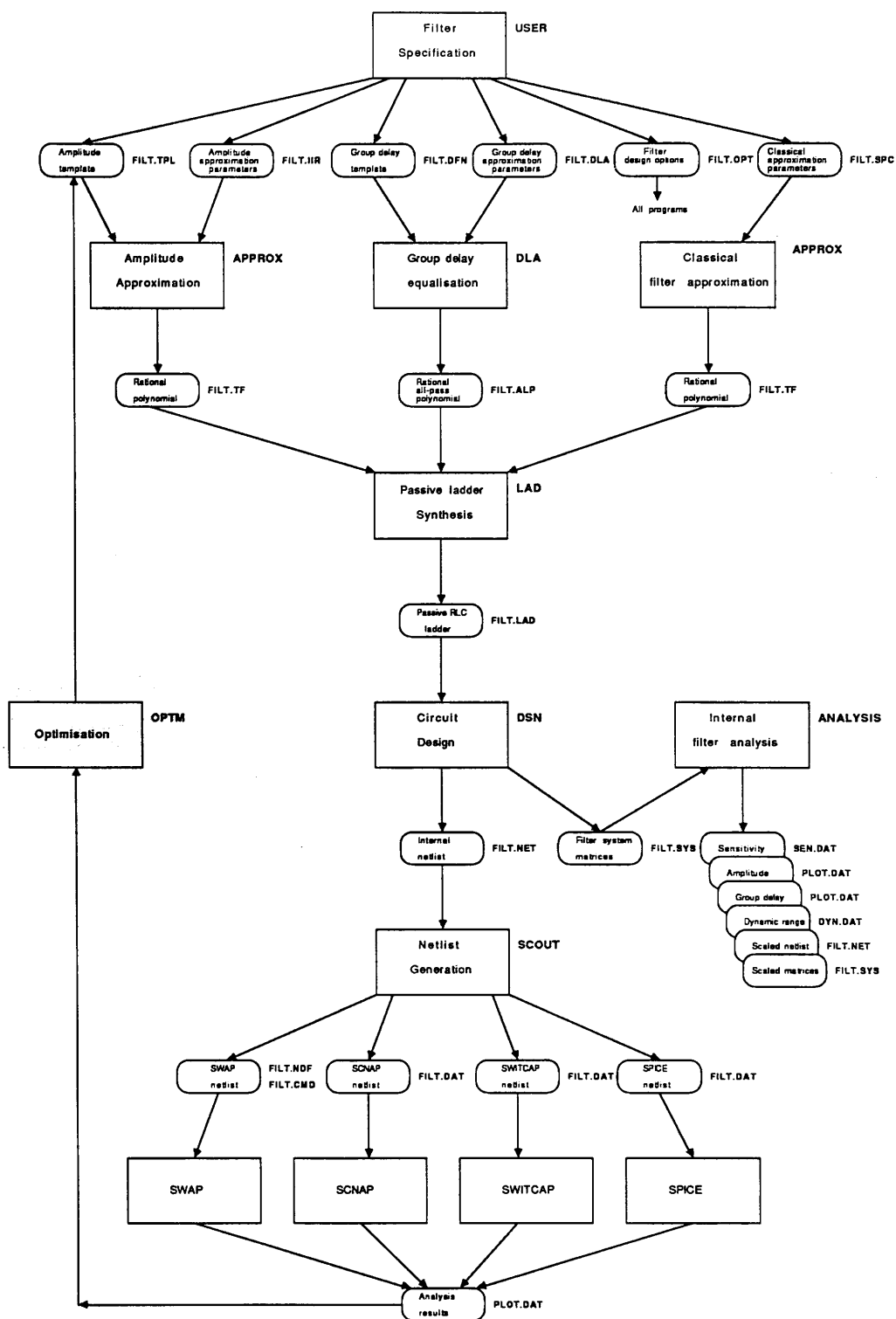


Fig. A.1 Internal structure of PANDDA program showing file usage

PANDA Version 1.000 16-Jun-89 AMSYS Filter Compiler									
DESIGN : Decoder Output Filter			DESIGNER : ncamos.filters.amsys.D07C			DATE 16 : 11 : 1989		TIME 12 : 10 : 38	
<b>DEFINITION</b>  ORDER : 5  ORDER & SA  ORDER & FS  <b>FS &amp; SA</b>		passband : 0.00  passband : 3400.00  passband : 3400.00		START : 10.00  STOP : 20000.00  NPOINTS : 200		LOG			
RIPPLE : 0.03  GAIN : 0.00  FCLK : 128000.00		LOWER BAND  stopband : 0.00  rejection : 0.00		UPPER BAND  stopband : 6000.00  rejection : 40.00		SIMULATION  STOP : 20000.00  NPOINTS : 200			
<b>CLASS</b>  LOWPASS  HIGHPASS  <b>BANDPASS</b>  BANDSTOP		<b>APPROXIMATION</b>  ELLIPTIC  CHEBYSCHEV  INVCHEBY		<b>MISCELLANEOUS</b>  TYPE  STRUCTURE  FUNCTIONS  LIGHTING  WRAPPING  E VALUES		<b>EXECUTE</b>  SYNTHESISE  PLOT  REALISE  SCHEMATIC  SWAP  LAYOUT			
5th order filter 8 zeros at DC Finite zero pair at 634.48Hz Finite zero pair at 9675.11Hz Pole pair at 3884.24Hz Q 3.61 Pole pair at 3287.45Hz Q 0.91 Pole at 2664.74Hz 5th order filter 8 zeros at DC Finite zero pair at 6308.48Hz		<b>Filter Classes:-</b> ELLIPTIC : Most commonly used filter shape. : Ripple in passband, Rapid roll off. CHEBYSCHEV : All pole filter, ripple in passband. INVCHEBY : Meet same attenuation spec as chebychev. : Better group delay performance. BUTTERWORTH : Maximally flat passband. BESSEL : Maximally flat group delay response. : Slow roll off LEGENDRE : Monotonic passband with most rapid roll off : Design arbitrary filter response.		dd order filter. ce required 1 2 43.52 units 2 1 Section 1 22.8 units Section 2 28.7 units Section 3 10.3 units total capacitance used is 53.793812 units writing swap files writing ALF file					

Fig. A.2 Screen display of PANDDA showing menus and help facility

and bandstop realisation by ladder networks uses new design techniques

Approx. type : [ELLIPTIC, CHEBYSHEV, INVCHEBY, BUTTERWORTH, BESSEL, LEGENDRE, IIR]

The first six are classical approximation forms. (Fig. A.2). The last allows the passband and stopband specifications to be tailored to arbitrary attenuation boundaries.

Order : [2-30]

Orders of filters may reliably be designed in this range. Even order designs will often require canonic ladder filter design techniques. Odd order bandpass or bandstop filters (parametric) are not designed at present.

Defn type : [ORDER&SA, ORDER&FS, FS&SA]

The specification of a classical filter may be done by fixing any three of the four parameters:

1. order,
2. stopband edge frequencies,
3. passband ripple,
4. stopband attenuation.

The passband ripple is always defined in the present program leaving three possible ways of choosing the other two required parameters, a third being undefined. Under the IIR option the order, passband ripple and stopband edges are fixed leaving the stopband attenuation free.

Weighting : [FLAT, X/SINX, LDI, LDI&X/SINX, BANANA, OPTIMISATION]

This option defines the form of the amplitude weighting of the passband region.

The possibilities are:

1. FLAT - no weighting,
2. X/SINX - inverse sinc(x) weighting,
3. LDI - LDI termination error correction,
4. LDI&X/SINX - 2. and 4. combined,

5. BANANA - whimsical sagging passband,
6. OPTIMISATION - weighting defined by external template.

Warping : [NONE, BILINEAR]  
Compensation for frequency axis distortion of sampled-data filters.

Sampling frequency, passband ripple, stopband attenuation, lower/upper passband/stopband edge frequencies : standard parameters. The upper edge frequency of the highest band is always at the Nyquist frequency  $f_s/2$ .

With IIR approximation type selected the following additional parameters become available

No. Iterations : [5-10]  
Parameter controlling the number of iterations between passband and stopband of approximation algorithm. It may be necessary to allow more iterations for sharp transition band or high order filter (normally  $<10$ ).

Grid size : [30-100]  
Parameter controlling number of search points evaluated in order to find ripple extrema. For a narrow band filter the parameter may have to be increased at the penalty of longer run times.

Accuracy : [ $10^{-1}$ - $10^{-5}$ ]  
Maximum relative error in positions of minima to template boundaries. Related to grid-size. Increased grid-size will allow minima positions to be determined more accurately allowing the terminating accuracy to be reduced.

Further commands available under IIR filter definition are required to set up the passband and stopband characteristics. The filter is now regarded as a series of

bands whose characteristics may be set up independently. A template is defined in each band as a series of piece-wise linear points on upper and lower boundaries between the band edge frequencies. An example template and definition are given in Fig. A.3. Notice that in the stopband the lower boundary is, in reality, always  $-\infty$ dB, but is set to  $-120$ dB for convenience. The following options may be also be set in either stopband (SB) or passband (PB) mode.

Band type : [EQUIRIPPLE, MAXFLAT, GENERAL]

Three attenuation characteristics are definable

1. EQUIRIPPLE - rippling function like elliptic passband (not necessarily equal).
2. MAXFLAT - maximally flat as in Butterworth.
3. GENERAL - arbitrary osculatory band defined by a series of high order touch points incident to upper passband boundary or lower stopband boundary (0). List of touch point orders must be entered, all even except at extreme frequencies 0 or  $f_s/2$ .

Band order : [0-30]

Order of band. This controls the order of the polynomial approximating the band. The total stopband order should be less than or equal to the total passband order for a realisable SC filter.

Commands are available to insert, delete and clear template points.

Delay approximation offers a series of options

Filter class : [ALLPASS]

At present group delay approximation is done by equalisation due to an allpass function.

Design mode : [EQUALISER, INDEPENDENT]

The group delay may be approximated independently or to equalise the group delay peaking due to a pre-designed amplitude filter.

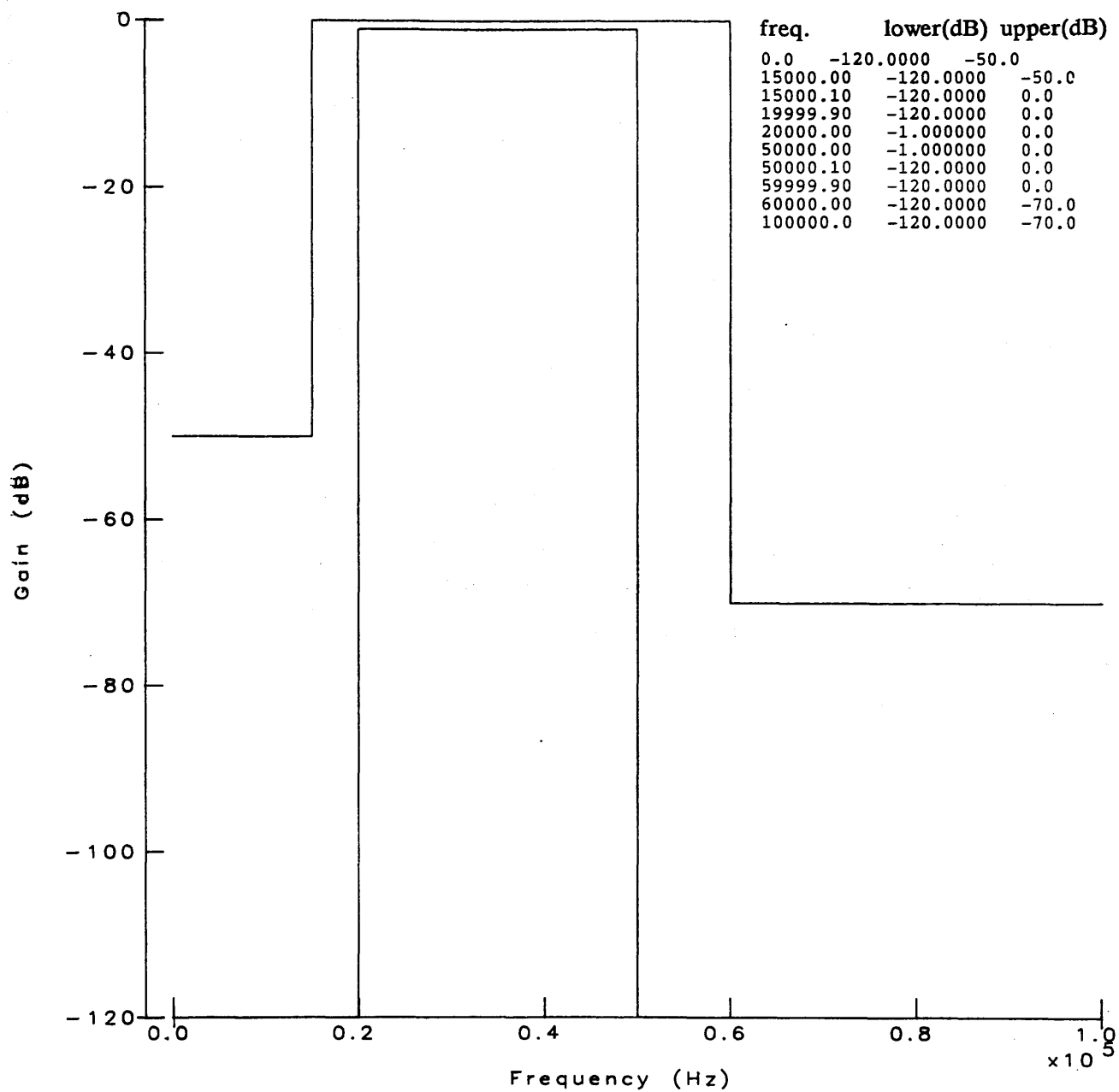


Fig. A.3 Filter template with numeric description (inset)



Approx. type : [CLASSICAL, GENERAL]

Classical group delay equalisation is done to approximate constant delay by an equiripple function. However, general equalisation may be to arbitrary boundaries and may include high order touch points.

Order : [1-30]

Order of the allpass function.

Edge frequencies : [0-fs/2]

Equalisation is done over a single frequency band Normally inside the passband edges of an amplitude filter. Multi band equalisation may be done by cascading equalisers.

Remez iterations : [1-10]

Parameter controlling maximum number of Remez iterations of approximation algorithm. May need to be increased for high order examples.

Scaling iterations.: [1-10]

Parameter controlling number of iterations to determine constant delay offset.

Gridsize, accuracy : as before

Delay

: Classical delay equalisation parameter specifying acceptable delay ripple over the frequency range. Otherwise delay specified by template.

As before commands are available to insert, delete and clear template points. The lower delay boundary may have an arbitrary constant offset which will be ignored.

### Filter Attributes

Title : [automatic]

A filter title will be generated automatically from

the present value of the filter options e.g.  
6th order elliptic highpass LUD ladder SC filter

Implementation : [SC, RLC, ACTIVE-RC]

Filter implementation may be switched-capacitor, digital, passive RLC or active-RC. Active-RC networks are at present only available for passive ladder simulation. Digital design is planned.

Ladder : [LUD, LEFT-DIRECT1, LEFT-DIRECT2, LEAPFROG, RIGHT-DIRECT1, RIGHT-DIRECT2, TWINTOR]

Passive ladder simulation methods (Fig. A.4). Left-direct and right-direct belong to the categories of type-E or type-F coupled-biquad. Twintor is only suited to bandstop simulation.

Input stage : [ONE-PHASE, TWO-PHASE]

The type of input stage to a ladder SC filter can be selected. A two-phase input implies that a sample-and-hold circuit must be added - a sizeable overhead for a small order filter. It may be dropped by adopting a single phase input with the penalty of LDI-type frequency response distortion.

Ladder type : [DOUBLY-TERMINATED, SINGLY-TERMINATED]

Resistive termination type of passive RLC ladder. Doubly-terminated ladders are known to have near optimal passband sensitivity. However singly-terminated structures have excellent dynamic range and can improve capacitance spread of an SC simulation.

Synthesis mode : [AUTOMATIC, INTERACTIVE, EXPERT]

This parameter controls the degree to which a user need guide the passive ladder synthesis operation. Automatic synthesis implies no intervention at all, producing a standard ladder structure. Interactive synthesis allows the zero

PANDA Version 1.000 16-Jun-89 AMSYS Filter Compiler					
DESIGN : Decoder Output Filter		DESIGNER : ncamos.filters.amsys.D07C		DATE 16:11:1989	TIME 12:10:38

<b>DEFINITION</b>  ORDER & SA  ORDER & FS  <b>FS &amp; SA</b>	ORDER : 5  <b>ORDER &amp; SA</b> RIPPLE : 0.03  GAIN : 0.00  FCLK : 128000.00	passband : 0.00  <b>LOWER BAND</b> stopband : 0.00  rejection : 0.00	passband : 3400.00  <b>UPPER BAND</b> stopband : 6000.00  rejection : 40.00	START : 10.00  <b>SIMULATION</b> STOP : 20000.00  NPOINTS : 200 LOG
---------------------------------------------------------------------------------	----------------------------------------------------------------------------------------------------	-------------------------------------------------------------------------------------	--------------------------------------------------------------------------------------------	---------------------------------------------------------------------------------------

<b>CLASS</b>  LOWPASS  HIGHPASS  <b>BANDPASS</b>  BANDSTOP	<b>APPROXIMATION</b>  ELLIPTIC CHEBYSCHV INVCHBY BUTTERWORTH BESSEL LEGENDRE <b>IIR</b>	<b>MISCELLANEOUS</b> TYPE <b>LEAPFROG</b> STRUCTURE RC1 RC2 OPTIONS TWINTOR WEIGHTING BIQUAD-E BIQUAD-F WARPING <b>BIQUAD-A</b> OPT FILE VALUES	LUD LD1 LD2 <b>EXECUTE</b> SYNTHESISE PLOT REALISE SCHEMATIC SWAP LAYOUT
------------------------------------------------------------------------------------	-----------------------------------------------------------------------------------------------------------------	-------------------------------------------------------------------------------------------------------------------------------------------------------------------------	-----------------------------------------------------------------------------------------------------

5th order filter 0 zeros at DC Finite zero pair at 6300.48Hz Finite zero pair at 9675.11Hz Pole pair at 3884.24Hz Q 3.61 Pole pair at 3287.45Hz Q 0.91 Pole at 2664.74Hz 5th order filter 0 zeros at DC Finite zero pair at 6300.48Hz	<b>WARNING</b> Odd order filter. Total capacitance required 48.78 units 1 2 43.52 units 2 1 Section 1 22.8 units Section 2 28.7 units Section 3 10.3 units total capacitance used is 53.793812 units writing swap files writing ALF file
------------------------------------------------------------------------------------------------------------------------------------------------------------------------------------------------------------------------------------------------------------------	---------------------------------------------------------------------------------------------------------------------------------------------------------------------------------------------------------------------------------------------------------------------

Fig. A.4 Filter realisation options

sequence to be defined. Expert synthesis mode allows both the zero sequence and the types of two-port sections to be defined.

**Biquad** : [TYPE-E, TYPE-F, AUTOMATIC SELECTION]

A biquadratic cascade may be composed entirely of type-E or type-F topologies as in the first two parameters. Alternatively, an automatic selection of biquad topology can be made in order to minimise the cost in capacitance spread.

**Pole-zero pairing** : [NONE, RING, STATISTICAL, EXHAUSTIVE, INCREASING-Q]

The poles and zeros of a given transfer function can be paired to reduce the capacitance spread of a biquad SC realisation:

1. NONE - no pairing done, initial sequence employed.
2. RING - n-pairings tried according to simple modulo shift-test rule. No changes in sequence.
3. STATISTICAL - a random selection of 100 pairings is tested.
4. EXHAUSTIVE - all  $n!$  possible pairings are tested. Not useful above 14th order due to excessive computation required.
5. INCREASING-Q - poles are ordered by increasing Q-factor from input to output. Minimum noise rule.

**Ideal** : [IDEAL, NON-IDEAL]

For the purposes of network simulation the circuit realisation may be ideal or non-ideal. For switched-capacitor circuits switches are given finite on-resistance and amplifiers finite gain and bandwidth.

**OA Paras.** : [GAIN, BANDWIDTH]

D.C. gain and 3dB bandwidth of operational

amplifiers. Typical values are shown in Fig. A.5.

Switch Res. : [ON-RESISTANCE, OFF-RESISTANCE]

Unit C : [1pF-1F]

For an ideal SC network the default unit capacitor value is 1F. For a non-ideal network the value is 1pF.

Max. CSpread : [10000]

Parameter controlling maximum tolerable capacitor. If any capacitor exceeds this value it is deleted from the circuit. Normally, this is only required to delete capacitors cancelled by zeros at  $\pm 2fs$ .

Scaling : [ON, OFF]

Scaling for maximum dynamic range and minimum capacitance spread may be switched off or on.

Output form. : [SCNAP, SWITCAP, SWAP, SPICE]

Netlist output format. Active-RC networks may be analysed by SCNAP or SPICE. Switched-capacitor networks by SWAP, SWITCAP or SCNAP.

Scaling range : [1.0-10.0]

Factor controlling frequency limits over which dynamic range scaling is performed. Expressed as a factor of current passband width i.e. 1.1 is scaled between 10% outside passband edges.

Scaling error : [0-60dB]

Allowable loss of dynamic range as trade-off with capacitance spread of SC filter. Often 6dB is the most useful value as it can half the largest capacitor ratio in the filter.

Filter stage : [AMPLITUDE, GROUP-DELAY EQUALISER]

The filter stage that is currently being compiled.

PANDA    Version 1.000    16-Jun-89    AMSYS Filter Compiler

DESIGN : Decoder Output Filter

DESIGNER : ncamos.filters.amsys.D07C

DATE    16 : 11 : 1989

TIME    12 : 10 : 38

DEFINITION

ORDER & SA

ORDER & FS

**FS & SA**

ORDER : 5

passband : 0.00

passband : 3400.00

START : 10.00

RIPPLE : 0.03

LOWER BAND

UPPER BAND

SIMULATION

GAIN : 0.00

stopband : 0.00

stopband : 6000.00

STOP : 20000.00

FCLK : 128000.00

rejection : 0.00

rejection : 40.00

NPOINTS : 200

LOG

CLASS

LOWPASS

HIGHPASS

**BANDPASS**

BANDSTOP

APPROXIMATION

ELLIPTIC

CHEBYSCHV

INVCHBY

BUTTERWORTH

BESSEL

LEGENDRE

**IIR**

MISCELLANEOUS

TYPE

STRUCTURE

OPTIONS

Maximum capacitance spread (units) : 1000.00

Unit capacitor (F) : 2.00E-013

On resistance (ohms) : 1000.00

Off resistance (ohms) : 1.00E+007

Opamp gain : 30000.00

Opamp bandwidth (Hz) : 2.80E+006

EXECUTE

SYNTHESISE

PLOT

REALISE

SCHEMATIC

SWAP

LAYOUT

5th order filter

0 zeros at DC

Finite zero pair at    6300.48Hz

Finite zero pair at    9675.11Hz

Pole pair at    3884.24Hz    Q 3.61

Pole pair at    3287.45Hz    Q 0.91

Pole at    2664.74Hz

5th order filter

0 zeros at DC

Finite zero pair at    6300.48Hz

43.52 units    2    1

Section 1    22.8 units

Section 2    28.7 units

Section 3    18.3 units

total capacitance used is    53.793812 units

writing swap files

writing ALF file

Fig. A.5 Non-ideal circuit parameters

At present it may either be an amplitude filter or a group delay equaliser. In future, this may be extended to anti-aliasing filters and decimators.

#### **A.1.2 Amplitude approximation (APPROX)**

This program will design a transfer function to filter amplitude specifications. If the approximation type belongs to a classical form then a series of explicit formulae are available for the pole and zero positions. A report is given of the achieved order, passband and stopband edge frequencies, passband ripple and stopband attenuation. This is very fast and reliable up to extremely high orders ( $> 50$ ). When the approximation belongs to the general IIR category a Remez-type optimisation algorithm is invoked. The transfer function is then fitted within an amplitude template (Fig. A.4). In both cases the output is a factorised transfer function scaled to maximum transmission of 0dB.

#### **A.1.3 Group delay approximation (DLA)**

This program designs an allpass group delay function of a specified order within specified bounds. An iterative Remez-type algorithm is once again employed, giving a report of convergency. The output is a factorised allpass transfer function in the same form as the amplitude transfer function above.

#### **A.1.4 Prototype design (LAD)**

This program is an implementation of the classical insertion loss synthesis method for passive ladders. It takes a normalised factorised transfer function and transforms it into the component values of a passive ladder prototype. Negative element values may be synthesised from poles placed on the real axis of the  $s$ -plane. All polynomials are maintained internally in factored form to preserve accuracy. The program can be coupled to an iterative passive ladder design stage for further accuracy refinement.

#### **A.1.5 All-pass ladder design (ALPLAD)**

A special singly terminated ladder is required for efficient design of SC all-pass ladder simulations. This program is a specially modified version of the previous one.

#### **A.1.6 Transfer function plotting (TFPLOT)**

Evaluate the factorised transfer function over a specified frequency range with a certain number of points. This is a very fast way of viewing the filter transfer function. Both group delay and amplitude are plotted (Fig. A.6).

#### **A.1.7 Circuit design (DSN)**

Designs an SC circuit to simulate the current transfer function or passive prototype. The circuit is scaled for maximum dynamic range and minimum capacitance spread. A report of the saving in total capacitance by dynamic range optimisation or pole-zero pairing is issued. An internal netlist of the designed filter in block format is produced.

#### **A.1.8 Internal filter analysis (ANALYSIS)**

Analyses the current filter design from its matrix system description. The amplitude and group delay are evaluated. Sensitivity of amplitude and group delay with respect to component value deviations are also calculated according to a variety of different norms. The dynamic range performance of the filter is also estimated by recording the minimum internal voltage levels. A rescaled filter matrix system and netlist are also produced.

#### **A.1.9 Network linker (LINKER)**

This program links netlists together. Networks can be added in series or parallel. This is primarily of use to cascade group delay equalisers with their amplitude filter.

#### **A.1.10 Netlist output (SCOUT)**

Translate the internal filter netlist to external form suitable for a network analysis program or a layout synthesiser. An analysis range is prompted for. Redundant components are eliminated at this stage. A report of the final cost of the filter in components and total capacitance is issued (Fig. A.7). A typical netlist is shown in Fig. A.8.



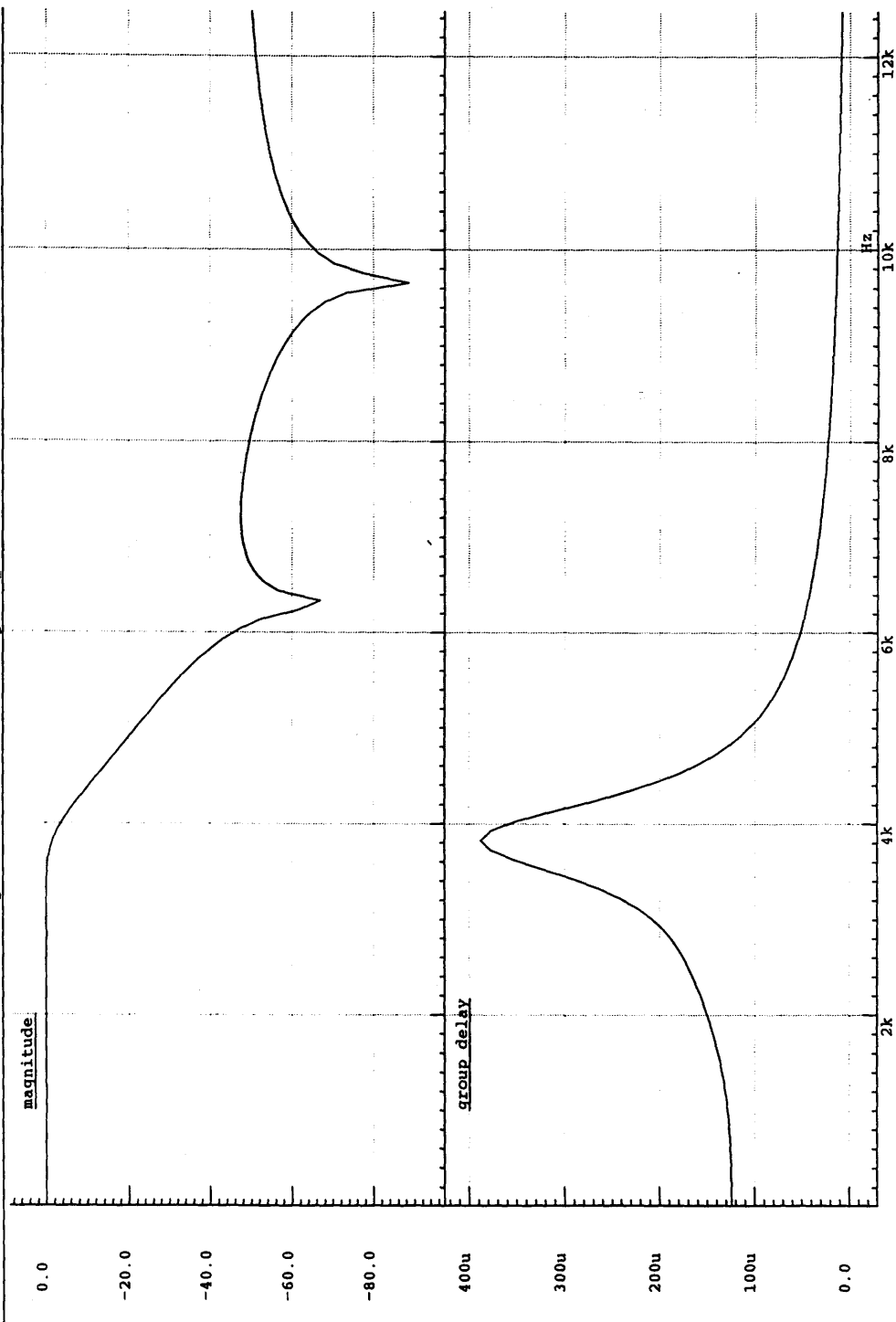


Fig. A.6 Display of filter amplitude and group delay response

#### **A.1.11 Optimisation (OPTM)**

Create error function between analysed filter performance and ideal specified passband response. This function will pre-warp the original filter template.

#### **A.1.12 Schematic generation**

GEC Research have written software which will generate circuit schematics of SCF designs (Fig. A.9).

#### **A.1.13 Automatic layout**

GEC Research has added the facility of automatic layout of the filter networks to PANDDA (Fig. A.10). Further description of PANDDA in its industrial environment can be found in the advertising material of Fig. A.11.

PANDDA -- Switched Capacitor Filter Output -- PANDDA  
Version 1.0 (c) R. K. Henderson 13-NOV-89 20:16:09

Design : 14th order elliptic bandpass type-e biquad sc filter

Output file format : SCNAP

Start frequency ? <0.1000E-01>

Stop frequency ? <0.1000E+06>

Number of points ? <201>

! Total capacitance = 320.1165units  
! Capacitance spread = 43.53361units  
! Average capacitor = 7.807721units  
! Number of capacitors = 41  
! Number of switches = 48  
! Number of op-amps = 10

**Fig. A.7 Report from filter output program (SCOUT) showing filter statistics**

```

! Total capacitance = 32.41205units
! Capacitance spread = 5.782805units
! Average capacitor = 2.315146units
! Number of capacitors = 14
! Number of switches = 20
! Number of op-amps = 3
statistics

title '3th order elliptic lowpass leapfrog ladder sc filter'
analyze
  freq 0.1000000E-01 10000.00 lin 201
  output 2
end

timing
  def
    T = 0.2500000E-04
  end
  even T (0 0.0) (1 1.0) (2 1.0)
  odd T (0 1.0) (1 0.0) (2 0.0)
end
clock waveform definitions

subckt opamp 1 2 3 4 (gain, BW)
  r 1 0 500M
  r 2 0 500M
  r 1 2 2M
  vccs 1 2 5 0 1.0
  r 5 0 gain/100
  c 5 0 50/PI/gain/BW
  vccs 5 0 3 4 4/3
  r 3 4 75
end
op-amp model definition

circuit
  def
    ron = 1000.000
    roff = 0.1000000E+08
  end
  switch resistances
  vs 1 0 ac 1.000000 0.0
  opamp 0 3 4 0 (100000.0, 10.00000)
  opamp 0 5 6 0 (100000.0, 10.00000)
  opamp 0 7 2 0 (100000.0, 10.00000)
  opamp 0 22 21 0 (1.000000, 0.1000000E+09)
  c 9 10 0.2242162E-11
  c 9 12 0.2242162E-11
  c 13 14 0.1435307E-11
  c 15 14 0.1000000E-11
  c 17 10 0.1435307E-11
  c 19 12 0.1000000E-11
  c 4 3 0.5645035E-11
  c 6 5 0.5782805E-11
  c 2 5 0.1478378E-11
  c 6 7 0.2121926E-11
  c 2 7 0.4028968E-11
  c 22 0 0.1000000E-11
  c 23 5 0.1000000E-11
  c 24 10 0.2000000E-11
  s 4 9 odd
  s 9 0 even
  s 10 5 even
  s 10 0 odd
  s 12 7 even
  s 12 0 odd
  s 6 13 odd
  s 13 0 even
  s 14 3 odd
  s 14 0 even
  s 2 15 odd
  s 15 0 even
  s 6 17 even
  s 17 0 odd
  s 2 19 even
  s 19 0 odd
  s 1 22 odd
  s 21 23 even
  s 21 24 odd
  s 24 0 even
end
switches

```

Fig. A.8 Netlist of filter in SCNAP format

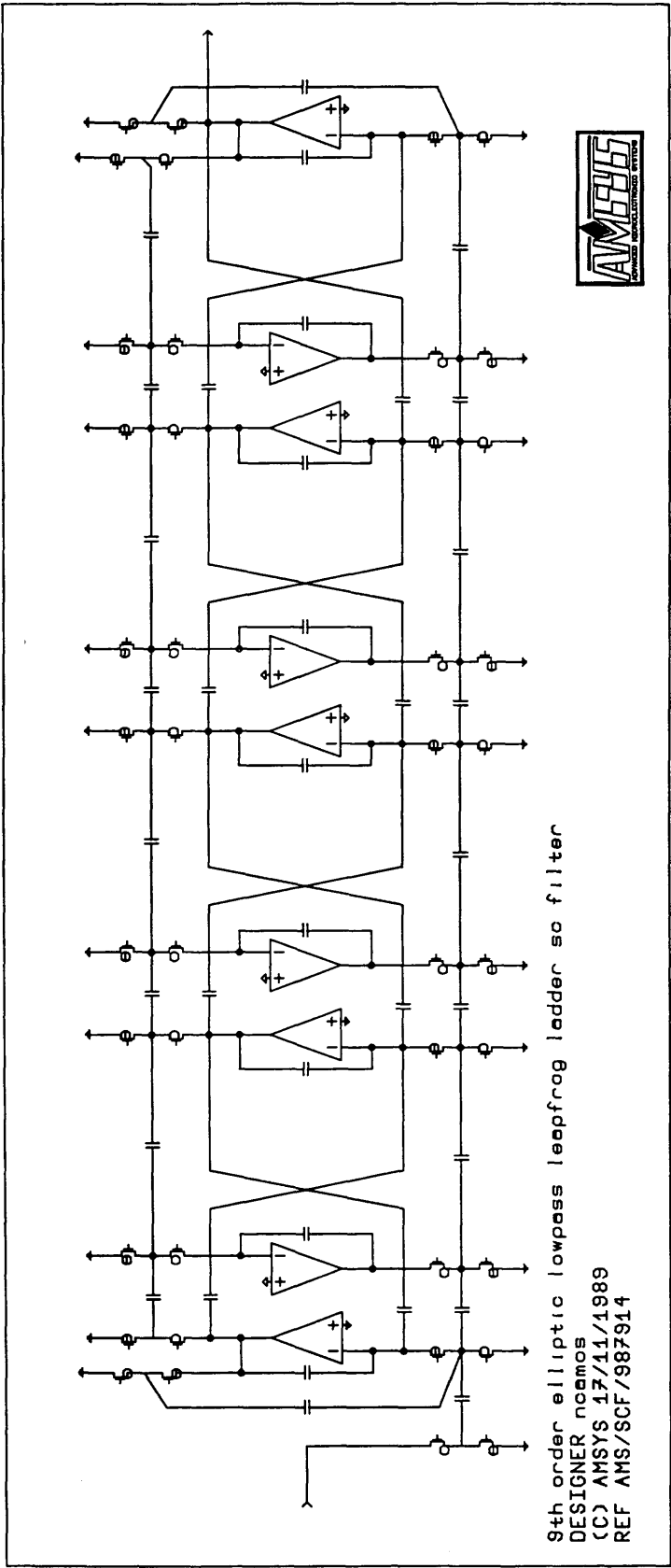
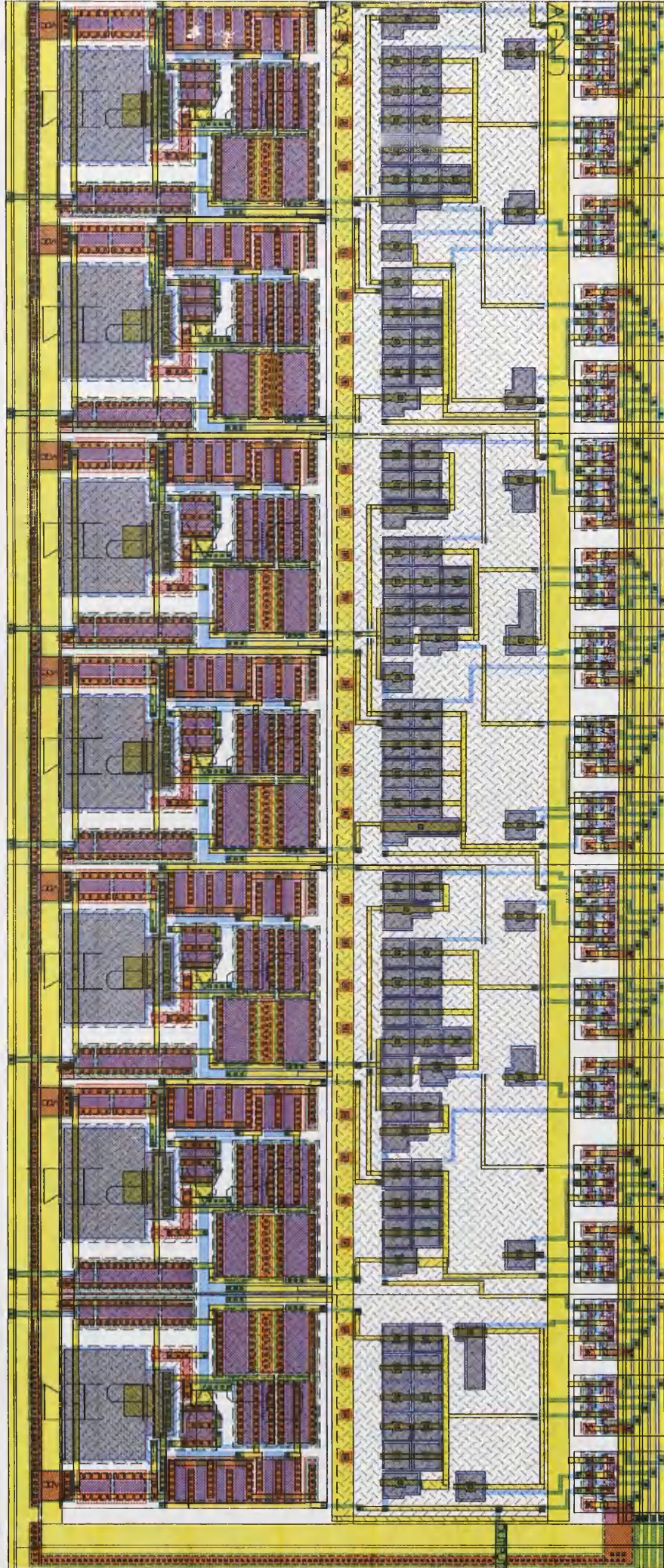


Fig. A.9 Automatic schematic generation of a 9th order leapfrog SC filter





© General Electric Company PLC, 1989

Fig. A.10 Automatic layout of 8th order biquad SC filter

### Background

- Work performed in the area of switched capacitor filters since 1979
- First SCF's implemented on silicon in 1981
- System chips designed including SCF's
  - ♦ PCM Combo
  - ♦ V22 bis Modem Front End
  - ♦ Speech codecs
  - ♦ Echo cancelling transceiver
  - ♦ SCF ASICs

### Upper limits of performance achieved

- 20<sup>th</sup> Order voice band filters
- Simpler filters at cutoff frequencies up to 250KHz
- Low distortion filters (THD typically less than -90dB)
- Low noise filters (Dynamic range typically 90dB)
- Multiple filters on a chip maintaining > 70dB crosstalk isolation
- Full continuous time anti-aliasing and anti-imaging filters also provided.

### SCF Design and Compilation suite

AMSYS has developed an extensive SC Filter compiler suite that allows rapid design and layout of both standard SC Filters and high complexity, arbitrary specification filters.

The whole suite is presented in a menu-driven environment running on Apollo workstations and allows a system designer to specify his requirements interactively with AMSYS. The following features are supported :

- Low-pass, band-pass, high-pass, band-stop and all-pass types
- Standard Butterworth, Chebyshev, Elliptic, Bessel etc approximations
- General amplitude responses specified by arbitrary piecewise linear templates and degree of flatness of frequency bands.
- Superimposed weighting functions e.g. sincx, LDI terminations etc
- Group-delay equalisation using all-pass functions
- Cascaded biquad and several ladder based configurations available
- Automatic generation of SCF schematic diagrams
- Detailed simulation of real effects in SCFs via SWAP<sup>1</sup>
- Automatic generation of SCF layout for biquads

Note 1      SWAP is a trademark of Silvar Lisco.

Advanced Microelectronic Systems  
PO Box 227  
East Lane  
Wembley  
Middlesex HA9 7TZ

Tel : 01 - 908 9200  
Fax : 01 - 904 7582  
290889 - 110

© The General Electric Company plc, 1988. This document gives only a general description of the product(s) or service(s) and shall not form part of any contract. From time to time changes may be made in the products or services or conditions of supply.

Fig. A.11 AMSYS advertising material



### Integrated filters


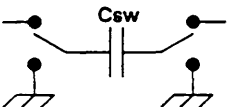
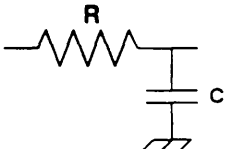
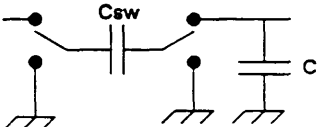
Traditional techniques for the implementation of filters in PCB or thick-film hybrid based systems have relied on accurate LCR or RC time constants to produce accurate filter responses. Passive filters and thick-film hybrids are expensive, and must be trimmed in production to meet performance requirements. Stability and long-term reliability of such systems can also be a problem.

Typical CMOS processes cannot integrate inductors, and the absolute accuracy of resistors and capacitors is not well controlled, leading to RC time constants with a tolerance typically worse than  $\pm 40\%$  which is also temperature and signal-level dependent. Audio-frequency time constants also require large RC values and consequently high silicon area.

### Switched-capacitor filter techniques

Switched-capacitor filter techniques have been developed over the last 10 years, and are particularly suitable for integrated circuit applications which require precision filtering. The basic principles are essentially very simple.

Consider a simple resistor and first-order RC filter network in passive and switched-capacitor forms.

Passive network :	Switched-capacitor equivalent :
 $I = (V_{IN} - V_{OUT}) / R$	 <p>For each switch transition, a charge <math>Q</math> flows  <math>Q = C_{sw} (V_{IN} - V_{OUT})</math>          If the switches are clocked at a rate <math>F_{clock}</math>, the charge flowing per second is given by</p> $I = (V_{IN} - V_{OUT}) \cdot C_{sw} \cdot F_{clock}$
 <p>Time constant = <math>RC</math></p>	 <p>Time constant = <math>C / (C_{sw} \cdot F_{clock})</math></p>

Provided the capacitors are switched at a rate much higher than the signal frequency, switched-capacitor time constants depend only on the matching accuracy of capacitors and the clock frequency. Very complex filtering functions can be performed based on extensions to this technique. There are two main approaches, usually starting from a passive LCR ladder filter :

- Simulate the passive ladder voltages and currents directly.  
There are several techniques available, leading to filters with theoretically low sensitivity to component values, although in practice such structures are only used in the design of lowpass filters due to problems with their implementation on silicon.
- Decompose the passive ladder into its poles and zeros, and implement pole-zero pairs as biquadrate sections.  
This is a very popular technique, as it is relatively easy to automate the design and layout of any filter shape in such an architecture. Allpass filters can also be designed for group-delay equalisation.

Advanced Microelectronic Systems  
 PO Box 227  
 East Lane  
 Wembley  
 Middlesex HA9 7TZ

Tel : 01 - 908 9200  
 Fax : 01 - 904 7582  
 280388 - 103

© The General Electric Company plc, 1988. This document gives only a general description of the product(s) or service(s) and shall not form part of any contract. From time to time changes may be made in the products or services or conditions of supply.



## SWITCHED-CAPACITOR FILTERS – PERFORMANCE

These performance figures are intended to give a general guide to the capabilities of switched-capacitor filters on a particular process, and apply only to the process specified below.

**Process**                      *Generic 3 micron double poly single metal p-well CMOS process.*

### General points

- Any filter shape can be synthesised using AMSYS proprietary software.
- There is no limitation on the order of the filter. Filters from 2nd to 20th order have been implemented.
- Several filters can be implemented on the same chip.  
50 orders of filtering on a chip is not unusual.

### Performance guidelines

These figures indicate performance levels for a typical filter in the given technology. Some performance figures are highly dependent on the filter type.

- 5V or 10V operation
- Maximum cutoff frequency                      30kHz to 50kHz  
Can be higher depending on application and filter complexity.
- Clock to cutoff frequency ratio                      >20  
Lower values make anti-aliasing more difficult.
- DC offset voltage                      10mV
- Current consumption                      100µA per filter order
- Power supply rejection                      Dependent on filter complexity. Figures on request.
- Slew rate                      >5V/µs
- Dynamic range                      >70dB dependent on filter complexity.
- Crosstalk between filters on same chip                      >70dB dependent on chip complexity.
- Typical standard amplifier performance

SC filter amp	Signal voltage range	Vdd – 0.5V Vss + 0.5V
	Drive capability	100kΩ 20pF
	Unity-gain bandwidth	3MHz
Standard off-chip driver	Signal voltage range	Vdd – 0.5V Vss + 0.5V
	Drive capability	<1kΩ 400pF
	Unity-gain bandwidth	4MHz

The standard amplifiers above are designed to meet the performance levels required for the majority of filter applications. Other amplifiers are available with higher drive level, voltage range and unity-gain bandwidth.

Advanced Microelectronic Systems  
PO Box 227  
East Lane  
Wembley  
Middlesex HA9 7TZ

Tel : 01 – 908 9200  
Fax : 01 – 904 7582  
280388 – 109

© The General Electric Company plc, 1988. This document gives only a general description of the product(s) or service(s) and shall not form part of any contract. From time to time changes may be made in the products or services or conditions of supply.

## SWITCHED-CAPACITOR FILTER SYNTHESIS

### Features

- Starting point – LCR ladder or pole-zero specification file from AMSYS passive filter synthesis software.
- Choice of biquad or several ladder realisations, including LDI and Bilinear.
- Rapid estimation of silicon area.
- Simulation of ideal and non-ideal frequency, impulse response and sensitivity analysis, using state-of-the-art simulator – Silvar Lisco SWAP™.
- Parasitic capacitance extraction, back-annotation and resimulation of physical circuit layout.
- Automatic generation of schematic diagram.
- Automated layout of filter cells.
- Automatic layout generation of continuous-time anti-aliasing and smoothing filters.

SWCAPFS Version 1.100b 28-Jan-88 AMSYS Switched-Capacitor Filter Synthesis			
DESIGN : LOWPASS7		DESIGNER : Neil Amos	DATE : 18-Feb-1988 15:36:19
FILTER : LOWPASS	INPUT : LCR	CIRCUIT : (BIQUAD)	TOTAL CAPACITANCE = 241 units
TYPE : CAUER	POLE/ZERO :	AM-DS1	LARGE CAPACITORS = 53.7 26.0 24.1 units
ORDER : 7	UNITCAP DIMENSION (um) : 25	AM-DS2	AREA ESTIMATE = 1400 x 660 um = 924000 sq um
PASSBAND EDGE = 3400.0	UNITCAP VALUE (pF) : 0.40	AM-LUF	CIF FILE = LOWPASS7.CIF
STOPBAND EDGE = 7000.0	CLOCK FREQUENCY : 100000.00	IM-OF	SWAP FILE = LOWPASS7.HOF
		IM-ICS	ALF FILE = LOWPASS7.ALF
		IM-LUD	
		LOI	
		ALLPASS	

### Capability

The AMSYS switched-capacitor filter synthesis software is an integrated CAD package to generate switched-capacitor filter blocks from an LCR ladder or pole-zero specification, usually defined using the AMSYS passive filter synthesis suite. Customers can call on the extensive expertise within AMSYS to assist and advise on switched-capacitor filter specification and realisation, and integrate such filters into larger systems with associated anti-aliasing and smoothing filters.

The synthesis of the switched-capacitor filter design has been completely automated, the program allowing designers to select the particular filter topology which results in the lowest silicon area or gives the lowest sensitivity to capacitor values. Theoretically, ladder structures have lower sensitivity than cascaded biquad realisations, but are normally only used in lowpass filters due to silicon implementation problems. Biquadratic sections can be used to synthesise any filter response, including allpass sections.

The software runs on Apollo workstations, and produces a switched-capacitor filter topology with full dynamic range scaling within seconds. The resulting circuit may then be simulated to include non-ideal effects such as opamp gain-bandwidth and switch resistance.

Ideal and non-ideal simulation responses can be compared before and after layout, so that any parasitic capacitances occurring in the integrated circuit layout of complex filter structures can be removed prior to manufacture.

Switched-capacitor filters up to 20th order have been implemented successfully using this synthesis package.

Advanced Microelectronic Systems  
PO Box 227  
East Lane  
Wembley  
Middlesex HA9 7TZ

Tel : 01 - 908 9200  
Fax : 01 - 904 7582

280388 - 102

© The General Electric Company plc, 1988. This document gives only a general description of the product(s) or service(s) and shall not form part of any contract. From time to time changes may be made in the products or services or conditions of supply.

## APPENDIX B : ANALYSIS OF DISTRIBUTED—RC NETWORKS

### B.1 Distributed—RC networks

Active filters with distributed RC components have found application recently as anti—aliasing/smoothing filters in analog sampled data systems [1]. The choice of a distributed RC network over a discrete network has the following advantages.

1. The passband is flatter for a distributed RC network compared with a discrete network with the same  $-3\text{dB}$  corner frequency, while the stopband rolloff is much steeper.
2. A large reduction in silicon area due to the overlap of resistance and capacitance areas.
3. Elimination of substate power supply coupling of discrete polysilicon resistor realisations.

Some additional improvement in the frequency response of the distributed network is possible if the distributed RC components are tapered: a steeper rolloff in low pass filters and a narrower rejection band in notch filters may be obtained [2]. Commonly available circuit analysis programs are not able to analyse tapered components so that the potential benefits of tapering have not been realised in current designs [3–4]. An interesting recent development concerns the use of distributed—RC elements to design accurate continuous—time integrator structures whose time constants track with temperature and processing variations [5].

### B.2 Program for the analysis of distributed—RC networks

A computer program capable of analysing networks of discrete and distributed RC components in the frequency domain has been written. The distributed RC components may be tapered in a uniform, linear or exponential manner.

The program is capable of producing a frequency analysis of linear networks of discrete and distributed components. Inputs are requested interactively from the user. A file containing a network description and (possibly) some default analysis options must be written. Once the program is run, the user may specify the input and output filenames, the frequency range and the type of frequency step, and the output nodes of the network. Any network file may then be loaded and analysed and the results viewed at the terminal or written to an output file. The output of the program is a list of the magnitude and phase of the voltages at the

output nodes of the network. The magnitude may be in dBs or absolute and the phase is in degrees.

The program is capable of analysing the following lumped elements.

1. Inductors
2. Capacitors
3. Resistors
4. Independent a.c. voltage and current sources
5. Controlled sources (VCVS, CCVS, VCCS, CCCS)

The program is capable of analysing the following distributed elements.

1. uniform RC lines (URC)
2. linearly tapered RC lines (LRC)
3. exponentially tapered RC lines (ERC)

The definition of these RC lines allows for an arbitrary number of tap points on the surface of the distributed resistor.

The main stages in the analysis procedure are given below.

*Step 1: read a network description from an input file.*

*Step 2: check network topology and build a list of node numbers used.*

*Step 3: form MNA system matrices for discrete components*

$$(G + sC)V = W$$

where  $G$  and  $C$  are modified nodal admittance matrices and  $W$  is an excitation vector.

*Step 4: pre-process distributed RC components. This involves splitting tapped lines into individual distributed sections and pre-calculating constants used very frequently in later calculations.*

*Step 5: form a system of complex linear equations describing the network at frequency  $\omega$ ,*

$$(G + j\omega C + D_{re} + jD_{im})V = W$$

where  $D = D_{re} + jD_{im}$  is a nodal admittance matrix of the distributed components in the circuit. This is formed by calculating the real and imaginary components of the  $y$ -parameters of the distributed components and adding them into the system matrix [2]. These  $y$ -parameters have no constant or linearly

*dependent on frequency terms and so must be recalculated at each new frequency. In the case of the linearly tapered RC lines this involves evaluating Bessel functions by a series approximation.*

*Step 6: LU factorise the MNA matrix using the Crout method.*

*Step 7: solve for the node voltages by forward and backward substitution.*

*Step 8: repeat from Step 5 at each new frequency of interest*

### B.3 Analysis examples

A series of analyses of circuits containing distributed—RC lines is illustrated. Fig. B.1 gives a comparison of the results of a SPICE analysis of a uniform distributed RC line simulated as a succession of many RC sections with that of an exact model [4]. A large number of RC sections is required to produce a realistic analysis result, at great cost in computer time. Fig. B.2 shows that by increasing the degree of taper ( $\tau$ ) of a linearly tapered distributed RC line the roll-off can be increased [2]. Fig. B.2 shows a simple distributed—RC notch circuit, variation of the taper factor can greatly increase the selectivity. Finally the frequency response of a 3rd order lowpass filter is shown in Fig. B.4 with two sets of optimised component values [6].

### REFERENCES

- [1] B. K. Ahuja, "Implementation of active distributed RC anti-aliasing/smoothing filters", IEEE J. Solid-State Circs, vol. SC-17, no. 6, Dec. 1982.
- [2] W. M. Kaufman and S. J. Garrett, "Tapered distributed filters", IRE Trans. on Circ. Theory, ct-8, pp. 329-336, 1962.
- [3] K. Singhal and J. Vlach, "Approximation of nonuniform RC distributed networks for frequency and time domain computations", IEEE Trans. on Circ. Theory, Vol CT-19, No.4, July 1972
- [4] L. P. Huelsman and W. J. Kerwin, "Digital computer analysis of distributed-lumped-active networks", IEEE Journal of Solid State Circuits, Vol. SC-3, pp26-29, Mar. 1968
- [5] J. M. Khoury and Y. P. Tzividis, "Active URC circuit realisation of arbitrary rational transfer functions in s", Proc. ISCAS, pp. 1071-1074, Portland, Oregon, May 1989.
- [6] M. E. Mokari-Bolhassan and T. N. Trick, Correspondence, IEEE Trans. on Circuit Theory, Jan. 1971, pp297-298

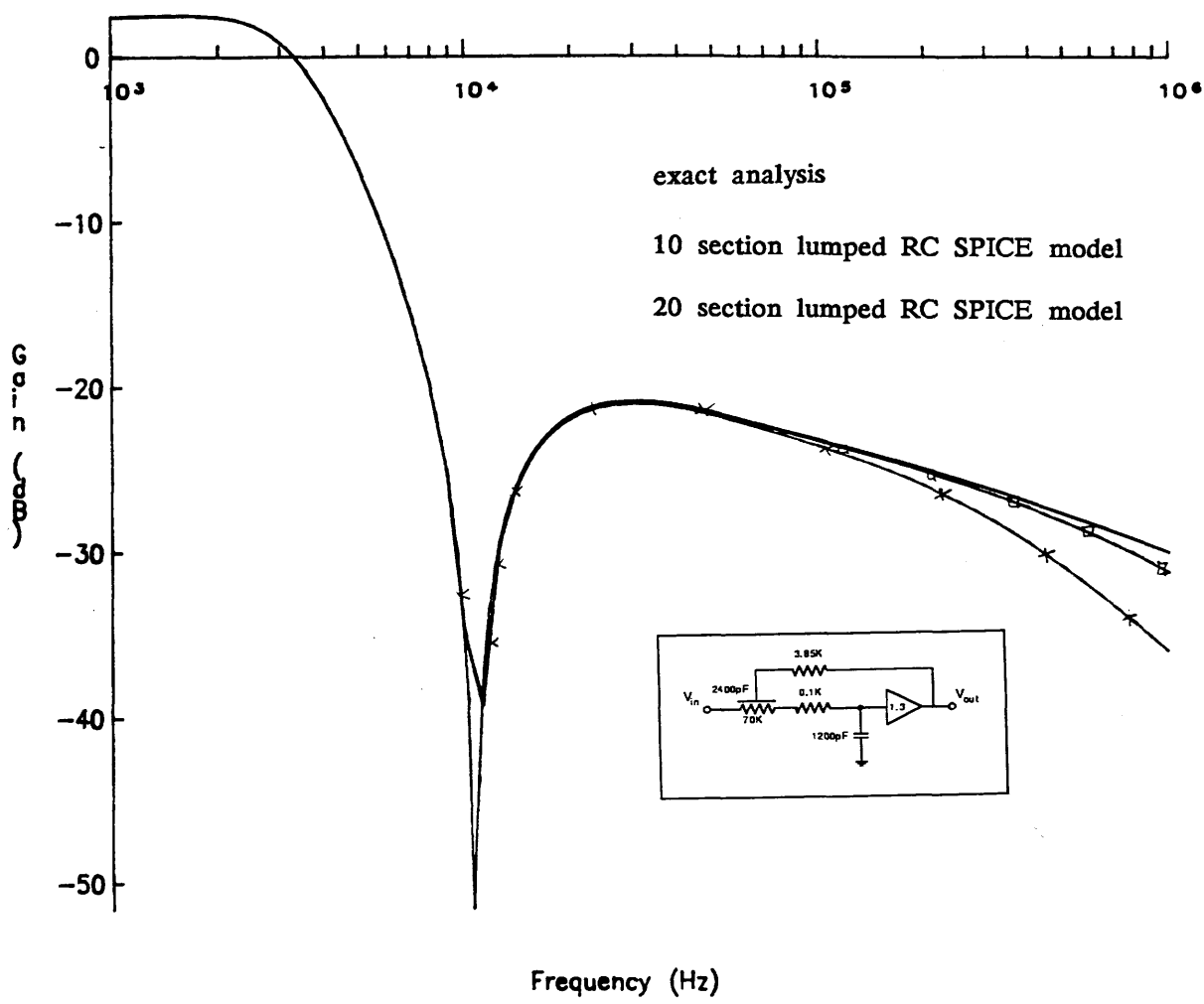


Fig. B.1 Comparison of approximate (SPICE) analysis of URC network with exact response

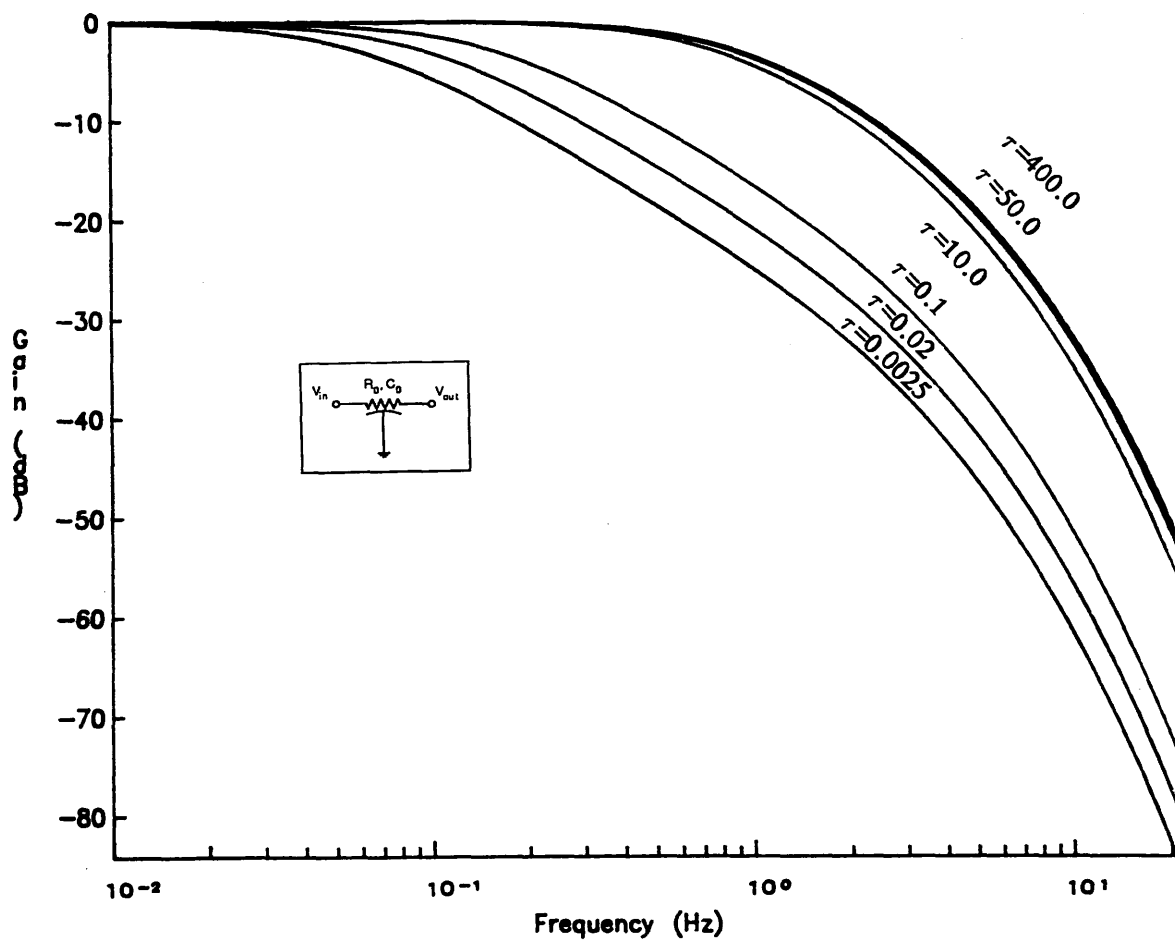


Fig. B.2 Variation of frequency response of linearly tapered distributed-RC line with taper factor

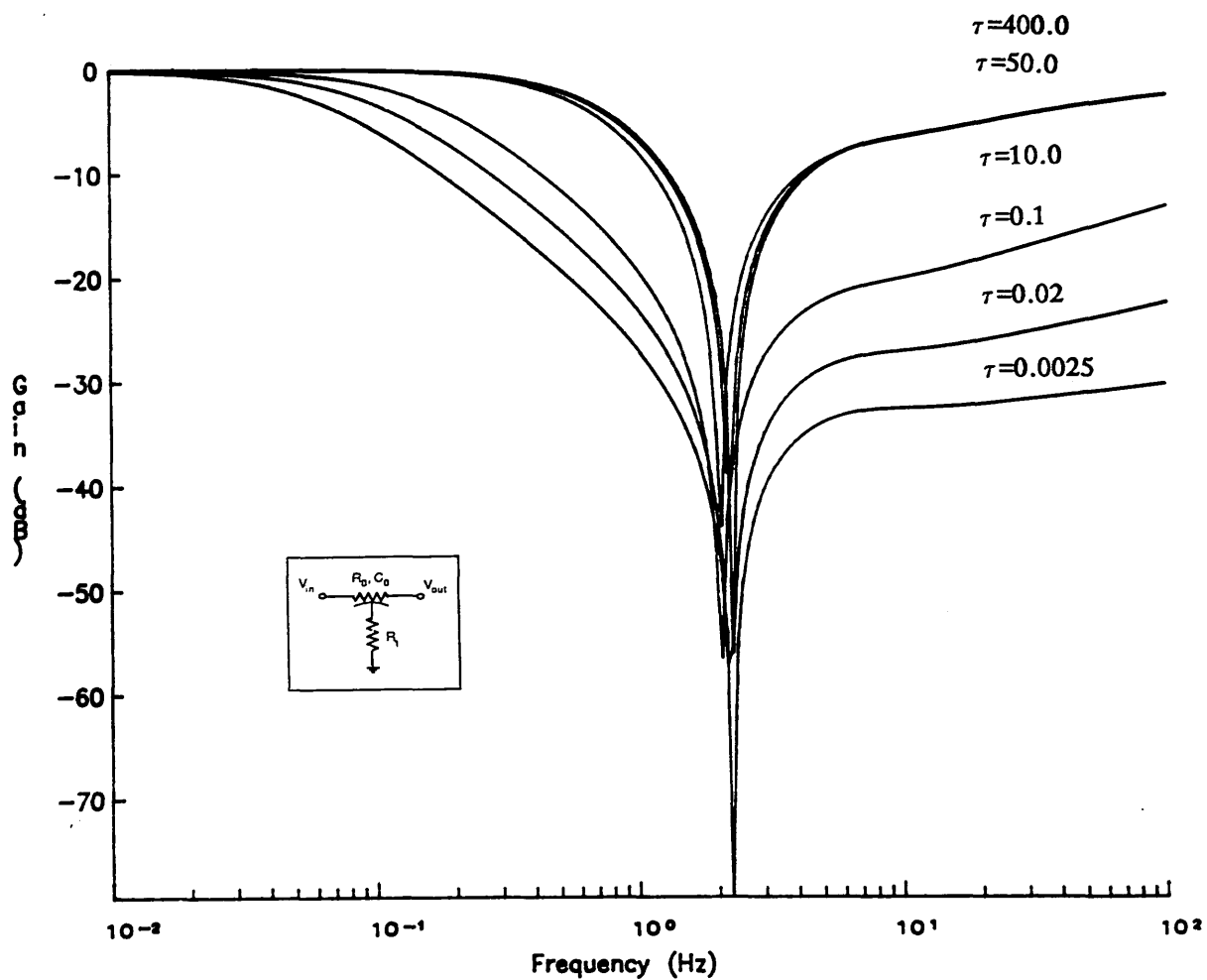


Fig. B.3 Linearly tapered distributed RC notch circuit with various taper factors



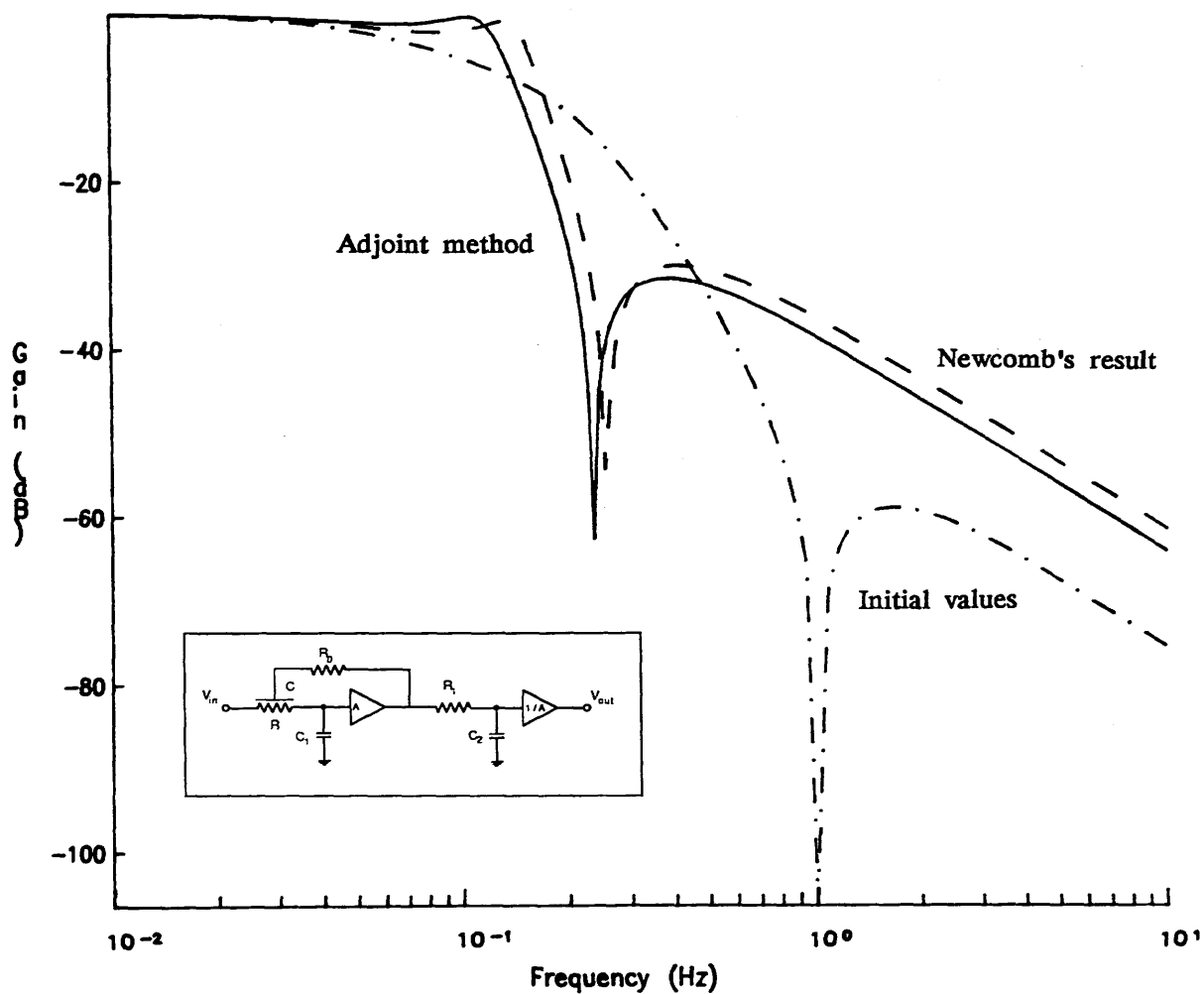


Fig. B.4 Frequency response of various 3rd order lowpass URC filters